HARD TURNING OF MARTENSITIC AISI 440B STAINLESS STEEL

Kehinde K. Sobiyi

A thesis submitted to the Faculty of Engineering and the Built Environment, University of the Witwatersrand, Johannesburg, in fulfilment of the requirements for the degree of Doctor of Philosophy in Metallurgy and Materials Engineering

Johannesburg, 2015

DECLARATION

I declare that this thesis is my own, unaided work. It is being submitted for the Degree of Doctor of Philosophy in Metallurgy and Materials Engineeringat the University of the Witwatersrand, Johannesburg. It has not been submitted before for any degree or examination at any other University.

_____

(Signature of candidate)

_____day of _____year_____

ABSTRACT

Hard turning has been in use for some time to achieve close dimensional tolerances to eliminate time consuming and costly grinding operations. The most widely used cutting tools for finish machining of hardened steels under dry cutting conditions are the ceramics and PcBN cutting tools.

The purpose of this study was to investigate the machinability of hardened martensitic AISI 440 B stainless steel (HRC 42-44) using commercially available cutting tools: alumina based ceramic and PcBN, by hard turning under different machining conditions, by providing an in-depth understanding of wear mechanisms of these cutting tools. The study also developed a serrated chip formation mechanism of the workpiece and provided a deep understanding of the chemical interaction between workpiece and cBN cutting tools, through microstructural analysis of the adhered layer on the worn cutting tool.

Experimental studies on the effects of cutting parameters on the tool wear mechanism, cutting forces; surface roughness, dimensional accuracy, and chip formation mechanism were investigated.

The characterization of the workpiece, cutting tools, chips and wear scars on the cutting tools was performed using an X-ray diffractometer, and optical, scanning and transmission electron microscopes, as well as an energy dispersive spectroscope (EDS).

The cutting speeds selected for testing the cutting tools were in the range of 100 m/min and 600 m/min, depending on the type of parameter investigated. Two depths of cut, 0.1and 0.2 mm, and three feed rates, 0.05, 0.1 and 0.15 rev/min, were selected for the experiments.

Experimental results showed that the flank wear in the PcBN cutting tool is lower than that of the mixed alumina, with PcBN showing better wear resistance at all cutting conditions (about five times longer in some instances). Apart from the cutting speed, the feed rate was found as a parameter that directly influences the flank wear rate of the cutting tool.

The wear mechanism for the ceramic cutting tool is predominantly abrasive wear, and for PcBN tools it was adhesive wear and abrasive wear. The abrasive wear was caused by hard carbide particles in the workpiece material resulting in grooves formed on the flank face.

There was formation of a transferred layer followed by plastic deformation of the workpiece material on the rake face of the PcBN tool when cutting at low cutting speed and feed rate. At much higher cutting speeds, some form of chemical wear preceded by adhesion and abrasion was the main tool wear resulting from the chemical affinity between the PcBN tool and the workpiece.

Better surface finish (Ra) was recorded for mixed ceramics but with deteriorating surface topography. The increase in the cutting speed results for improvement in the surface finish produced by both cutting tools was investigated. The final part, using the PcBN cutting tool, produced better dimensional accuracy resulting from its better wear resistance at the flank face. The results also show that good dimensional accuracy can be achieved with cBN tools using a CNC machine with high static and dimensional stiffness coupled with high precision hard turning.

The influence of cutting conditions on the chip formation showed production of continuous chip at a cutting speed of 100 m/min and segmented chip at higher cutting speeds above 200 m/min by both cutting tools. The increasing cutting speed affects the formation of shear localised chips with rapid increase in shear strain rate and degree of segmentation at cutting speeds higher than 200 m/min. The microstructure of the chip produced shows the distinct carbide grain in the martensite of the work material with intense shear localisation in the primary deformation zone of the cutting tool and formation of white layer in the secondary deformation zone.

The microstructure of the crater of the worn PcBN cutting tool at cutting speeds of 100 m/min and 600 m/min were studied in detail. A situ lift-out technique, in a Focused Ion Beam/SEM instrument, was used to produce thin foil specimens, which were taken out of the crater face of the PcBN tool and observed using SEM and TEM. The SEM and TEM study showed evidence of chemical interaction between the work material and the PcBN tool. Fe from the work material was found in the vicinity of TiC and AlB grains of the PcBN tool, with TiC having greater affinity for Fe. Oxidation of the elements was common in all Fe-rich areas. The microstructure of the worn PcBN cutting tool at the cutting speed of 600 m/min showed deeper penetration of Cr and Fe into the cBN tool, which was not easily detected by SEM at the cutting speed of 100 m/min.

The hard turning operations using the PcBN cutting tool for substituting traditional machining operations was successfully performed in the industrial environment. The overall surface finish and dimensional accuracy generated during the application of CBN-100 for machining within the industrial environment on specified mass produced shape showed a component acceptable tolerance range with good surface finish similar to that of the grinding operation.

DEDICATION

To Mofiyinfoluwa, Mofopefoluwa, Moranuoluwa, Moposoreoluwa, Darasimi

ACKNOWLEDGEMENTS

I thank Almighty God for his grace and favours during my PhD studies.

My deepest gratitude goes to my supervisors, Prof. Iakovos Sigalas and Prof. Guven Akdogan for their strong and endless support, encouragements, fruitful discussions and patience throughout the duration of my studies towards my thesis. It was a privileged to work with them and to share from their valuable expertise.

I am grateful to Dr Matthias Herrmann for his fruitful discussions and contributions. I am also grateful to Dr. Peter Olubambi and Dr. James Wesley-Smith for their valuable help in scanning electron microscopy and transmission electron microscopy investigations.

I give my specialthanks to the personnel of Castco Precisions Pty Ltd., most especially Mr. Yunus Turan for allowing me to conduct some experimental works using their facilities, providing me an opportunity to have an industrial experience in machining and other technical assistance provided.

I would also like to take advantage of this opportunity to thank the staff and students of the School of Chemical and Metallurgical Engineering for their contributions to this research project.

I will like to thank Dr. Olugbenga Johnson for his inputs and assistance with microstructural analysis of my specimens.

I wish to thank the project sponsors, DST-NRF Centre of Excellence in Strong Materials, University of the Witwatersrand, Johannesburg, and Element Six Pty Ltd., for funding this research.

Lastly, I take this opportunity to express my gratitude to my family for unfailing encouragement, prayers and support**.**

CONTENTS

LIST OF FIGURES

LIST OF TABLES

LIST OF ABBREVIATIONS

Aluminium Oxide	Al_2O_3
Axial Force	F_f
Built Up Edge	BUE
Built Up Layer	BUL
Cubic Boron Nitride	cBN
Computer Numerical Controlled	CNC
Energy Dispersive Spectroscope	EDS
Energy Dispersive X-ray Spectroscopy	EDX
Focused Ion Beam	FIB
High-Speed Steels	HSS
Polycrystalline Cubic Boron Nitride	PcBN
Polycrystalline Compact Diamond	PCD
Radial Force	F_r
Secondary electron	SE
Scanning Electron Microscope	SEM
Scanning Transmission Electron Microscope	STEM
Tangential Force	F_c
Transmission Electron Microscope	TEM
Titanium Carbide	TiC
Titanium Nitride	TiN
Tungsten Carbide	WC
X-Ray Diffraction	XRD
Zirconium dioxide	ZrO_2

1 INTRODUCTION

1.1 GENERAL BACKGROUND AND JUSTIFICATION OF THE RESEARCH

In the last few decades, hard turning has fast become an attractive alternative route for finish production of parts made from hardened steels, as opposed to grinding. Hard turning has been in use for some time to achieve close dimensional tolerances to eliminate time consuming and costly grinding operations. Hard part turning allows machinists to simplify their processes and still achieve the desired surface finish quality. This form of machining is a finishing or semi-finishing operation that depends on geometrical accuracies, surface topography and integrity of the subsurface layer of the final part produced (Ko and Kim, 2001).

The acceptability of hard turning over the grinding process must satisfy the workpiece high quality requirements such as form and size accuracy, surface finish and surface integrity. These requirements are mainly determined by the following conditions: machining parameters, tool materials, cutting edge geometry, properties of the machine tools, and the geometric shape of the workpiece (Tonshoff, et al., 1995; Ko and Kim, 2001).

The advantages of hard turning as a potential replacement over grinding for hardened steels includes: lower machining costs, increased flexibility of the machining technology, few process steps, shorter set up times and the optional use of coolant, the latter offering a more environmentally friendly operation (Konig, et al., 1990a; Tonshoff, et al., 2000; Housheng, et al., 2007; Sieben, et al., 2010).

The cost consideration associated with hard turning compared to grinding is for finish production of parts as illustrated in Figure 1–1. From the figure, it follows thatthe overall cost ofthe finish-turning of a gear blank (hardness of about 62 HRC) using a PcBN cutting tool was less than that of grinding.

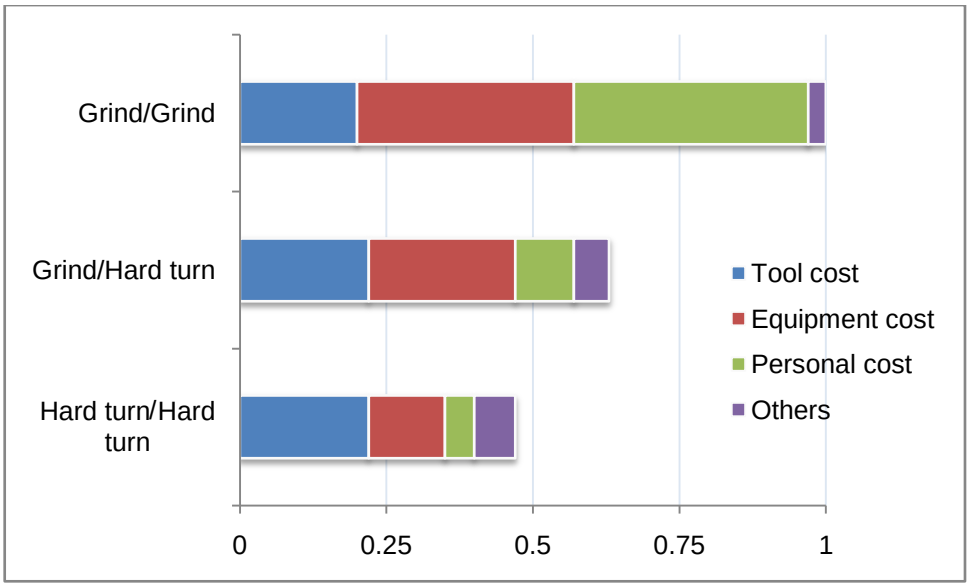

Figure 1-1Cost comparison between hard turning and grinding (Adapted from Eredel BP, 1998)

Current techniques used to manufacture parts from hardened materials aresimplified by hard turning and involve three sequential steps:heat treatment to the required hardness, rough machining of the hardened steel, and finish machining to the required dimensional accuracy (Noordin et al., 2007). Figure 1–2 shows the sequential steps in hard turning as compared with conventional turning steps. Parts hard turned are usually machined in a highly tempered or hardened state with geometrically defined cutting tools (Ko and Kim, 2001).

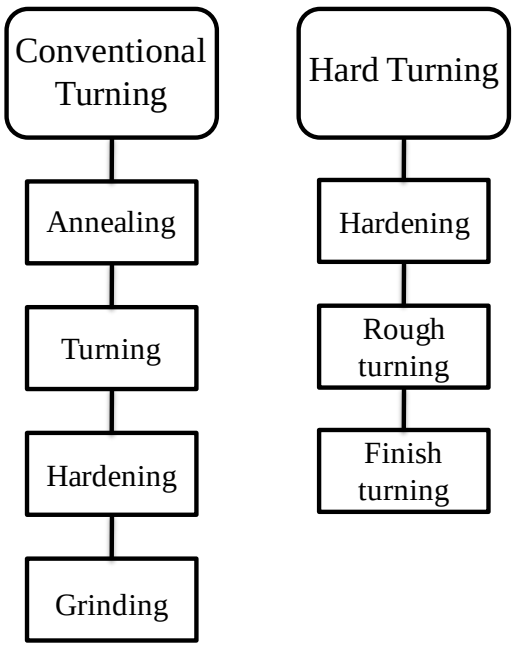

Figure 1-2 Sequential steps for conventional and hard turning (Adapted from Dograet al.,2010)

Hard turning is commonly used for producing parts such as gears, bearings and shaft-type automotive drive-train components. The types of materials that can be cut by the hard turning method are growing in number and applications as a result of advances in recent research. The most common hard turned material is stainless steel,owing to its wide application in the automotive and tool and die industries (Grzesik, 2008). The main demand in product quality in the mould and die industry is often geometrical precision anddimensional accuracy (Yih-Fong, 2006). In addition, these high performance parts require high wear resistance and compressive strength.

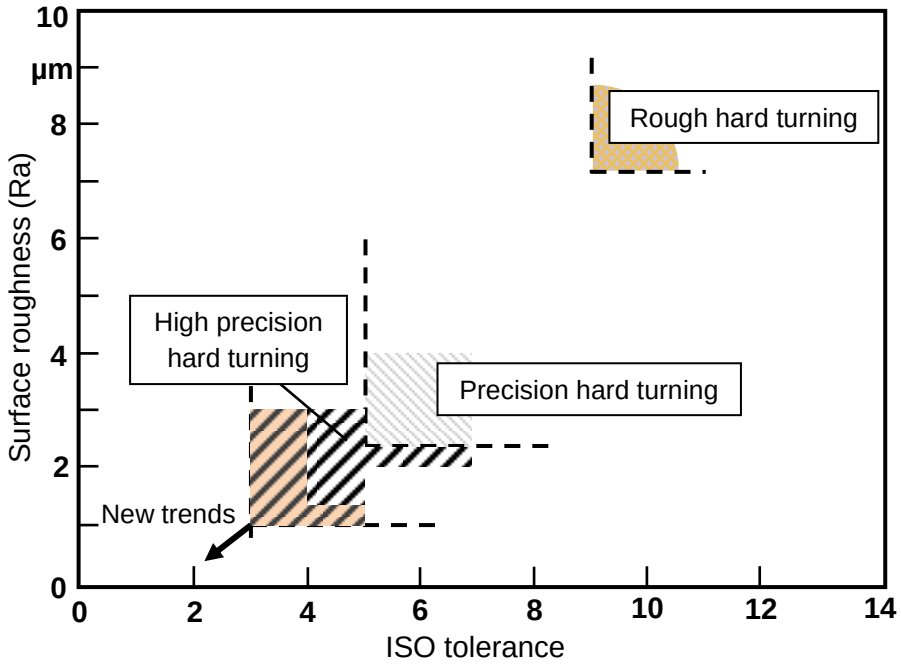

Figure 1-3Achievable surface roughness and ISO tolerance in hard turning (Adapted from Bryne et al., 2003)

Figure 1–3 shows the trends of hard turning fromprecision hard turning to high precision hard turning. It has been demonstrated that during high precision machining using a cBN cutting tool under specific machining conditions, values of 1 µm Rz (equivalently 0.1 µm Ra) and correspondingly IT3 dimensional tolerance are possible (Grzesik, 2009).

Machining of hardened parts does not involve turning alone but also other machining processes,such as milling, drilling, broaching, threading, and reaming. These operations are also performed using PCD, PcBN, Ceramics and Cermetcutting tools.

As shown in Figure 1–4, awide range of machining operationscan be performed on lathes, on hardened transmission parts,including longitudinalcontinuous and interrupted turning, facing and boring, as well as grooving and threading.

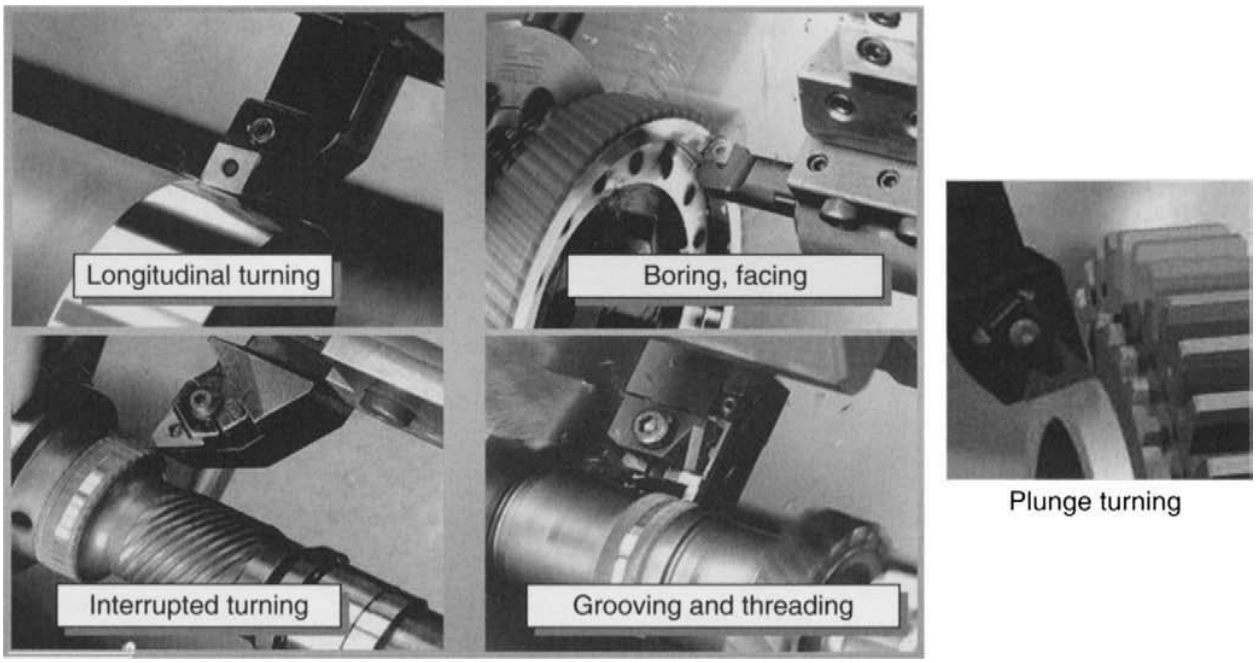

Figure 1-4Machining applications on the lathe including boring, threading and hard turning (Courtesy, Grzesik, 2008)

Generally, for many hard parts, relatively high accuracy can be achieved during hard turning, but sometimes important problems arise with surface integrity, especially with changes of subsurface microstructure (white layer), and undesirable patterns of residual stresses which reduce the fatigue life of the machined surfaces (Grzesik, 2008).

The various workpiece materials involved in hard machining include hardened cast irons, alloy steels,hard-chrome-coated steels, bearing steels, case-hardened steels, tool steels, superalloys,nitrided irons and heat-treated powder metallurgical steels (Abrao et al., 1995; Chou and Evans, 1997; Luo et al., 1999; Richt, 2009; Sales et al., 2009).

Of all the stainless steel alloys, martensitic stainless steelis an appropriate type of stainless steel for hard turning since it can be easily hardened by quenching and tempering, and therefore it can achieve high strength and hardness levels (Sourmail and Bhadeshia, 2005). Martensitic stainless steels are generally known to be chromium steels with higher carbon content when compared to austenitic and ferritic stainless steels (Bramfitt, 2002). The family

relationship of martensitic stainless steel is shown in Figure 1–5. The relationship includes the modification ofeach grade and its added advantage. Among the martensitic stainless steels, AISI 440 B possessesgood mechanical properties owing to its high chromium content and high carbon content (lower than AISI 440C). Martensitic stainless steels are widely used in engineering applications such as steam and water valves, pumps, turbines, compressor components, shafting, cutlery, surgical tools, bearings, aerospace applications and plastic moulds(Hassan and Tamizhmanii, 2010; Sobiyi et al. 2015). The typical microstructure of martensitic stainless steel is shown in Figure 1–6 (Barlow and Du Toit, 2011).

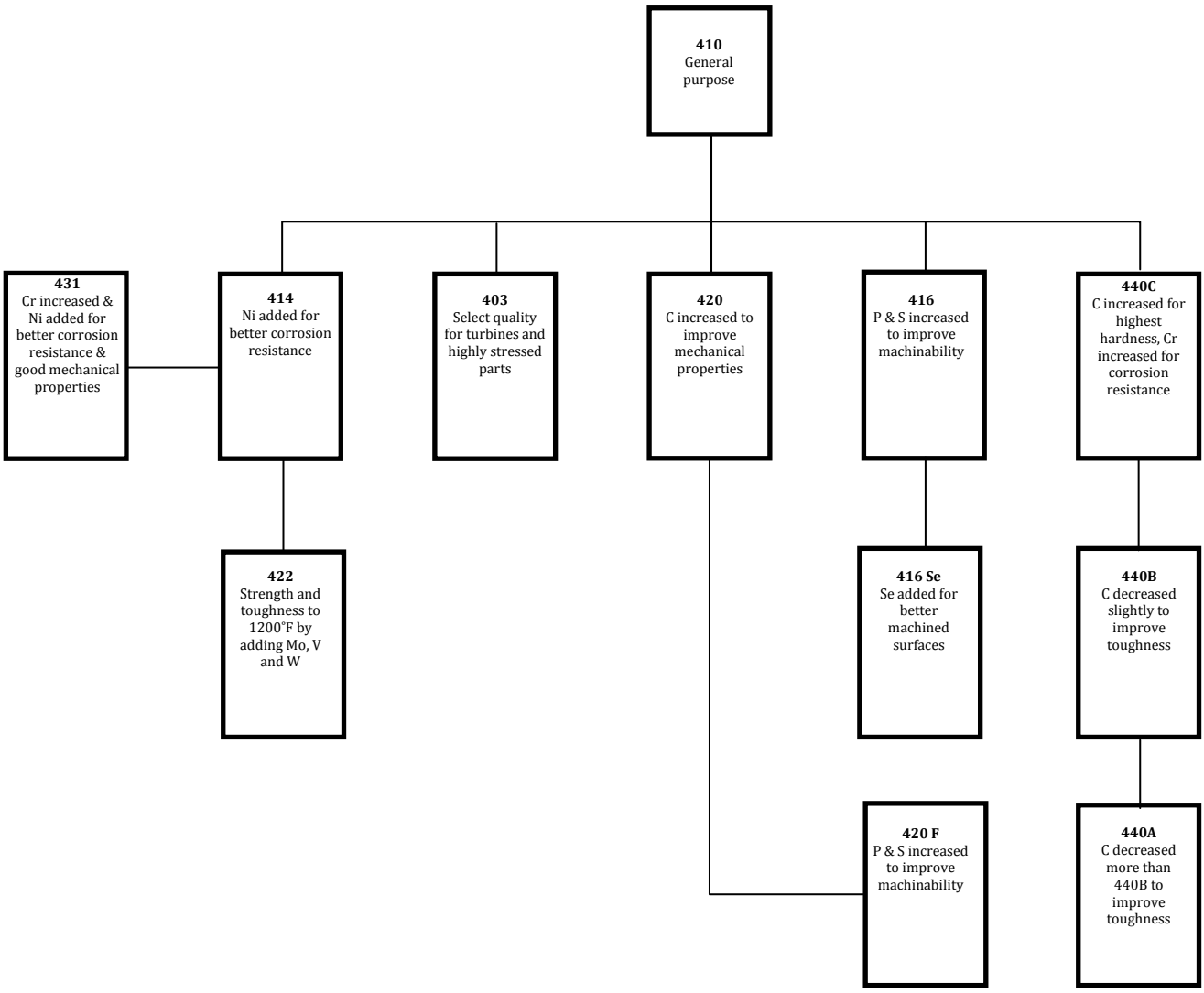

Figure 1-5Family relationship of standard martensitic stainless steel (Adapted from Bramfitt, 2002)

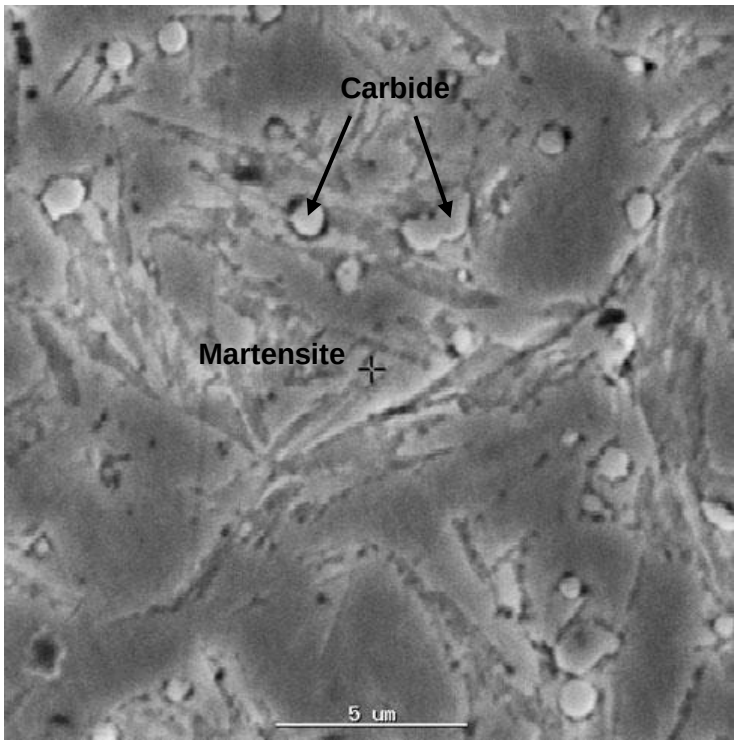

Figure 1-6Microstructure of AISI 420 martensitic stainless steel consisting of 100% martensite (Courtesy, Barlow and Du Toit, 2011)

Hard turning of steels was made possible through the development and implementation of tougher tools with high abrasion resistance and high heat conductivity. The development of PcBN and ceramics as super hard cutting tool materials made it possible to machine these steels close to thedimensional tolerance achievable by the grinding process.In finishing and continuous cutting, alumina-based ceramics reinforced with titanium carbide (Al_2O_3/TiC) are suitable because of theirresistance to thermal and mechanical shocks. Polycrystalline cubic boron nitride (PcBN) cutting tools are suitable for both continuous and interrupted cutting, depending on the cBN grade of the insert during finishing and roughing operations, because of their superior fracture toughness, high hot hardness and low solubility in iron (Konig et al., 1990b; Rech and Moisan, 2003).

Alumina-based ceramic composites are widely used for machining alloy steels of hardness ranging from 34 HRC to 66 HRC, but they have drawbacks such as lower fracture strength, toughness and thermal shock resistance, therefore leading to chipping of the cutting edge of the cutting tool and or tool fracture. All these factors make them unsuitable for interrupted cutting (Kumar et al., 2006; Zhou et al., 2010).

In addition to the chemical stability of PcBN at temperatures below 1200 ºC, cutting tool inserts made from this material are recommended for continuous and interrupted cutting of cast irons and steels with hardness values ranging from 50 to 65 HRC, during roughing and finishing operations (Huang and Liang, 2003; Lima et al., 2005).

In hard turning, the cutting tool is subjected to cutting forces that are concentrated over a relatively small contact area on the rake face and the flank. The chip also slides over the rake surface and the machined surface rubs upon the flank surface of the cutting tool. High temperatures are developed over the contact surfaces. The cutting tool is also subjected to mechanical and thermal shock when it enters and exits from the cut. So, the cutting tools wear out, and under these adverse conditions even fracture occurs and precious machining time is lost in changing the tool, thus affecting the final part produced.

The final machining part is dependent on the insert types, machine tool condition, performance andmachining methods, as well as edge preparation, where the edge reinforcement with -20 degrees chamfer is normally recommended for machining hardened steels (Grzesik, 2008).By proper selection of tool material, tool geometry, and cutting conditions, plastic deformation and mechanical failure can be prevented. However, tool failure through gradual wear cannot be avoided completely. This makes the study of tool wear so important.

Despite the significant advantages of hard turning, this type of machining process cannot replace all grinding operations, and its implementation as ultra-precision machining is not widely spread because of its limited turning accuracy (Pavel et al., 2005). Despite these evident advantages, industrial implementation of hard machining has not increased in comparison with its potential applications. The clearly unsatisfactoryindustry level of acceptance of hard machining technology can be attributed partly to insufficient knowledge of tool wear, the component behaviour of hard machined surfaces, and the uncertainty about the attainable accuracies-to-size (Risbood et al., 2002; Pavel et al., 2005).The characteristics of turning as opposed to grinding for geometrical accuracies are the higher cutting force, single point form generation and excessive tool vibration.

The dimensional tolerances that can be achieved in hard turning are around ±0.050 mm, and some machinists (by using diamond tip cutters) may achieve±0.040 mm. On the other hand,it

is often required to achieve dimensional tolerances below ±0.010 mm. Thus hard-turned components may still need to be finished on a grinder to achieve the required tolerances.Any improvement in the hard turning process to establish tolerances near the ±0.010mm range will result in significant cost savings and give a competitive advantage to machining companies.

1.2 OBJECTIVES

The aims of the research were to:

a. Investigate the feasibility of using PcBN and Al_2O_3basedcutting tools for hard turning of martensitic AISI 440B stainless steel
b. Investigate the effects ofmachining parameters such as, feed rates, depth of cut and cutting speed on the cutting forces, surface integrity.
c. Provide an in-depth understanding of wear mechanisms and failures of PcBN and Al_2O_3based cutting tools when machining AISI 440B.
d. Propose a method for determining the out of roundness and dimensional accuracy during hard turning with the goal of producing a final part at extreme tolerance of $\pm$ 0.010 mm.
e. Develop serrated chip formation mechanism for the workpieceand provide in-depth understanding of the mechanism of the chip formation through microstructural analysis of the shear localized band during serrated chip formation.
f. Provide a deep understanding of the chemical interaction between workpiece and cBN cutting tools, through microstructural analysis of the adhered layer on the worn cutting tool using both Fused iron beam scanning electron microscopy (FIB/SEM) and transmission electron microscopy (TEM) techniques.
g. Explore the application of hard turning of AISI 440Busing PcBN cutting tool in the industrial environment.

2 LITERATURE REVIEW

2.1 MACHINING

Machining is a manufacturing process based on removing unwanted and excess material from a workpiece in the form of relatively thin layerscalled chips. The material removal processes are generally of three machining classes: conventional, abrasive and non-traditional machining, as described in Figure 2–1 (Groover, 2010). A machining process is normally referred to as metal cutting, if the work material is a metal (DeGarmo et al., 2003; Trent and Wright, 2000; Stephenson and Agapiou, 2006). Most metals, hard or soft, ductile or brittle, cast or wrought, with high or low melting point, can be machined to different sizes or shapes.

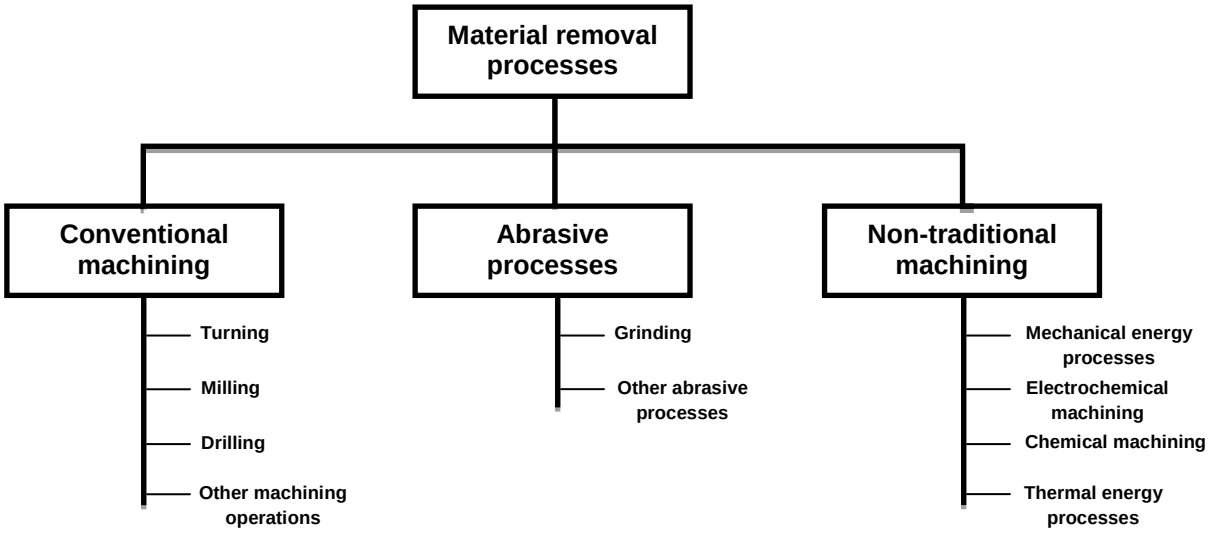

Figure 2-1 Material removal process (Adapted from Groover, 2010)

Compared to most other relative shaping processes, metal cutting operation provides high accuracy, which therefore it makes it a suitable operation for producing parts that require high dimensional accuracy. The most common metal cutting operations include: turning, boring, drilling, milling, broaching and shaping(Groover, 2010; Stephenson and Agapiou, 2006).

Turning is the most common operation in metal cutting. The turning operation is carried out using a lathe, where the work material is held on the chuck of the lathe while it rotates, and the tool is held rigidly on the tool post. The cutting tool moves constantly across the work

material either vertically or horizontally in the X, Y and Z axes. In turning, the major parameters involved include three factors: the cutting speed, *V*, (the rate at which the uncut surface of the work material passes the cutting edge of the cutting tool); the feed rate, *f*, (the distance moved by the cutting tool in axial direction at each revolution of the work material); and the depth of cut, *d*, (the thickness of the material removed measured in the radial direction) (Trent and Wright, 2000). The turning operation configuration of the major parameters is shown in Figure 2–2. Where $D_o$is the diameter before cut, $D_f$is the final diameter, *d*is the depth of cut, *f*is the feed,*L*is the workpiece length and *V*is the workpiece rpm.

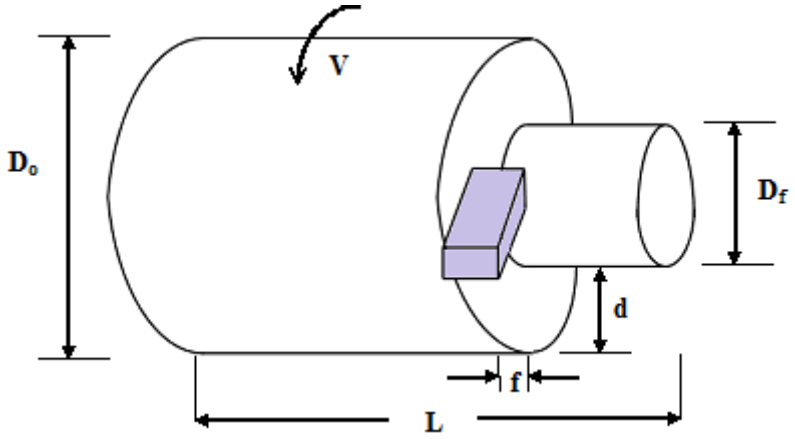

Figure 2-2 Diagrammatical illustration of turning operation

The relationship between tool life, machining productivity and surface finish is affected by tool geometries, material removal rates and material characteristics (Astakhov and Davim, 2008).

The localised shear deformation on the work material, just after the cutting edge of the cutting tool passes, describes the fundamental mechanism involved in metal cutting. The cutting tool is wedge-shaped, and it is forced symmetrically into the material being cut and then moved parallel to the edge, slicing the material into two pieces by removing a thin layer from the thick work material body (Trent and Wright, 2000). A chip is formed during the relative motion between the cutting tool and the workpiece, which induces a primary shear deformation. As the chip is cut, the chip flows over the cutting edge of the cutting tool. A secondary shear deformation is experienced through shearing process (Stephenson and Agapiou, 2006).

The primary mode of plastic deformation is dislocation slip.There is a mutual dependence in the plastic deformations in the primary and secondary shear zones. The primary shear zone influences the deformation in the secondary shear zone.In the primary shear zone, the shear plane angle is directly influenced by the deformation and friction at the tool–chip interface, thus influencing the heat generation and strain in the primary shear zone (Trent and Wright, 2000; Stephenson and Agapiou, 2006).

A relatively low amount of energy is required to form a new surface, and this is insignificant compared to the energy required to plastically deform the whole of the material removed (Trent and Wright, 2000).

2.2 REVIEW OF HARD TURNING

Studies on several factors in hard turning of hardened steelare available in the research literature: on wear characterisation of PcBN, on surface integrity and chip formation, on optimisation design parameters, on tool edge geometry effects on surface finish, and on the effects of coatings on the surface finish(Shihab et al., 2014). Much work is yet to be done on improvements in the dimensional accuracy of parts produced by hard turningandon the full in-depth understanding of the wear characteristics of cutting tools when machining AISI 440 B. Work on machining of the following alloys has been reported: AISI 52100, AISI 4340, AISI 1050, AISI 9310, AISI 4320, AISI 440 C, M2 and M50 (Pavel et al., 2005; Caydas, 2009; Hasan and Thamizhmanii, 2010).There are studies on martensitic stainless steel (AISI 440C and AISI 410), with reports on the toolwearmechanism,failure modes and surface roughness during hard turning usingPcBN and ceramic cuttings tools (Kumar et al., 2006; Thamizhmanii and Hasan, 2008; Hasan and Thamizhmanii, 2010).

This chapter reviews the literature pertaining to the tool wear mechanisms, surface integrity, tool failure modes and dimensional accuracy.

2.3 TOOL MATERIALS FOR HARD TURNING

Cutting tools that are generally used for machining are designed to meet a significant set of requirements. Some of the essential properties include: high compressive strength, adequate impact resistance, low interface friction, thermal shock resistance, chemical inertness at

working temperatures, good abrasion resistance, high deformation resistance, high thermal conductivity, high stiffness to maintain accuracy, dimensional quality in terms of size, and high hardness and toughness at elevated temperatures of the cutting tool (Byrne, 2003). The toughness of the cutting tool is indicated by the critical stress intensity factor, which describes the stress concentration required at the end of a crack to extend that crack (Friemuth, 2002).

When steel is machined, the temperatures at the chip–tool interface can be about 1000°C, and considerably higher when exotic materials are machined, particularly if heat is applied to help soften the work material (Rech, 2006). In manufacturing, higher productivity is sought; this involves high machining speed, which generates high temperatures at the cutting tool tip; this creates increasing demands on the high-temperature properties of the tool materials.

During dry machining, high-speed machining or high-performance machining, cutting tools are also subjected to high stresses. An ideal cutting material normally combines properties such as high hardness with good toughness and chemical stability, the hardness and toughness represent opposing properties. Figure 2–3 shows the properties of widely available cutting tools in relation to hardness and toughness. However, there is no perfect cutting material that has been developed to meet all three requirements simultaneously. In order to merge some of the characteristics mentioned, wear resistant coatings are combined with a tough substrate material (Mohlfeld, 2000; Byrne et al., 2003).

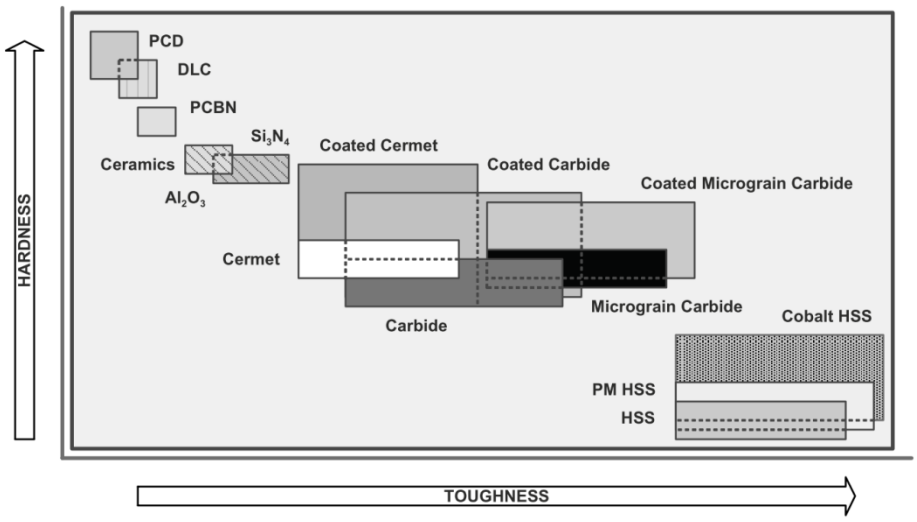

Figure 2-3Tool materials as a function of hardness and toughness (Astakhov and Davim, 2008)

There are several machining operations involved in hard turning. These are: milling, turning, broaching, drilling, threading and reaming.Several cutting tool materials have also been used for performing these operations (Grzesik, 2008). Some common cutting tools that have been used for hard machining operations are: carbides, PCD, cermets, ceramics and PcBN. Carbides, ceramics and PcBN are more commonly used based on their advantages as compared to diamond and cermets. Diamond is no longer used in machining hardened steel owing to its high affinity to ferrous materials, especially at high cutting speeds, thus causing severe chemical wear in the cutting tool (Neo et al., 2003). Cermets have their drawback based on the relatively poor abrasive wear resistance when compared to PcBN and ceramics, and they are only applicable in instances when turning through a hard case into a soft core (Gosiger, 2012). Abrasion wear resistance has been described as an important property of a cutting tool for machining of hardened materials. The comparison of the abrasive wear resistance of cutting tools used during hard turning is shown in Figure 2–4.

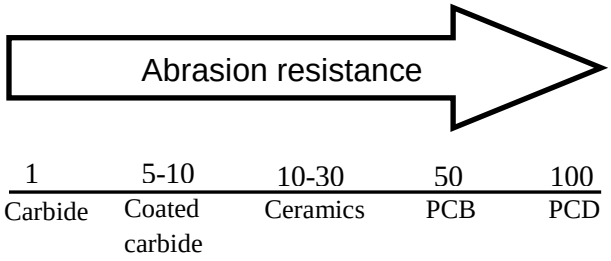

Figure 2-4 Comparison of abrasive wear resistance of tool materials (Adapted from Stephenson and Agapiou, 2006)

The relative comparison between different cutting tools and their propertiesis illustrated by Stephensonand Agapiou(2006).

2.3.1 Cermets

Cermets are ceramic–metal combination materials containing both a ceramic (non-metallic) phase and a free metallic phase. The ceramic phase consists of ceramic hard materials with titanium nitride as a major constituent, and carbonitrides of titanium, tungsten carbide, vanadium, molybdenum, tantalum, aluminium and niobium in their solid solutions. The metallic phase consists of nickel alloyed with a constituent of the ceramic phase and cobalt (Ber and Porat, 1990;Gruss and Friederich, 1994;Seah et al., 1995).

Cermets were developed to have intermediate properties of both metals and ceramics, by having the toughness of metals and the hardness of ceramics. The toughness of cermet inserts was improved by the addition of tungsten carbide and tantalum carbide (Gruss and Friederich, 1994). The metal binder in cermets is a ductile, tough phase. The ceramic part of the cermet composite serves as a resistance to abrasive wear while nickel and cobalt contribute to plastic deformation resistance (Gruss and Friederich, 1994; D' Errico et al., 1997).

Cermet owes its high hothardness to the primary component of its hard particles-TiC. In 1973, Japanese manufacturers added TiN to the hard particle portion, and that provided a finer microstructure and improved high temperature strength and oxidation resistance. New cermets with improved binders provides better impact-resistant,making it more suitable for milling and interrupted turning.

Compared to the conventional WC based hardmetals, Ti(C,N)-based cermets can provide smooth surface finish, excellent chip control and close tolerance, andoffer geometric accuracy in workpieces, variable speed range capability and low price (Gruss and Friederich, 1994;Ettmayer et al., 1995;Jung and Kang, 2004; Zhang et al., 2009;Buchholz et al, 2012 Peng et al., 2013). Because of these advantages, cermet cutting tools are replacing WC–Co hardmetals in applications such as high speed cutting and semi-finishing operations of both carbon and stainless steels (Ettmayer et al., 1995; Zhang et al., 2009).Generally,cermetsare less expensive compared to coated carbides,but they still lack the toughness of WC-Co based materials, making them unsuitable for roughing operations.

Fundamentally, during finishing operations, oxidation resistance of cermetsreduces notching at the cutting edge of the tool, and this reduces damage to the machined part surface being produced (Ettmayer et al., 1995).

Cermets are generally classified into two major categories, titanium nitride (TiN) and TiC-based materials. Typical schematic representation of TiCN-based cermets cutting tool microstructure is shown in Figure 2–5.

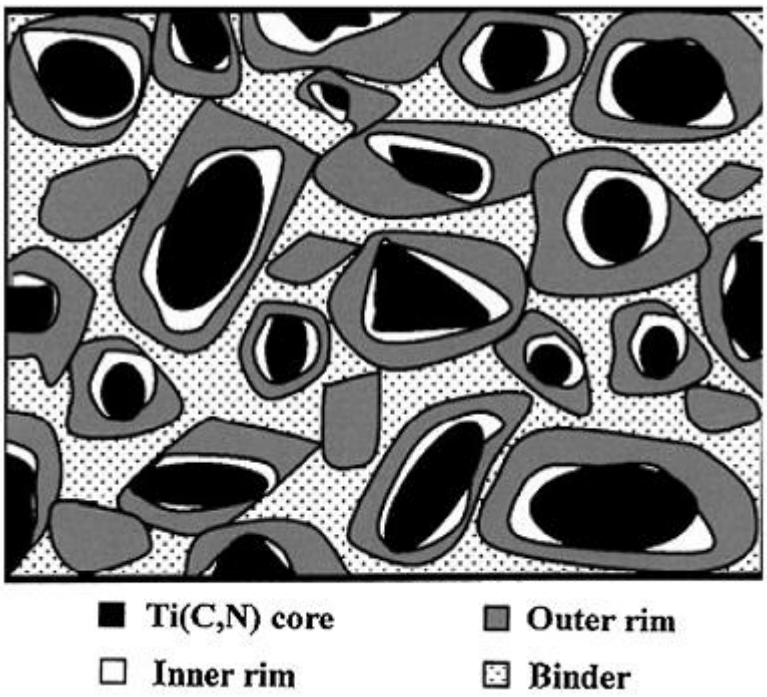

Figure 2-5 Schematic representation of the microstructure of a TiCN-based cermets (Courtesy, Ahn and Kang, 2000)

However, TiCN possesses the properties of both TiC and TiN, such as high hardness,excellent wear resistance, good corrosion resistance, good chemical stability, and high thermal andelectric conductivity (Liu et al., 2004).

Compared with TiC-basedcermets, TiCN-based cermets have much higher transverse rupture strength, much higher thermal conductivity, higher high-temperaturehardness, and better resistance to oxidation. TiCN-based cermets have a better resistance to high-temperaturecreep deformation when compared to TiC-based cermets, owing to the muchfiner grains of the hard-phase in these materials. The higher enthalpy in the formation of TiCN, as compared to that of TiC, makes it more difficult for the formation of scaling, oxidation layers, crescent depression and built-up edges during machining applications (Peng et al., 2013).

TiCN-based cutting tools have become the better choice for cutting some materials with high hardness and highstrength that cannot be machined by TiC-based cuttingtools. The same tools are better at producing excellent surface finish and better dimensional deviation with the machined part. In industrial applications, the TiCN-based cutting tool is gradually replacing TiC-based cermets (Pastor, 1987; Peng et al., 2013)

Cermets have also been found to be suitable for continuous cutting of case-hardened materials.

2.3.2 Carbides

Cemented carbides tools have been the most used and popular cutting tool in the machine shop worldwide, accounting for up to 75% of indexable inserts (Hallberg, 2010; Noordin et al., 2012). Cemented carbide tools have undergone significant developments over the years by coating them to improve their hardness and toughness. Solid carbide tools with TiAlN and TiCN layer coatings are generally used as drills, mill cutters, and taps for machining hardened materials up to 65HRC.

Tungsten carbides properties depend on the grain size, binder(cobalt) alloy content, and the addition of tantalum carbide, titanium and other alloying elements. Carbide tool materials with small grain size have better hardness and abrasive resistance, but they have lower resistance to thermal shock compared to larger grain sized carbides.To further prevent galling or hot welding, tantalum/niobium and titanium carbides are added to the binder system of the cutting tool.Coatings are normally applied on cutting tool materials to either improve the surface strength and/or reduce the friction at the chip–tool interface (Sales et al., 2009).

Sales et al.(2009) investigated the performance of coated cemented carbide (TiN/Al_2O_3/Ti(C,N) coating,mixed ceramic (Al_2O_3+TiC) and PcBN-H (90% cBN) for machining W320 hardened steel. The authors found that the above cemented carbide cutting tool produced best tool wear resistance at low cutting speeds (60 and 90m/min) as a result of its good toughness and relatively good hardness, but, when used at higher cutting speeds (150 and 200 m/min), the cemented carbide tool had a shorter tool life owing to the accelerated wear caused by decrease of hardness at the high temperature generated at the tool–chip interface.

The wear mechanisms of the worn cemented carbide cutting tool as observed by the authors showed that chipping, abrasion and adhesion wear were most dominant. Crater and flank wear were dominant tool wear modes. Abrasion wear on the flank face is a result of hard carbides contents in the workpiece material, such as; SiC, Mo_2C,Cr_7C_3, VC and Fe_3C. The hard

particles were removed from the surface of the workpiece by chipping; theseparticles can be sandwiched between workpiece, the toolflank face and the chip-tool rake face, thus creating amedium three-body abrasion system.

However, the removal of the coatings on the cutting tool occurred at high cutting speed; the mechanism of removal was micro-chipping and plastic deformation.Figure 2–6 shows the crater and flank face of worn cemented carbide.

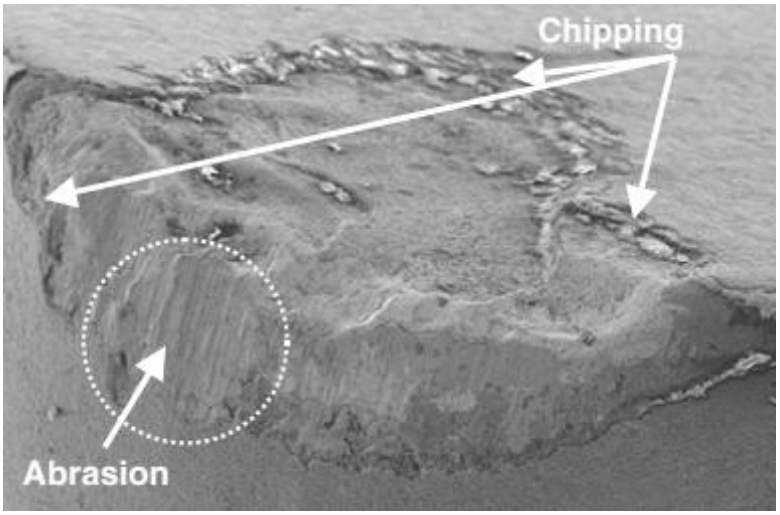

Figure 2-6Abrasion and chipping wear on worn cemented carbide cutting tool (Courtesy, Sales et al., 2009)

Jiang et al. (2006)analysed machining of hardened AISI 4340 steel using WC-Co cutting tools coated with cBN–TiN.The wear mode observed was the crater and flank wear with the flank wear predominant; the abrasive wear pattern resulted from the rubbing of the tool cutting edge and flank against the workpiece material (martensite). The tool–workpiece interface did not experience significant heating during the machining process resulting from the low thermal conductivity of the cBN composites in the cBN–TiN coating, thus, the integrity of the TiN binding phases is retained.

When compared to the commercially available PcBN cutting tool, cBN–TiN coated carbide insertsshowed less flank wear resistance but superior crater wear resistance, owing to good lubricity provided by the TiN capping layer.However, the surface roughness produced using the cBN–TiN was poor compared to the PcBN cutting tool.

Noordin et al. (2012) investigated the machining of martensitic stainless steel, AISI 420, using a carbide tool with TiAlN coating. The authors adopted empirical models to measure the tool's performance by quantifying the effect of the cutting parameters to the tool's life and the surface roughness of the machined workpiece. Under selected cutting parameters, the tool life was observed to beproportional to bothcutting speed and feed. In their investigation, the cutting speed was observed havingstronger influence on the tool life compared to other cutting parameters. However, thecutting force reduces with increasing cutting speed andincreases with increasing feedrate, while the surface roughnesswas directly proportional to feedrate and inversely proportional to cuttingspeed.

2.3.3 Ceramics

Ceramics used for hard turning are of different grades: aluminiumoxide-basedand siliconnitride-based grades, and mixed and reinforced grades. The characteristics that make ceramics suitable for machining of hard materials is the high wear resistance, good thermal stability and high hot hardness.Ceramics are replacing carbide tools in many machining applications because of their hardness and chemical stability. Ceramics have superior mechanical properties compared to carbides, most especially at a higher cutting temperature. Ceramics have the ability of retaining theirhardness and stiffness at temperatures up to 1500˚C, and they are also chemically inert to many materials at such high temperaturesowing to theirstrong covalent and ionic chemical bonds (Smallman and Ngan, 2007; Walker et al., 2011). However, ceramics have their own setbacks: low fracture toughness, tendency of failure by chipping, and poor resistance to mechanical and thermal shock (Stephenson and Agapiou, 2006). The physical and chemical properties of ceramics cutting toolsare shown in Table 2–1.

Table 2-1 Physical and mechanical properties of ceramics cutting tools (Whitney, 1994)

Properties			Oxide ceramic Al_2O_3		Whisker-reinforced ceramic Al_2O_3	Oxide ceramic Al_2O_3		Silicon nitride ceramic Si_3N_4
			+3.5 % ZrO_2	+15 % ZrO_2	+15 % ZrO_2 +20 % SiC Whisker	+10 % ZrO_2 +5% TiC	+30 % Ti (C,N)	+10% Y_2O_3
Density	ρ	g/cm^3	4.0	4.2	3.7	4.1	4.3	3.3
Vickers hardness	-	-	1730	1750	1900	1730	1930	3.3
Bending strength	σ_{bB}	N/mm^2	700	800	900	650	620	800
Thermal expansion	α	$10^{-6}K^{-1}$	8	8	-	8	8	3.4
Thermal conductivity	λ	W/m.K	16.4	15	32	14.7	20	
Fracture toughness	K_{IC}	$N.m^{1/2}/mm^2$	4.5	5.1	8.0	4.2	4.5	7.0
Young modulus	*E*	$10^3.N/mm^2$	380	410	390	390	400	
Compressive strength	σ_{dB}	N/mm^2	5000	4700	-	4800	4800	-

Ceramics cutting tools are usually made of Al_2O_3 and Si_3N_4 based materials. The commonly available ceramic grades are shown in Figure 2–7. The grades exist in two major categories, oxidic (cutting tool materials based on Al_2O_3) and non-oxidic ceramics (silicon nitride-based cutting tool material).

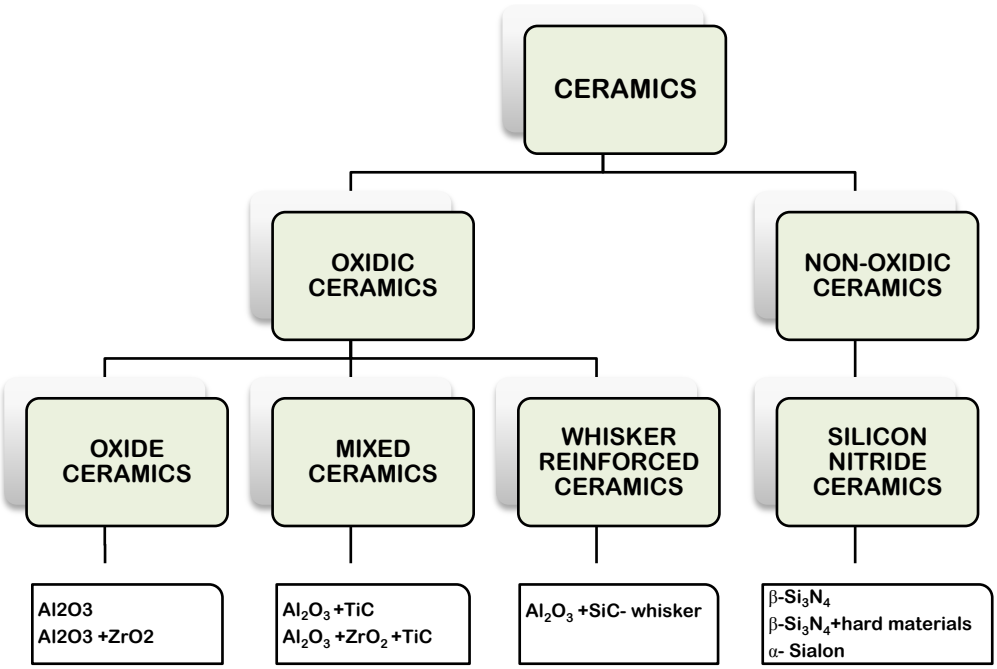

Figure 2-7 Classification of ceramics cutting tool (Adapted from Klocke, 2011)

Mixed type grade of ceramics with TiC content and micro grain structure is widely used forcontinuous or slightly interrupted hard machining of cast irons and steels. Ceramics are not often used for machining requiring an extreme high tolerance (not tighter than 0.025mm) as in the case of PcBN (Grzesik, 2008).

2.3.3.1 Oxide Ceramics

Oxide ceramics are normally made of a combination of aluminium oxide and finely distributed zirconium dioxide (about 3–15 %) added to enhance the toughness of the cutting insert. The phase transformation of zirconium dioxide (ZrO_2) is responsible for the toughness enhancing effect of the dispersed zirconium dioxide particles in the aluminium oxide matrix.

ZrO_2 exists inthe form of a tetragonal lattice modification during sintering at a temperature range of 1400–1600°C, which transforms during cooling into monoclinic (low-temperature)modification, followed by a volume expansion. The transformation temperatures are dependent on ZrO_2 particle size. Lower transformation temperature is achieved with smaller particle size. During the transformation process, various specific mechanisms of actions are involved which ultimately absorb fracture energy.The speed of crack development is reduced by the stress-induced transformation of small ZrO_2 particles; this gives rise to micro-cracking and crack branching, and as crack diversion. At a higher level of energy, critical cracks develop, thus leading to improved ductility and increased fracture resistance (Claussen et al., 1984).

The application of oxide ceramics is mainly for roughing and finishing during turning operations and for grooving of grey cast iron and nodular cast iron with the absence of coolant. Oxide ceramics are normally not recommended for milling operations. The comprehensive selection for ceramics application by Sandvik is shown in Table 2–2 (SandvikCoromant).

Table 2-2 Application of different types of ceramics (Sandvik Coromant)

GRADE	WORKPIECE MATERIALS	CUTTING PARAMETERS	CUTTING CONDITIONS
Oxide ceramics	Steels (below 35 HRC), cast iron hardened steels	High speeds, light to medium feeds	Finish turning, requires rigid setup, no coolant
Mixed ceramic	Hardened cast irons, high temperature alloys	High speeds, low feeds	Finish turning, light interrupted cut, milling, no coolant
Whiskered reinforced Al_2O_3	High temperature alloys, hardened steels, cast iron	Medium to high speeds, light to medium feeds	Rough turning/milling, interrupted cutting
Silicon nitride	Cast iron	Medium to high speeds, low to medium feeds	Rough and semi-rough turning and milling, with or without coolant

2.3.3.2 Mixed Ceramics

Al_2O_3-based ceramics are considered to be suitable tool materials for machining hardened steels because of their high hardness, wear resistance, heat resistance and chemical stability (Kumar et al., 2003; Liu and Ai, 2005). However, the intrinsic drawbacks of Al_2O_3-based cutting tools, such as lower strength, lower fracture toughness and lower thermal shock resistance, usually make them more susceptible to excessive chipping or fracture when machining hardened materials. This is especially true at interrupted cutting; this regime leads to short tool life. Conventionally, Al_2O_3-based ceramic tool materials were strengthened and toughened by the addition of micro-sized particles like ZrO_2, TiC, TiN, (W, Ti)C, Ti(C, N), TiB_2, SiC, orSiC whiskers, to improve the mechanical properties. Thus the abrasive and erosive wear resistance increases with the improved hardness and toughness (Kumar et al., 2006; Asian et al., 2007; Davim and Figueira, 2007; Grzesik and Zalisz, 2008).

Mixed ceramics are produced by the combination of aluminium oxidewith other hard substances (in proportions between 30% and 40%) such as titanium carbide and/or titanium nitride or compounds. Higher hardness than that of oxide ceramics is obtained by embedding the hard particles into the aluminium oxide matrix. Mixed ceramics possess better thermal properties than oxide ceramics, but the tendency of TiC to oxidise limits the thermal loading capacity of the resulting composites. Newly developed mixed alumina grades consist of very fine grains extremely homogenously dispersed in the oxide matrix. This results in significantly higher hardness, heat resistance and fracture toughness compared to previously

manufactured mixed ceramics grades. Mixed ceramics were previously mainly used for finishing operation of hardened steel and chilled cast iron, at high cutting speeds (Schneider and Richter, 1999).

The toughening or strengthening mechanisms of these ceramic composites are phase transformation toughening, whisker toughening and particle dispersion strengthening or toughening, as well as synergistic toughening by multiple agents or mechanisms, with the main toughening indicators being crack bridging, crack deflection, whisker pull-out, etc. However, these extrinsic effectsare limited in magnitude, especially in strengthening introduced by micro-sized secondary phase particles and whiskers.

The research activity in ceramic nano-composites was pioneered by Niihara and Nakahira (1990), who first revealed that a dispersion of 5 vol.% of SiC nanoparticles into Al_2O_3 increased the room-temperature strength from 350 MPa to1.0 GPa. An important indicator of the strength increase is the transition in fracture behaviour from intergranular to transgranular crack propagation, and the strengthening mechanism is believed to be chiefly owing to generation of thermal mismatch dislocations around the second phase particles (Pezzotti and Muller, 2002; Awaji et al., 2002). The author and co-researchers (Song et al., 2002) developed an Al_2O_3/TiCnano-composite ceramic tool material by adding TiCnano-particles into the Al_2O_3matrix, with remarkable increase in flexural strength yet slight increase in fracture toughness over that of the Al_2O_3/TiC micro-composite ceramic tool material. Similar phenomena have been found for Al_2O_3/SiCnano-composite ceramics by other researchers (Davidge et al., 1997; Derby, 1998). It seemed that the toughening effect of these secondary phase nano-particles was debatable for Al_2O_3-based ceramics.

Research in recent years revealed that the addition of secondary phase particles with multi-modal particle size distribution was an effective method for improving both the fracture toughness and flexural strength of Al_2O_3-based ceramics simultaneously. By adding micro-sized TiC and nano-sized TiN particles into Al_2O_3matrix, Huang et al.(2007) developed multi-scale Al_2O_3/TiC/TiNmicro-nano-composite ceramic tool materials with significantly improved flexural strength and fracture toughness relative to the Al_2O_3/TiC micro-composite ceramic material. Co-existence of both intergranular and transgranular fracture modes were observed on the fracture surface.

An understanding of the failure mechanisms in cutting processes is the prerequisite for not only the proper application but also the development of Al_2O_3-based ceramic tool materials. In continuous turning of steels, the typical wear types of ceramic tools are crater wear, flank wear and depth of cut notch wear, which are sometimes accompanied by chipping, even flaking, under hard turning conditions (Zhao et al., 2010). The total tool wear generally observed in any cutting tool can be divided into two main broad categories, the chemical wear (adhesion, dissolution or diffusion wear) and mechanical wear (abrasion and fracture wear) (Kumar et al., 2006). The wear mechanism usually varies accordingly with the location of the worn area (e.g. tool nose, rake face, flank face, etc.); furthermore, a change in cutting condition especially in cutting temperature would lead to the transition in the predominant wear mechanism. Built-up layer or transfer layer were often observed on the rake face; however, their formation mechanisms and the consequent influence on tool wear would be different (Grzesik and Zalisz, 2008). Additionally, it was concluded that notch wear mostly occurred in machining hard materials using ceramic tool materials with low toughness (Kumar et al., 2006).

In intermittent turning, investigations of the cutting performance and failure mechanisms of Al_2O_3-based ceramic tools have been published (Zhao and Ai, 2006).

2.3.3.3 Whisker-reinforced ceramics

Whisker-reinforced ceramics consist mainly of aluminum oxide with about 20–40% silicon carbide whiskers. The toughness of the ceramic material is enhanced by the whisker-reinforcement, owing to the high strength of SiC whiskers and a relatively weak bond between the SiC whiskers and the Al_2O_3 matrixachieved by incorporating whiskers into the oxidic ceramics matrix. The cutting tool is manufactured through hot pressing. Whisker-reinforced ceramics have fracture toughness up to 60% higher than mixed ceramics.The whiskers bring about more rapid transport ofheat from the highly thermally loaded cutting areas owing to their high thermal conductivity as well as a more uniform distribution of mechanical loads in the cutting tool material; this results inimproved fatigue limits and thermal shock resistance.

Whiskered ceramics are far better suited for machining hard ferrous materials and nickel base alloys, but do not work satisfactorily on ferrous materials below 42HRC, because of a chemical reaction between the tool and the workpiece at the cutting edge. New whisker reinforced ceramic materials are being developed which are stronger and more chemically inert thus making it more compatible for machining a wider range of work materials including ferrous metals.

A whisker-reinforced Al_2O_3 insert can turn 45-65 HRC hard materials up to about four times faster than coated carbides and eight times faster than uncoated tungsten carbides (Momper, 1987).

2.3.3.4 Non-oxidic ceramics

Ceramics based on silicon nitride (Si_3N_4) are found to be more popular cutting tool materials among the non-oxidic ceramics materials: carbides, nitrides, borides and silicates. Properties such as increased toughness, improved thermal shock resistance, higher fracture resistance, higher hot hardness and high temperaturestrength make non-oxidic ceramics strong competitors to the oxidic ceramics. The significantly higher fracture resistance is based on the needle-like shape of the hexagonal β-Si_3N_4 crystals as opposedto the globular Al_2O_3grains when compared to oxide and mixed ceramics. The microstructure is made up of mechanically interlinked components as a result of the non-directional growth of the needle-shaped crystals, thus producing tool materials with excellent strength. The favourable thermal shock resistance as compared with the oxide and mixed ceramics results from the low thermal expansion of the silicon nitride ceramics (Trent and Wright, 2000; Klocke, 2011).

Silicon nitride ceramics can be subdivided into three groups, based on their chemical compositions and crystallographic structure (Trent and Wright, 2000):

- Group 1: β-Si_3N_4 + binder phase (Y_2O_3, MgO, Al_2O_3)
- Group 2a: α sialon (α–Si_3N_4 + Al_2O_3 + AlN) + binder phase (Y_2O_3), Group 2b: (α + β) sialons (α Si_3N_4 + Al_2O_3 + AlN) + additive (e.g. ytterbium)+ binder phase (Y_2O_3)
- Group 3: β silicon nitride + hard materials (e.g. TiN, ZrO_2, SiC-whiskers) + binder phase

Mostof the commercially available Si_3N_4 cutting tool materials belong to Group 1, while Group 2 materials are usually designated as Sialons (Si-Al-On). Sialons are silicon nitride based cutting materials with oxygen and aluminum included as substitutional ions. Sialons are normally produced using similar processes for making cemented carbide. The starting material such as silicon nitride, alumina and aluminum nitride with alloying elements containing Y_2O_3 are milled together, dried, pressed and sintered at a temperature of about 1800˚C. During sintering, the oxide Y_2O_3reacts to form silicate, in liquid form, whereby nearly full density is achieved. After sintering, the liquid solidifies during cooling as a glassy phase bonding together the silicon nitride-based crystals (Trent and Wright, 2000).

The shapes of α-sialon mixed crystals are globular, while the β-sialonismixed crystals. In comparison to Group 1 materials, sialons are more chemically stable, harder, and have better resistance to oxidation.The main application of Si_3N_4 cutting tool materials is in machining of grey cast iron, with preference to the tougher silicon nitride ceramics of Group 1.

High cutting speeds, feeds and large volume removal ratescan be realized when machining cast iron materials in smooth and interrupted cut owing to the high fracture toughness of the silicon nitride tools (Konig and Lauscher, 1986; Schneider and Richter, 1999).

Sialons are mainly useful for roughing and finish turning of nickel-based alloys. They can be applied at much higher cutting speeds compared to carbide tools. However, sialons have lower wear resistance in comparison to oxide ceramics as a result of their strong affinity to iron and oxygen during machining conditions. Improvement of sialons properties is possible through applications of coatings such as: TiN, TiC, TiCN and Al_2O_3; these are applied in different layer thicknesses and combinations (Schneider and Richter, 1999).

2.3.4 Polycrystalline diamond (PCD)

Polycrystalline diamond (PCD) is a synthetic composite cutting tool material manufactured by the bonding of micron sized diamond crystals during sintering under high pressure and temperature in the presence of a solvent/catalyst metal, usually cobalt or cobalt/nickel alloy (Philbin and Gordon, 2005; Hsu et al., 2013).

During the sintering process, the interstitial spaces in the PCD grains are predominantly filled with cobalt binder, which is used as a solvent catalyst in the synthesis process. The individual diamond grains bond to each other, resulting in tough, hard material with the ability of retaining its shape and strength if some of the metal phase is removed. This is unlike cemented carbide: when the binder phase is removed the PCD grains separate from each other and from the base material(Anthony, 1990; Philbin and Gordon, 2005).

PCD is an excellent material for machining in situations in which high stress loads are generated. This is owing to the mechanical properties typical of diamond. The PCD crystals are randomly oriented to eliminate any direction for crackpropagation, resulting in extreme hardness of high transverse rupture strength, and thus great wear resistance.

PCD tool materials typically have a higher thermal conductivity and abrasion resistance (up to 500 times more) than those of tungsten carbide. PCD tools have replaced tungsten carbide, ceramics and natural diamond in high performance applications in turning, milling, slotting, boring and chamfering of materials such as high-silicon aluminium, metal matrix composites (MMC), ceramics, reinforced epoxies, plastics,engineered wood products,and carbon-fibre-reinforced plastics (CFRP) (Astakhov and Davim, 2008).

The selection of PCD grades for specific applications is generally dependent on the tool life expectations and surface finish requirements. Generally, fine grade PCD designed with small diamond particles exhibits greater abrasion resistance, thus better tool life when compared to larger diamond particle, but its use results in a smooth cutting edge, making it suitable for producing parts with superior surface finish. PCD normally has medium toughness but it is very hard and has good abrasion resistance.New prime grades of PCDs which rely on structural changes that enhance toughness are currently developed in order to further improve the fracture toughness of this material.

Polycrystallinediamond tools are normally cheaper than the monocrystalline tools,especially if the tool bit is larger than 2 mm. Applications in the manufacturing industry where mirror polished surface is not required make use of polycrystalline diamond tools. Monocrystalline diamonds are used for all those applications where a mirror polished surface is necessary, which can only be achieved with a grainless diamond cutting edge (Weinz, 1980).

Today PCD is widely used for machining applications such as rock drilling (Okubo et al., 1999; Clayton et al., 2005; Hamadeet al., 2010), machining of titanium alloys (Konig and Neises, 1993a; Ezugwu and Wang, 1997, Nurul Amin et al., 2007, Da Silver et al., 2013) and abrasive silicon–aluminium alloys when surface finish and accuracy are critical. PCD is not recommended for machining ferrous alloys owing to the poor chemical compatibility between the cutting tool and workpiece materials leading to high chemical wear. However, certain classes of cast iron can be machined using PCD with cutting speeds in the range of200–500 m/min (Gimenezet al.,2007).

Zhang et al. (2011) investigated the machining of a hardened stainless steel (Stavax) using commercial PCD tools under Ultrasonic elliptical vibration cutting (UEVC) technique. From the study, they concluded that the UEVC technique produces smaller cutting forces (or specific cutting energy) thus generating less heat in the tool andworkpiece interface, and achieving better surface roughness when compared to the conventional cutting techniques.

2.3.5 Polycrystalline cubic boron nitride (PcBN)

Boron nitride (BN) is a synthetic polymorph material. According to Heath (1986), boron and nitrogen can be formed into a compound by the chemical reaction shown in Equation 2–1.

$$BCl_3+NH_3 = BN+3HCl \quad \text{.....} \quad (2\text{-}1)$$

Boron nitride can be typically found in four crystalline forms, according to different pressure and temperature conditions. The forms are: cubic (cBN), hexagonal (hBN), rhombohedral (rBN), and wurtzitic (wBN). The denser ultra-hard forms of boron nitride are the cBN and wBN (Liu et al., 1995).

Boron nitride (BN) is a soft, slippery, friable substance and exhibits a hexagonal structure. Under high temperature and pressures (temperatures in the range 1400–1750°C and pressure of the order of 5-8 GPa), hBN can be transformed into cBN as shown in Figure 2–8(Heath, 1989).

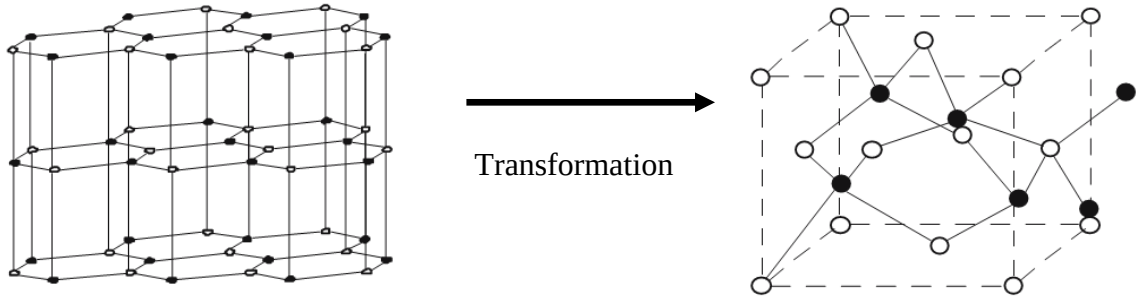

Figure 2-8 Transformation of hexagonal boron nitride to cubic boron nitride (Adapted from Heath, 1989)

Solvents or catalysts, mostly metals, are generally added to hBN in order to increase the transformation rate and also effectively reduce the required pressure and temperature to a more easily attainable level of about 6 GPa and 1,500°C, respectively. The cBN can be liberated and recovered for subsequent processing after the grains grow, by dissolving unwanted matrices (Heath, 1989; Lopez et al., 2011).

cBN tool is a superabrasive material which is second in abrasive resistance and hardness only to diamond. cBN is produced under high temperatures and pressures. cBN tools also have an important advantage over diamond tools, namely chemical inertness with steel (Huang et al., 2007).

cBN has very good mechanical properties which are attributed to its crystalline structure and its covalent link (Lopez et al., 2011). The physical properties of cBN are as follows: density, 3.48 g/cm^3, thermal conductivity 13 W/cm°C at room temperature, hardness, 4,500 HV, Young's modulus, 71×10^3N/mm^2, and thermal expansion 4.7×10^{-6}/°C from room temperature to 800°C.

PcBN is a composite material consisting of cubic boron nitride (cBN) grains in a binder matrix. Commercially manufactured PcBN tool products are generally called CBN tools; they are available at variable cBN contents with some additives. PcBN materials are categorized into two, namely, high cBN content material or low cBN content. High cBNcontent grades contain the cBN grains with a metallic or ceramic binder(s) (such as cobalt, W-Co-Al, Ti-Al and Al ceramic) and have approximately 0.8–0.95 volume fraction of cBN grains. Low cBN content grades can contain from 0.4–0.7 volume fraction of cBN and have a ceramic based binder such as Titanium carbide (TiC), Titanium nitride (TiN) or AlN (Harris et al., 2004,

Lahiffet al., 2007, Huang et al., 2007, De GodoyandDiniz, 2011). High cBN content and Co matrix grade is recommended for interrupted cutting of iron castings, while for finishing operations, low cBN content and ceramic matrix are recommended.

Research to date has found that low cBN content materials provide the best performance in hard turning in terms of tool life and surface finish (Lahiff et al., 2007)

During the sintering of PcBN cutting tool materials, with more than 0.8 volume fraction cBN grain, cBN grains form a skeletal structure with considerable cBN phase contiguity. But, the contiguity of cBN is limited when the volume fraction of cBN grains is lower (0.4–0.6) (Can and Andersin, 2006).Ultrafine powders of a secondary hard phase are purposely incorporated in the binder phase as grain growth inhibitors, to prevent or reduce grain growth of the binder phase during the high temperature–ultra high pressure process when the volume fraction of the cBN grains in the PcBN cutting tool material is less than 0.7.

For applications such as turning, milling and drilling of pearlitic iron castings, both grey and ductile, PcBN is normally recommended. PcBN is not suitable for machining ferritic iron castings, because of its high reactivity of ferrite with cBN, which degrades the cBN owing to diffusion of boron within the ferritic matrix (Lopez et al., 2011).

PcBN cutting tools are fabricated in the form of substrate backed or master blanks compact structures. The making of PcBN cutting tool material consists of sintering randomly orientated cBN grains, typically mixed with various binder phase precursors, as mentioned above. The latter is necessary because sintering of highly pure cBN compacts is generally difficult because of the predominant covalent atomic bonding of cBN, thus requiring high temperature and ultra-high pressure conditions for full densification (Can and Andersin, 2006). To overcome this problem, binders are used as sintering aids for obtaining fully dense PcBN cutting tool materials (Heath, 1989).

In the making of PcBN cutting tool materials, composites or compounds of Group 4, 5 or 6 transition metals are most frequently used as binder phases. Among these particular compounds, TiC and TiN exhibit the highest chemical activity towards cBN material (Benkoet al., 1999; Benkoet al., 2001). Among binder phases that are often used in the

synthesis of PcBN cutting tool materials TiC with Al compounds, TiN with Al compounds, Al (AlB_2, AlN, α AlB_{12}), W–Co and Al compounds are commonly used (Harris et al., 2004).

During this high temperature–ultra high pressure sintering, new phases are formed as a result of chemical reactions between cBN grains and the sintering binder. In selection of the appropriate binder phase, thefundamental understanding of their mechanisms of formation and prediction of these new phases is of critical importance (Benko et al., 1999). The performance of PcBN cutting tool materials is dependent upon the bulk mechanical properties and the interactions of microstructural constituents of the tool and the work material can be vital to cutting tool performance (Chou et al., 2003).

Once PcBN is produced, the master blanks or substrate backed structures are cut into smaller blanks before being ground into shapes and sizes as tips for cutting tool inserts. PcBN cutting tools are available in either solid form or tips brazed to the solid blank (usually carbides) (Liu et al., 1995). The brazed tips result in a stronger cBN blank and allow more of the generated heat to be absorbed (Grzesik, 2009).

PcBN is an ideal cutting tool material for machining iron-based workpiece materials, most especially hardened steels, where excellent surface finish is required, but the cost of the cutting tool is an important consideration in a production environment.

In the literature, parameters such as the cutting edge geometry, cBN content, coating type, grain size of cBN, type of binder, use of coolingmethods and variation in cutting parameters have significant influence on cBN tool performance (Konig et al., 1990; Lin and Chen, 1995; Chou et al., 2003) as indicated in Figure 2–9.

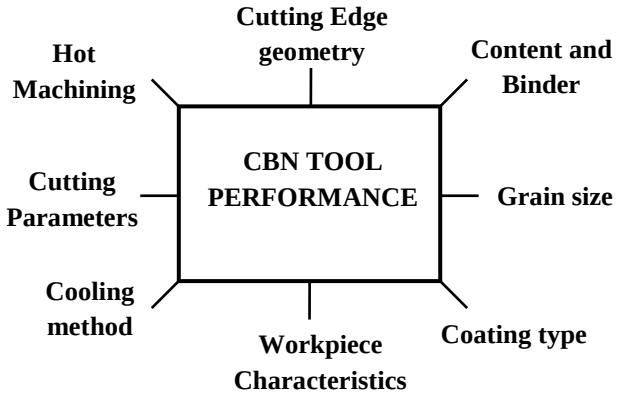

Figure 2-9Factors affecting cBN tool performance (Adapted from Dogra et al., 2010)

Generally, PcBN is normally recommended for hardened materials with hardness up to 70 HRC to generate surface finish down to Ra of 0.3 μm. Low content cBN is better suited for machining owing to better shock resistance, wear resistance and chemical stability, while high content cBN is more suitable for hard cast-iron and high-temperature alloys owing to its toughness.

2.4 TOOL WEAR

The most important consideration in testing and selection of any cutting tool is the tool life. This is widely studied in many cutting tool materials. Generally, the cutting tool fails from wear, fracture or plastic deformation. The type of tool wear according to the ISO standard is shown in Figure 2–10.

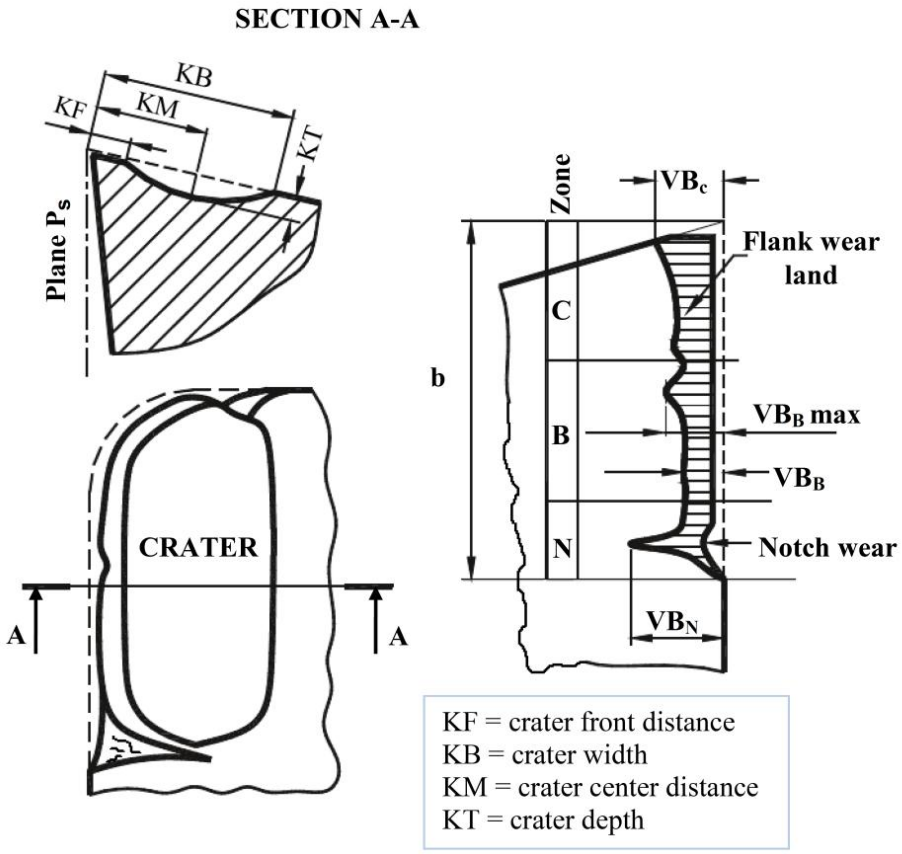

Figure 2-10 Flank wear and crater wear according to ISO 3685 Standard (Adapted from ISO 3865 standard)

The dominant wear mechanisms with their corresponding cutting speeds and temperatures were illustrated by Opitz and Konig, (1967) and Hastings and Hastings and Oxleyn (1976). At low cutting speeds and temperatures, abrasion wear dominates, followed by adhesion at moderate speeds and temperatures and, at high speeds and temperatures, diffusion wear.

The cutting edge of any cutting tool is subjected to a combination of high temperatures, high stresses, and in some cases chemical reactions which cause wear of the cutting tool as a result of one or several mechanisms. The mechanisms causing tool wear depend on the cutting geometry, tool and workpiece material combination, and the environment, as well as the thermal and mechanical loadings encountered. The main observed wear patterns common with tool wear are flank wear, crater wear, notch wear,chipping, thermal shock cracks, nose wear, tool breakage, and built-up edge (North, 1989; Klimenko et al., 1992; Lahiffet al., 2007).

The typical wear patterns generated in finish machining of metal cutting are illustrated in Figure 2–13 (Chou and Evans, 1997).

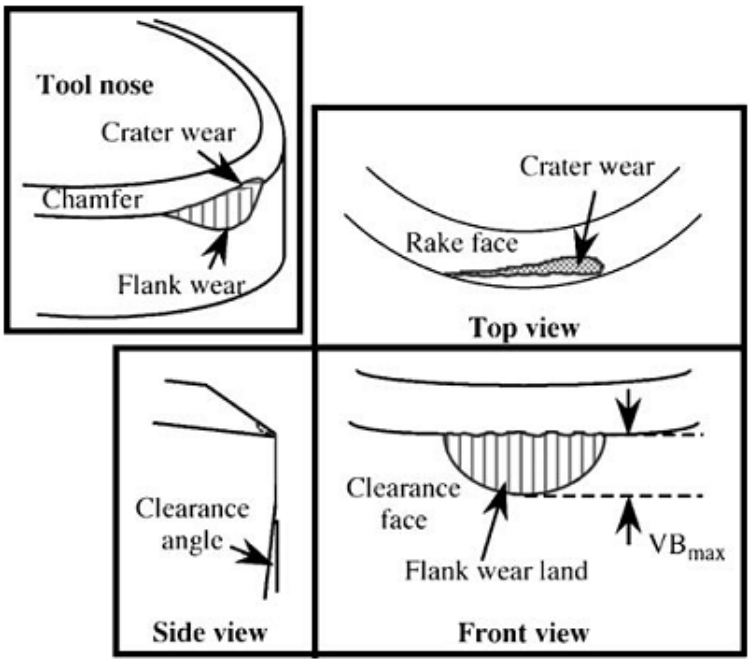

Figure 2-11 Typical wear patterns on a cutting finishing tool (Chou and Evans, 1997)

In hard interrupted turning, the tool wear is a combination of both abrasive and adhesion wear owing to the tribological effect resulting from high temperature (Rech and Moisan, 2003). In hard turning, PcBNis still the most successful cutting tool. The use of Mono-crystalline Diamond (MCD) and Mono-crystalline Cubic Boron Nitride as cutting tools for ultra-precision machining to achieve high accuracy had been investigated, but attempts to introduce them in this application have not been successful owing to the rapid wear rate of the cutting tool, and the difficulty associated with its production (Konig, 1993).

The tool wear is generally classified either according to the region on the cutting tool affected or by the physical mechanisms producing it (Cook, 1973; Wright and Bagchi, 1981). The flank and crater wear are the most commonly produced wear on the tool face.

Flank wear can be easily observed on the rake face of the cutting tool and it is produced during rubbing of the wear land against the machined surface, as a result of abrasion of the cutting edge. The flank wear is the most commonly observed for tool wear as a result of its occurrence in all machining operations. The flank wear increases over a period of time till the critical wear is reached (point where the tool edge is no longer useful owing to either excessive wear or poor surface quality of the machined part).Flank wear occurs mainly when

the flank face rubs against the spring-backed workpiece surface and it can be minimized by raising the tool hardness under elevated temperatures.

Crater wear, measured by the crater depth (KT), is produced on the rake face of the cutting tool but normally does not have a serious effect on the tool life of the tool except when it is excessive, thus leading to deformation or fracture of the tool and weakening of the cutting edge. Crater wear is caused by chemical, physical, and/or thermo-mechanical interactions between hot metal chip removed during cutting action and the rake face of the cutting tool. A crater is caused as a result of one dissolution of the tool material into the chip, adhesion between the insert and the chip owing to micro-welds, abrasion of the cutting tool by free/embedded abrasive particles, and tribo-chemical reaction between the chip and cutting tool rake face (North, 1989). However, an increase in the crater wear reduces the cutting force and effective rake angle of the cutting tool (Stephenson and Agapiou, 2006).

Other forms of the tool wear on the surface of the cutting tool are: notch wear, nose radius wear, thermal and mechanical cracking, edge built up, edge chipping, tool fracture and plastic deformation, as illustrated in Figure 2–11.

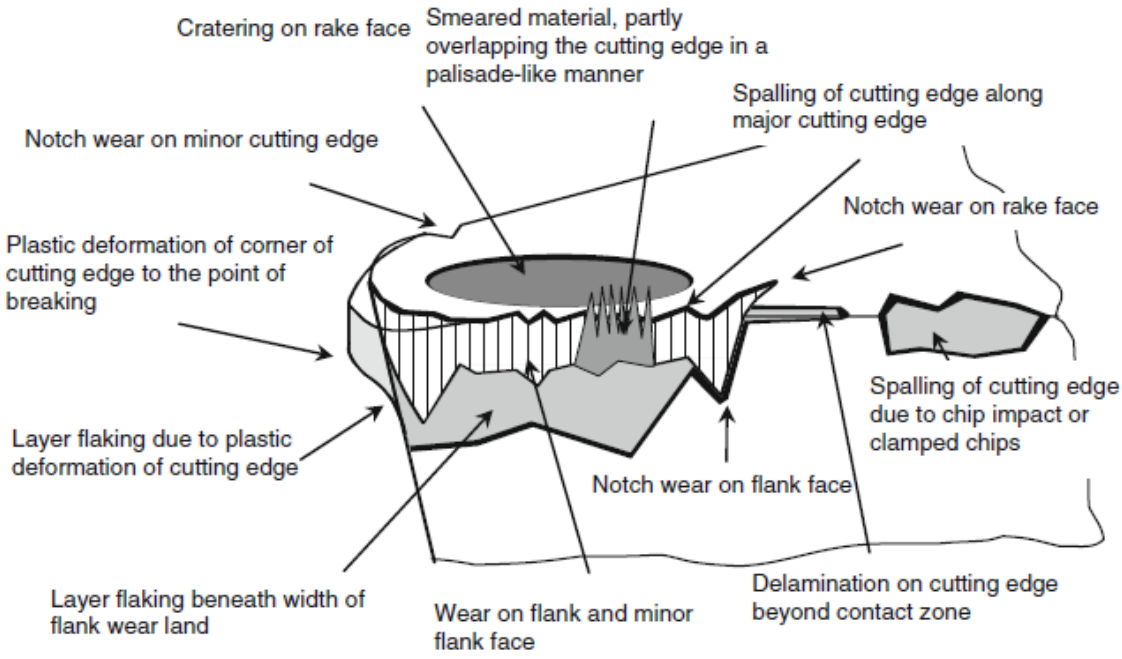

Figure 2-12 Wear Forms on cutting tool (Courtesy, Klocke, 2011)

The notch wear is common with parts made from work hardening materials, or with hard surface layer, as a result of abrasion between the cutting tool and the workpiece (Lee et al.,

1979).Thermal and mechanical cracking results from cyclic loading of the cutting tool during machining of materials with high chip-tool temperatures or during interrupted cutting. The cracks lead to rapid chipping or tool fracture. They can be reduced by using a tool material grade with high thermal shock resistance or by reduction in the cutting speed (Wayne and Buljan, 1990).

Edge chipping occurs as a result of one or combination of these factors: cutting work materials with hard or abrasive particles in the metal matrix, tool vibration owing to excessive cutting forces, low system stiffness, and cutting with brittle tool materials such as ceramics or PcBN. Poor surface finish is produced with chipped tools.

Built-up edge mostly occurs when cutting soft materials and at low cutting speeds, since it depends on the ductility of the work material and the tool-chip friction (Trent and Wright, 2000). The work material that is being cut adheres to the cutting edge. The effect of built up edge includes the following two results: reduction in machining accuracy as a result of changes in the feed rate, and poor quality of surface produced (periodical breaking and reform, creating irregularities on the work surface). Built up edge is undesirable during machining and can lead to increase in the effective rake angle of the cutting tool and the reduction of cutting forces.

The basic mechanisms that dominate tool wear are as follows:

- Diffusion wear – caused by chemical loading on the tool and cutting material;
- Oxidation wear – causing gaps to occur in coated film and resulting in a loss of the coating at elevated temperature;
- Fatigue wear – a thermo-mechanical effect and leads to the breakdown of the edges of the cutting tool;
- Adhesive wear – occurs at low machining temperatures on the rake face of the tool and leads to the formation of a built up edge (BUE), and the continual break down of the tool edge itself;
- Abrasive wear – affected by hardness of the work material and closely related to the distance of cut as well as hardness, shape and distribution density of theabrasives(Dolinsk and Koac, 2006; Arsencularatne, 2006).

2.4.1 Abrasive wear

Abrasion wear is seen as grooves primarily on the flank face of the cutting tool. Abrasive wear is usually the form of wear that determines the tool life at low and medium cutting speeds and is the primary cause of flank, nose radius and notch wears in cutting tool.

Abrasion wear occurs during the sliding movement of loose hard particles penetrating into the surface of the stressed cutting tool material, thus creating grooves and removing material from the surface of the cutting tool. The abrasive particles are usually found as iron carbides in cast iron. The abrasive particles are also found in the chip (oxides, carbides, nitrides), martensite, austensite, hard phases in the steel, and sands inclusions from sand cast parts in foundry (Bergman et al., 1994).The hard abrasive particles in the work material can play a significant role in the wear of the tools, under the conditions of sliding.

The material damage process falls into three categories, micro-plowing, micro-cutting and micro-cracks. In ductile materials the micro-plowing and micro-cutting are thepredominant wear processes.The material is plastically deformed within the created groove and drawn towards the groove edges during micro-plowing (ZumGahr, 1987).
Because of the hard workpiece material structure of the martensitic stainless steel, there is a rubbing action between the tool flank and the hard martensitic workpiece; the hard abrasive particles in the workpiece material can play a significant role in the wear of the tools by removing material in the flank side of the cutting tool. This is the main cause of the abrasive wear (Luo et al., 1999; Narutaki et al., 1979; Konig et al., 1984; Poulachon et al., 2004; Hasan and Thamizhmanii, 2010).

2.4.2 A**dhesive wear**

Adhesion involves the formation of micro-welds between two different bodies during friction (mechanical adhesion of workpiece material that is plastically deformed), with atomic interactions(thermally induced diffusion processes, electron exchange orelectric polarization). During adhesion, small particles removed from the cutting tool material welds to the cutting chips flowing over the face of the cutting tool (Cook, 1973).

The adhesion coefficient (strength of adhesion bond) is defined as the ‘quotient of the normal force F_N with which two solid bodies inrelative motion are pressed against each other and the opposing force F_A that mustbe applied to undo the bond formed by adhesion’ (Habig, 1980).

Significant adhesion is responsiblefor the formation and growth of BUE, in which material is transferredfrom the workpiece into the cutting tool (ZumGahr, 1987). Adhesive wear is usually seen as a smooth wear on the flank or crater face of any cutting tool. Adhesive wear can further lead to chipping of the cutting tool. Built-up edges are described as highly reinforced layers from the machined work material bonded on the cutting tool edge,which function as a new cutting edge. Steel materials such as ferritic and austenitic steel, have a great tendency of adhesion with cutting tool materials owing to its high ductility.

2.4.3 Oxidation wear

Oxidation wear occurs when there is a chemical reaction between the cuttingtool material and atmospheric oxygen. Oxidation wear changes the properties of the external boundary layer of the tool and occurs near the surface of the cutting tool, where a hot area of the cutting tool within the tool chip is exposed to the atmosphere. Oxidation wear is responsible for severe depth of cut notch usually, seen as discoloration in the wear area of the tool.

Oxidation wear is common with cemented carbides and tungsten carbide tools resulting from high cutting temperature and atmospheric oxygen. However, this form of wear is not common for tool steels, aluminium oxide based ceramics and high speed steels since their heat resistance is exceeded before their surfaces can be strongly oxidized(Konig et al., 1984; König and Neises,1993b).

2.4.4 Diffusion wear

Diffusion wear is thermally activated wear whereby the elements of the cutting tool material diffuse or go into a solid solution with the work material, as a result of contact with the cutting chip leaving the cutting zone. Diffusion in the reverse direction is also possible. This wear leads to serious cratering of the cutting tool and tool surface weakness resulting from decrease in hardness and resistance to abrasion at the rake face of the cutting tool (Habig, 1980).

The schematic diagram of diffusion wear occurring when machining with uncoated cemented carbide is shown in Figure 2–12 below, and the reactions are as follows;

- diffusion of Fe into the binder phase Co
- diffusion of Co into the steel, with the formation of mixed crystals from Fe and Co
- dissolution of tungsten carbide to form mixed and double carbides in the form of $(FeW)_6C$, Fe_3W_3C, and $(FeW)_{23}C_6$.

In Figure 2–12, iron is seen to diffuse from the work material into the cutting tool, and carbon and cobalt into the work material. Since the carbon concentration in the workpiece material (steel) is lower than the one in the carbide tool, the carbon released during the dissolution of tungsten carbide migrates into it. The resultant iron diffusing from the work material into the tool forms iron mixed carbides (Klocke, F, 2011).

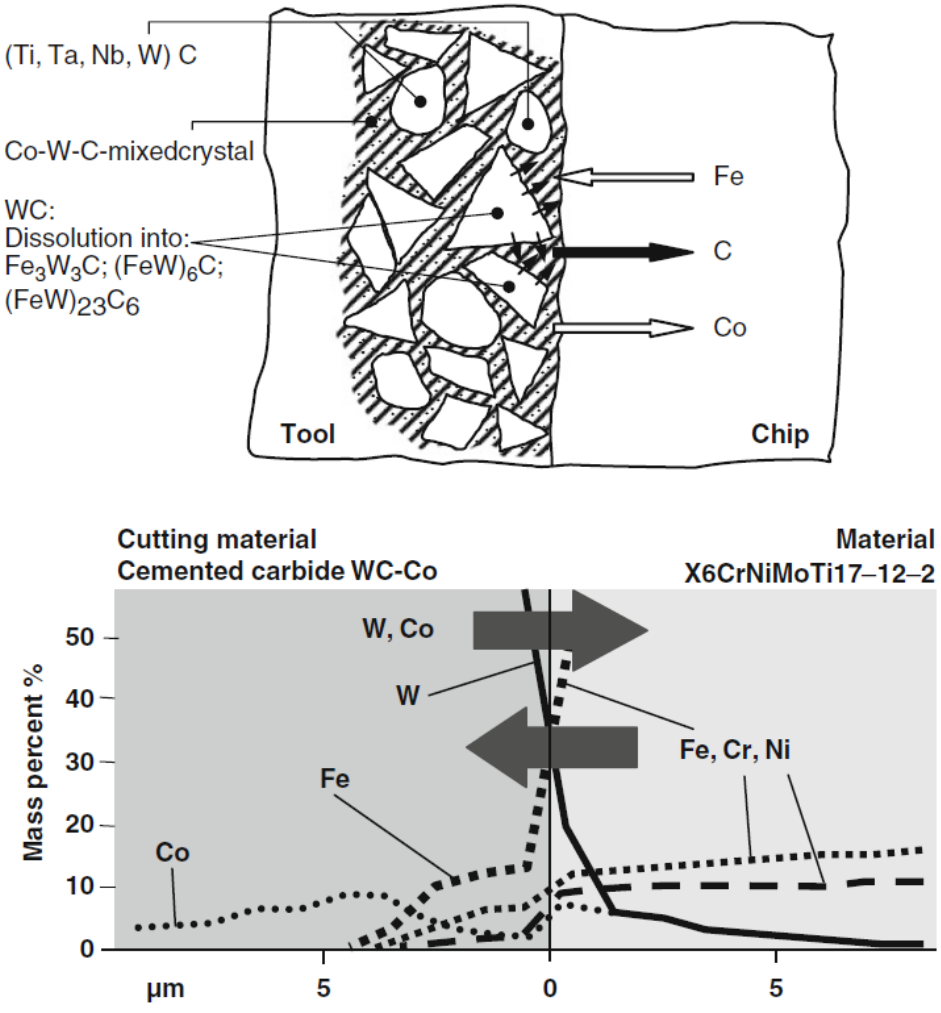

Figure 2-13 Schematic diagram of diffusion in cemented carbide cutting tools (Klocke, 2011)

2.4.5 cBN and Ceramics wear

2.4.5.1 cBN wear

The main wear mechanisms in cBN turning hardened steels are generally considered to be a combination of abrasion, adhesion and diffusion, and the wear mechanism is dependent on the cutting conditions, tool geometry and material properties of the tool and the workpiece (Huang and Liang 2004a; Huang et al., 2007; Wang et al., 2008; Hasan and Thamizhmanii, 2010). The predominant wear mechanism for PcBNtools is abrasion (Hasan and Thamizhmanii, 2010).Some studies on the use of PcBN cutting tools for machining hardened steels are presented below.

In the study conducted by Thamizhmanii and Hassan (2008) on the use of cBN and PcBN cutting tools on surface roughness and flank wear during hard turning of martensitic AISI 440 C stainless steel, they found that there was more flank wear on the cBN tool when compared to the PcBN cutting tool, which was owing to more abrasion and diffusion. The wear was mainly owing to abrasion by hard martensite particles in the work material. The flank wear was less in the PcBN tool at high speeds. They concluded that the effect of cutting temperature has significant influence on the tool wear.

The cBN content and nature of the binder in use in PcBN significantly affect the wear rate of the cutting tool. PcBN with low cBN content and ceramic bonding phase has substantially better performance for finish hard turning than PcBN with high cBN content and PcBN with a cobalt bonding phase owing to its lower thermal conductivity (Konig et al., 1993). The lower cBN content permits longer machining time owing to its slow wear rate, thus hard turned parts have higher surface quality and better dimensional accuracy in comparison to parts machined with higher cBN content cutting tools (Konig et al., 1993).

Many studies have been carried out in the intermittent (or interrupted) hard turning with cBN tools, with the concentration on the effects of cBN content, wear mechanisms, cutting speed and frequency of interruption on tool life (Chou and Evans, 1997; Ko and Kim, 2001). The factor used for determining tool life was flank wear rather than tool fracture in these studies probably owing to the higher value of cutting length ratio (that is, the ratio of the cutting length to air-cutting length).

Liew et al. (2003), investigated the wear of different grades of PcBN cutting tools (BN 100, BN 250, BN 300 and BN 600 with volume of cBN of 85, 60, 60 and 90 vol. % respectively), during machining of modified AISI 420 stainless steel (hardness of 55HRC). They observed that the wear resistance of BN 100, BN 250 and BN 300 tool grades at the flank face were similar and lower compared to BN 600 grade. With the BN 250 and BN 300 grades, the authors found no fracture on the rake faces, and the increase in the size of the cavities (fine-scale damage on the tool rake face) with cutting distance was also found to be significantly less than the ones found using BN 100 grades. They attributed this to the BN 250 and 300 grades possessing greater bonding strength, smaller grain size and lower thermal conductivity. They concluded that porosity, bonding strength of the grains in the tool, ductility, and thermal conductivity had a significant effect on the fracture resistance of the cutting tool.

Ko and Kim (2001) studied the surface integrity and machinability in intermittent hard turning of a ball bush made of AISI 52100. These authors observed that a low-content cBN tool is superior to one with highcBN content in terms of tool wear and surface integrity for intermittent hard turning. Also that the low-content cBN tool is superior to one with high cBN content at higher cutting speeds, while at low cutting speeds the reverse is found to apply. This is ascribed to the high thermal conductivity of the high cBN content cutting tool which helps reduce the effect of thermal shock. The vulnerability of cBN to chemical attack by ferrous alloys is another important factor in explaining these differences.

2.4.5.2 Ceramics wear

The most dominant tool wear associated with the use of ceramic tools (Al_2O_3) in hard part turning are the abrasion and adhesion wear (Caydas, 2009). Some studies on the wear of ceramics are presented below.

Kumar et al. (2006) studied the tool wear of an alumina-based ceramic in comparison with a composite ceramic made of alumina mixed with zirconia, as well as alumina mixed with Ti [C, N], and SiCwhisker reinforced alumina on martensitic stainless steel SS 410 (60 HRC). They observed that alumina-based ceramic cutting tools are affected by flank wear at low cutting speed and crater/notch wear at higher cutting speeds. The alumina ceramic mixed with Ti [C, N], performed best owing to its ability to retain hardness at elevated temperatures.

In another study, Grzesik (2009) reported that TiC-reinforced alumina, (Al_2O_3+TiC) wears in a mode involving abrasion, plastic flow, adhesive fracture and tribological effects, which all depend on the mechanical and thermal conditions generated during the machining test. PcBN is found to have better tool wear resistance compared to ceramic cutting tools (Sales et al, 2009).

Zhao et al. (2010), investigated the cutting performance, failure modes and mechanisms of wear of Al_2O_3–WC–TiC ceramic tool(TiC 24%, WC 16%), Al_2O_3/(W, Ti)C ceramic tool and cemented carbide tool for both continuous and intermittent turning of hardened AISI 1045 steel (40 – 44 HRC). They observed that under continuous turning conditions, the Al_2O_3–WC–TiC ceramic tool had better wear resistance than the Al_2O_3/(W, Ti)C or the cemented carbide tool as a result of its high fracture toughness. The wear resistance was lower than that of the Al_2O_3/(W, Ti)C tool during interrupted cut at speed of 110 m/min. The authors attributed the longer tool life of the Al_2O_3–WC–TiC tool to its synergistic strengthening/toughening mechanisms induced by the WC micro–particles and TiCnano-particles. This microstructure and composition resulted in, mixed modes of intergranular and transgranular fracture, matrix grain refining, dislocation pinning, crack deflection, crack bridging and crack branching.

2.4.6 Influence of coatings and cutting conditions on surface integrity

Research by Rech and Moisan (2003) on the effect of feed rate and TiN coatings when turning case hardened steels showed that feed rate is the major parameter influencing surface roughness. TheTiN coatings were found to improve the surface roughness of the produced surfaces. The surface roughness of any machined product is strongly influenced by cutting parameters such as speed, feed and depth of cut (Surjya and Chakraborty, 2005).

Benga and Abrão (2003) investigated the effect of cutting speed and feed rate on surface roughness and tool life using three-level factorial design after machining hardened 100Cr6 bearing steel (62–64 HRC) using ceramic and cBN tools. They found that feed rate was the most significant factor affecting surface finish while the cutting speed had little influence on surface finish. However, surface finishimproves with increase in cutting speed and decreases

with an increase in feed rates (Lima et al., 2005; Bouachaet al.,2010). Changes in depth of cut normallydo not show any significant effect on surface roughness (Bouachaet al.,2010).

As observed by Thamizhmanii and Hasan (2008b), cBN tools produced low surface roughness at high cutting speeds with low feed rate, whereas the PcBN tools produced high surface roughness for the same operating parameters. The authors concluded that surface roughness is mostly dependent on formation of built up edge, temperatures at tool tip and flank wear of the tools investigated.

Zhou et al. (2010) studied turning of hardened AISI 52100 (60–62 HRC) using PcBN cutting tools, under dry and flood cooling conditions. They observed that use of coolant improved the dimensional tolerance by keeping the temperature at the tool–chip interface low, thus minimising the thermal distortion of the work piece. The dimensional tolerance was also found to vary with the length of cut. Zhou et al. (2004) observed that tool wear up to 0.2mm can lead to dimensional error of 25 µm on a comparative study between hard turning and grinding AISI 5115 (62-64 HRC). In addition they observed that the tool clamping system had significant effect on the dimensional tolerance, with the magnetic clamping system found to produce better dimensional accuracy compared to 3 and 6 jaws clamping systems.

2.5 EFFECT OF VIBRATION AND TOOL GEOMETRY

Workpiece and tool vibration can lead to irregularity of machined shape as well as surface damage of the machined workpiece. Vibrations can also lead to increased tool wear rate and tool breakage. In hard turning, when the requirements are high precision in dimensions and shape, self-exited vibration of the machining set-up can be a major factor affecting the level of accuracy of the part produced (Kopac et al., 2006).

Konig et al. (1993) noted that hard finish comparable to grinding it is not always abletoachieve the high degree of geometric accuracy required owing to thermal effects and stiffness of the machine tool system; if these factors can be carefully controlled, it is possible to produce parts with high precision.

Micro geometry of a cutting edge plays an important role on the workpiece surface properties and the performance of the cutting tool (Tonshoff et al., 1995). Generally, cutting tools such

as the ceramics and PcBN are designed with certain micro edge geometry with a process called edge preparation. It is known that sharp tools are not durable enough for most of the machining operations. Thus, different types of tool edge preparations such as chamfer, double chamfer, chamfer+hone, hone, and waterfall hone edge design have been introduced by manufacturers. In order to improve the overall quality of the finished component, tool edge geometry is carefully designed. Thedesign of the cutting edge may affect the chip formation mechanism and therefore help reduce cutting forces, thus increase the tool life (Arazzola and Ozel, 2007).

When cutting hardened steels, the use of chamfered edges and negative rake and inclination angles help to increase the machining forces. In addition, the use of large nose radius together with low depths of cut leads to low side cutting edge angle values (irrespective of the selected tool holder geometry), thus resulting in high thrust forces.

Diniz et al. (2009)also performed hard turning experiments using a high cBN content tool (cBN-H) and low cBN content tool(cBN-L) tool with chamfered and rounded edges on continuous, semi-interrupted and interrupted surfaces on one cutting speed. They observed that the chamfered geometry was the best choice for all kinds of surfaces, with the rounded geometry producing good results on interrupted surfaces.

Large nose radius and cutting edge angle values may improve the surface finish of the machined part provided tool vibration can be avoided (Lima et al., 2005). The nose radius of PcBN inserts directly affects the tool life as well as the surface roughness of the product (Noordin et al., 2007). A larger nose radius produces a fine surface finish, but also increased specific cutting energy (Kopac et al., 2006).If the radius is too large, the contact area of the cutter would be too large, which may result in chatter, which is harmful to the turning process. The risk of microchipping is reduced by honing of the cutting edge (Yih-Fong, 2006).

Tools with multi radii (wiper) geometry have been provided by tool manufacturers in order to improve productivity of hard turning. The wiper inserts combine the high feed capability and high quality surface finish produced by large round inserts. This tool geometry has wiper radii adjacent to the nose radius, and it has little or no clearance angle to improve finish by burnishing action by the flank face of the insert (Noordin et al., 2007). Recently, both cBN and mixed ceramic are offered in wiper configuration with special *Xcel* geometry or

smoothing micro-edges with the smaller approach angle resulting in a reduced chip thickness relative to the feed rate (Grzesik, 2009).

Figure 2–14 shows a multi-radii cBN cutting tool corner containing,(a) a small smoothing part of the radius (r_{bo}) parallel to the feed direction and (b) a more universal design of a wiper corner with both right handed and left-handed wiper segments.
In this figure, $r_{\varepsilon 1}$ and $r_{\varepsilon 2}$are the radii of wiper curvature, $R_z$is valley-to-peak height, and r_{bo} is the radius of smoothing part.

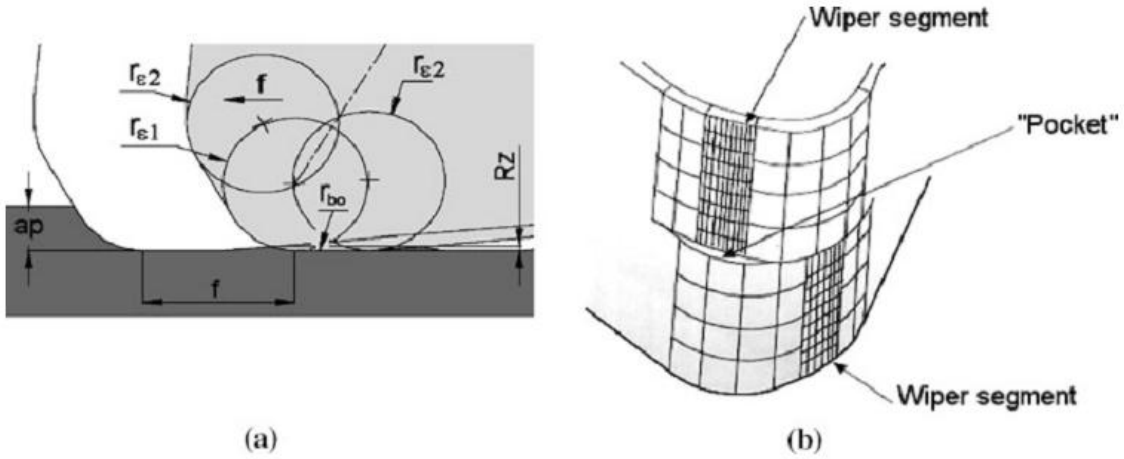

Figure 2-14 PcBN wiper inserts (a) one-handed design, and (b) two-handed (Grzesik and Wanat, 2006)

Figure 2–15 shows the new design of solid cBN inserts having a straight part of the cutting edge blending into a wiper. The cutting edge of the wiper insert has a smaller approach angle (Kr) compared to conventional cutting edge, thusreducing the depth of cut where constant chip thickness is achieved. Higher feedrates up to 0.4 mm/rev can be applied when using wiper inserts as a result of the smaller approach angle.

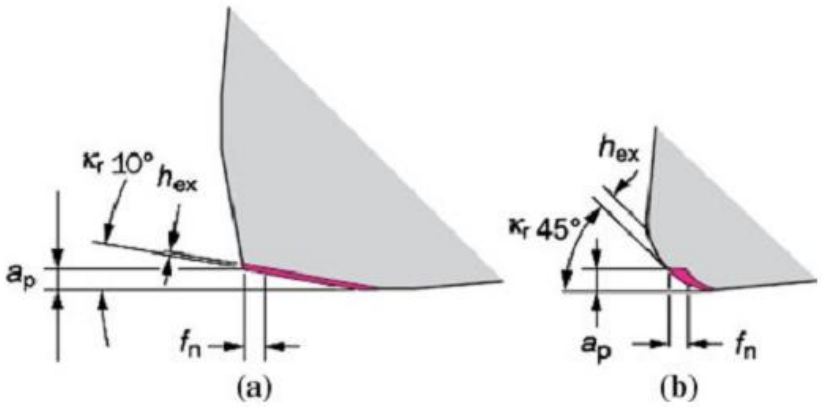

Figure 2-15 Comparison of chip thickness and Excel geometry for (a) wiper and (b) conventional corner (SandvikCoromant)

Thiele and Melkote (1999) investigated the effect of cutting edge geometry and workpiece hardness on surface generation in finish hard turning. They found that increasing the edge hone radius tends to increase the average surface roughness. They attributed this to the increase in the ploughing component compared to the shearing component of deformation. The effect of edge hone on the surface roughness decreased with increasingworkpiece hardness.

2.6 CUTTING FORCES

Cutting forces are sometimes used for evaluating the performance of the cutting tool during finish hard turning of theworkpiece within the selected range of cutting parameters (Trent and Wright, 2000; Bartarya and Choudhury, 2012)

The energy consumption, tool and workpiece deflections and power requirements of the machining process are determined by the cutting forces. The cutting forces are normally measured using the dynamometer. The most commonly available instrument for this purpose is the quartz dynamometers, with high stiffness, good thermal stability and high broad frequency range response, and which exhibit little static crosstalk between measurements in different directions (Stephenson and Agapiou, 2006).

Figure 2–16 shows the schematic diagram of the component forces that can be easily measured acting on the tip of a single point cutting tool, where F_c is the cutting force and F_t thrust force. The analysis of the cutting force during orthogonal cutting is shown in Figure 2–

17. The forces are perpendicular to one another, and combined they act on the tool as a resultant force. The component forces acting are the longitudinal feed or axial force,F_x, the cutting force (radial), F_y, and the tangential force,F_z. The radial and cutting force is proportional to the tangential cutting force; the proportionality factor is dependent on the lead angle and the depth of cut (Sobiyi, 2011).

The cutting force is a product of the contact area (A_r) of the rake face of the cutting tool to the workpiece and the shear strength of the work material at the surface (K_r). It is given in Equation 2–2 (Trent and Wright, 2000).

$F_y = K_r A_r$ ... .….. …… (2–2)

For cases where the rake angle is 0° (during roughing operation), the cutting force F_y, is an indication of the drag created by the chip as it flows away from the rake face of the cutting tool.

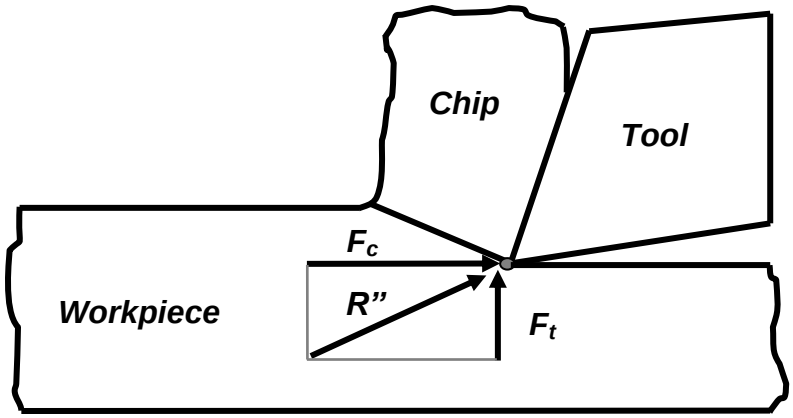

Figure 2-16Component forces acting on the single point cutting tool (Adapted from Sobiyi, 2011)

During finishing operations, where the depth of cut is very small, the radial and axial cutting forces usually approach or even exceed the tangential force. Several factors affect the cutting forces during machining. For a given material, the tool forces are influenced by the tool geometry, with the rake angle the most important parameter. An increase in the rake angle reduces both the cutting force and the feed force, which eventually leads to fracture of the tool. The cutting force is also dependent on the width of the cut and the feed rate. The cutting force increases most especially with the feed rate (Stephenson and Agapiou, 2006). The forces

divided by the depth of cut is an important parameter determining breakage or chipping of the cutting tool and this is calculated from Equation 2–3 (Stephenson and Agapiou, 2006).

$$F = dC_1 V^a a^b (1 - sin\ \alpha)^c \quad \text{…….} \quad (2–3)$$

where *F* is the cutting forces normal or parallel to the tool rake face, *V*, the cutting speed, *a*, the uncut chip thickness, *d*, the width of cut, and α the normal rake angle.

During hard turning with ceramics and PcBN, negative rake angles are normally used owing to their lack of toughness. During machining of slender shapes, higher cutting forces make negative rake angle unsuitable, thus leading to distortion as a result of the higher stresses experienced by the tool. As the tool wears, the cutting forces normally increase, thus the clearance angle is destroyed and the contact area between the tool and work material increases.

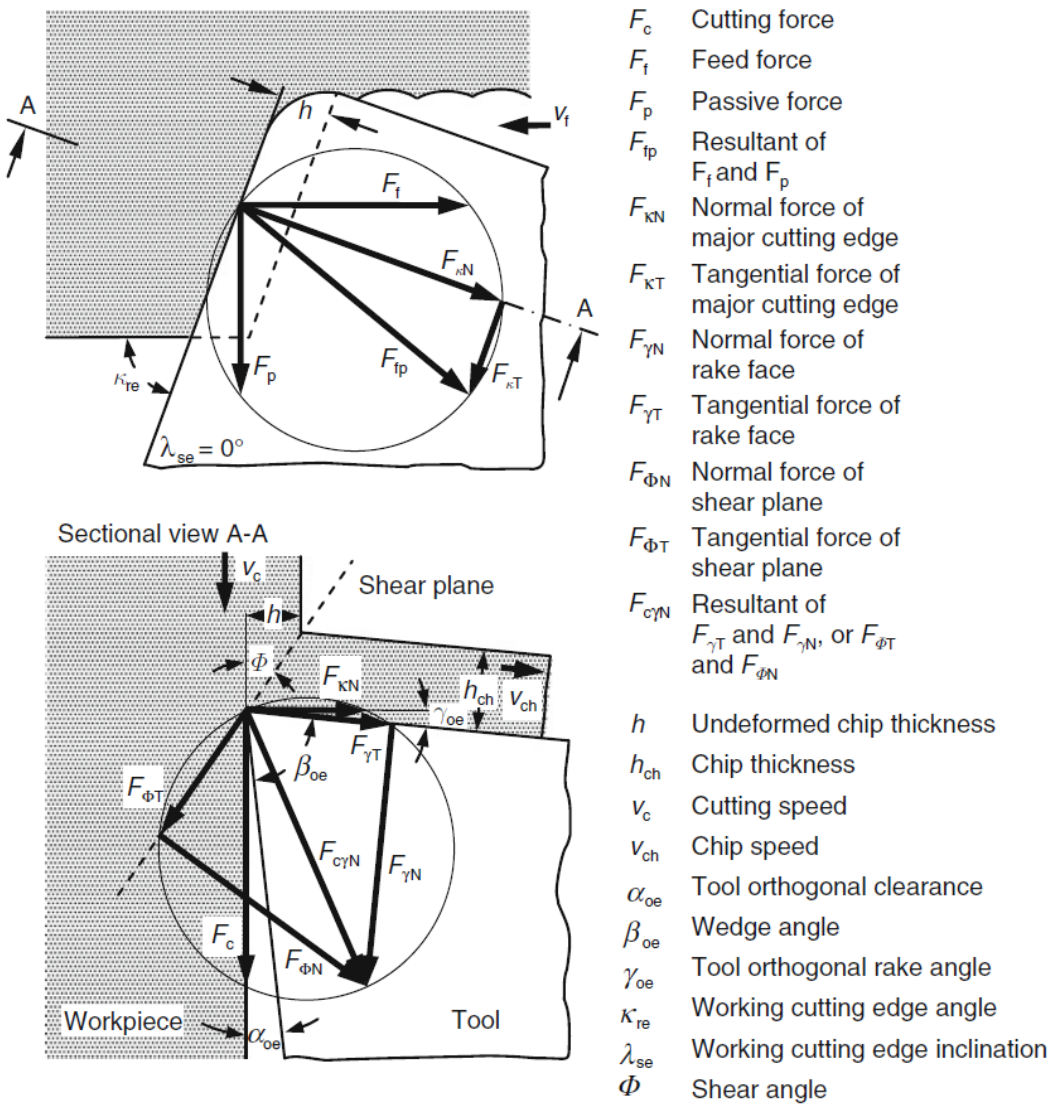

Figure 2-17 Force analysis during orthogonal cutting in the working plane (Courtesy, Klocke, 2011)

Several studies on cutting forces have been conducted on the effect of cutting forces during machining of hardened steel.

Generally in finish hard turning where depth of cut is normally smaller than the nose radius of the cutting tool, the cutting force (radial component) of tool force is found to be the most dominant (Konig et al., 1984; Zhou et al., 2004; Huang and Liang, 2005; Karpat and Ozel, 2007; Fnideset al., 2008, 2011; Suresh et al., 2012). The radial component increases significantly with flank wear rate, and it is as a result of spring-back of the work material (Nakayama et al., 1988). Consequently, cutting speed does not have a significant influence on the cutting force (Lalwaniet al.,2008; Bouachaet al.,2010).

The primary cause for size error in hard machining is large thrust force. The radial and tangential components of the cutting force depend on the tool rake angle; these components do not increase with the hardness of the workpiece material when rake angle is zero, but with an angle of –20°, these components significantly reduce with hardness (Nakayama et al., 1988).

The cutting forces in hard turning are higher compared to conventional cutting, owing to the hardness of the workpiece; this results in reduction of the performance of the cutting tool (Suresh et al., 2012)

Suresh et al. (2012) investigated the variations in cutting conditions on the cutting forces during finish hard turning AISI52100 grade steel. They observed the thrust force (radial component) as the dominant cutting force with interrupted turning. Variation in the feedrate and depth of cut do influence the cutting forces, with the depth of cut having significant effect. They concluded that the thrust force increases with an increase in the cutting length as the wear rate progresses, resulting from an increase in contact area between the land ofthe tool flank and the workpiece.

Hard turning of martensitic AISI 440 C stainless steeland SCM 440 alloy steel using a cBN cutting tool was investigated by Thamizhmanii and Hasan (2008a). The authors found a direct relationship between the cutting force and flank wear. High cutting speed and feed rates, owing to softening of chips at the cutting zone, resulted in a lower cutting force, less distortion of workpiece and improved surface roughness while turning of AISI 440 C stainless steel.

Luoet al. (1999) investigated the relationship between cutting forces and during hard turning AISI 4340 steel using mixed alumina tools. They observed that an increase in the workpiece hardness results in an increase in the cutting forces. Similar results were observed by Bouachaet al.(2010) during hard turning of AISI 52100 bearing steel using a cBN cutting tool. In conventional turning of the same material, an increase in hardness shows a decrease in the cutting forces. Figure 2–18, shows the effect of hardness and cutting speed on component forces acting on the cutting tool.

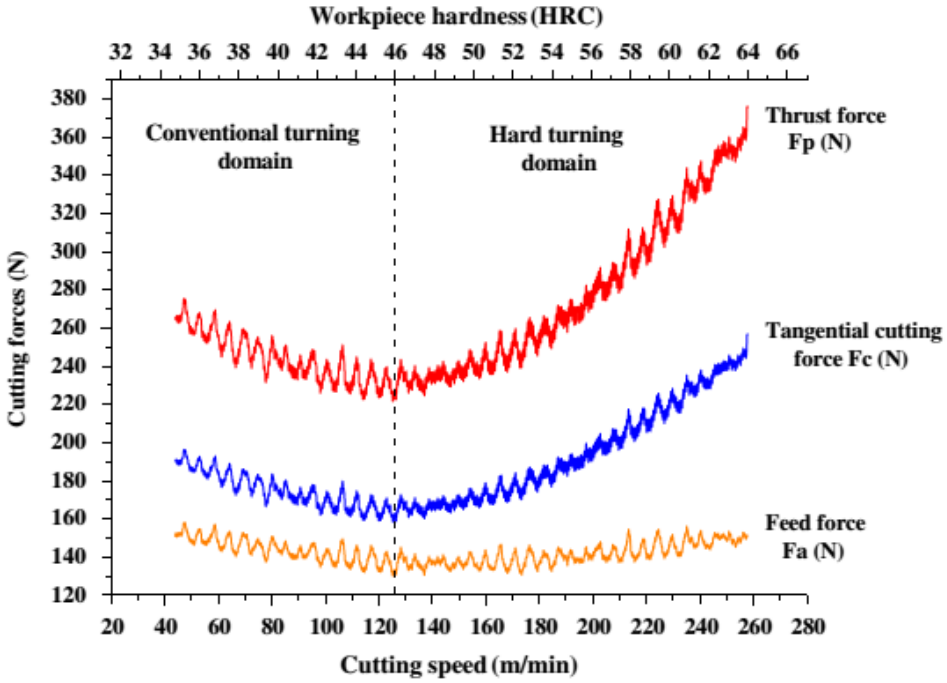

Figure 2-18 Effect of cutting speed and workpiece hardness on component forces of cBN cutting tool (Bouachaet al., 2010)

Fnideset al. (2011) investigated the machining of hardened AISI H11, hot work tool steel using mixed alumina cutting tools. They found that in dry hard turning of this steel, the radial force is not always the predominant force as suggested by other authors. At axial depth of cuts between 0.3mm and 0.45 mm and feed of 0.16 mm/rev, the tangential force becomes dominant followed by the radial and axial forces respectively. The previous study on the same workpiece and cutting tool material showed that the increase in the feed rate increases the component cutting forces, with the tangential force showing the highest amount of increase (Fnidesetal., 2008).

2.7 CUTTING CHIP

During all machining operations, cutting chips are produced from the work material during shearing action by the cutting tool. The chips are produced in different shapes and sizes as shown in Figure 2–19. Chips are formed by shearing of the workpiece material from the region of the cutting tool edge to the top surface of the tool where the chip finally leaves the tool. During the same machining conditions, different types of chips can be formed. In many cases the change in the chip results from the wear progression of the cutting tool. The chip formation is dependent on other conditions, such as material properties, cutting parameters

and the contact area between the rake face and chip. The best chip is described as favourable for the tool system, machined surface and machine tool. Chip forms can be improved by the use of chip breakers.

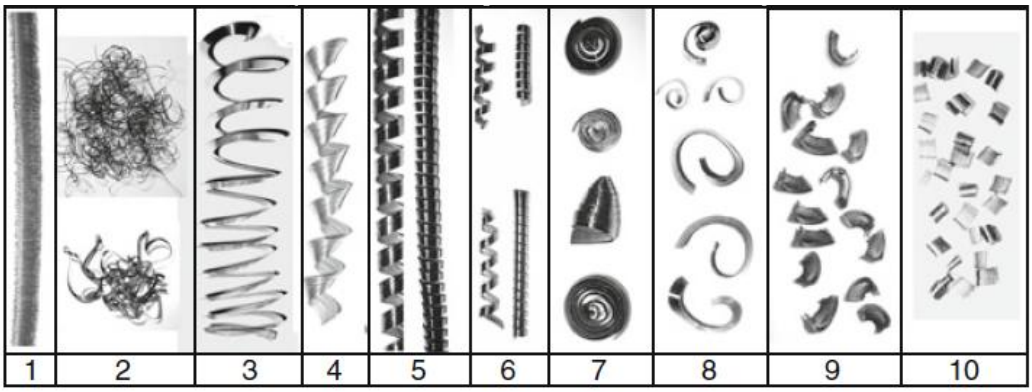

1 Ribbon
2 Snarled
3 Flat helical
4 Angular helical
5 Helical
6 Helical chip segment
7 Cylindrical helical
8 Spiral chip
9 Spiral chip segment
10 Discontinuous

Figure 2-19 Chip forms (Adapted from Klocke, 2011)

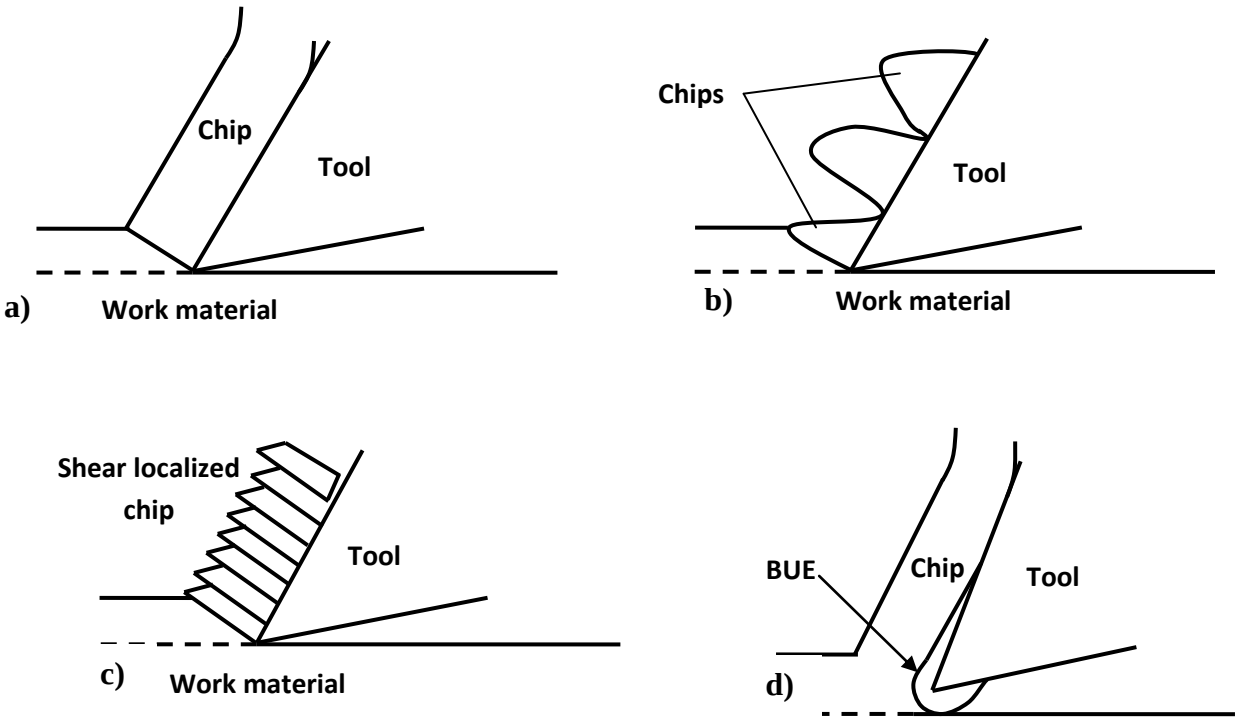

Figure 2-20 Chip types, a) continuous, b) discontinuous c) Lamellar and d) continuous with BUE

The cutting chips are categorised into four types as shown in Figure 2–20, according to Ernst (1938) and Merchant (1945) and other widely observed sources (Barry and Bryne, 2002; Stephenson and Agapiou, 2006).

The continuous chips are the most desirable type of chips, formed when the material has sufficient deformabilityand also by uniform friction conditions between the tool and the chip resulting in an evenly deformed chipmaterial structure.

The discontinuous chip is formed by fracture mechanism when brittle materials with uneven microstructure such as brass are machined at low cutting speeds by fracture mechanisms. The chips formed are torn off from the surface.

Lamellar chip formation is usually observed when machining titanium alloys, hardened materials and stainless steels at high cutting speeds. It is characterized by narrow bands of an unevenly deformed materialstructure alternating with larger regions of the under-deformed material. This particular chip is characterized by localized shear bands; the chip is formed when the yield strength of the workpiece material decreases with increasing temperature, thus the narrow bands in front of the tool are weaker than the surrounding material (Xie et al., 1995).

Continuous chips with built up edge consist of chip segments that are separated from the tool chip contact area in the shear plane and then welded together. They are mostly produced when machining soft ductile materials and also at extremely low cutting speeds.

Most chips are rough on their free surface and smooth on the side in contact with the cutting tool. The grains in the chips normally deform in narrow bands and may change through the thickness of the chips, most especially when cutting at low cutting speeds. The plastic deformation on the tool occurs in two regions, the primary zone and secondary zone. The primary zone stretches from the tip of the cutting tool to the free surface of the chip, while the secondary zone occurs at the tool chip interface (Stevenson, 1992).

2.7.1 Chip formation

The chip formation theory is derived from the shear plane theory, whereby the deformation takes place in the shear plane. The shear plane is inclined toward the cutting edge plane *Ps* by

the shear angleϕ (see Figure 2–21). The chip formation is generally observed in detailed machining studies. In the chip formation, the mean chip thickness is the most important parameter. In orthogonal cutting, the chip thicknessis always thicker than the feed and equal to the undeformed chip thickness.

The ratio of the undeformed chip thickness or depth of cut (t_1) to the deformed chip thickness (t_2) is given as the chip thickness ratio*r* as shown in Equation 2–4.

$$r = t_1/t_2 \quad \text{..... (2–4)}$$

The chip thicknessratio is normally related to the tool rake angle α and the shear angle ϕ as shown in Equation 2–5.

$$\tan\phi = \frac{r\cos\alpha}{1-r\sin\alpha} \text{..... (2–5)}$$

The shear area Aϕ in the shear plane can be calculated as shown in Equation2–6,where *b* is a constant.

$$A\phi = b.\frac{t_1}{\sin\phi} \text{..... (2–6)}$$

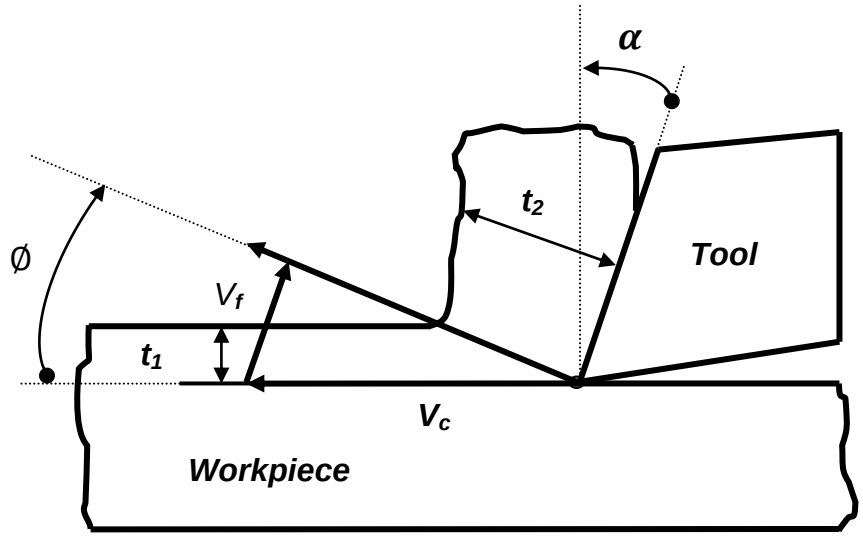

Figure 2-21 Chip velocity plan in orthogonal cutting (Adapted from Merchant, 1945)

The shear plane angle is small if the chip thickness is small, thus the chip movement from the tool face is slow; however, with a large shear angle and a high velocity, a thin chip is produced.

The relationship between the velocity of the chip flowV_f and shear angle ϕ is shown in Equation 2–7, with the schematic diagram of the chip velocity plan shown in Figure 2–21.

$$V_f = {Sin\ \phi . Vc}/{\text{Cos}(\phi - \alpha)} \quad \text{..... (2–7)}$$

where $V_C$is the cutting velocity.

Chip formation has been studied extensively during machining of hardened materials. The formation of segmented chips is one of the primary characteristics during hard turning (Rect, 1964; Boothroyd and Knight, 1989; Shaw et al., 1998).

During hard turning operations, high compressive stresses are experienced owing to the negative rake angles of the cutting tools. The compressive stress leads to the formation of cracks instead of plastic deformation owing to the brittleness of the hardened steel at the chip primary shear plane, whereby the crack initiates from the free surface of the chip and goes deeper towards the tool nose. At this stage, plastic deformation and simultaneous heating occur within the material and the cutting tool as well. The process repeats itself in a cyclic manner after the chip segment has slipped, with another new crack initiated (Konig et al., 1990; Dogra et al., 2010).

For hardened material, there is a formation of saw-tooth chips as a result of the poor ductility of the work material, thus lower cutting forces are experienced,even though the material is of high strength.During saw-tooth chip formation,there exists a catastrophic failure within the primary shear zone of the hard materials,which is attributed either tocyclic crack initiation and propagation or to theoccurrence of a thermo-plastic instability (Barry and Byrne, 2002).

The adiabatic shear theory for the chip segmentation processduring hard turning was introduced by Recht (1964). Many aspects of the cutting process are further determined by the process of plastic deformation in the cutting zone. The solution to some aspects of the cutting

process, such as heat generation, cutting forces and surface quality, depend critically on understanding the chip formation process (Cep et al., 2008).

Lin et al. (2008) investigated the turning of AISI 4340 using a low content cBN tool.They observed continuous chip formation at low cutting speeds and saw-tooth formation at high cutting speeds. They concluded that transition of the chip type occurs between 80 and 130 m/min, with the increase in the cutting speed being the significant factor for the increase in segmentation of the chips produced. The transition in the type of the cutting chips generated can also be attributed to the condition of the tool edge and the cutting forces generated, an increase in work hardness, undeformed chip thickness flank land width, and a decrease in chip tool angle (El-Wardany et al., 2000; Dogra et al., 2010).

Nelslusan et al. (2012) investigated the chip analysis during turning of hardened (62 HRC) and annealed 100 Cr6 rolled bearing steel using mixed ceramic insert at a cutting speed of 100 m/min and feed rates of 0.05–0.271 mm/rev. Theseauthorsfound that segmented chips (thin and long) were formed during the turning of hardened steel.The chip ratio was smaller than 1, whereas thick, short continuous chips with chip ratio more than 1 were formed with the annealed steel. An increase in cutting speed results in more continuous chip. The chip form during hardened steel turning was attributed to low intensity of plastic deformation, though within localized areas of the segmented chip, the plastic deformation was extremely high. The chips formed also have a very high shear angle with cyclic frequency ranging between 14 and 90 kHz.

Similarly, saw-tooth chips were produced in orthogonal cutting of the 100Cr6 steel (hardness of HV730) by Poulachonet al. (2001). During the turning of the same material, high mechanical and thermal stresses were experienced on the machined surface owing to direct stresses in the region of 4000 MPa. The tangential stress was caused by the friction coefficient between 0.2 and 0.3, with thermal stresses as a result of the friction between the workpiece and flank wear land (Konig et al., 1993)

The characteristic phenomenon of material side flow generated during hardturning operations is attributedeither to the squeezing effect of the workpiece material between the machined surface and toolflank land or originating from the flow of plastically deformed material through the worn trailing edge to the side of the tool when the chip thickness is less than a

minimumvalue (Kishawy and Elbestawi, 1999). This effect results indeterioration of the surface finish because the squeezed, flake-like,hard and very abrasive material in the workpiece is loosely attached to the machined surface along the feed marks. This is normally significant with high cutting speed and large tool nose radius,and it becomes aggressive with increasing tool wear.

2.8 SURFACE INTEGRITY

The performance of the machining process in any machining operation can be described by the surface integrity of the resulting part.Surface integrity can be defined as the topological, chemical, mechanical and metallurgical condition of a manufactured surface with its relationship to its performance (Griffiths, 2001).

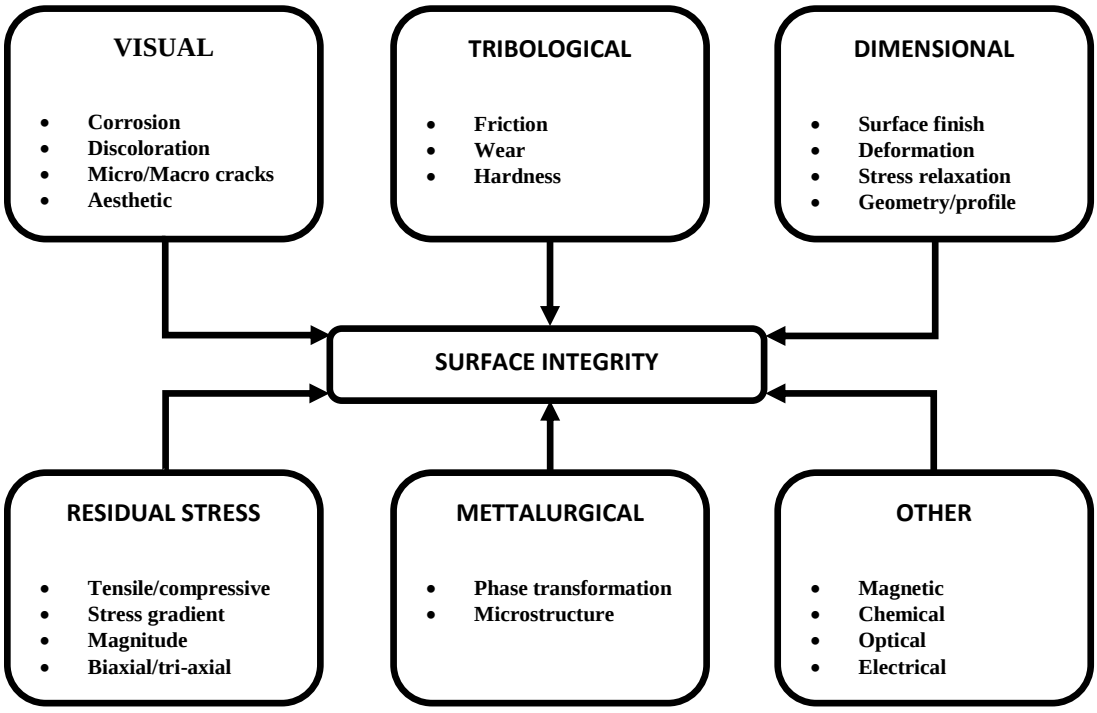

gure 2-22Factors that describe the surface integrity of a machined part (Adapted from ASM Handbook, 1994)

Surface integrity investigations can be divided into two, namely: the external aspects (topography, texture, and surface finish) and the internal subsurface aspects (metallurgy, hardness and residual stress) (Griffiths, 2001).

The key factors, visual, dimensional, residual stress,tribological, metallurgical and others, describe the concept of the surface integrity of a finished material, and they are shown in Figure 2–22.

The topography of the machined surface is shown in Figure 2–23. The topography of a surface is made up of a combination of three main features: surface roughness, surface waviness and surface form (ASM handbook, 1994; Griffiths, 2001). The features are explained below:

- Surface roughness refers to the high frequency irregularities on the machined surface which are usually caused by the interaction of the cutting tool and material's microstructure. These interactions are functions of feed rate and particle size.
- Surface waviness refers to the texture on the surface on which the surface roughness is superimposed. It is caused by a combination of one or more of the following: workpiece deflection, instability of the cutting tool and drive screw errors.
- Surface form is the overall shape of the surface, neglecting both waviness and roughness, caused principally by thermal distortion or wear, or by both.

The lay (L) is the direction of the dominating pattern of the machined method, while the flaws (F) include foreign material, scratches, inclusions,cracks, micro-holes and other defects on the machined surface.

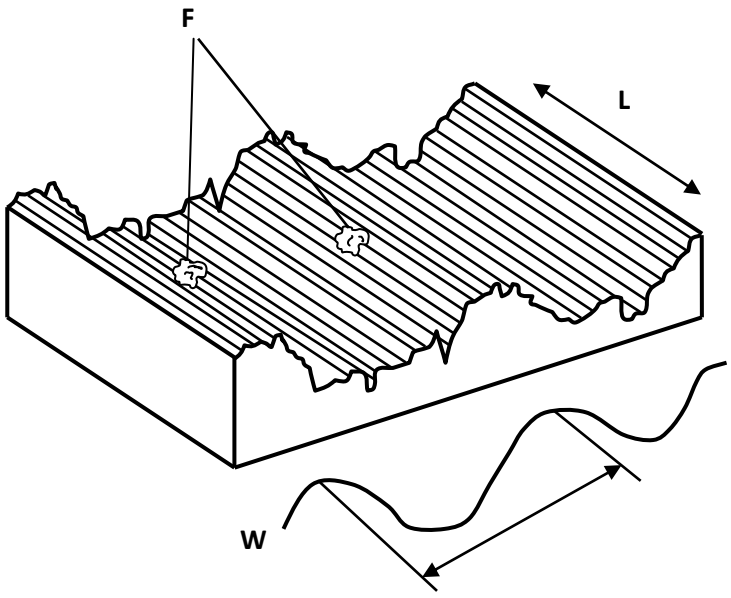

Figure 2-23 Typical surface produced after machining, showing its topography (F- flaws, L- lay, R- roughness and W- waviness) (Adapted from Griffiths, 2001)

The final surface roughness obtained after machining operation may be considered a sum oftheoreticaland natural components. The theoretical components influence the surface roughness resulting from the geometry of the tool, feedrate and cutting speed, whereas the natural component is affected by a couple of effects such as tool wear, built-up edge, chatter, inaccuracies in machine-tool movement, and so on.

The effect of the tool geometry on the surface finish of a machined part is illustrated in Figure 2–24.Better surface finish are generally produced using round inserts compared to the single point cutting tool resulting from the larger effective feed indicated in the figure as *f*. The cutting edge of the cutting tool has significant influence on the final part surface produced, where different shapes and sizes of feedmarks are produced by the cutting tool.a)

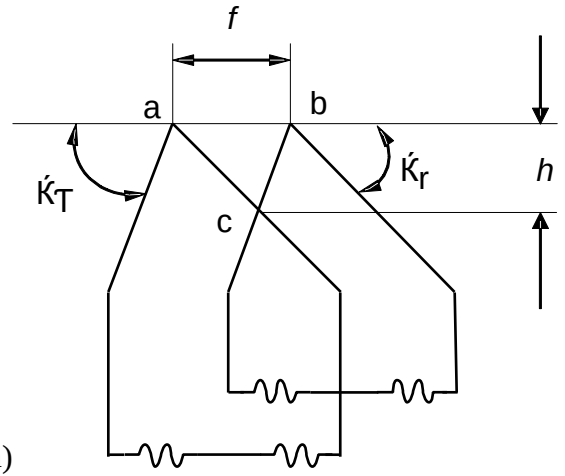

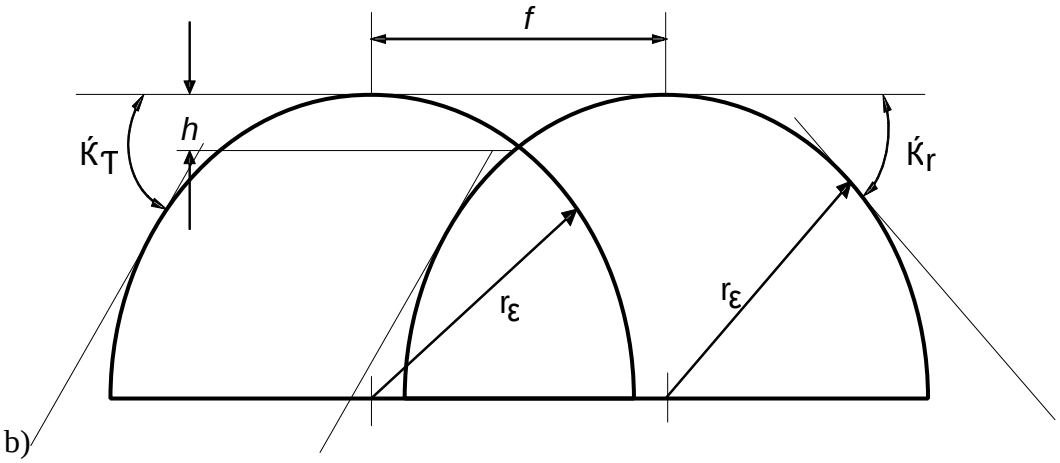

b)

Figure 2-24 Typical feedmark produced by different cutting geometry (a) single point and (b) round(Adapted from Thomas, 1999)

The surfaces generated by hard turning are normally defined by the cutting tool geometry (feed rate and nose radius) unlike grinding, where surface finish is determined by the size, shape, hardness, and distribution of abrasive grains in the grinding wheel, and hardness (Dawson and Kurfess, 2000).

Surface roughness is indicated by specific parameters, such as: arithmetical mean roughness (Ra), maximum height(Ry), ten-point mean roughness(Rz), mean spacing of profile irregularities(Sm), mean spacing of local peaks of the profile(S) and profile bearing length ratio(tp). The arithmetical mean centre-line average roughness value (Ra) as shown in Figure 2–25, for a randomly sampled area, is mostly used as an indication of the surface roughness. This parameter can be calculated using Equation 2–8. For hard turning conditions, Equation 2–9 is mostly appropriate (Dawson and Kurfess, 2000).

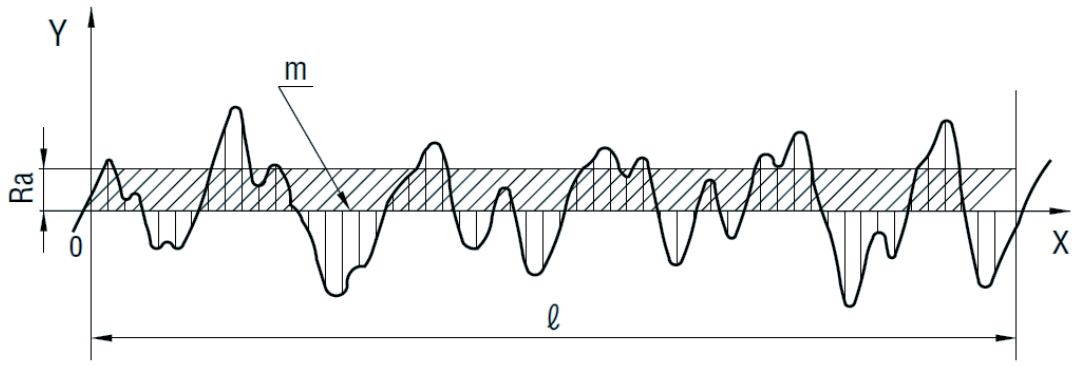

Figure 2-25 Indication of surface roughness using arithmetic mean roughness value (Ra)

$$R_a = \frac{1}{L}\int_0^L |y(x) - y_{avg}|dx \quad \text{..... (2–8)}$$

$$R_a = \frac{f^2}{18.\sqrt{3}.r\varepsilon} \quad \text{..... (2–9)}$$

where$f$ is the feed rate and$r\varepsilon$ is the nose radius of the cutting tool.Equation 2–9 clearly shows that the surface roughness increases with increasing feed rate and a large tool nose radius reduces the surface roughness of the workpiece. The principal parameters affecting the surface finish of turned components that have been widely recognized are the feed rate and the nose radius (Abrãoet.al., 2011).

Several papers have been published on surface finish produced by hard turning. Some of these reviews are presented below.

Rech and Moisan (2003)investigated the influence of feed rate and cutting speed on the surface finish of 27MnCr5 steel case hardened to 850 $HV_{0.3}$ when turning with PcBNinserts. They observedplastic flow caused by high temperature and pressure on the freshly machined surface. When machining at low cutting speed and feed rate, compressive residual stresses were induced and low surface roughness *R*a values below 0.2 µm were recorded on the machined surface. They concluded that feed rate isthe major parameter that influences the surface roughness,while cutting speed is the major parameterthat influences the residual stress level. Moderate surface roughness of Ra between 0.3 and 0.5 µm was reported by Lima et al. (2005) for low feed rateduring turning tests, using AISI D2 cold work tool steel (58 HRC) using mixed alumina inserts.

Grzesik and Wanat (2006) assessed the surface finish produced during hard turning of AISI 5140 (DIN 41Cr4) hardened to 60 HRC using mixed alumina cutting tool (conventional and wiper geometry) by comparing the roughness parameters produced. For conventional cutting tools with feeds between 0.04 and 0.4 mm/rev the values of Ra parameter changes from 0.24 to 5.47 µm, whereas a lower measure of roughness value was recorded for the wiper insert. The comparison curve is shown in Figure 2–26.Consequently, a better surface finish was obtained with the wiper ceramic cutting tool during finish hard turning of AISI D2 cold-work die steel (60 HRC), using the mixed alumina cutting tool with conventional and wiper geometry (DavimandFigueira, 2007; Gaitondeet al., 2009)

Similarly, the same cutting tool (mixed ceramics) was used for turning X38CrMoV5-1 steel hardened to 50 HRC (Fnideset al., 2008). They investigated the effect of feed, cutting speed, depth of cut and flank wear rate on the surface roughness produced. The authors observed an increase in surface roughness with increase in feed rate and flank wear, but there is no definite effect of depth of cut on the roughness, while the effect of increase in cutting speed only improved the surface roughness up to a certain point; the roughness value depreciated beyond this value owing to vibration of the tool.

Abrãoet al. (2011) investigated the influence of cutting tool materials (mixed-alumina, TiN-coated mixed-alumina tools) when turning case-hardened (66 HRC) DIN 19MnCr5 steel.

They noticed that the coated ceramic produced a better surface finish, probably owing to its superior wear resistance, which maintained the integrity of the cutting edge for a longer period.

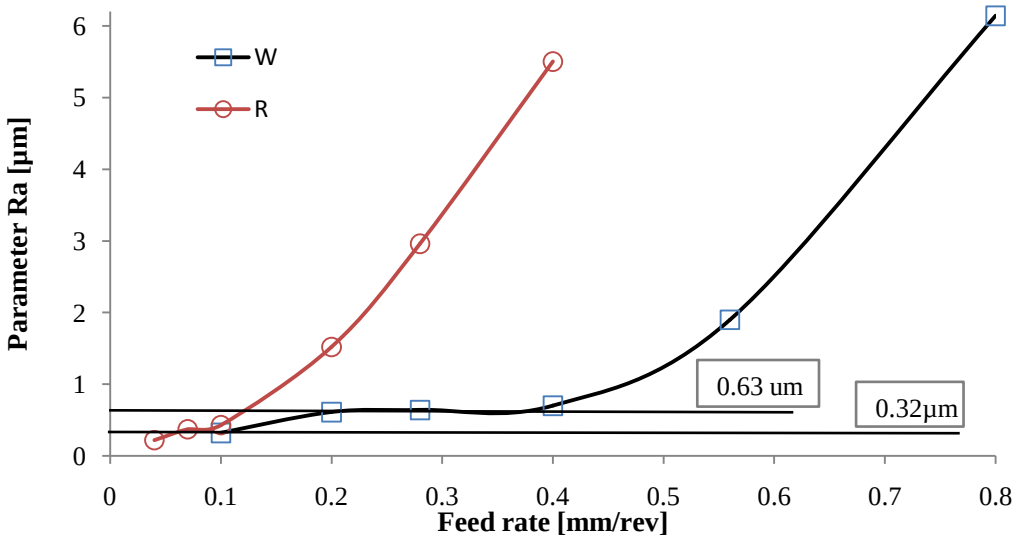

Figure 2-26Surface roughness produced by conventional (R) and wiper insert (W) (Adapted from Grzesik and Wanat, 2006)

Abraoet al. (1995) investigated the influence of PcBN (high and low cBN content) and ceramics (mixed alumina, whisker-reinforced alumina and silicon-nitride based) tool materials, and cutting speed on the surface roughness during finish hard turning of AISI H13 hot-work die steel withhardness of 52 HRC and AISI E52100 bearing steel (62 HRC). The authors found that the low cBNcontent and the mixed-alumina tools provided superior surface finish for both work materials with roughness value (*R*a) as low as 0.14 µm. This value was however achieved at cutting speed of 200m/min in the case of the tool steel and at 70 m/min for the bearing steel. During the turning of hardened bainite steel using a PcBN cutting tool at different cutting speeds, the best surface finish (*R*a = 1.7 µm) was achieved at a cutting speed of 170 m/min (Jacobson et al., 2002)

Avila andAbrao, (2001) carried out a comparison between the performance of different cutting fluids when turning hardened AISI 4340 steel (49 HRC) with mixed-alumina tools. The authors observed that, at high cutting speeds, the use ofcutting fluids resulted in lower scatter in the roughness of the machined surface. They concluded that emulsion cutting fluid produced better surface finish compared with the synthetic cutting fluid but, occasionally, dry machining produced much better surface finish.

Coelhoet al.(2004) investigated the surface finish of Inconel 718 (44 HRC) using ceramic and PcBN inserts with various geometries (square, round and triangular) and two edge preparations (sharp edge with chamfer of 20° × 0.1 mm and honed edge with chamfer of 15° × 0.15 mm). The round insert produced the lowest surface roughness values owing to its small radius (6mm). Consequently, the surface finish Ra produced by mixed alumina was lower than that achieved with SiCreinforcedalumina and PcBN tools, as well as when honed edge was used. Similarly, lower surface roughness was obtained by round inserts compared with square inserts, and inserts with honed edge in comparison with sharp and chamfered edges, during turning of the same material (at hardness of 35 HRC) (Arunachalamet al., 2004). The authors concluded that the poor surface finish obtained using chamfered tools was attributed to the higher cutting forces and, in the case of sharp tools, excessive chipping of the cutting edge.

Thamizhmaniiet al., (2008), investigated the turning of AISI 440C material (hardness between 45 and 55 HRC) using cBN tool. They deduced that the best cutting condition for producing surface roughness of 23 µm was a high cutting speed of 225 m/min with feed rate of 0.125 mm/rev.

Benga and Abrao (2003)adopted the surface response methodology in order to identify the optimal machining parameters that can produce lower surface roughness values when turning DIN 100Cr6 bearing steel(62 HRC) using mixed alumina, whisker-reinforced alumina and PcBN tools. They observed that the lowest feed rate resulted in lowest surface roughness, with roughness value (*R*a) of 0.25 µm. The optimum cutting speed ranging between Vc= 116 and 130 m/min was obtained for the mixed-alumina and PcBNinserts.At cutting speeds above this range, vibrations were generated impairing surface finish. However, the whisker-reinforcedalumina produced the lowest surface (cutting speed *V*c= 100 m/min), probably owing to the high tool wear rates observed when cuttingspeed was elevated, leading to rapid deterioration of the cutting edge.

The study of the influence of workpiece hardness on the surface finish on hardenedAISI 4340 with hardness of 42 and 50 HRC, machined with coated carbide and PcBN inserts respectively, showed that a PcBN tool produced the lowest roughness despite higher toolwear rate. This is attributed to the nose radius (r_{ε}= 1.6 mm) of the PcBN insert, which is larger than

that of the coated carbide (r_{ε}= 0.8 mm) and also higher cutting forces recorded when turning thesofter material with PcBN (Davim and Figueira, 2007).

Investigationson hardened materials on the surface roughness produced by milling (Elbestawiet al., 1997; Koshy et al., 2002) and drilling operations (Sharman et al.,2008) are also available in the literature.

2.9 DIMENSIONAL DEVIATION

In hard turning, high accuracy of the critical elements of the machine tool is of outmost importance in order to produce components parts with quality comparable to that obtained through grinding.

Compared to grinding operations, turning and milling can offer much higher metal removal rates with similar surface roughness values. However, equivalent dimensional accuracy is not readily achievable owing to the fact that single point cutting requires a minimum depth of cut, possibly because of elastic deformations of the machine tool and workpiece as a result of high cutting forces (Tönshoffet al., 1986). Consequently, the high cutting forces normally result in machine and cutting tool vibrations, thus leading to dimensional and geometric alterations (Almeida and Abrao, 2002).

It has also been reported that under favourable conditions PcBN and conventional ceramic cutting tools can achieve tolerances down to ±10 μm. Considering the maximum level of quality to be expected when using currently available lathes, geometric tolerances corresponding to ISO IT6 are normally achieved, and this tolerance level is considered insufficient to replace many grinding operations (Konig et al., 1993; Almeida and Abrao, 2002).

Some of the studies on the influence of cutting tool on dimensional tolerance during hard part turning are presented below.

Almeida and Abrão, (2002) investigated the possibility of achieving high dimensional accuracy by turning tests of AISI 5115 steel subjected tocarbonitriding (in order to reach a surface hardness of 66HRC) by comparing mixed alumina, coated mixed alumina and PcBN

with grinding. They made comparison of the dimensional deviation of the parts produced. In the study, the tolerance range of ± 0.05mm was adopted. For all the cutting tools, the tolerances of the machined components remained within the recommended range as expected by the authors, with the results obtained in case of mixed alumina being better compared to those obtained with the coated mixed alumina tools.

Regarding the dimensional tolerance produced after turning with PcBN and grinding with alumina wheels, a lower scatter was produced with the PcBN cutting tool but both processes produced deviation within the allowable range (see Figure 2–27). Regarding roundness and straightness deviations, tight tolerances where derived by both processes. The deviation values for turning against grinding operation are given as: 8µm against 18µm for roundness, and 4 µm against 11 µm for straightness.

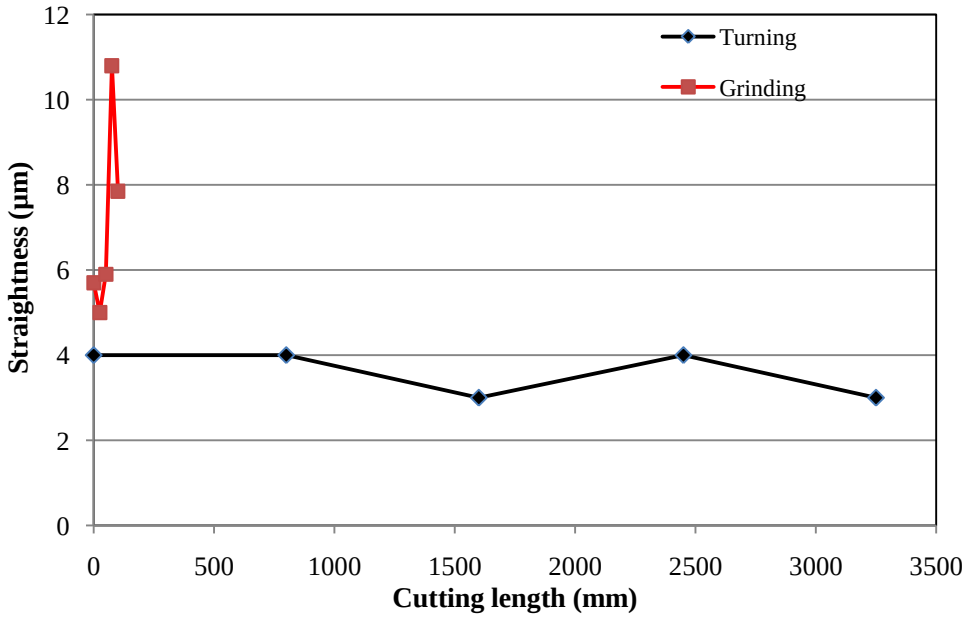

Figure 2-27 Dimensional deviation between PcBN turning and grinding (Adapted from Almeida and Abrão, 2002)

Matsumotoet al.(1999), compared hard turning with PcBN with grinding on the roundness deviation of bearing elements(58–62 HRC). They found that tighter tolerances were obtained with hard turning, owing to the accuracy of the machine toolsemployed, although the deviationsgenerated by both operations were within the component acceptable tolerance range.

Abrãoet al. (2011)investigated the influence of cutting tool wear on the geometric and dimensional deviation by conducting turning tests on case-hardened DIN 19MnCr5 steel using PcBN. The authors found that the dimensional deviation was within the acceptable tolerance level (IT5) at length of cut of 1600 mm but, after this point, the deviation increased drastically, as a result of the wear of the cutting tool. Regarding the geometric deviation, i.e. the roundness and concentricity, the tool wear had minimal effect on the roundness (minimum variation of 4 μm), while the effect was higher on the concentricity, thus increasing continuously with increasing cutting length. Figure 2–28 shows the effect of the cutting tool wear on the geometrical deviation.

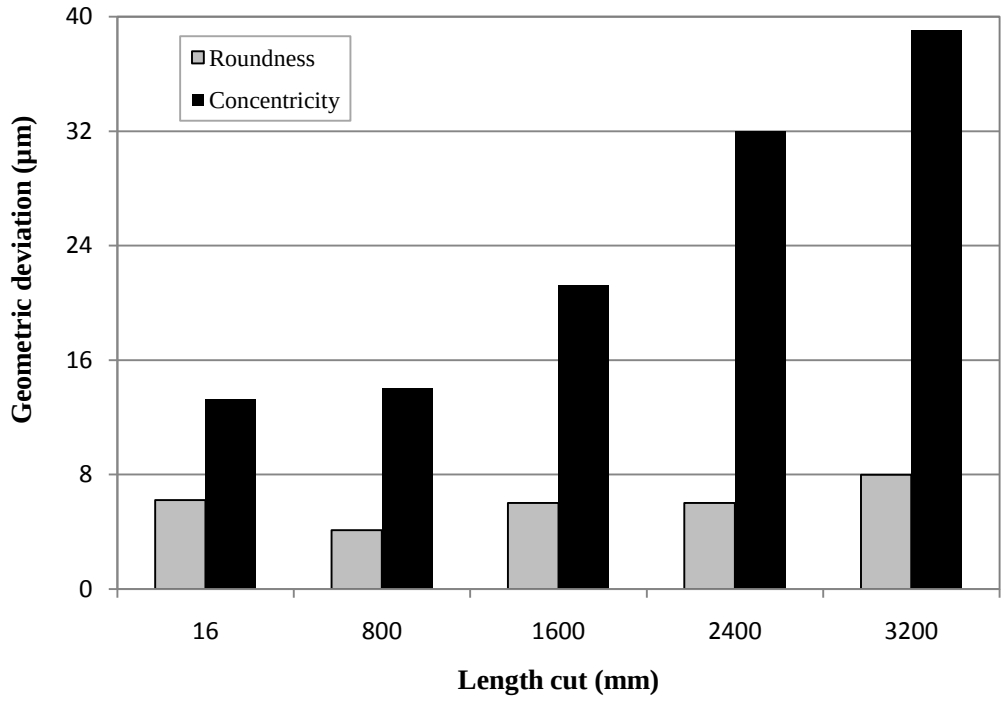

Figure 2-28 Effect of tool wear on the geometrical deviation using PcBN (Adapted from Abrao et al., 2011)

2.10 STATISTICAL METHODS

The Taguchi method is commonly used to optimise the cutting parameters in turning operations with surface roughness mostly used for investigating the effect of various process parameters on the product (Yih-Fong, 2006). Taguchi methods can be used for achieving high precision accuracy if process parameters are carefully controlled (Konig et al., 1993).

Yih-Fong (2006) studied the use of Taguchi on high dimensional precision cutting of hardened steels and reported that the most important control factors for dimensional precision of CNC turning process were: coatings, insert shape, and chip breaker geometry.

Other statistical methods, such as ANOVA and MRA, have been used for accessing the predominant factors for the wear of cutting tools and surface integrity of the hard turned parts (Kumar et al., 2006; Gopalsamy et al, 2009).

2.11 FIB-SEM

2.11.1 FIB SEM Equipment

The focused ion beam (FIB) instrument is becoming popular for specimen preparation in scientific and technological disciplines. FIB has simplified transmission electron microscopy (TEM) specimen preparation, with the huge potential in nanotechnology, micro-machining and tomographic characterization (Orloff, 2002; Giannuzzi and Stevie, 2005; Dacian and Pang, 2013). The easy preparation of site-specific cross-sections of any independent material is also possible with the FIB technique (Phaneuf, 1999; Jian, 2006). The semiconductor industry was first to apply the FIB technique (Wirth, 2009).

Giannuzzi and Stevie (2005) described the different FIB techniques that can be applied in material science. The description includes the lift-out technique, which was considered for this study.

Some major problems with conventional argon ion milling such as the poly-phase materials with different hardness, is overcome with FIB. TEM foil preparations are extremely challenging for inclusions in meteorites and the preparation of dust particles, but they are easily facilitated by the use of FIB (Lee et al., 2003; Graham et al., 2004).

The FIB device operates on a basic principle where sputtering atoms bombard the target materials with accelerated heavy ions. A high current density FIB from a liquid metal source such as gallium is used for milling micron-sized structures from integrated circuits (Puretz et al., 1984). Gallium has a low melting point of 29.8 °C. Solid Gallium metal is heated to its melting point and the melted Ga wets the tungsten needle after flowing to the tip of the needle by surface tension. At the end of the tungsten tip, a strong electric field of about 108 V/cm is applied and this causes the liquid Ga to form a point source (2–5 nm diameter), which extracts

ions from the narrow tip. The basic requirement of the sputtering process is an indication of the continuous flow of liquid Ga to the tip, replacing the extracted Ga^+ ions and resulting in a constant ion current (Wirth, 2009).

During bombardment of solid materials with gallium ions, the target material interacts with the ions, causing energy loss of the ions; there is momentum transfer from the incident ion to the target atoms as a result of elastic collision of the ions, which is called a sputtering process. During the sputtering process, there is an ion implantation caused by the incident Ga^+ ions losing their kinetic energy through collision. X-rays, secondary electrons, plasmons and phonons are produced as a result of inelastic scattering of the incident Ga^+ ions with the target material. In single beam FIB instruments, secondary electrons are used for imaging by collecting them with a continuous dynode electron multiplier (CDEM) detector (Giannuzzi and Stevie, 2005; Wirth, 2009).

2.11.2 FIB *ex-situ* lift-out of the TEM foil

FIB technique can be used to prepare electron-transparent membranes suitable for further TEM investigations. Possible investigations using these membranes include the following: electron diffraction, EEL spectroscopy, conventional bright- and dark-filed imaging, analytical electron microscopy (AEM), high-angle annular darkfield electron microscopy (HAADF), and high-resolution transmission electron microscopy (HRTEM). The process of the lift-out procedure is explained below.

It takes about 4hr to mill a standard TEM foil with typical dimensions of 15–20 µm× 10 µm× 0.150 µm. A thickness of approximately 80 nm can be achieved (Angseryd et al., 2009b).Before the milling process, a thin (1–2 µm) protection layer of platinum or tungsten metal is deposited onto the area of interest where the foil is to be cut.

During the final stage of the preparation with the foil thickness of less than 500 nm, the layer of the platinum metal is important because it protects the foil from being sputtered by the Ga^+ ion beam (Lee et al., 2007). The milling process usually starts at the front of the Pt-strip and another similar cut is made at the back of the strip.

The Pt-strip is completely cut through at the end of the foil preparation process, and the foil is ready for lift-out. The sample is then removed from the FIB device, after completion of the milling process (Lee et al., 2007; Wirth, 2009). A special manipulator is used for picking the lift-out of the foil from the excavation site, where electrostatic forces will attach the foil to the tip of the manipulator. Finally, the foil is attached to the standard TEM copper grid for TEM investigation.

2.12 TEM INVESTIGATION OF WORN cBN TOOL

Several papers have been published using the TEM for investigation of PcBN cutting tools materials microstructure (Walmsley and Lang, 1987;Klimenko et al., 1992; Benko et al., 2003;Rong and Yano, 2004;Weidow, 2005; Zhao and Wang, 2007; Gimenez et al., 2007; Flink et al, 2009;Angseryd et al., 2009b, Angseryd and Andren, 2011; Bushlya et al., 2013).

Authors reported that the sample preparation for PcBN material for TEM is difficult owing to crack formation and uneven thinning caused by high hardness and built-in stresses. In order to successfully perform energy filtered TEM (EFTEM) and electron energy loss spectroscopy (EELS) studies, very thin samples are normally required (Angseryd et al., 2009a).

Angseryd et al. (2009b) investigated the microstructure of the worn PcBN cutting tool after it was used for turning hardened steel (20NiMoCr65) using FIB combined with SEM and TEM. They observed a chemical reaction between the PcBN cutting tool and the work material, with an adherent layer from the work material on the PcBN. Some small amount of Al, was found in the adherent layer close to the cutting tool, and in the interface between the cutting tool and the adhered layer. They suggested that the Al was probably from the cutting tool material. The authors also found traces of Mn and Si close to the interface between the PcBN and the adhered layer but did not find elements such as B,N or Ti in the adherent layer.

The study by Flink et al. (2009), on worn ($Ti_{0.83}Si_{0.17}$) N coated sintered cBN insert after turning of case hardened steel, showed the presence of nitrogen from the cutting tool material in the adhered layer from the workpiece material, resulting from the chemical interactions between the coatings in the cutting tool and the workpiece. Formation of oxides on the rake face of the cutting tool result from the presence of oxygen picked up from the machining environment.

2.13 INDUSTRIAL APPLICATIONS OF CUTTING TOOLS

In metal cutting, three basic types of production are common. The basic types include: production of many small parts using different materials (job shop production), production of complex parts in small volumes, and mass production of complex parts in large volumes. In job shop production, general purpose and CNC machines are commonly used, where traditionally, only small volumes of complex parts can be produced. Today, the CNC machines are becoming popular for mass production of identical parts, typically carried out using specially designed machine systems. Automotive engines, transmission components, and military and aerospace components can be manufactured easily using the numerically controlled parts. For reliable and efficient machining operations with good surface finish and accuracy, the selection of the right tool geometries, cutting speeds, feed rates and depths of cut are essential, coupled with good control and tool monitoring systems (Stephenson and Agapiou, 2006).

2.13.1 Production machine tools

Production machine tools are used to perform one or more sequence operations requiring high volume identical parts, usually in thousands. Series of simple machines and mechanisms are used in the production process of obtaining the identical parts. During production, parts are normally transferred between stations using two basic classes of machines, conventional (inline) transfer machines and the rotary transfer machines (Boothroyd and Knight, 1989).The rotary transfer machine uses the rotary indexing (parts mounted are transferred by rotation via machining stations) and centre column systems. The centre column machines are used for heavy parts with the rotary transfer for the small and light parts production (Boothroyd and Knight, 1989; Rao, 2013).

The conventional transfer machines are designed to produce large volumes of single parts with long market cycle lives. These machines lack flexibility and in the event of breakdown of any of the stations, or tool changes, the entire system does not run (Stephenson and Agapiou, 2006, Rao, 2013).

2.13.2 CNC machine tools

These are advanced and numerically controlled machine tools useful for the production of complex parts. Cutting tools can be used simultaneously in complicated paths, in multiple axes motions (linear and rotary motions can be precisely controlled). The CNC is an economical machine for medium volume productions with consistent quality which ensures very minimal tool change (Stephenson and Agapiou, 2006). The basic component of these machines includes machine control units, programs of instruction, feedback devices and servo drives for each axis of motions (Jones and Bryan, 1987).Very complex shapes can be easily machined with the CNC depending on the number of machining centre axes. The development of CNC machines with multi-axes and multi-process workstation configurations makes high-speed manufacturing of precision parts such as complex aerospace components possible (Newman et al., 2008). Spindle speeds up to 40,000 rpm are possible with high-speed machining centres.

The CNC lathe has the ability to perform several machining operations, such as turning, facing, threading, cut-off, profiling and boring. Other operations, such as milling, drilling and tapping can also be achieved with the attachment of turrets equipped with additional powered spindles. Operations such as drilling, tapping and reaming can be performed using other machining centres (milling and boring machines) without the use of a CNC lathe. The performance of all the machining operations in a single step is now possible with hybrid machines which combine turning and other machining centres. Most conventional CNC machines have only three axes of motion, but higher axes machines (up to five axes) are also available. Some of the advantages of higher axes machines include maintaining high part precision, producing complex shapes and achieving higher productivity (Juneja et al., 2003; Bawa, 2004).

Several parts are combined to make up the production machine tool as listed below (Stepehnson and Agapiou, 2006).

- Machine tool structures
- Slides and guide-ways
- Spindles
- Coolant systems
- Tool changing systems (use of automate tool change systems).

2.14 ENABLING FACTORS IN THE MACHINE SHOP

In mass production of simple and complex components, the following factors are essential for good productivity and success in metal cutting: workpiece set-up, proper selection of cutting tools, effective coolants, machining condition optimizations (cutting speeds, feed and depth of cut), and tool changing sequences (Mookherjee and Bhattacharyya, 2001).

Workpiece clamping systems is one of the vital aspects in machining processes. Good choice of jaw and force for work clamping helps in reducing the effects of vibrations, ensure dynamic stability, part accuracy and consistency in the parts produced even after hundreds of pieces are already machined (Shao et al., 2013). In addition to this, machine rigidity, work holding rigidity, good damping characteristics, rigid cutting tools, and component part rigidity are part of the ideal machine used for hard turning.

The procedure for tool selection and optimization to ensure good productivity as designed by Kramer (1987) is shown in Figure 5–1. Selection decisions for cutting tool material are dependent on workpiece material, cutting tool characteristics, volumes of parts to be machined, types of production machines to be employed, surface integrity and the accuracy requirements of the final part (Mookherjee and Bhattacharyya, 2001). Carbide tools are mostly favoured in the machine shop for turning, milling, threading and boring using inserts owing to its numerous advantages, such as the low cost of inserts in comparison to some other tools, high transverse rupture strength, good hot hardness, and high fatigue and compression strength (Sales at al., 2009; Hallberg, 2010; Noordin et al., 2012). For high tolerance and surface finish, the work material is further subjected to grinding (Grzesik, 2008).

Good tool selection sequence provides means of optimizing the machining time, and this can be achieved by the experience of the machinist and also the shape requirements of the manufactured part (Lin and Yang, 1994). An important task in achieving an optimal machining sequence is the determination of optimal sequence cutting tools on the turret magazine of a CNC machine tool (Dereli and Fliliz, 2000). In turning operations, roughing operations are usually carried out first, and then followed by finishing operations.

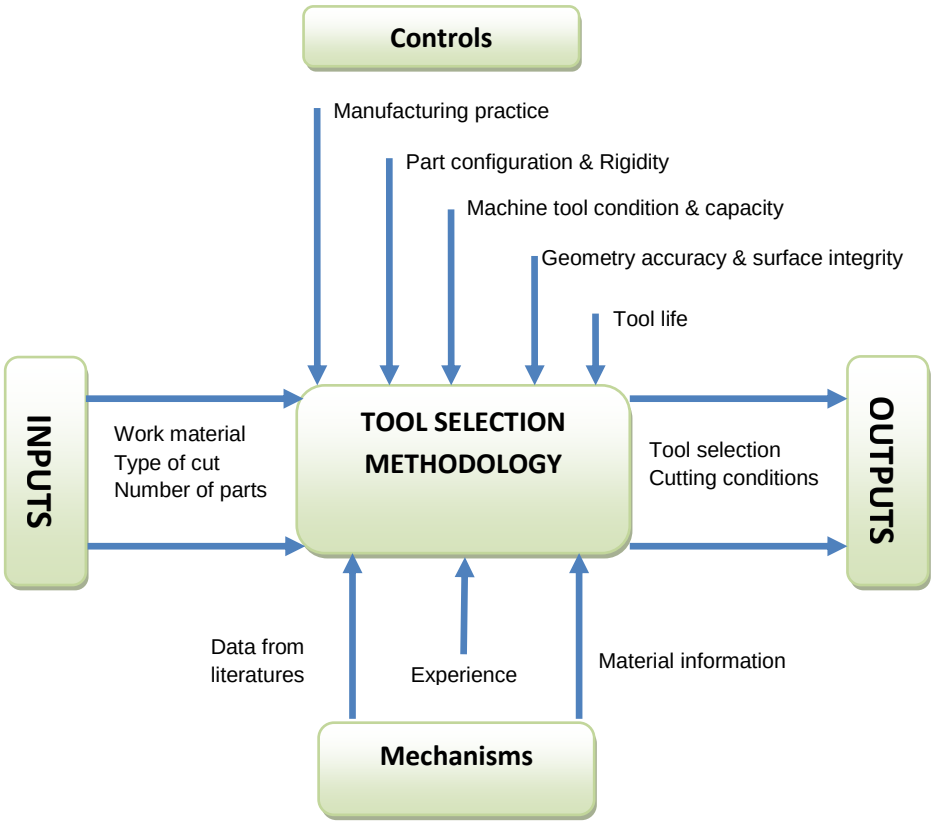

Figure 2-29 Tool selection procedure and optimization (Adapted from Kramer, 1987)

3 METHODOLOGY

3.1 WORKPIECE PREPARATIONS

The workpiece material was martensitic stainless steel AISI 440B (supplied by Bohler steel) widely used in engineering application, owing to its good mechanical properties as a result of its high chromium and carbon content. The carbon content is slightly lower compared to 440C stainless steel, in order to improve its toughness (Bramfitt, 2002). Its chemical composition in weight percentage is reported in Table 3–1.

Table 3-1Chemical composition of the AISI 440 B stainless steel in weight %

C	Cr	Mo	V	Si	Mn	Fe
0.9	17.5	1.10	0.10	0.45	0.40	Balance

The workpiece was through-hardened followed by tempering processes, which yielded a microstructure of tempered martensite to attain Rockwell hardness between 40 and 44 HRC. The workpiece was characterised for its microstructure and hardness. Its hardness was measured with a digital durometer (DM2-D 390). The properties of the martensitic stainless steel at 20°C are given in Table 3–2.

Table 3-2 Physical properties of AISI 440B stainless steel (Courtesy, Bohler steel)

PROPERTIES	VALUES
Density ($Kg.dm^{-3}$)	7.70
Specific heat ($J.Kg^{-1}.K^{-1}$)	430
Thermal conductivity ($W\ m^{-1}\ K^{-1}$)	15.0
Electric resistivity ($Ohm.mm^2.m^{-1}$)	0.80
Elastic Modulus ($X\ 10^3 N.mm^{-2}$)	215

For the microstructural investigation, conventional metallographic techniques were used for cutting, mounting(in Bakelite resin), grinding and polishing of the martensitic stainless steel samples. The stainless steel was ground with Silicon carbide paper (300–1200 grit, using water as lubricant, then polished using the finest particle size diamond paste and then etched using Villella's reagent (1 g picric acid, 4 mL HCl, 96 mL ethanol) to reveal its microstructure.

10 mm thickness from the workpiece material (300XØ50 mm) was cut for hardness testing, five different points were tested on the surface and the average was recorded for each test. The microstructure was first observed under the optical microscope (Olympus BX 41M)followed by a more detailed examination using the scanning electron microscope (SEM, Joel JSM 7600F).

3.2 EXPERIMENTAL PROCEDURES

Dry finish turning tests were performed on the martensitic AISI 440B stainless steel using two different cutting tools. The tools tested were commercially available cutting tools, PcBN (CBN–100) and Ceramics (CC 650), supplied by Seco Tools Inc. and Sandvik Coromant. The composition of each cutting tool is in Table 3–3 below. The properties of the cutting tools are presented in Table 3–4. In the context of this study, the CBN–100 term will be used for PcBN and CC650 will be used for the mixed alumina.

Table 3-3 Composition of cutting tools

Cutting tool	Supplier	Composition
PcBN (CBN-100)	SECO Inc.	cBN (50%)+TiC(40%)+WC(6%)+AlN,AlB_2(4%) average grain size of cBN is 2µm
Ceramics (CC 650)	Sandvik, Coromant	Al_2O_3(70%)+TiN(22.5%)+TiC (7.5%) average grain size of Ti(C,N) is 4µm

Table 3-4 Cutting tools properties (Kumar et al., 2006; Bushlya et al., 2014; Secomax, PcBN Technical guide)

Type of cutting tool	Al_2O_3+Ti (C,N)	cBN-100
Density (gcm^{-3})	4.15	4.28
Hardness (HV)	1800	3660
Thermal conductivity ($W\ m^{-1}\ K^{-1}$)	24	44
Transverse rupture strength (MPa)	550	-
Young Modulus (GPa)	440	587
Fracture toughness ($MPa\text{-}m^{1/2}$)	4.0	4.04
Coefficient of thermal expansion ($K^{-1}X10^{-6}$)	8.6	4.7

The machine used to conduct the turning tests was a CNC Turn Master LA 200 L Liouy–Hsing lathe, with a 14.72 kW power output, maximum speed of 4500 rpm and using a Fanuc O*i*-TB CNC controller. This lathe consists of a 3-jaw hydraulic chuck, an 8-position hydraulic turret and a hydraulic tailstock.

Cutting speeds selected for testing the cutting tools were in the range of 100 m/min to 600 m/min depending on the type of parameter investigated.Two depths of cut were selected for the experiments,0.1 and 0.2 mm, and three feed rates, 0.05, 0.1 and 0.15 rev/min.

The cutting conditions used for the experiments were appropriate for finish cutting and are given in Table 3–5.

Table 3-5 Turning conditions

Tool	**Mixed ceramic, PcBN**
Cutting speed, *Vc* (m/min)	100, 150, 200, 300, 600
Feed, *f* (mm/rev)	0.05, 0.1, 0.15
Depth of cut, *d* (mm)	0.1,0.2

The cutting tool inserts were secured onto a tool holder as shown in Figure 3–1. The tool holder in the experiments was CSDNN 2525 P09, which matched the insert types used (SNGN 090308S - 01020). The geometry angles of the inserts resulted in a rake angle of -6°, a back rake angle of -6°, a clearance angle of 6° and anapproach angle of 45°. The inserts were square shaped with 0.8 mm nose radius (honed, chamfer 0.1 mm x 20˚).

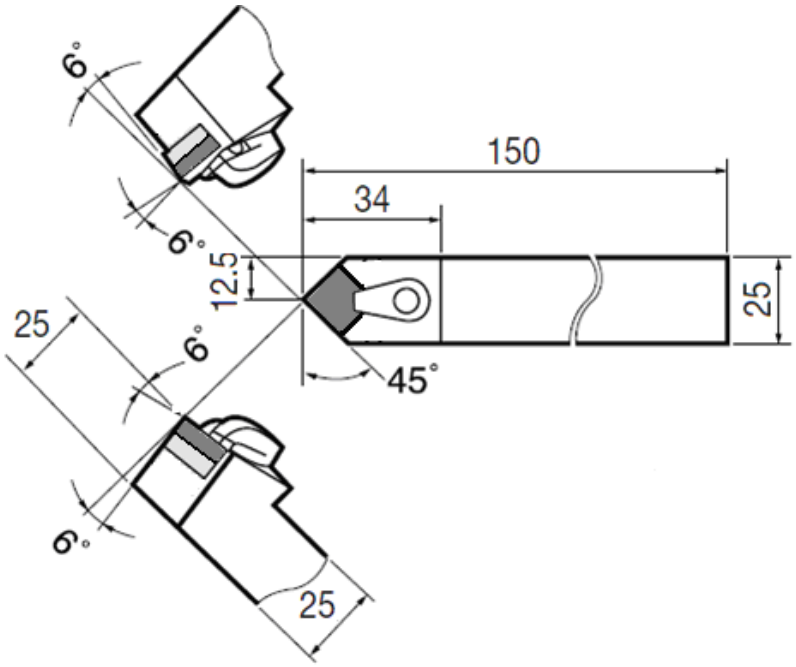

Figure 3-1 Tool holder specification (Courtesy, Katuku, 2009)

The diameter of the workpiece tested was 50 mm and the cutting length 200 mm. Before actual testing, the oxidized layer present on the workpiece surface was eliminated by removing a 1 mm thick layer of the material surface. Figure 3–2 shows the experimental set-up.

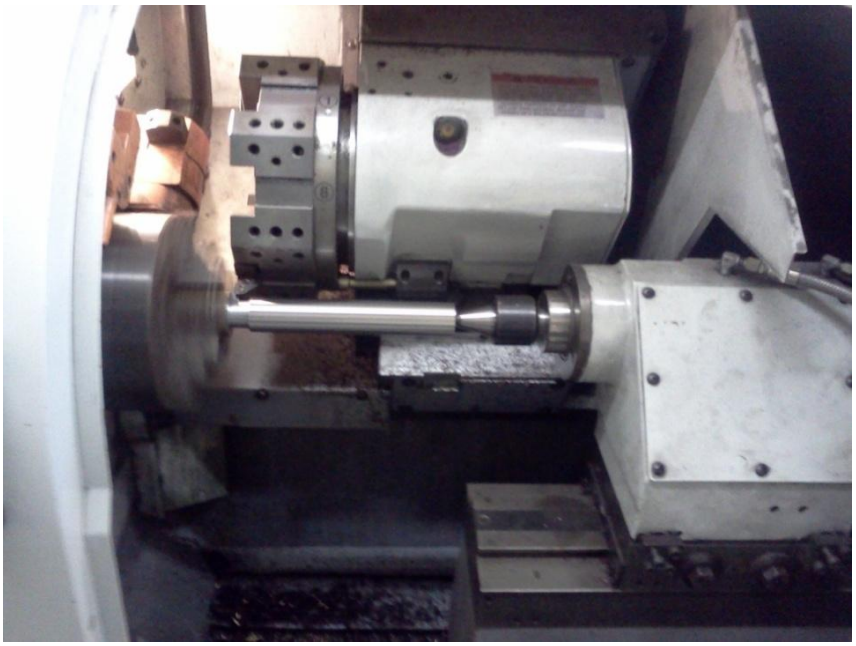

Figure 3-2 Machining experimental set-up

After turning over a certain cutting distance, the turning operation was stopped to allow the insert to be removed from the tool holder, and the flank and crater wear scars were observed under the optical microscope to measure the size of the flank wear scar; the average of three wear scar measurements was taken as the corresponding wear scar's width for that particular cutting length, time and speed. After the measurement, the insert was carefully replaced in the tool holder and the cutting operation resumed. This process was repeated till the tool wear criterion was reached.

Each cutting length was performed at least twice in order to ensure reproducibility and consistency of the results. The wear on the ceramics cutting tools was plotted together with that of the PcBN cutting tools in order to compare the wear resistance of the two types of tools.

Pass lengths were increased in steps and the cutting time corresponding with each pass length was calculated in order to plot graphs of flank wear against cutting time and flank wear against cuttingdistance for each cutting speed investigated. The cutting time t_c was calculated using Equation 3–1.

$$t_c = \frac{0.06\pi d_1 l}{V_s f} \ldots\ldots\ldots\ldots\ldots\ldots\ldots\ldots\ldots\ldots\ldots\ldots\ldots\ldots\ldots\ldots\ldots\ldots\ldots\ldots\ldots\ldots (3-1)$$

where: t_c refers to the cutting time in seconds, d_1 refers to the diameter of the workpiece in mm at the start of the cut, *f*, feedrate, *l* refers to the pass length (mm) and *V*s refersto the surface speed of the workpiece in m/min. The conversion factor of 0.06 allows for unit conversion to time in seconds by compensating for the set parameters with a different base unit, m/min, as opposed to mm per second.

The cutting time *t*(s) corresponding to a complete experiment was the cumulative time calculated from the total number of cuts *i* after each pass using Equation 3−2.

$$t = \sum_i t_i \ldots\ldots\ldots\ldots\ldots\ldots\ldots\ldots\ldots\ldots\ldots\ldots\ldots\ldots\ldots\ldots\ldots\ldots\ldots\ldots\ldots\ldots (3-2)$$

The cutting length $\boldsymbol{l_c}$ (mm) was calculated from the cutting speed *V* (m/min) and cumulative cutting time *t* (s) using Equation 3−3.

$$l_c = \frac{Vt}{60} \ldots\ldots\ldots\ldots\ldots\ldots\ldots\ldots\ldots\ldots\ldots\ldots\ldots\ldots\ldots\ldots\ldots\ldots\ldots\ldots\ldots\ldots (3-3)$$

The metal removal rate *MRR* (cm^3/min) was calculated from the feed f (mm/rev), cutting speed V (m/min), and depth of cut d (mm) using Equation 3−4.

$$MRR = Vfd \quad (3-4)$$

The volume of metal removed *MR* (cm^3) was calculated from the cutting time t (s) and metal removal rate *MRR* (cm^3/min) by using Equation 3−5.

$$MR = \frac{MRR.t}{60} \quad (3-5)$$

The tool wear was measured according to the ISO 3685:1993 standard,[1] and subjected to average flank wear width (VB_b) within the nose radius of the tool. The criterionfor cutting tool flank wear scar size states that a 300 µm wear scar is the point at which the cutting tool is no longer useful and cannot provide a good surface finish. However, for this study, the turning test was stopped when the flank wear scar size reached 200 µm.

The tool wear was evaluated using an optical microscope (Olympus BX 41M coupled to an Olympus Camedia Camera and connected to a computer using image analysis software AnalySIS®). The wear scars were inspected and analysed using anultra-high resolution field emission scanning electron microscope (SEM), Joel JSM 7600F, in order to understand the wear modes and mechanisms that affected the tool's performance. The cutting condition assumed for the experiments was a finish cutting. EDX analysis was used to confirm plastic deformation and adhesion based on the build-up of material on the flank and rake face. The optical 3D image of the machined surfaces was taken using an Olympus LEXT OLS410 3D laser measuring microscope.

[1]**Tool life testing with single-point turning tools, ISO Standard 3685:1993(E), 1993**

3.3 CUTTING FORCE MEASUREMENT

The three components of the cutting forces, radial force (F_r), tangential force (F_t), and feed force (F_f), were recorded using a standard quartz 3-component dynamometer (Kistler 9257B) equipped with Dynoware software (type 2825A 1-2) allowing measurements from -5 to 5 KN. The dynamometer has sensitivities of - 7.955 pC/N, - 7.95 pC/N and - 3.715 pC/N respectively for the x-axis, y-axis, and z-axis in the calibrated range 0-500 N. The multi-channel charge amplifier is shown in Figure 3−3.

Figure 3-3 Kistler multi-channel charge amplifier

Evaluation of the static and dynamic cutting forces corresponding to a specific time was obtained from the analyzed cutting force signals. The static cutting forces were estimated as the average of the signals, F_{r_i}, F_{t_i} and F_{f_i} as shown in Equations 3−6 to 3−8.

$$\bar{F_r} = \frac{1}{N}\sum_{i=1}^{N} F_{ri} \quad \ldots\ldots\ldots\ldots \quad (3-6)$$

$$\bar{F_t} = \frac{1}{N}\sum_{i=1}^{N} F_{ti} \quad \ldots\ldots\ldots\ldots \quad (3-7)$$

$$\bar{F}_f = \frac{1}{N}\sum_{i=1}^{N} F_{fi} \dots\dots\dots\dots\dots\dots\dots\dots\dots\dots\dots\dots\dots\dots\dots\dots. \quad (3-8)$$

where N is the number of cutting force data as recorded.

The dynamic cutting forces were estimated as the variation from the static cutting forces shown in Equations 3−9 to 3−11.

$$\bar{F}_{rd} = \sqrt{\frac{\sum_{i=1}^{N}(F_{ri} - F'_{ri})^2}{N}} \dots\dots\dots\dots\dots\dots\dots\dots\dots\dots\dots\dots\dots.. (3-9)$$

$$\bar{F}_{td} = \sqrt{\frac{\sum_{i=1}^{N}(F_{ti} - F'_{ti})^2}{N}} \dots\dots\dots\dots\dots\dots\dots\dots\dots\dots\dots\dots\dots.. (3-10)$$

$$\bar{F}_{fd} = \sqrt{\frac{\sum_{i=1}^{N}\left(F_{fi} - F'_{fi}\right)^2}{N}} \dots\dots\dots\dots\dots\dots\dots\dots\dots\dots\dots\dots\dots.. (3-11)$$

The force signals were obtained over the period of time taken to cut one pass on the cutting length (200 mm) on the workpiece. The variations of the cutting forces associated with the tool wear on a single pass were recorded till end of the tool life of the cutting tool. The influence of adhesion of chips on the rake face, and chip segmentation on the cutting forces, were detected by analyzing the dynamic cutting forces.

3.4 SURFACE ROUGHNESS MEASUREMENT

Instantaneous roughness criteria measurements (arithmetic mean roughness, Ra), for each cutting condition, were obtained by means of a Bondetec roughness meter. The length examined was 3 mm with a basic span of 0.8 mm. Maximum measurable values for Ra and Rt

were 40 and 160 mm respectively. This roughness was directly measured on the workpiece held between the chuck and tailstock, along the length of the bar, without dismounting from the lathe, in order to reduce uncertainties owing to resumption operations. The measurements were repeated three times at three reference lines equally positioned at 120° from each other on the surface of the workpiece, and an average of these values was taken as the result. The optical 3D image of the OD was taken using an Olympus LEXT OLS410 3D laser measuring microscope.

3.5 CHIPS

3.5.1 Chip analysis

Chip formation mechanism plays an important role in determining cutting forces, specific shearing energy consumed in the deformation process and the resulting surface generation mechanism. Figure 3−4 shows the systematic approach used to analyse the chips generated during the hard turning operation for this study. The chip morphology was observed using the optical microscope (Olympus BX41M), followed by an analysis of chip segmentation frequency and of the chip forms (revealing the presence of saw-tooth chips).

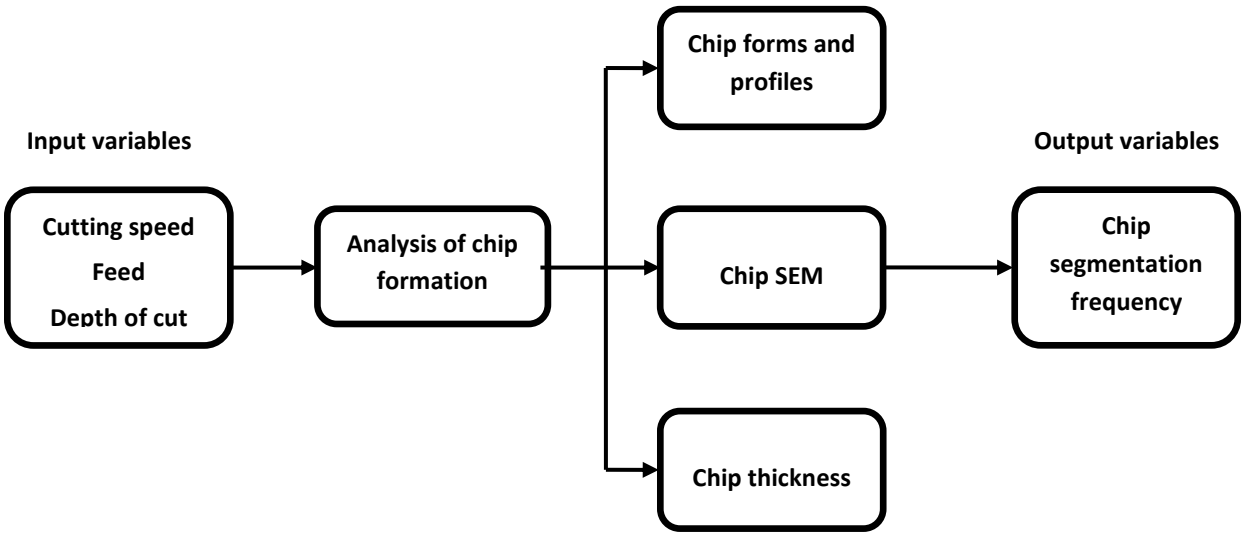

Figure 3-4 Chip analysis

The experimental output variables for this investigation are: chip dimensions, which include pitch of the chip outer surface profile (the maximum and minimum height), chip thickness ratio measurement and SEM morphology of the chips. Optical and SEM microscopy

micrograph were used to analyse the variables. The obtained data were used for developing a chip formation modeland the determination of the chip segmentation frequency. The chip thickness ratio was determined from the measured chip thickness as well as the chip width using the optical microscope.

Small straight segments (5 mm length) of the chips were cut from the ones produced during the turning tests and used as sample preparation to determine the chip segmentation related parameters. These chip segments obtained were embedded in a resin mouldin a hot mounting press. The chip samples were mounted so that the transverse section in the X-X direction (shown in Figure 3–5) was exposed for the measurement. The chip mounts were first ground manually with water using waterproof SiC papers(grit 320 to 1000), and later, cloth polishing of the mounted samples (using 1 μm diamond paste) was carried out to obtain a scratch-free surface. The chips were very thin; therefore the polishing was carefully done to reveal the chip cross-section of interest. For microstructural examination of the chips, the mounted and polished chip was etched with a Villella's reagent for 10 seconds. The etched chip samples were observed under the ultra-high resolution field emission scanning electron microscope (Joel JSM 7600F) also to reveal the details on a transverse facet of the chip morphology and microstructure.

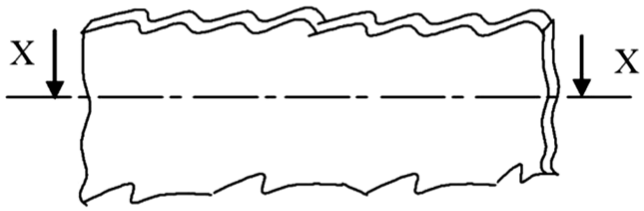

Figure 3-5 Schematic view of chip cross section

The chip morphology was monitored to capture the range of cutting speed atwhich the transition from continuous to shear-localized chip formation occurred. The morphologyof the upper- and underside of chips was investigated without any preparation toassess qualitatively the tribology atthe tool–chip interface, particularly with regard to the temperature at this interface.

3.5.2 Characterization of chip formation

The characterization of the continuous chip is expressed as the chip deformation (shear strain and the shear strain rate). The chip ratio (r) and other related parameters, namely deformation angle (φ), chip speed (V_{ch}), shear speed (V_{sh}) and shear strain (γ) can be calculated from the chip thickness (t_c) (see Equation 3–7).

$$r = \frac{t_c}{t} \quad \ldots \ldots \ldots \ldots \ldots \ldots \ldots \ldots \ldots \ldots . (3-12)$$

where t is the uncut chip thickness, given as $f \sin K_r$ (Astakhov., 2006), K_r is the cutting edge angle.

The shear angle φ can be derived from Equation 3-8.

$$\tan \varphi = \frac{\cos \gamma_n}{r - \sin \gamma_n} \quad \ldots \ldots \ldots \ldots \ldots \ldots \ldots \ldots . (3-13)$$

whereγ_n is the rake angle and V_c the cutting speed. The chip speed V_{ch} is given by Equations 3–9, and shear speed by Equation 3–10.

$$V_{ch} = \mathrm{V_c} \frac{\sin \varphi}{\cos(\varphi - \gamma_n)} \quad \ldots \ldots \ldots \ldots \ldots \ldots \ldots \ldots . (3-14)$$

$$V_{sh} = \mathrm{V_c} \frac{\cos \gamma_n}{\cos(\varphi - \gamma_n)} \quad \ldots \ldots \ldots \ldots \ldots \ldots \ldots \ldots . (3-15)$$

The shear strain γ and shear strain rate $\dot{\gamma}$ and the thickness of the shear zone s are given in Equations 3–11, 3–12 and 3–13 respectively.

$$\gamma = \frac{\cos \gamma_n}{\sin \varphi \cos(\varphi - \gamma_n)} \quad \ldots \ldots \ldots \ldots \ldots \ldots \ldots \ldots . (3-16)$$

$$\dot{\gamma} = \frac{\gamma \mathrm{V_c} \sin \varphi}{s} \quad \ldots \ldots \ldots \ldots \ldots \ldots \ldots \ldots . (3-17)$$

$$\mathrm{s} = \frac{\mathrm{h}}{5.9 \ \sin \varphi} \quad \ldots \ldots \ldots \ldots \ldots \ldots \ldots \ldots . (3-18)$$

The characterization of the serrated chips is expressed as frequency of serration, deformation of serrated chip and degree of segmentation. The frequency of serration F, is given by

Equation 3–14 as the number of segments produced per unit time, where d is the pitch of serrated chip (see Figure 3–6).

$$F = \frac{V \sin \varphi}{d} \quad \ldots \ldots \ldots \ldots \ldots \ldots \ldots \ldots \ldots \ldots \ldots \ldots \ldots \ldots \ldots \ldots \ldots \ldots \ldots \ldots \ldots \ldots \ldots \ldots \ldots \ldots . (3-19)$$

The degree of segmentation *G* can be calculated from Equation 3–15.

$$G = \frac{(h_1 - h_2)}{h_1} \quad \ldots \ldots \ldots \ldots \ldots \ldots \ldots \ldots \ldots \ldots \ldots \ldots \ldots \ldots \ldots \ldots \ldots \ldots \ldots \ldots \ldots \ldots \ldots \ldots \ldots . (3-20)$$

where h_1 is the higher part of the chip and h_2 the height of the continuous part of the serrated chip as shown in Figure 3–6.

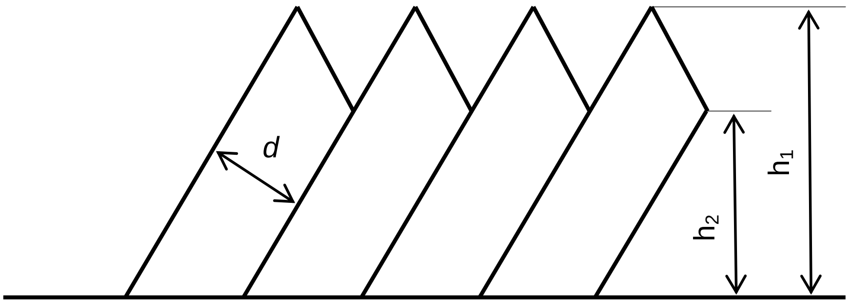

Figure 3-6 Serrated chip illustration

The degree of segmentation of the serrated chip is usually different from that of segmented chip when observed by metallurgical examination (He et al., 2002; Qibiao et al., 2012). The serrated chip is therefore transformed from the continuous chip, and the model of serrated chip formation is shown in Figure 3–7.

The serrated chip deformation in terms of the shear strainγ_{se} and shear strain rate$\dot{\gamma}_{se}$ is given in Equation 3–13 and Equation 3–14 respectively. The chip length, measured from different points is shown in Figure 3–7.

$$\gamma_{se} = \frac{2h|l_{EF} \sin \varphi - h|}{d(l_{EF} + l_{GH})^2 sin^2 \varphi} \quad \ldots \ldots \ldots \ldots \ldots \ldots \ldots \ldots \ldots \ldots \ldots \ldots \ldots \ldots \ldots \ldots \ldots \ldots \ldots \ldots \ldots . (3-21)$$

$$\dot{\gamma}_{se} = \frac{4h^2V|l_{EF} \sin \varphi - h|}{d^2(l_{EF} + l_{GH})^2 sin^2 \varphi} \quad \ldots \ldots \ldots \ldots \ldots \ldots \ldots \ldots \ldots \ldots \ldots \ldots \ldots \ldots \ldots \ldots \ldots \ldots \ldots \ldots . (3-22)$$

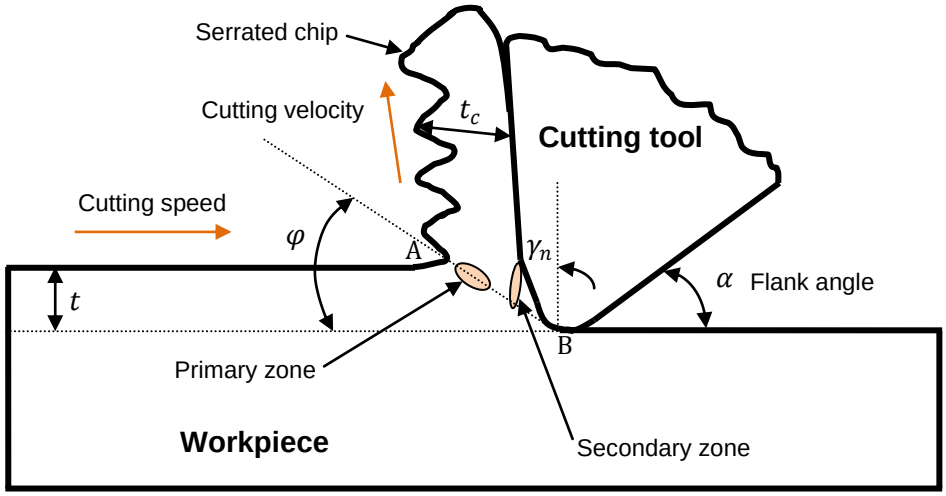

Figure 3-7 Serrated chip model formation

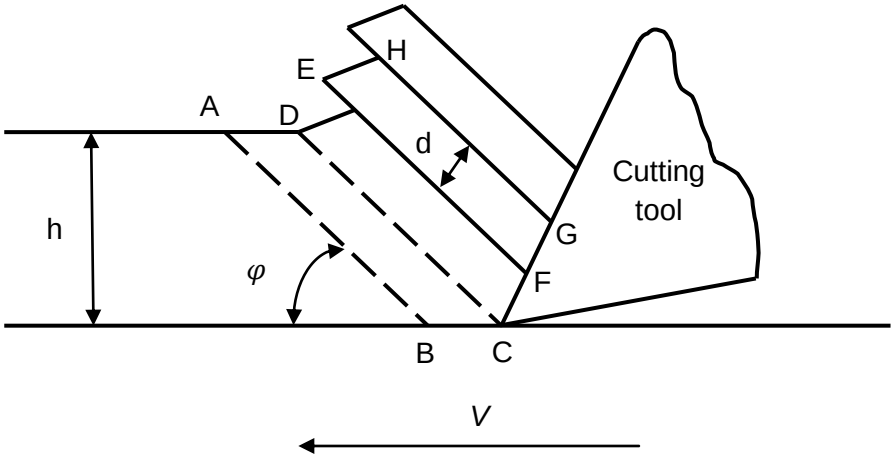

Figure 3-8 Measurement of chip length

3.6 SAMPLE PREPARATION FOR TEM

The preparation of thin foil specimens was done using a lift-out technique in the FIB-SEM. The instrument used for obtaining the lamella from the cutting tool rake face was a Carl Zeiss AURIGA® cross-beamFused ion beam Scanning electron microscope (FIB-SEM) workstation with a GEMINI FE-SEM column (Carl Zeiss, Germany). The macro-manipulator used on the FIB-SEM was a Nano Control NC40 (Kleindiek Nanotechnik, Germany).

Thin foils were obtained from the worn cutting tool samples and observed under the transmission electron microscope.

The thin foil samples were taken fromacross the crater formed on the rake face close to the cutting edge of the worn PcBN tool. The difficulty associated with using conventional means of sample preparation methods, where cutting lubricants are applied during cutting and polishing, are easily overcome using the FIB-SEM, most especially in the area of this study where anadherent layer is formed on the cutting tool edge. It is possible to avoid bigger detrimental impact on the sensitive surface layers, resulting from the use of a spark cutter for cutting PCBN materials (Angseryd et al., 2009b).

The cBN cutting tool samples were inserted in the FIB-SEM where the *in-situ* lift-out was performed. An electron assisted platinum deposition was done, followed by a thicker ion assisted Pt deposition, in order to protect the surface of the area of interest on the rake face of the tool,and to enable the welding of the lamellae on the microprobe. Pt deposition used as a protective layer is about 400 nm thick.

Milling and polishing were carried out with gallium ions. Two trenches were milled on both sides of the Pt layer using a high current of Ga ions, then the material beneath and on the sides of the specimen was milled leaving the specimen hanging ontwo thin strips on the sides. The accelerating voltage used for milling was 30 kV and the milling currents were varied: 4nA for coarse milling and 600 pA for fine polishing. The sample was later transferred to a Cu-grid using a micromanipulator (Omniprobe^{TM}) tool after milling and lift up from the cutting tool. The final step was thinning the specimen to electron transparency. Final polish was done with a 20 pA beam current. The high voltage used during milling causes some Ga ion implantation, re-deposition, and amorphous layer formation, which has a negative effect in the TEM analyses, especially at higher magnifications. The specimens were cleaned with Argon ion milling, using Gatan 691 Precision Ion Polisher System (PIPS) to reduce the problems on the surface. The SEM micrographs showing the lift-out procedure in steps are shown in Figure 3–9.

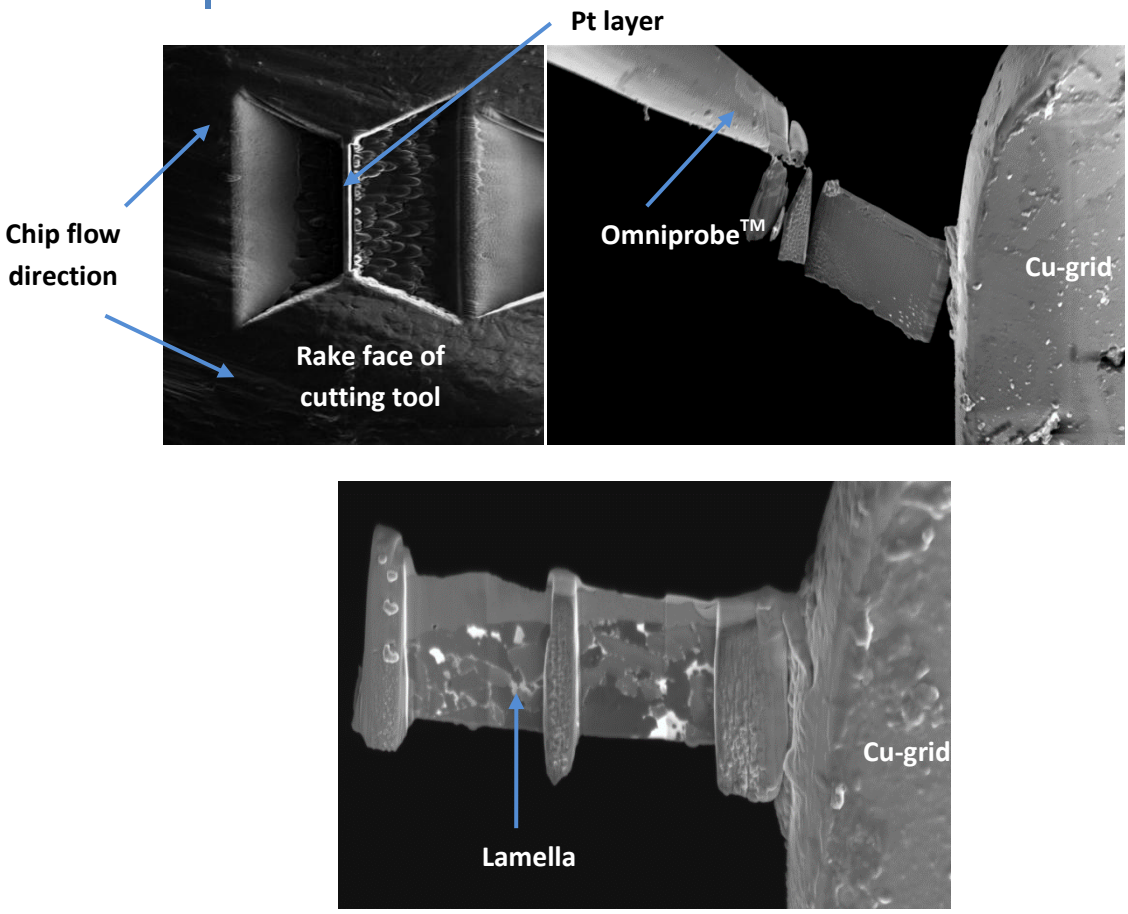

Figure 3-9 The step-by-step procedureduring the lift-out of the lamellae in the FIB-SEM: (a) Pt deposition on the site of interest and then cutting the side trenches and preparing for lift-out, (b) lamellae attached to the micro manipulator partially attached to the cupper grid and then cut loose, (c) the final the sample is attached to a copper TEM grid.

3.7 SCANNING ELECTRON MICROSCOPE (SEM)

The microstructure of the cutting tools (CBN-100 and CC 650), workpiece, worn inserts and chips were studied using the ultra-high resolution field emission scanning electron microscope (SEM), Joel JSM 7600F, equipped with an EDAX energy dispersive spectroscope (EDS), and WDS and EBSD analyzersconnected to a computer. Energy-Dispersive X-ray (EDX) point analysis was conducted on all specimens while EDX mapping was conducted for the thin foils obtained during lift-out. The SEM used for evaluation is shown in Figure 3–10.

Figure 3-10 Scanning electron microscope

3.8 TRANSMISSION ELECTRON MICROSCOPE (TEM)

Information about chemical composition (analytical electron microscopy AEM) and structural information (crystal structure) of a solid sample material in a nano-meter scale can be investigated using the transmission electron microscopy (TEM).
Three different techniques are used for obtaining the chemical information about the sample. They are energy dispersive X-ray analysis (EDX), high-angle annular darkfield imaging (HAADF), and electron energy-loss spectroscopy (EELS) (Williams and Carter, 1996).

Utilizing the EDX system of the microscope, chemical information may be obtained from the excited characteristic X-rays of the specimen. Element mapping and line scans with very high spatial resolution (a few nanometres) can be generated from a thin, homogeneous foil.

EELS is based on the acquisition of a spectrum of the inelastic scattered electrons and it is a complementary technique to EDX analysis (Williams and Carter, 1996; Brydson, 2001).

High angle annular darkfield (HAADF) detectors are used for imaging in the scanning transmission mode (STEM) of the microscope by collecting elastically and in-elastically scattered electrons. Images with very high resolution at atomic scale are generated using the high-resolution transmission electron microscopy (HRTEM).

TEM investigations require electron-transparent specimens (about 200nm in thickness) depending on the acceleration voltage of the microscope.

The lamella that was cut using the FIB-SEM was observed using a JEOL JEM 2100 High Resolution TEM, with a LaB_6 cathode. TEM was operated at 200 kV to view the lamella. Images were captured using a Gatan Ultrascan camera and Digital Micrograph software.

The TEM investigations involve: imaging, EDX, and Scanning TEM (STEM). The EDX was performed as EDX point analysis.

4 RESULTS AND DISCUSSION

4.1 WORKPIECE MATERIAL

Five different points were tested on the surface of the work material and the average was recorded for the hardness test. The results from the Vickers hardness test were converted to Rockwell using a conversion chart.

The average hardness of the workpiece material obtained was 430.1±13HV ≈ **43±13 HRC**

The SEM micrograph of the microstructure of the etched hardened stainless steel is shown in Figure 4–1a, EDX spectra of the martensite and carbides in the workpiece are shown in Figures 4–1b&c, and the XRD pattern is shown in Figure 4–1d. From the SEM micrograph, the microstructure comprises carbide precipitates in the tempered martensite of the workpiece. The carbides are seen in the form of spheroidal and elliptical shapes, while the martensite grains are needle-like in shape. The work material had undergone tempering and hardening by the supplier at temperatures of 538 ˚C and 1038 ˚C respectively (Bohler steel). Generally, the microstructure of martensitic stainless steel contains carbides such as M_7C_3, $M_{23}C_6$ and M_2C after tempering, where M represents Cr, Fe, Mo, V or other carbide-forming elements (Zheng-Fei and Zen-Gou, 2003; Bhadeshia and Honeycombe, 2006; Verhoeven, 2007; Salleh et al., 2009, Bushlya et al., 2014). The large complex primary carbide particles in the martensitic matrix of the AISI 440 B stainless steel were identified as $M_{23}C_6$ carbides based on the carbon chromium phase diagram and by EDS analysis of the carbides showing a high chromium carbide. The compositions of the carbides were analysed using EDS and they show a composition of 38at.% Cr, 24at.% Fe, 1.3at.% Mo, and fractional percentages of V and Ni. The complex cubic $M_{23}C_6$ carbides are the chromium rich carbides as confirmed by EDS results and as already reported in the literature (Salleh et al., 2009). The EDX shows the high peaks for Cr and Fe in the microstructure of the work material. The X-ray diffraction (XRD) used for identifying the phases in the workpiece microstructure is shown in Figure 4–1d. The result shows the FeCr Phase as predominant phase in the material which was confirmed by the EDX report.

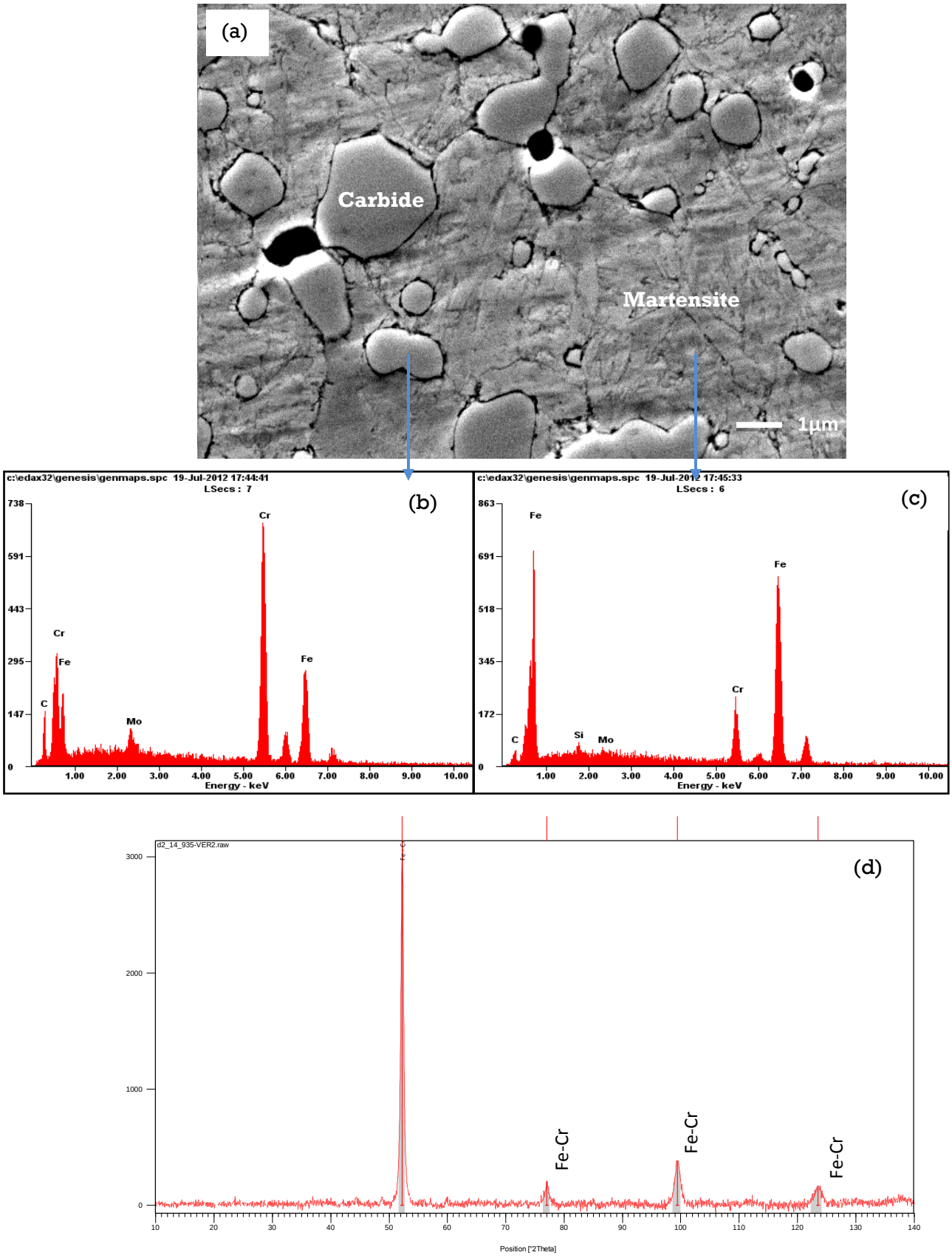

Figure 4-1 SEM, EDAX and XRD micrograph of etched martensitic stainless steel sample

4.2 CUTTING TOOL MATERIAL

The SEM micrographs and EDS spectra of selected spots in these micrographs of the received CBN-100 and CC650 cutting tools are shown in Figures 4–2 and 4–3 respectively. The EDS spot analysis confirmed the composition of the cutting tool inserts as supplied by the manufacturers. The microstructure of CBN–100 cutting tool (Figure 4–2a) shows two major interpenetrating uniformly dispersed continuous phases, namely cBN and TiC. The cBN grains are the dark phase whereas the TiC is the light grey phase. Also WC grains are seen as bright grey grains and the TiB_2 or Al-based phase appeared as dark grey grains in some areas within the microstructure. The EDS spot analysis confirmed the presence of these phases (see Figure 4–2b). The average cBN grain size was measured and found to be about 2 µm, which confirmed the information contained in the supplier's data sheet (SECOMAX). Similarly in Figure 4–3a the micrograph and EDS overall spectrum of CC650 cutting tool material is shown. In this, dispersed phases of Al_2O_3 and TiC/TiN are seen; the Al_2O_3 is seen as grey phase while TiC/TiN appears as a lighter one. Small traces of Tungsten carbide grains seen as bright grey phase were found in the microstructure of CC650 tool.

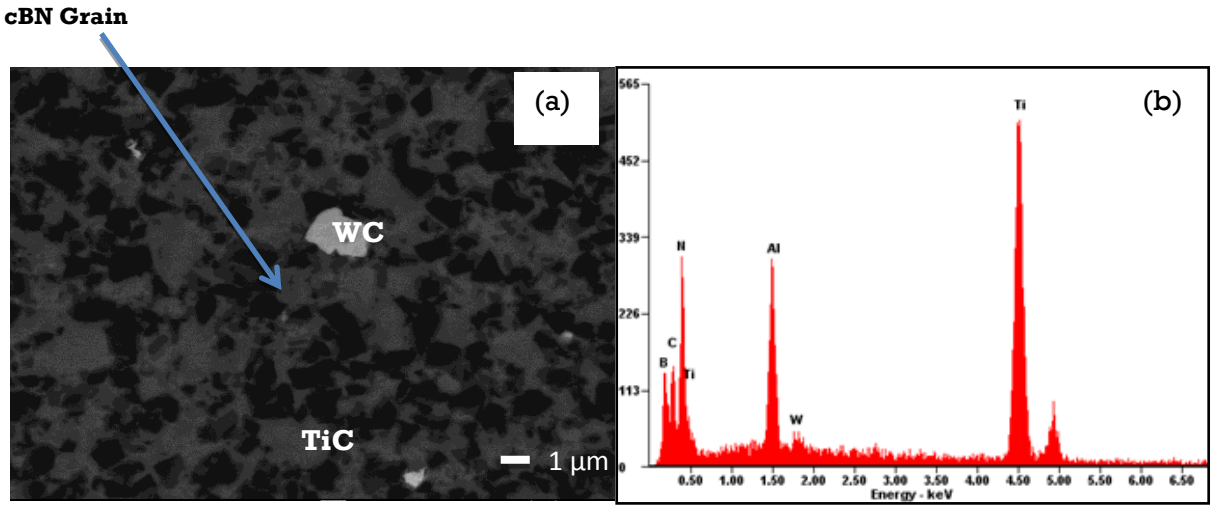

Figure 4-2 SEM micrograph and overall EDS spectrum of received CBN-100 cutting tool insert from SECO Tools

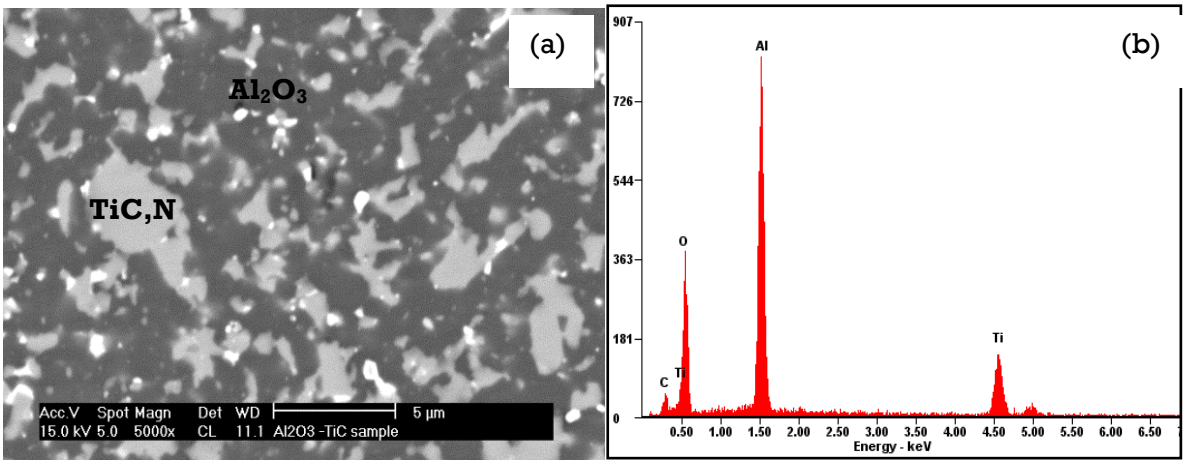

Figure 4-3 SEM image and overall EDS spectrum of received ceramic insert with composition of Al_2O_3 and TiC

4.3 MACHINING RESULTS

4.3.1 Tool wear

The turning tests carried out in this work are used for determining the evolution of different types of tool wear mechanisms operating at machining conditions that vary with respect to cutting speed, feedrate and depth of cut. In high speed machining, wear at the rake face of the cutting tool is more predominant. Thus, the tool life is determined by flank wear. Figure 4–4 shows the variation of the size of the flank wear scar (V_B) with cutting time with cutting speed as the parameter (100, 150 and 200 m/min) for CBN–100 and CC650. The tests were conducted at the feed rate of 0.1 mm/rev and depth of cut of 0.1 mm. The experiments were repeated three times under identical machining conditions. Similarly, Figure 4–5 shows the flank wear as a function of cutting length. From Figure 4–4, the time taken for CC650 to reach allowable maximum flank wear was 56 minutes, compared to about 261 minutes with CBN–100 when cutting at 100 m/min. This is about 5 times longer cutting time. Similarly, at the same cutting speed about 5 times more material is removed using CBN–100 (see Figure 4–5).

The results show that the flank wear increases with increasing cutting speed for both cutting tools. Generally, the tool life of any cutting tool is greatly affected by the cutting speed, thus the most significant factor affecting the tool life during machining of hardened steel (Poulachon et al., 2004; De Godoy and Diniz, 2011). CBN–100 however showed better wear resistance for all the cutting speeds; this is owing to its higher fracture toughness and the

ability to retain its hardness at elevated temperatures (higher hardness at both low and high temperatures), and thus it can withstand the high temperature generated at the tool–chip interface. For the ceramic cutting tool, at the tool–chip interface, the cutting temperature is very high resulting from the cutting speed, the layer on the tool face becomes soft with more accelerated wear, since the flank face can be easily abraded by the hard particles in the work material.

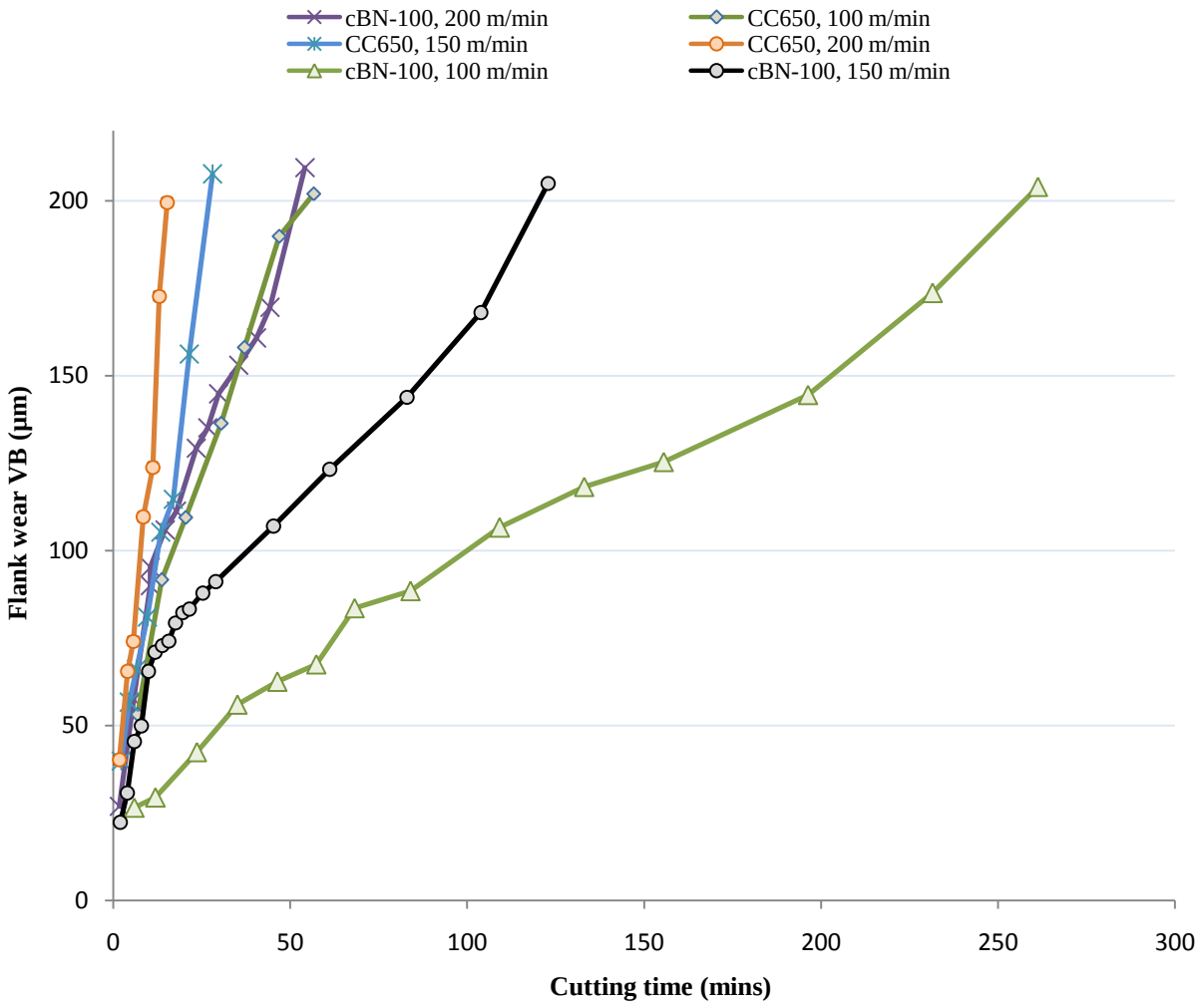

Figure 4-4 Evolution of flank wear at cutting speeds of 100, 150 and 200 m/min in relationship to cutting time

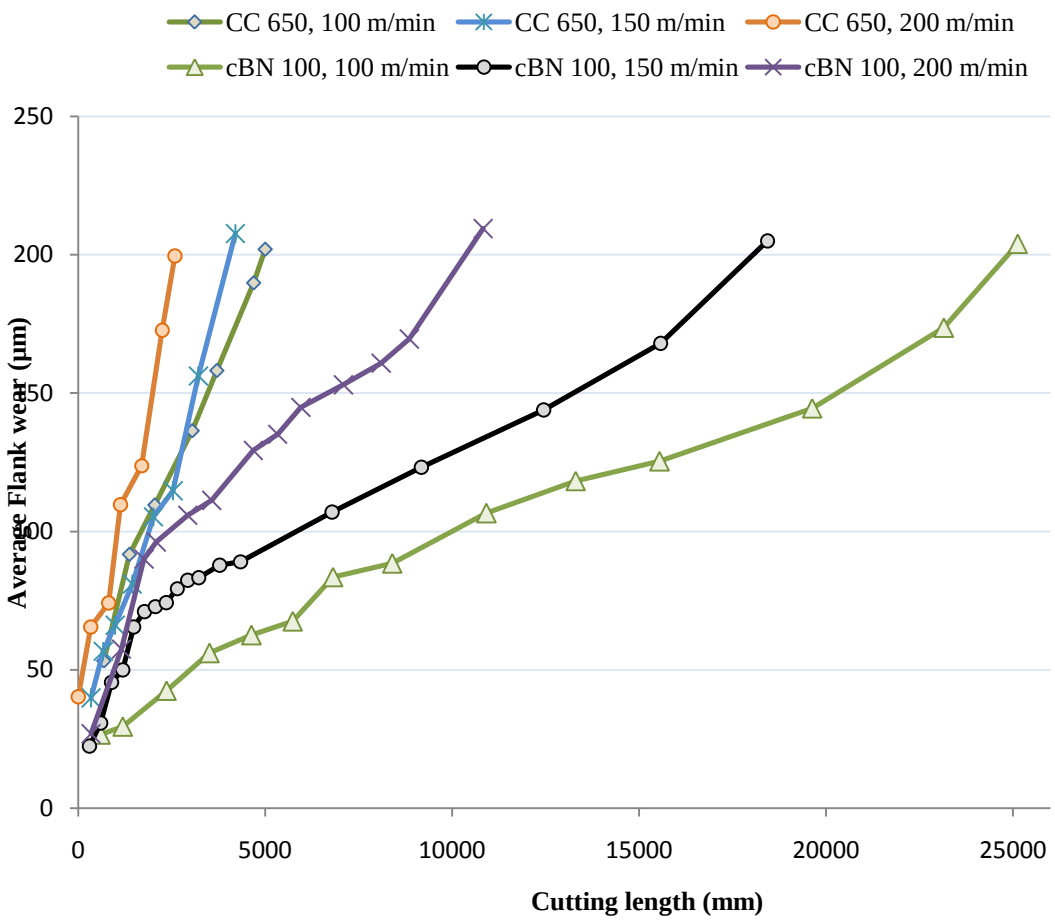

Figure 4-5 Evolution of flank wear at 100, 150 and 200 m/min in relationship with cutting length

At very high cutting speed (600 m/min), with the same feed rate and depth of cut as used in the previous experiment, rapid tool wear is experienced by both cutting tools. At this cutting speed, CC650 wear grew very rapidly and catastrophically from the initial cuts, and the workpiece finally collapsed by rupturing of the cutting edge at a machining time of 2.62 minutes as shown in Figure 4–6. In the case of CBN–100, there is excessive wear of the tool flank only towards the end of the tool life, though the cutting tool failure was also rapid as shown by severe chattering of the cutting edge.

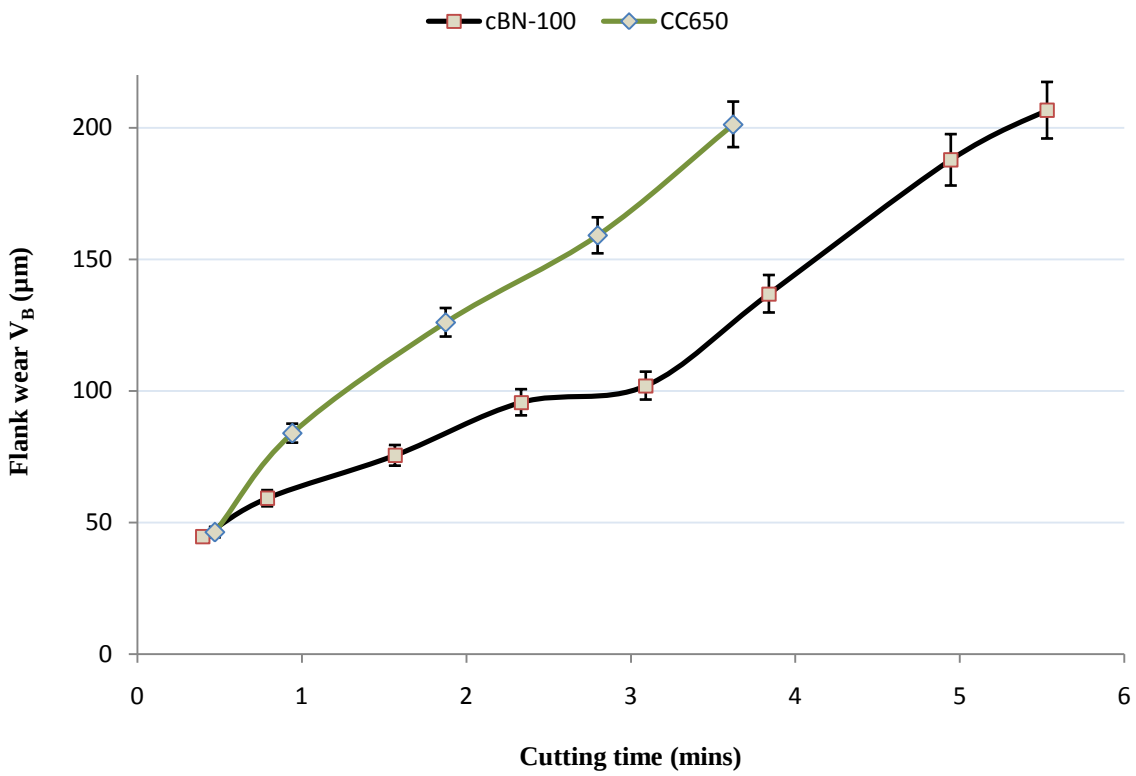

Figure 4-6 Flank wear at cutting speed 600m/min, feed rate=0.1 rev/mm, DOC=0.1 mm

The ratios of volume of metal removed per unit of flank wear for CBN–100 and CC650 are shown in Figure 4–7. The ratio of the volume of metal removed per unit of flank wear is assumed to be constant with time. This metric decreased rapidly with increasing cutting speed up to about 300 m/min, and more slowly at higher speeds. The amount of material removed by the cBN cutting tool is considerably higher than the CC650 cutting tool at speeds below 300 m/min. At higher cutting speeds beyond 300 m/min, the volume of material removed by cBN is relatively close to that removed by CC650, and at 600 m/min the volume is lower. This is owing to the rapid tool wear of the cBN tool at this cutting speed, where it is not able to handle excessive vibration as a result of its lower fracture resistance compared to mixed alumina (See Table 3-4). The recommended speed range for a high ratio of metal removed per unit flank wear is speeds below 200 m/min. However, for good surface quality, higher cutting speeds are recommended, where the surface roughness obtained at higher cutting speeds were better than the ones obtained at lower speeds.

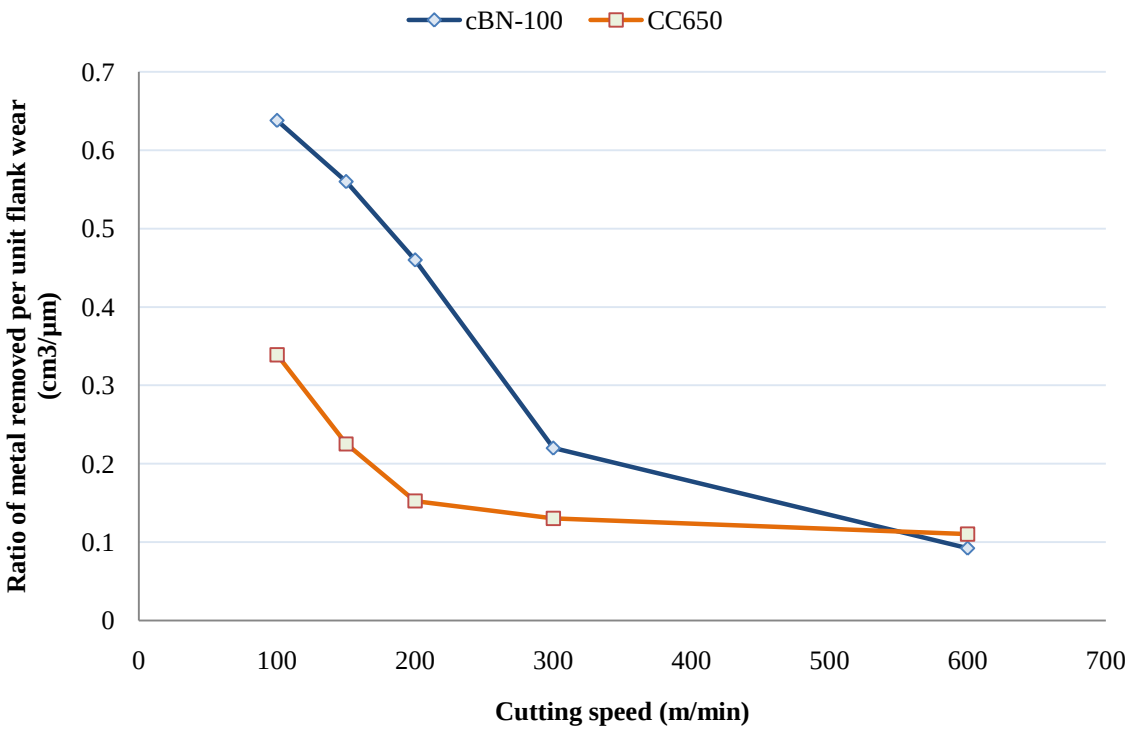

Figure 4-7 Effect of cutting speed on the ratio of volume removed per unit flank wear

The lives of both cutting tools at selected cutting speeds (100–600 m/min), feeds of 0.1 rev/mm and depth of cut of 0.1 mm are shown in Figure 4–8. This diagram shows the dramatic effect of the cutting speed on the cutting tool wear. It can be seen in Figure 4–8 that when the speed increases from 100 to 200 m/min, the tool life of CBN-100 decreased rapidly, but above the cutting speed of 200 m/min, the rate of decrease in the tool life with cutting speed was lower. A similar observation was made with the CC650 cutting tool. The CBN–100 exhibit much longer tool lives than CC650 cutting tools, as expected.

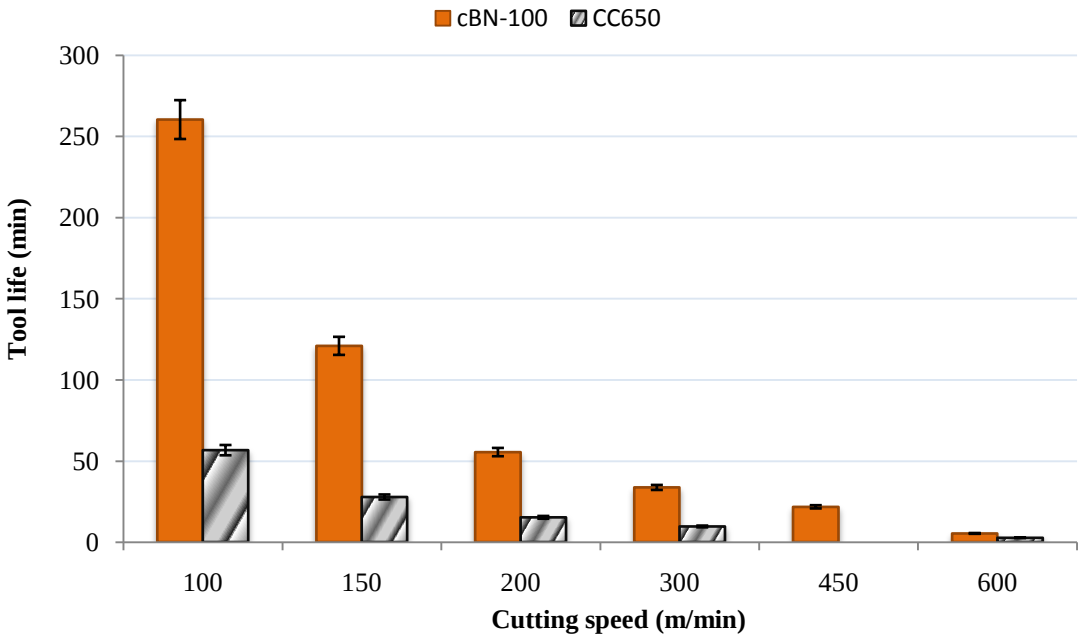

Figure 4-8 Average tool lives for CBN-100and CC650 cutting tools

Generally the feed rate has a direct influence on the productivity, quality and efficiency of machining. The increase in the feed rate normally increases the wear of any cutting tool, as long as the cutting speed and depth of cut are kept constant, thus having the effect on the parameters as listed earlier (Astakhov, 2006). Figures 4–9 and 4–10 show the flank wear as a function of cutting length for CBN–100 and CC650 respectively, with feed rate as the parameter. It is seen that the flank wear decreases with increasing feed rate for the CC650 cutting tool. When machining with CC650, there is a significant effect of feed rate increase on the wear rate, most especially with feed of 0.15 mm/rev. More material can easily be cut within the shortest time interval, while the wear rate improves. For the CBN–100 tool, the flank wear decreases initially with an increase in the feed from 0.05 to 0.1 mm/rev, and later increases with the feed of 0.15 mm/rev. The decrease in the tool wear is probably owing to the depth of the cold working material which is less than the uncut chip thickness, thus the tool wear rate decreases with the increase in the feed (Astakhov, 2006).The high tool wear experienced using CBN–100 at 0.05 mm/rev is as a result of tool vibrations. Often, increasing the feed rate reduces the intensity of vibrations that take place in machining, thus there is a reduction in the tool wear rate. The increase in the feed rate usually changes the ratio of the radial and axial forces that increases the dynamic rigidity of the machine tool (Markarow, 1976). It is generally believed that an increase in the cutting feed leads to an increase in the tool wear (Childs et al., 2000). However, as observed in this study, the reverse of this

phenomenon is observed when using the CC650 cutting tool; this could be a result of the cutting speed used for machining (100 m/min), which is relatively low; the actual cutting temperature at the cutting zone is lower than the optimal cutting temperature of the cutting tool.

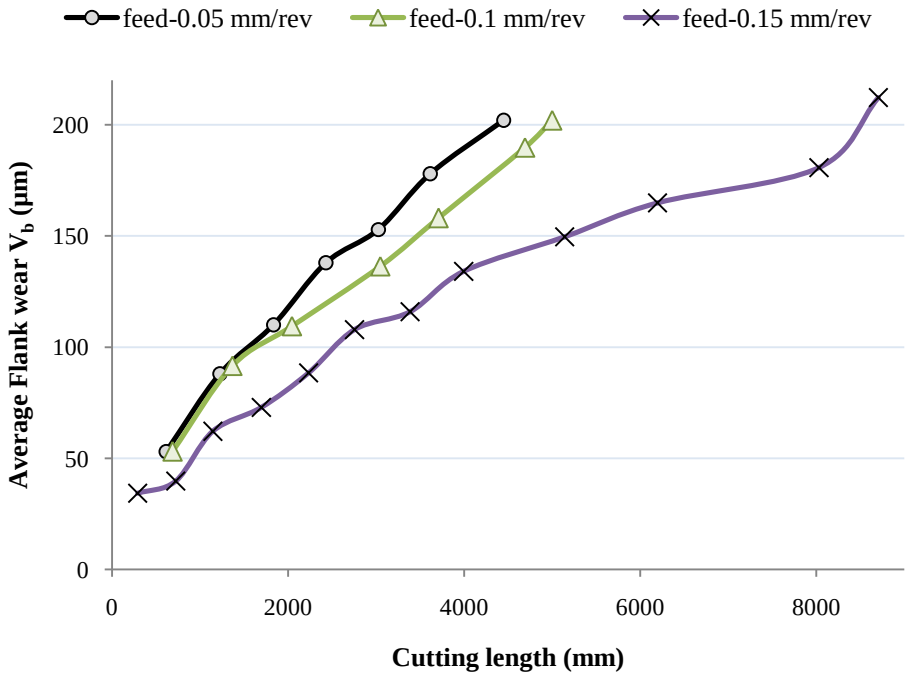

Figure 4-9 Effect of feed rate on tool wear for CC650, speed, 100 m/min, DOC 0.1 mm

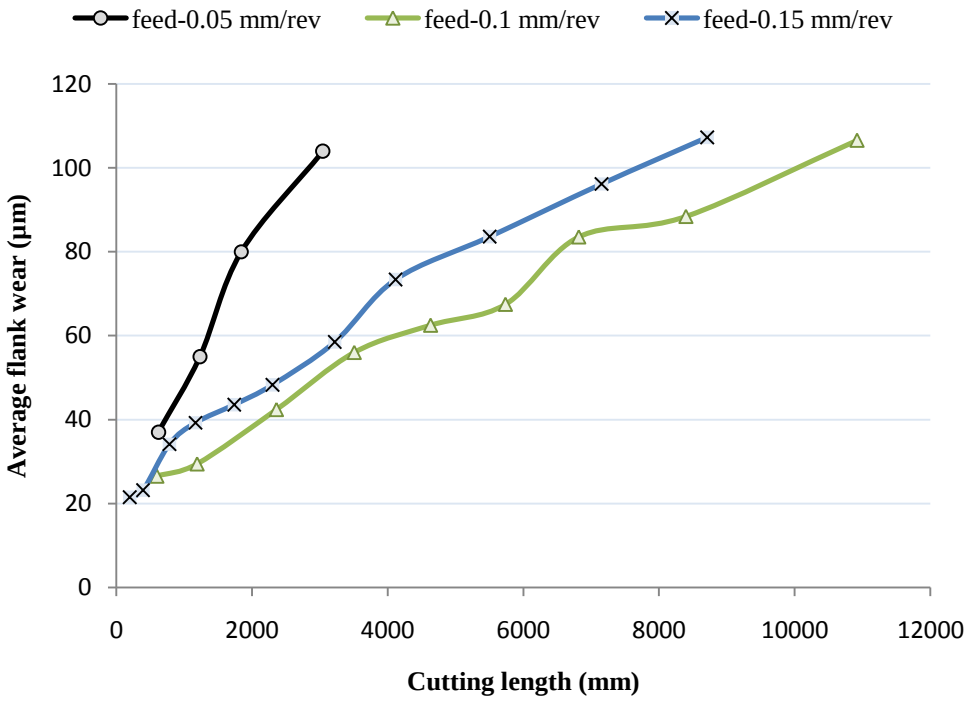

Figure 4-10 Effect of feed rate on tool wear for CBN-100, speed, 100 m/min, DOC 0.1 mm

The effects of depth of cut on the flank wear as a function of the cutting time for CBN–100 are shown in Figure 4–11. The flank wear increases with increase in the depth of cut, but the rate of increase is less significant when compared to the effect of increase in the cutting speed on tool wear rate. As seen in Figure 4–11, lower wear rate was recorded with depth of cuts of 0.2 mm initially compared to depth of cut of 0.1 mm, but after certain cutting distance and time (20 minutes), the wear rate increased.

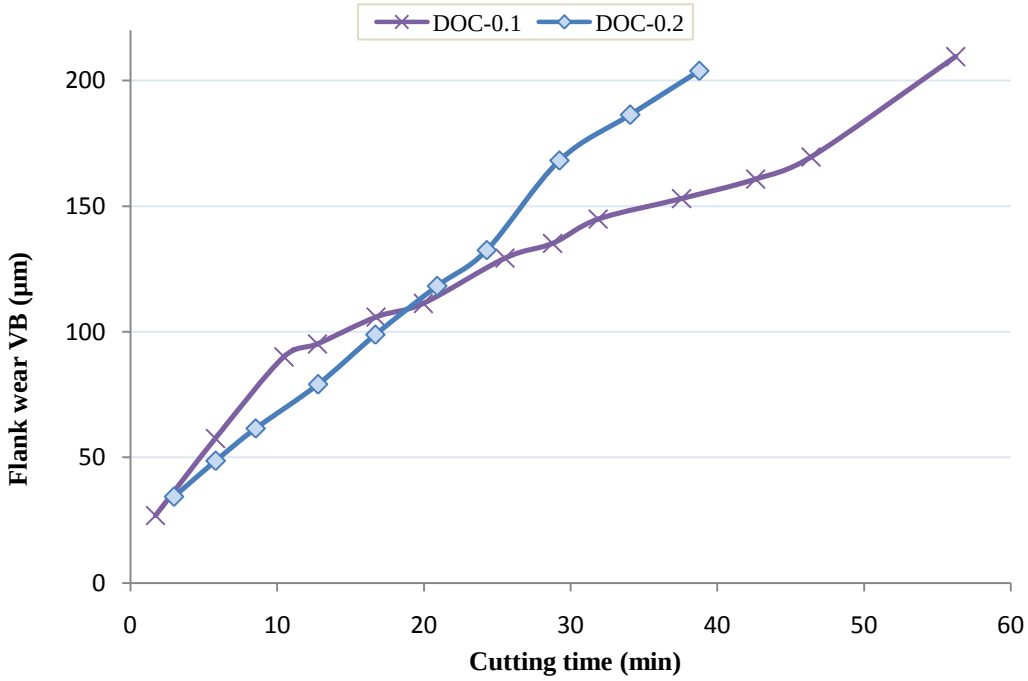

Figure 4-11 Effect of depth of cut on tool wear for CBN-100, speed 200 m/min, feed 0.1 mm/rev

In general, the CBN–100 cutting tool showed a better performance in all the cutting conditions investigated owing to its superior wear resistance and ability to retain its strength at higher cutting temperatures, but at low feeds the tool wear for PcBN is very high, probably as a result of its lower toughness. Therefore it cannot withstand high machine vibration with small feeds. However, for both cutting tools, the feed of 0.1 mm/rev recommended because of the moderate flank wear and better surface finish obtained at this feed by the cutting tools. There is a high impact loading on the tribological system, which is caused by micro and macro grooves on the workpiece surfaces, accompanied by a high temperature at the chip–tool interface. The high cutting temperature generated at the chip–tool interface, resulting from high speeds and feeds, leads to the accelerated tool wear of the CC650 owing to the

decrease of its hardness, poor thermal shock resistance and low fracture toughness (Lo Castco et al., 1993).

The results from the wear study clearly showed that the cutting speed had the most significant influence on the tool wear compared to the feed rate and depth of cut. The increase in the cutting speed for instance from 100 m/min to 150 m/min (See Figure 4–8), there is a drastic reduction in the tool life of the cutting tool, whereas, the increase in both feed and depth of cut shows slight influence in the tool wear for both mixed ceramics and cBN cutting tool. Based on the result of the tool wear study, the machining parameters recommended for machining hardened martensitic AISI 440 B is cutting speed of 100–150 m/min, depth of cut of 0.1 mm and feedrate of 0.1 mm/rev.

4.3.2 Wear mechanism of cutting tool

Figures 4–12 and 4–14 show the optical micrographs of CBN–100 and CC650 respectively. Figures 4–13 and 4–16 show the SEM micrographs of CBN–100, while Figures 4–15 and 4–18 show the corresponding SEM micrographs for CC650. All of these figures refer to the worn surfaces of the two cutting tools tested in this work. The EDS information of the rake face is shown in Figure 4–16 for CBN–100 and Figure 4–18 for CC 650 tools respectively. The SEM figures show cutting tool flank face and rake face when machined at cutting speed of 100 m/min. The most dominant wear modes, in both cutting tools, easily seen on the SEM micrographs, are the flank and crater wear. Abrasive wear mechanism is more predominantly observed for both cutting tools on the flank face but is moderate at the chip–tool interface on the rake face. Other wear mechanisms such as chipping, adhesion and plastic deformation were also observed on the cutting tools.

Figures 4–12 (a–f) clearly show smooth abrasive wear (marks parallel to the cutting direction) on the flank face. At the cutting speed of 200 m/min, the abrasive marks are coarse as a result of higher friction at the work material–cutting tool interface, compared to machining at the speed of 100 m/min. The grooves formed on the flank face of the CBN–100 tool result from the detachment of cBN grains from the bond caused by the hard particles ($M_{23}C_6$) in the work material. Smooth wear is normally observed with this particular cutting tool when cutting hardened steel as a result of the small feeds. The rubbing between the contacting surfaces of

the cutting tool and the workpiece and the high temperature at the chip–tool interface, create the environment where diffusion can take place in the cutting tool; however, because of this mode of wear, there is a possibility of chemical interaction between the cutting tool and the workpiece material. This wear phenomenon is normally reported when machining hardened steels using PcBN (Chou and Evans, 1997; Hasan and Thamizhmanii, 2010; Lahiff et al., 2007).

There is evidence of grooves on the top surface of the flank face at a cutting speed of 100 m/min at initial cuts, and this is later covered by adhered, plastically deformed material. The clearance face of the cutting tool at this speed shows brittle chipping. At feeds of 0.05 mm/rev, evidence of chipping on the clearance face was clearly observed. When the feeds and speeds were further increased, the chipping was reduced. On the rake face, at the cutting speed of 100 m/min, there is evidence of built up edge, moderate abrasion (cratering), and adhesion with transferred layer as observed during machining with the CBN–100 cutting tool, shown in Figures 4–16b and c. The adhesion of the workpiece material on both the rake face and flank face of CBN-100 cutting tool at elevated temperature and stresses, causes adhesive wear of the tool, This form of wear is mostly common at medium cutting speeds. The EDS information of the rake face of CBN-100 tool in Figures 4–16d and 4–17 respectively, shows evidence of Cr and Fe of the work material adhering on the both rake and crater face of the cutting tool. The adhered material consists of the constituents from the workpiece material with elements such as, Fe, Si, Cr, Mn and oxygen introduced during oxidation. From Figure 4–18c, there is evidence of grain pull-out from the cutting tool, which is carried away from the flank face.

\

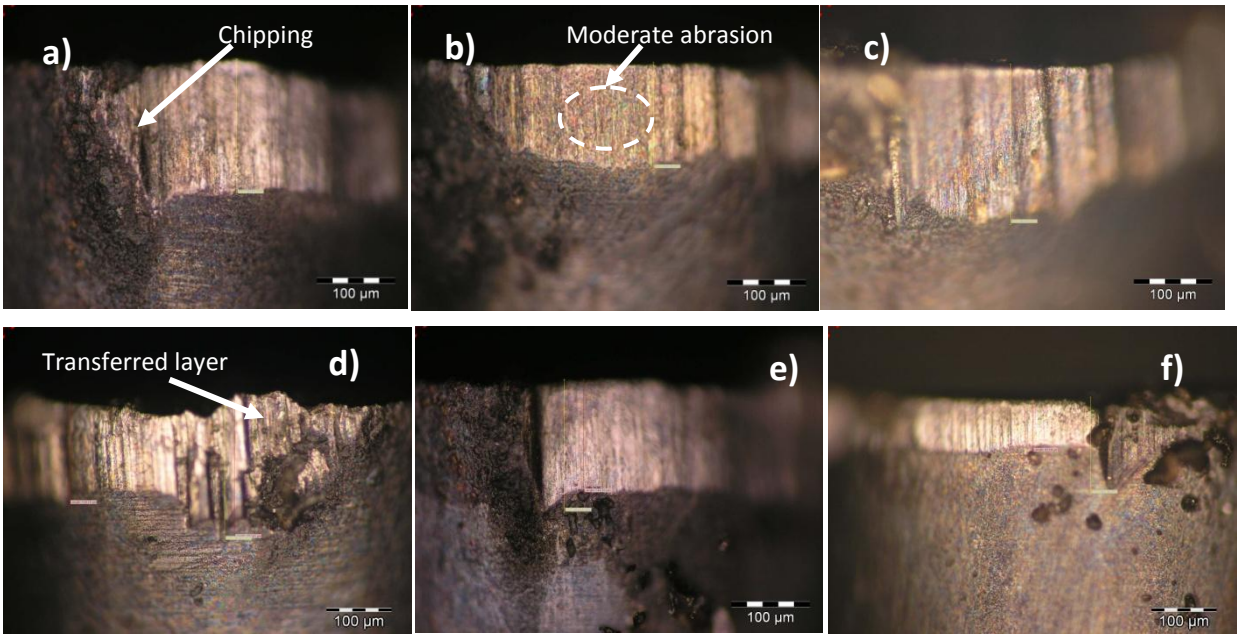

Figure 4-12 Optical micrograph of the worn CBN-100 cutting tool at varying cutting speed showing the cutting lengths at feed rate of 0.1 mm/rev a) 100 m/min; 25,125 m, b) 150 m/min; 18, 430 m, c)200 m/min; 10,829 m; varying feed rate at cutting speed of 100 m/mind) 0.05 mm/rev; 3,044 m, e) 0.1 mm/rev; 10, 920 m, f)0.15 mm/rev; 8,708 m

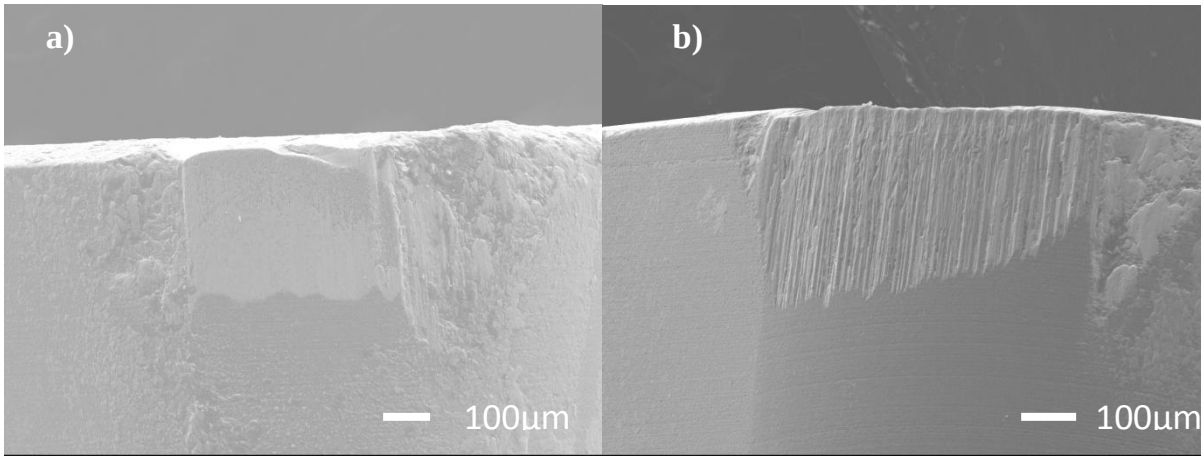

Figure 4-13 SEM micrograph of flank face of failed CBN-100 magnification X150 cutting tool a) 100m/min; 25, 125 m, b) 200m/min; 10,829 m

Figures 4–14a–f and 4–15a and b show the optical and SEM micrographs, respectively, of the worn CC650 cutting tool. The flank face shows more chipping and tool fracture when the machining speed increases (200 m/min) as shown in Figure 4-15b and c. The main wear mechanism observed is abrasive wear with deeper grooves when compared with the parallel marks on the flank face of the CBN–100 cutting tool. This could be a result of possible combination of the disintegration of oxides and carbides from the material and the abraded action of hard debris from the workpiece, being dragged across the flank face, thus removing

the tool material. However, the deeper marks, on CC650 cutting tool is as a result of the bigger carbide grains in the CC650 cutting tool, compared to the ones found in the CBN–100 tool.The higher chemical affinity of CBN–100 to the workpiece material makes it more susceptible to diffusion and chemical wear compared to CC650.On the rake face, there exist adhesion and crater wear, caused by rapid shearing of the successive layers of the cutting tool, thus forming deep craters. Usually, crater wear affects the cutting process resulting from the changing of the tool–chip interface geometry. Some of the factors that affect the crater wear are chemical affinity between the work material and the cutting tool, temperature at the tool–chip interface, and similar factors affecting flank wear which is activated by high cutting speeds and temperatures. Notch wear is mostly observed while machining hard materials using ceramic tools, most especially with low toughness (Kumar et al., 2006); however, that wear type was not observed in the present study.

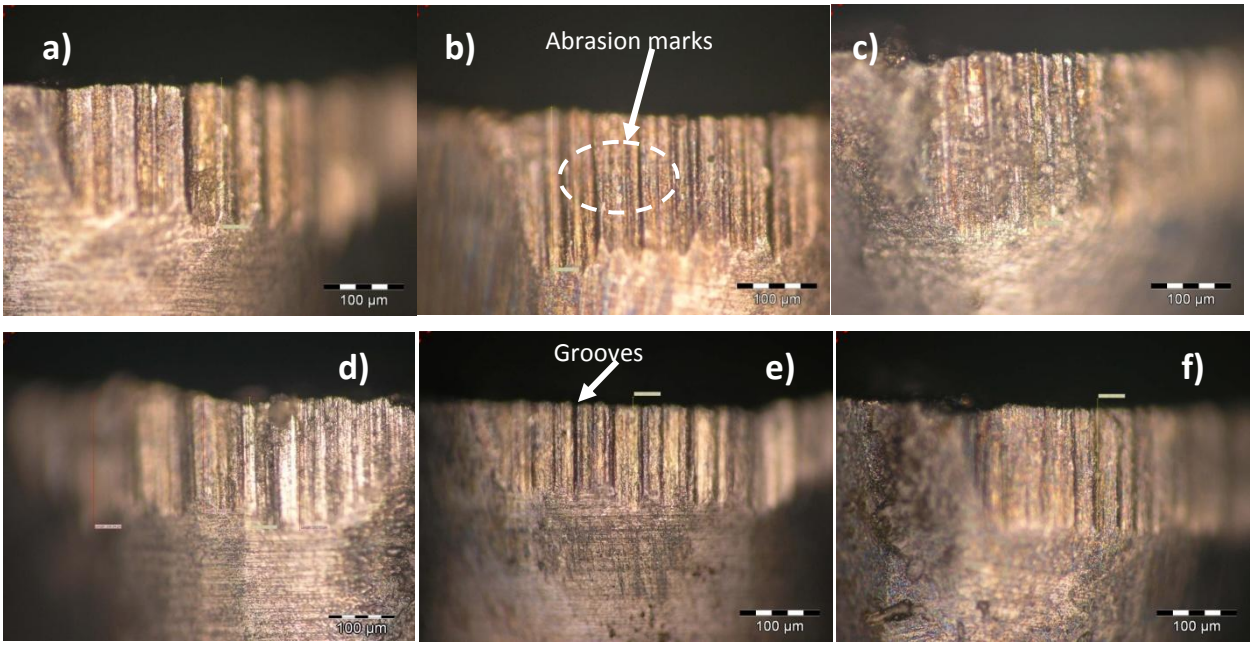

Figure 4-14 Optical micrograph of the worn CC650 cutting tool at varying cutting speed at cuttings lengths a) 100 m/min; 5,001 m, b) 150 m/min; 4, 203 m, c) 200 m/min; 2,589 m; varying feed rate d) 0.05 mm/rev; 4,446 m, e) 0.1 mm/rev; 5,001 m, f) 0.15 mm/rev; 8, 705 m

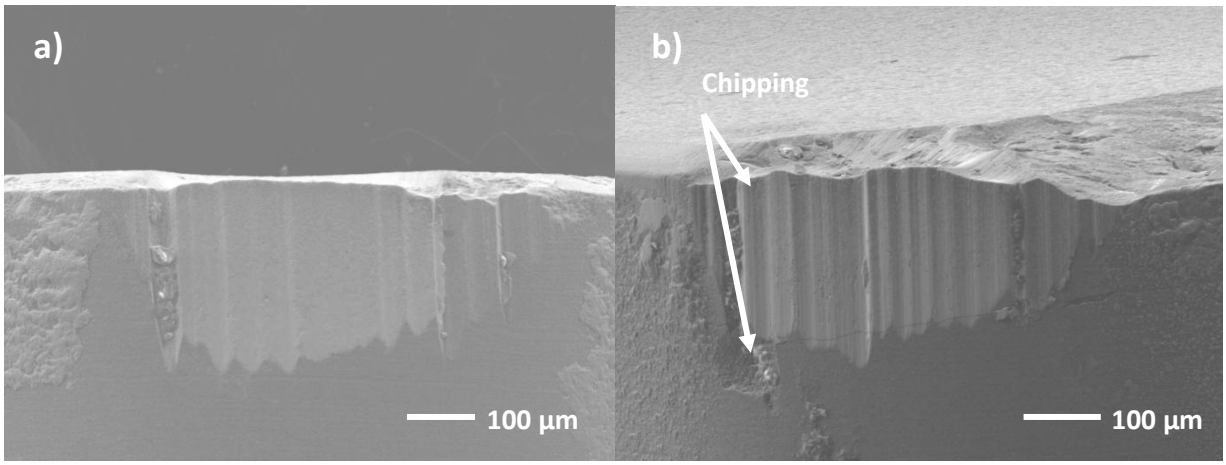

Figure 4-15 SEM micrograph of flank face of failed CC650 cutting tool A) 100m/min; 5,001 m, B) 200m/min; 2,589 m.

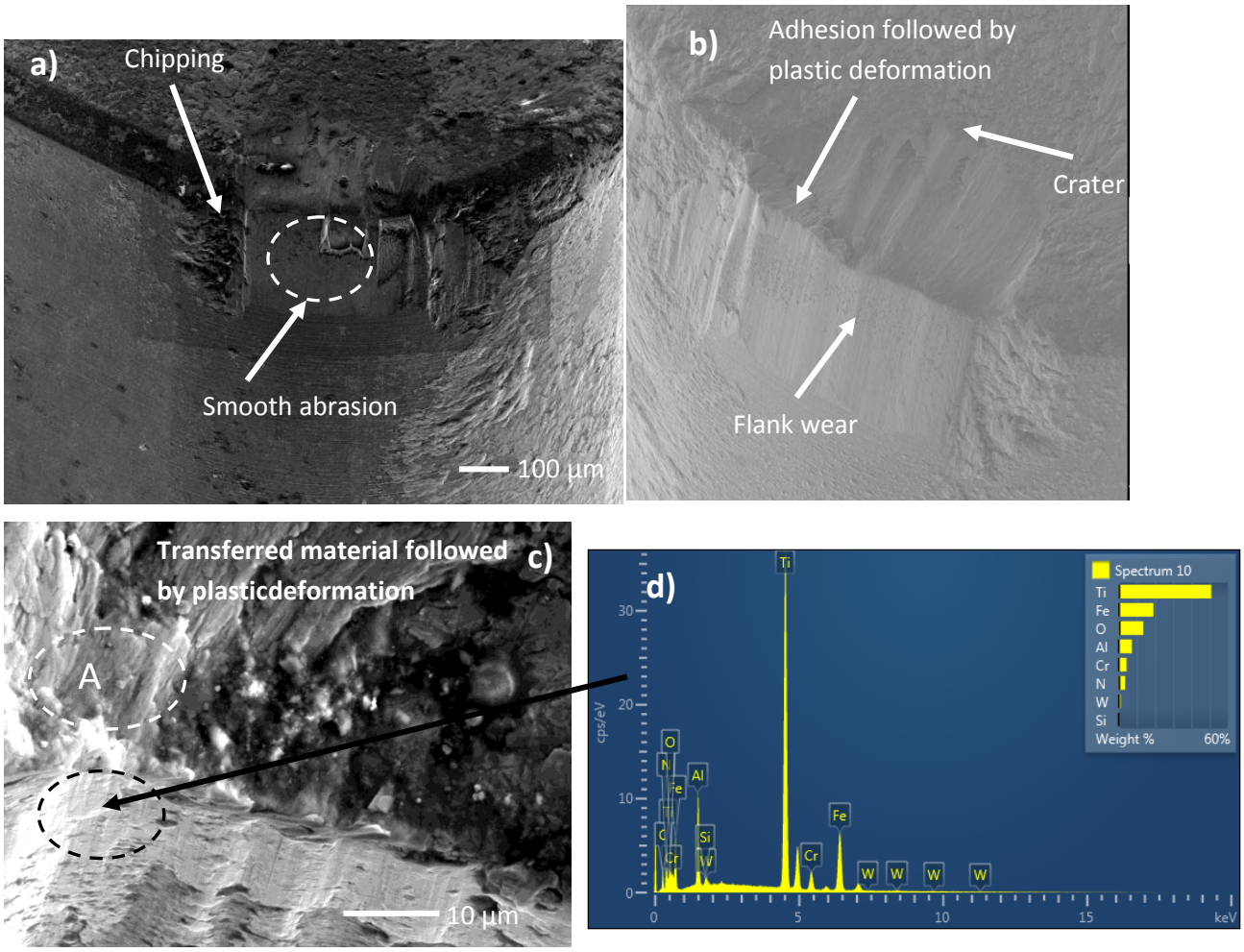

Figure 4-16 SEM micrograph and EDS of failed CBN–100 cutting tool, speed 100m/min, feed 0.1 mm/rev, DOC, 0.1 mm, Length, 25,125 m

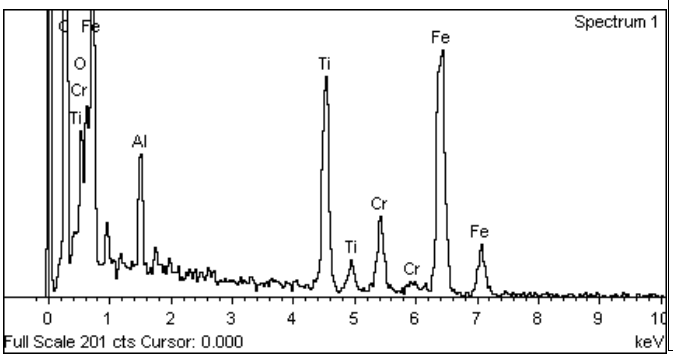

Element	Weight %	Atomic %
CK	64.48	65.35
OK	16.21	12.33
AlK	4.05	1.83
TiK	20.04	5.09
CrK	8.95	2.09
FeK	61.04	13.30
Totals	174.76	

Figure 4-17 EDS of Spot A of Figure 4-16 showing chemical affinity of work material on crater face

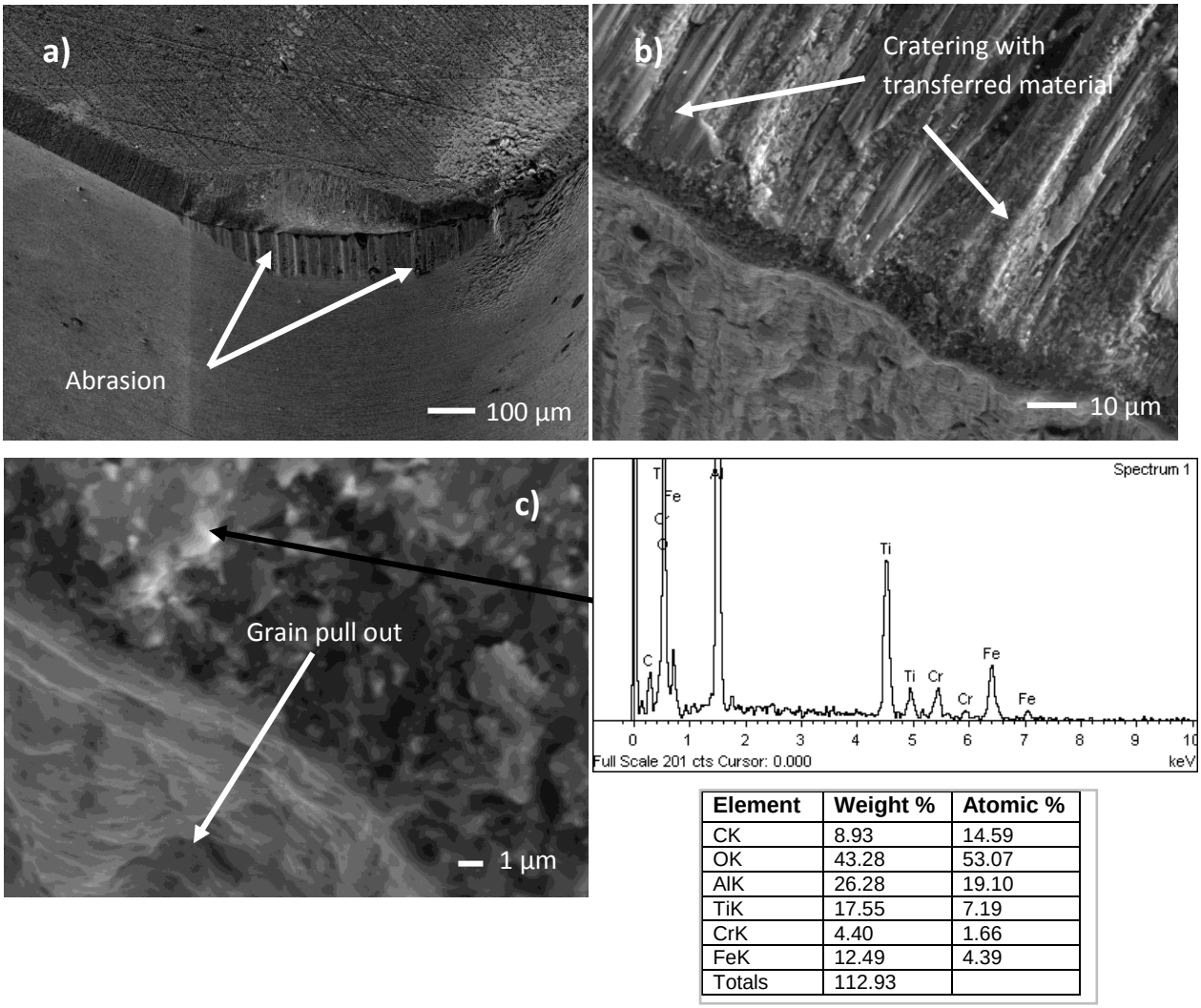

Element	Weight %	Atomic %
CK	8.93	14.59
OK	43.28	53.07
AlK	26.28	19.10
TiK	17.55	7.19
CrK	4.40	1.66
FeK	12.49	4.39
Totals	112.93	

Figure 4-18 SEM micrograph and EDS pattern of failed CC650 cutting tool, speed 100m/min, feed 0.1 mm/rev, DOC, 0.1 mm, Length, 5,001 m

Small elements of the work material can be found on the crater face of CC 650 as confirmed by EDS pattern (Figure 4–18). However, the extent of chemical affinity of CC650 to the

stainless steel material is very small in comparison to CBN–100, judging from the fact that the peaks of Cr and Fe are quite small in the case of CC650 cutting tool and also that the composition of the elements by atomic percentage was more in the case of CBN–100 (see Figure 4–17).The main wear mechanisms observed in this study in the rake face of the ceramic tool is one, or a combination, of diffusion, adhesion and abrasion.

The predominantly abrasive wear occurring on the flank face of both cutting tools is a result of the hard carbide particles within the *martensitic* matrix of the workpiece material, such as $M_{23}C$ (predominantly), SiC, Cr_7C_3, VC, Mo_2C, M_7C, M_2C and Fe_3C. This cause of wear is described by many authors as the significant major cause of wear during machining of hardened steels (Liew at al., 2003; Sales et al., 2009; Chou and Evans, 1997; Thamizhmanii and Hasan, 2008; Hasan and Thamizhmanii, 2010).

At increasing cutting speeds (between 300 m/min and 600 m/min), the crater depth increases, as observed, and typical wear on the rake face can be seen in Figures 4–19 and 4–21 for CBN–100 and CC650 respectively. The tool wear on the rake face is formed at some distance from the cutting edge, within the conventional cutting speed range and adjacent to the cutting edge during high cutting speed. Deeper grooves and the depth of wear area can be seen on the cutting edge of both cutting tools showing excessive wear. Crater wear occurs mainly owing to high cutting temperatures on the rake face. On the crater face of CBN–100 cutting tool there is still present some form of adhesion of the work material on the crater surface but with very small thickness. Debris or micro particles of the chips formed at high cutting speeds were deposited on the craters (see Figure 4–20). Abrasive marks can be clearly seen on the rake surface of the CC650 cutting tool at cutting speeds of 300 m/min and 600 m/min. The abrasive wear on this surface is aggravated owing to the reduction in the hardness of the cutting tool resulting from high cutting temperatures (Liu et al., 2002).

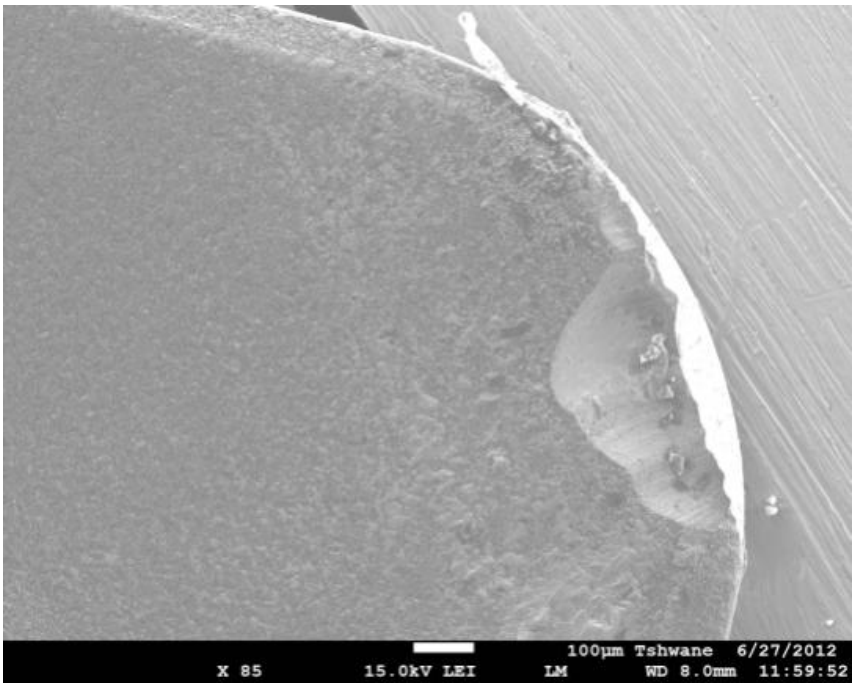

Figure 4-19SEM micrograph of crater face (CBN-100, speed 300m/min, a_p 0.1mm, feed 0.1 mm/rev)

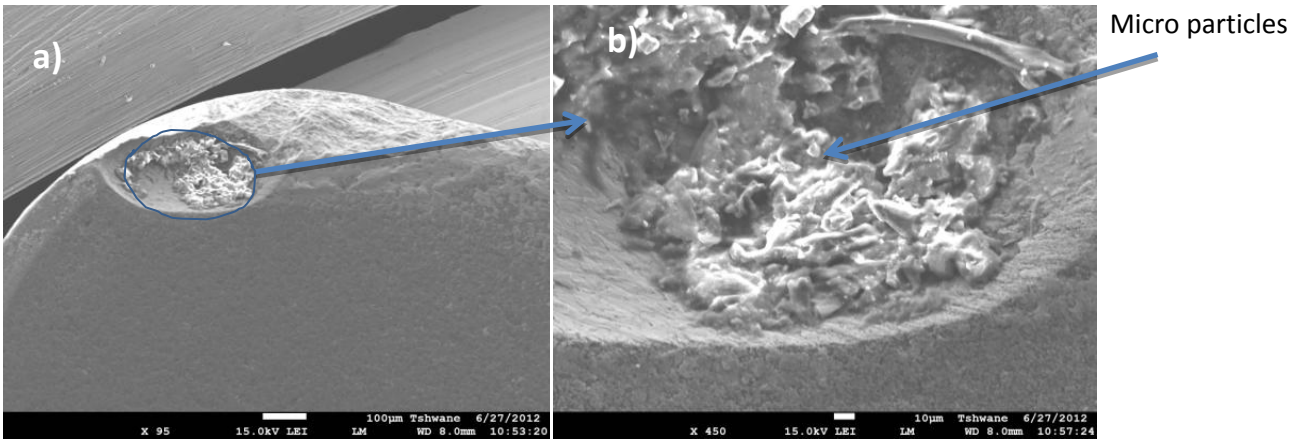

Figure 4-20 Crater face of failed CBN-100cutting insert (Speed 600 m/min, a_p 0.1 mm, feed 0.1 mm/rev)

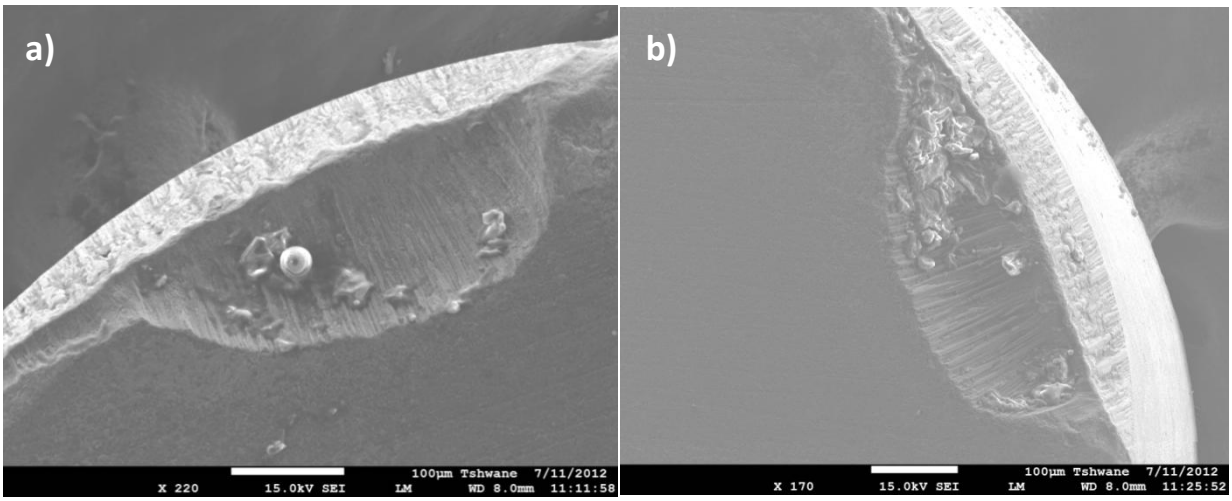

Figure 4-21 SEM micrograph of crater wear of CC650 tool, a) 300m/min, b) 600 m/min, a_p 0.1mm, feed 0.1 mm/rev

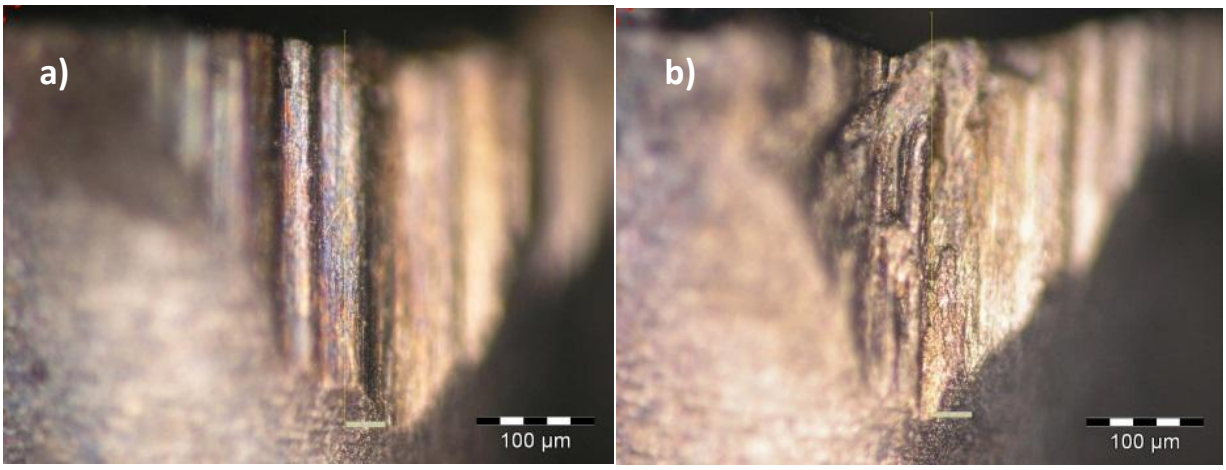

Figure 4-22 Flank wear images of CBN-100insert a) 100m/min b) 300m/min c) 600m/min

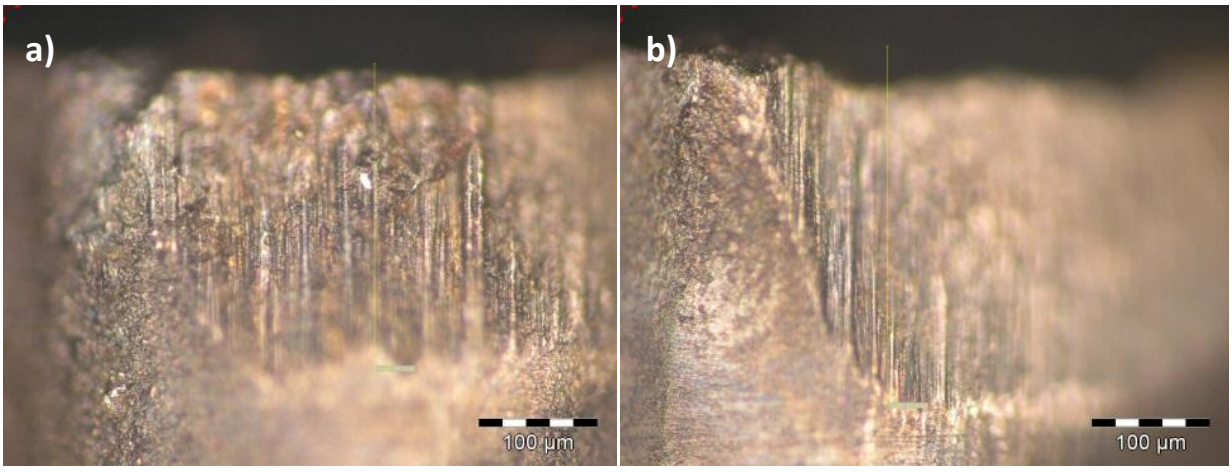

Figure 4-23 Optical micrograph images of flank wear of CC650 insert a) 300m/min b) 600m/min

The optical micrographs of the cutting tools machined at 300 m/min and 600 m/min are presented in Figures 4–22 and 4–23 for CBN–100 and CC650 cutting tools respectively. During high speed cutting, small chips of the cutting tool break off from the cutting edge as a result of possible transient thermal stresses and mechanical shocks owing to cyclic heating and cooling as the cutting tool enters and exits the workpiece.

It can be seen from Figure 4–23, the wear mechanism of the CC650 cutting insert is a combination of abrasive and chipping with abrasive wear more dominant, whereas for the cBN cutting tool, fracture is the dominant form of wear. The excessive chipping of the CC650 cutting tool is caused by abrasive wear, thus leading to flank wear.

The CBN–100 cutting tool failure is mainly by the maximum flank wear VB_{max}. The cutting edge of both cutting tools appeared jagged with depressions on the wear land. There exist small chips along the boundary of the minor and major flanks of the tools. The abrasive wear on the CC650 flank is more uniformly distributed when compared to that formed on the flank face of the CBN–100 tool. There, severe cracks, chattering and fracture are observed, most especially at cutting speeds of 600 m/min. Similar trends with PcBN were observed by Liu et al. (2002).

Generally, tools that are prone to fracture have low fracture toughness and transverse rupture strength (Kopac et al., 2006); this phenomenon was observed with CBN–100. In the case of CBN–100, there is weak mechanical strength resulting from the ineffective cBN crystal to crystal bonding (Deming et al., 1994).
The fracture toughness of both cutting tools is in the region of 4 $MPa\text{-}m^{1/2}$(see Table 3–4),which makes the tools highly prone to fracture at the flank face. This properties can be enhanced to improved the tools resistance to this particular wear, thus increase in their tool life.

The results in this study, based on the wear mechanism, CBN–100 or any PcBN with low cBN content are generally not recommended for machining martensitic stainless steels with hardness less than 45–50 HRC at high cutting speeds.

4.3.3 Forces

In turning operations, the cutting forces are critically important and sometimes used for evaluation of the performance of the machining process, because of their strong correlation with the tool's wear, cutting temperature, surface accuracy, tool breakage, and self-excited and forced vibrations (Shaw, 1984; Lalwani et al., 2008; Bartarya, and Choudhury , 2012)

The three cutting forces, namely tangential force (Fc), radial force (Fr) and feed/axial force (Ff), were measured during hard turning experiments. In each experiment, a fresh cutting tool was used and the experiments were repeated twice at each cutting condition in order to keep experimental error to a minimum. The cutting force information was based on a single pass of the cutting tool over the workpiece within a cutting distance of200 mm. The cutting forces were only investigated using the CBN–100 cutting tool to understand the effect of cutting

parameters on the cutting force and also the relationship between the cutting forces and tool wear.

As observed in the first test when cutting forces were varied with speed, the axial force was lower than both tangential and radial forces. The radial force (thrust force) is the highest (about twice the cutting force) observed in the experiment. This is in agreement with result obtained by Wuyi (2000); Ozel et al. (2005); Huang and Liang (2005); and Fnides et al.(2008) using PcBN for machining steel during finish hard turning. When machining within the limit of the nose radius, the thrust force was found to be the dominant force, followed closely by the tangential force (Nakayama et al., 1988; Fnides et al., 2008). Typical cutting forces obtained during the machining test are shown in Figure 4–24.

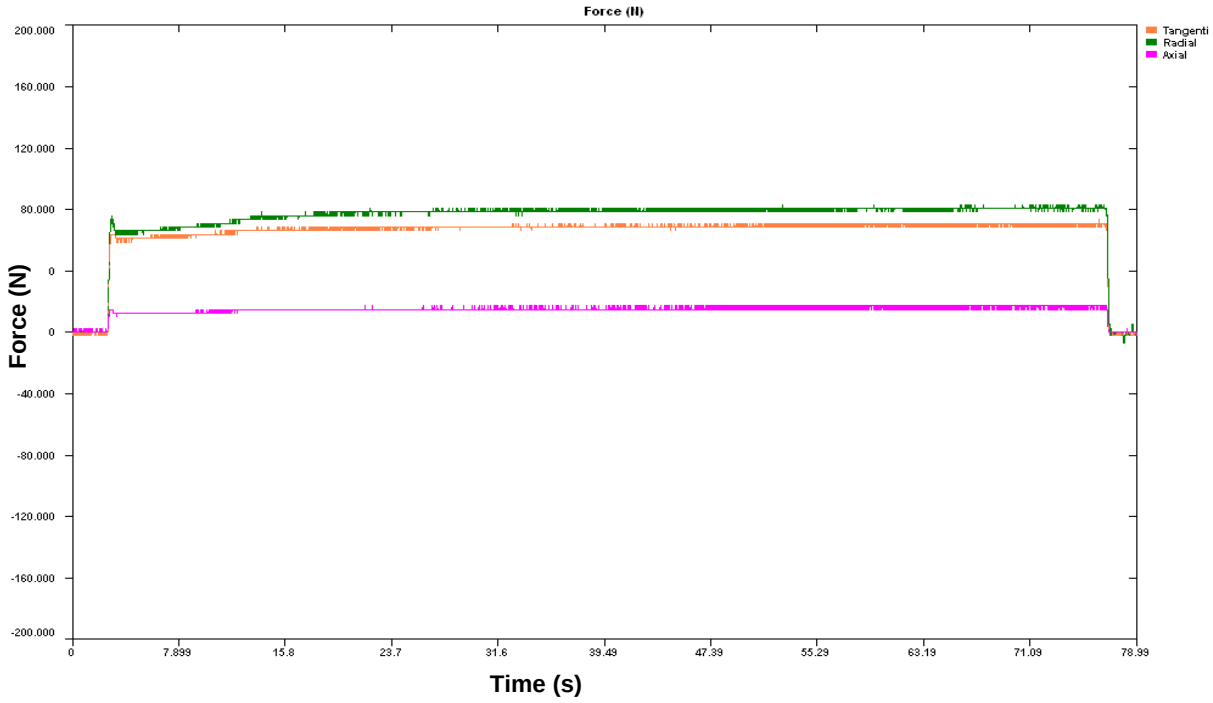

Figure 4-24 Cutting force using CBN-100 during a single pass length of 200 mm, Speed 100m/min, DOC 0.1mm, feed 0.1mm/rev

The effect of increase in cutting speed on the resultant cutting forces is presented in Figure 4–25. The cutting forces were obtained at constant feedrate of 0.1 mm/rev and depth of cut of 0.1 mm. As observed, the increase in the cutting speed leads to a decrease in the cutting forces. The highest radial cutting force recorded was 78.125 N and the lowest recorded was 46.367 N (at a speed of 400 m/min). The tangential and axial forces were in the range of 68.359 N–34.174 N and 14.648 N–7.324 N respectively. There is a minimal effect of the cutting speed on the axial force as observed when the cutting speed increases from 100 m/min

to 400 m/min. However, there is a decline in the cutting tangential and radial cutting forces with increasing cutting speed. Normally, it is expected that the cutting forces should reduce with increase in the cutting speed, since the temperature between the work and cutting tool increases and this leads to softening of the work material. The decrease in the cutting force at high cutting speed is essentially owed to the reduction of the rubbing between the chip and cutting tool, limited by the stabilization of the temperature at high cutting speeds. At high cutting speeds the degree of plastic deformation increases along with the cutting temperature, and the angle of shearing increases permitting the reduction of the area or section of shearing, and therefore of the cutting force (Kamruzzaman and Dhar, 2008).

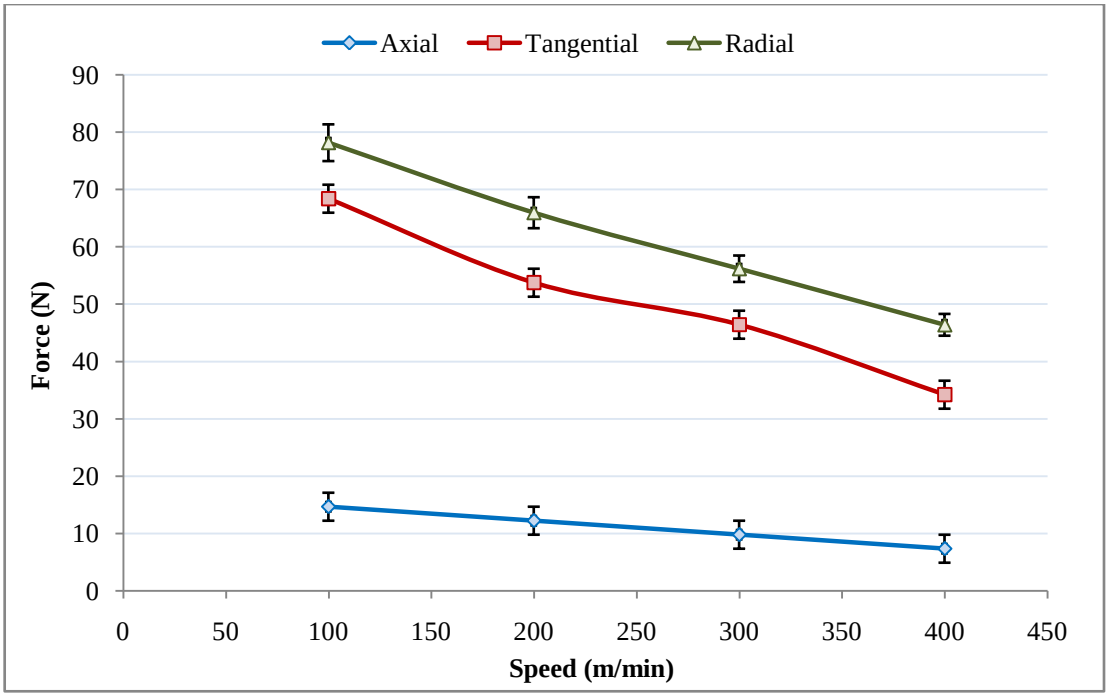

Figure 4-25 Cutting force variation at different speeds

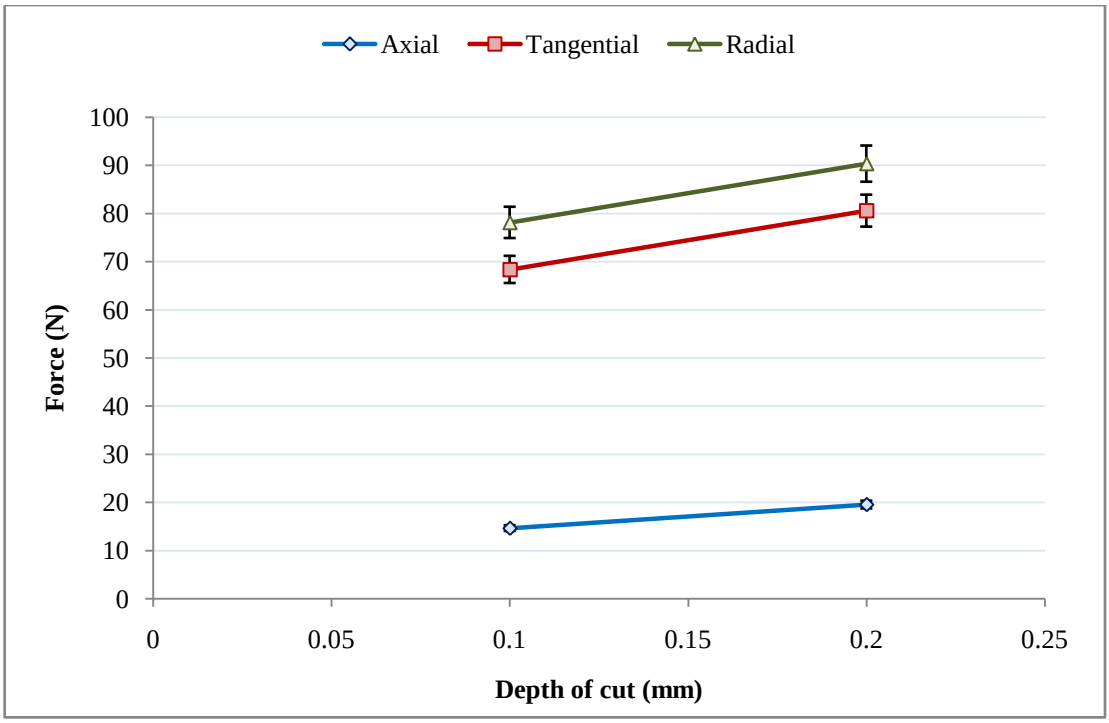

Figure 4-26 Effect of depth of cut on cutting force, speed 100 m/min, feed 0.1 mm/rev

The cutting forces increase with an increase in the depth of cut from 0.1 mm to 0.2 mm, as seen in Figure 4–26. The axial force remained lowest while the thrust force (radial force) was the highest. The tangential and thrust forces were found to increase by almost the same ratio as the depth of cut increases. This increase in the cutting force probably owes to the larger contact area of the cutting tool on the workpiece when the depth of cut is increased from 0.1 to 0.2 mm.

Figure 4–27 shows the cutting force as a function of the feed rate. The thrust (radial) force was recorded as the highest in the experiment, at about 119.6 N. Other cutting forces (tangential and axial) were lower than the cutting forces recorded at feedrate of 0.1 mm/rev. The thrust force reduces with an increase in the feed rate from 0.05 mm/rev to 0.15 mm/rev, but with the tangential and axial forces, this was not so as they increased when the feed was increased.

The high value of the thrust force at feed rate of 0.05 mm/rev, compared to its value at higher feed rates, is probably a result of the vibrations experienced when cutting at this feed and at a low cutting speed. The high vibration when cutting at low feed rate had been ascribed earlier to the low fracture toughness of a CBN–100 tool.

It is expected for the cutting force to increase with increasing feed rate (Ozelet al., 2005; Kosaraju et al., 2011). This was observed at 0.1 mm/rev feed.

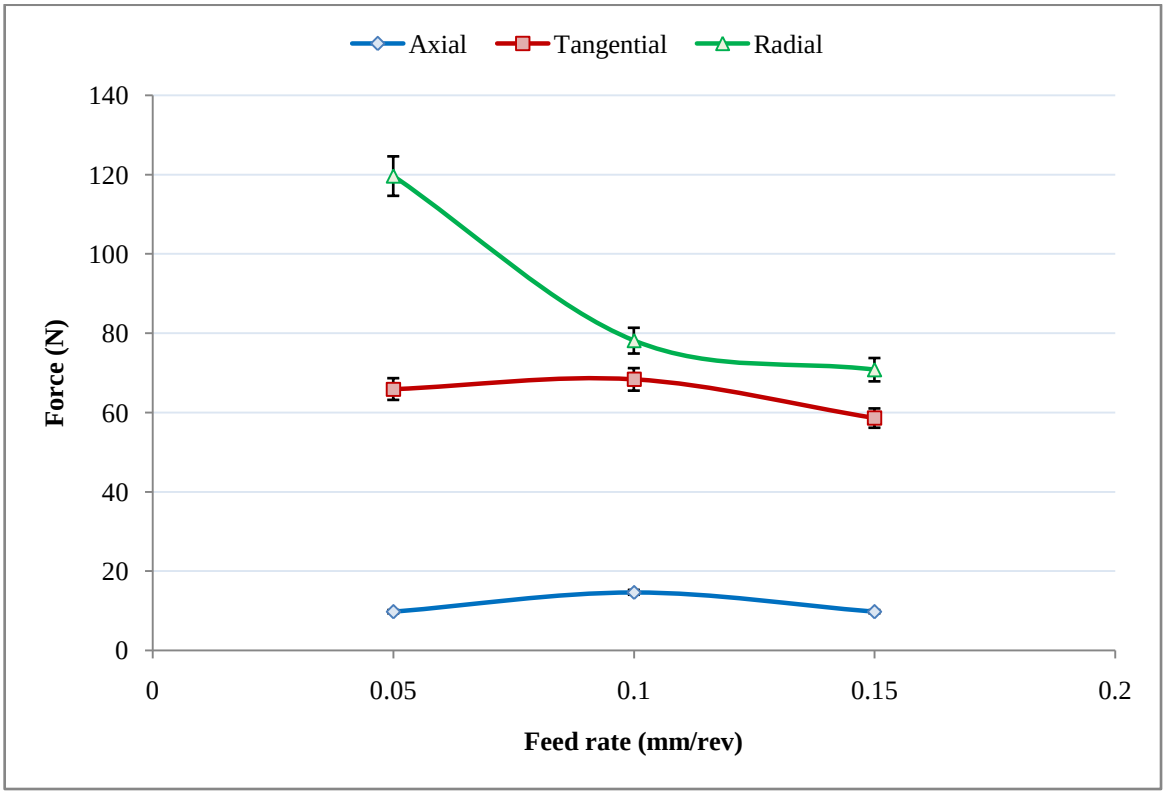

Figure 4-27 Cutting forces as a function of feed rate at100 m/min and DOC 0.1 mm

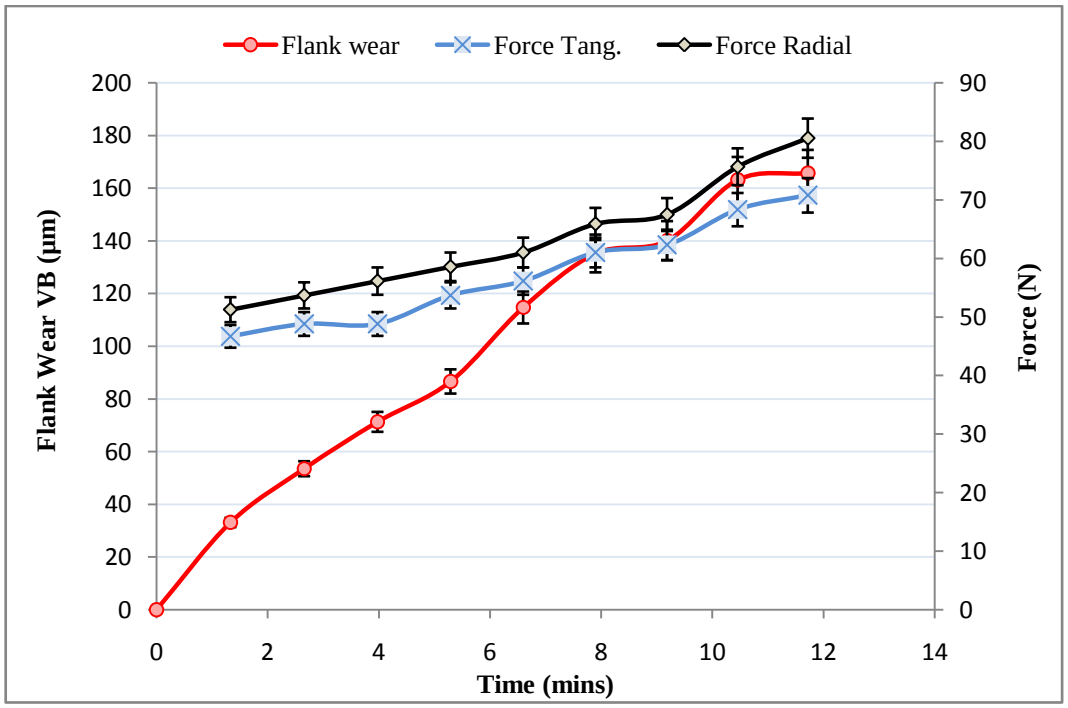

Figure 4-28 Forces and flank wear Vs cutting time for CBN-100 at 200 m/min cutting speed

Figure 4–28 shows the effect of machining time on the cutting forces in comparison to the flank wear scar size during machining of the work material using the CBN–100 cutting tool. The radial force (thrust force) is usually higher than the tangential cutting force (feed force) (typical observation during machining of hardened materials). The flank wear profile is similar to the cutting force profile. An increase in flank wear rate leads to a corresponding increase in the cutting forces. The mechanical loads (which are directly related to the cutting force) of the surface produced at the tool workpiece–interface are mainly affected by the flank wear, thus its effect on the cutting forces is significant (Dubec et al., 2013).

4.3.4 Effect of machining parameters on the surface roughness

Diameter error, geometric deviation and surface integrity are the key quality characteristics in a turning operation. Surface roughness in metal cutting is sometimes used for evaluating the cutting tool failure and it is also a good indication of the quality of the machined surface. The surface finish produced during hard turning while using the CBN–100 and CC650 were found to be generally satisfactory. The roughness value for the CBN–100cutting tool was similar at cutting speed of 100 and 150 m/min but it improved at 200 m/min. For the CC650 cutting tool, the Ra value was better at 100 m/min compared to higher cutting speeds. The minimum and maximum Ra values of 0.51 and 1.13 µm respectively were recorded for the CC650 tool, and 0.63 and 1.44 for the CBN–100tool.

The surface finish produced when using CC650 is found to be better compared to that obtained with the PcBN cutting tool at all the cutting speeds investigated (100, 150 and 200 m/min). Figures 4–29, 4–30 and 4–31 show the surface roughness variation with cutting length at different cutting speeds. At 100m/min the surface roughness produced by CBN–100 deteriorated rapidly from the first cut as the machining test progressed, while CC650 gave a fairly uniform Ra value over the cutting distance investigated. CC650 showed a much better surface roughness value at cutting speed of 100 m/min than CBN–100. At much higher cutting speeds (200 m/min), the Ra produced by both cutting tools were similar though the Ra produced by CC650 was slightly better than CBN–100 (see Figure 4-31). CC650 produced Ra of 0.5 µm in the initial cuts and later the surface started deteriorating as the flank wear increased at a cutting speed of 200 m/min.

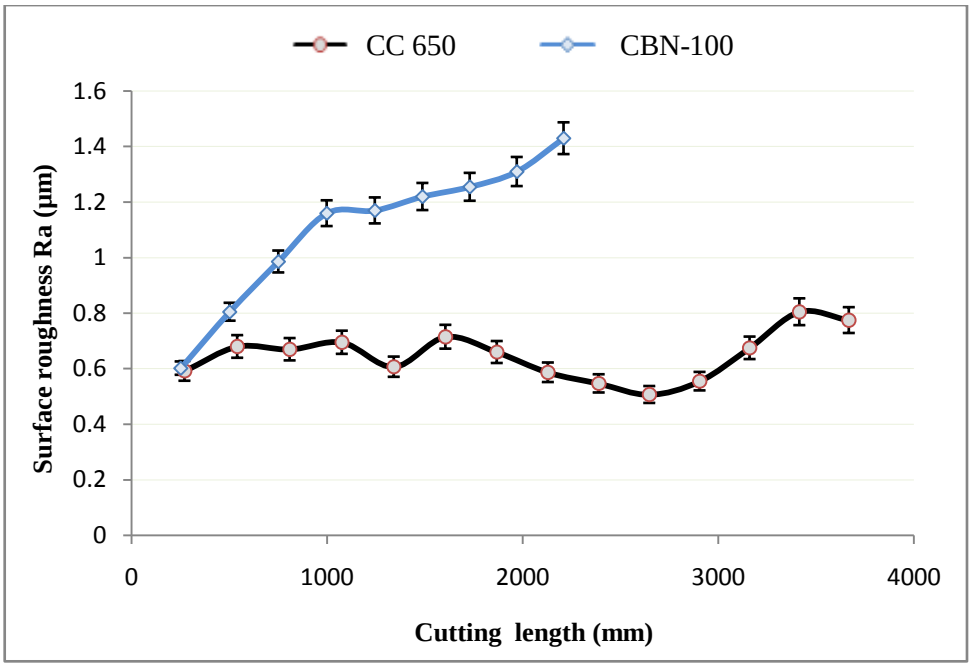

Figure 4-29 Surface roughness (Ra) produced at 100 m/min cutting speed, feed 0.1 mm/rev, DOC 0.1 mm

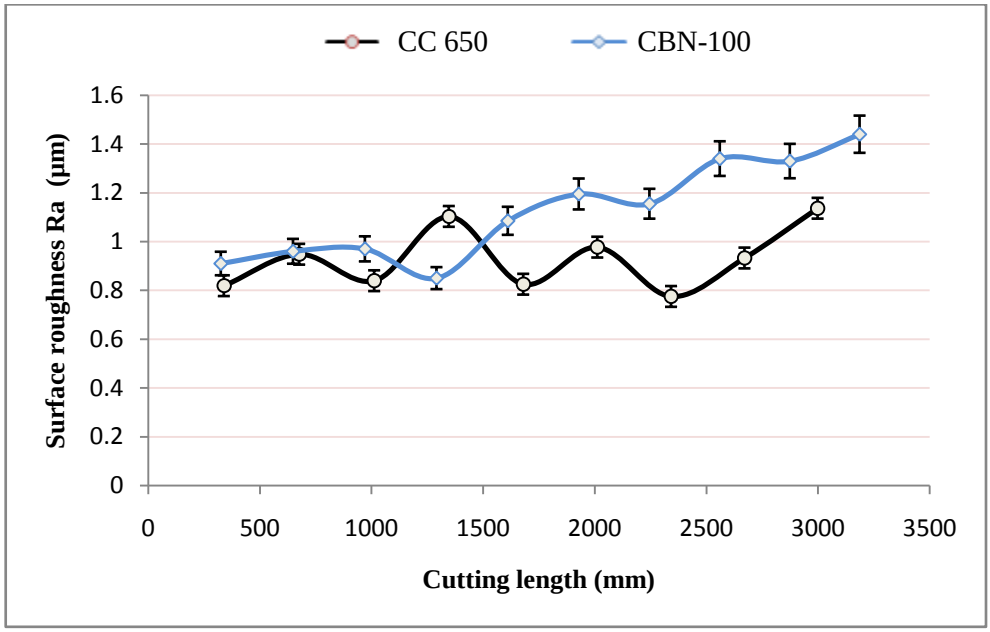

Figure 4-30 Surface roughness (Ra) produced at 150 m/min cutting speed, feed 0.1 mm/rev, DOC 0.1 mm

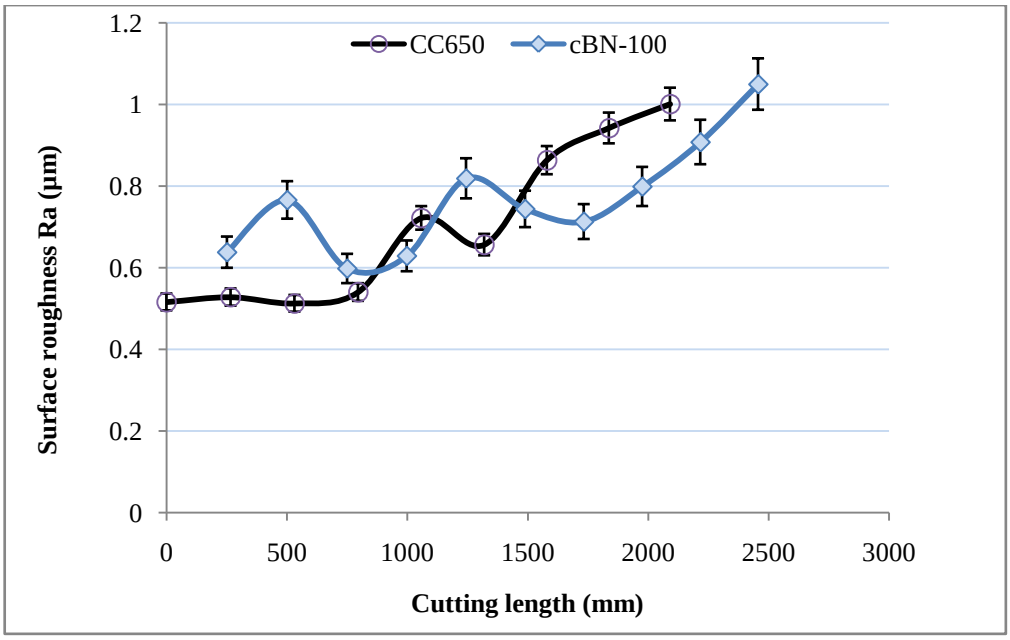

Figure 4-31 Surface roughness (Ra) produced at 200 m/min cutting speed, feed 0.1 mm/rev, DOC 0.1 mm

The typical Ra and Rz produced by CBN–100 at cutting speed of 160 m/min are shown in Figure 4–32. The arithmetic mean value Ra (arithmetic average roughness) was about 2.8 times lower than the Rz (maximum height of roughness profile) value. This shows that Rz is more sensitive than Ra to the changes in surface finish because maximum profile heights.

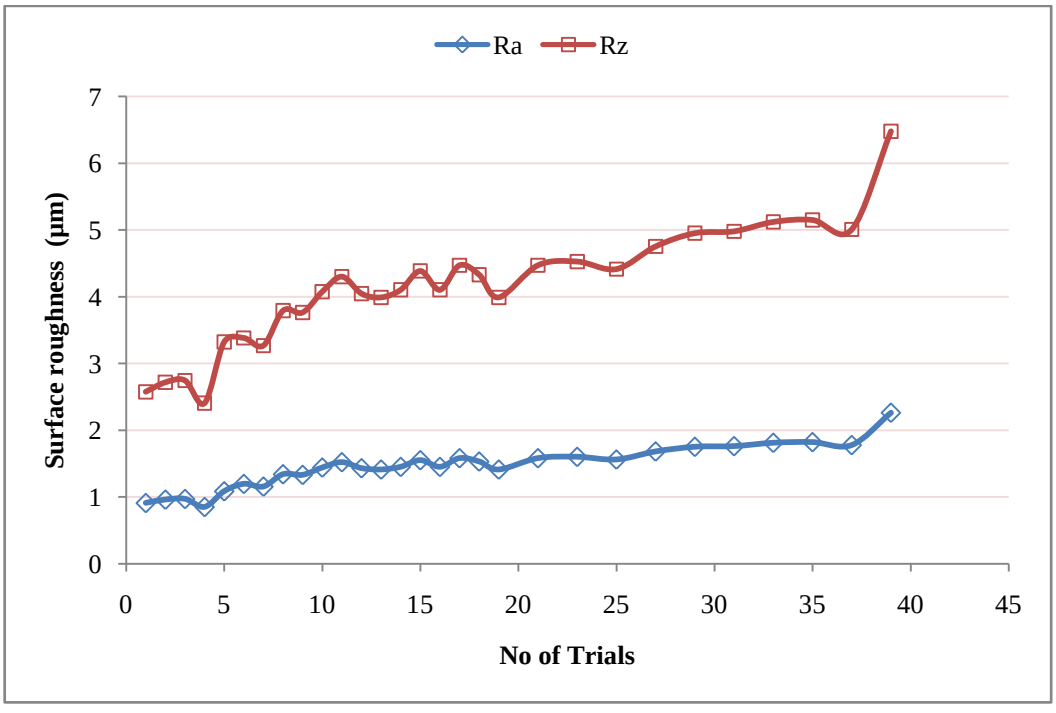

Figure 4-32 Typical Ra and Rz produced by CBN-100, speed 160 m/min, feed 0.1 mm/rev, DOC, 0.1 mm

The increase in the cutting speed resulted in an improvement in the surface finish produced by the CBN–100 cutting tool, whereas for CC650, the surface finish was moderate at the initial cuts, but increased with cutting speed as the tool was worn out, resulting in chatter marks and debris on the machined surfaces, as shown in Figures 4–33b and 4–34b. As reported by Stephenson and Agapiou (2006), cutting speed, feed rate and depth of cut have significant effects on the surface finish of the machined component. Based on Equation 2–9 (theoretical expression of surface roughness), the feed rate found to be the major parameter that influencing the surface roughness.

Figure 4–33 and 4–34 show the typical surface produced on the workpiece after machining using CBN–100 and CC650. Generally, machined surface topography consists of straight grooves in parallel direction to the cutting velocity; this was observed on all surfaces produced. Observed in Figure 4–33a and 4–34 are deeper feed marks on the surface with cBN–100. This is the reason for the higher surface roughness obtained with the cBN compared to the CC650 cutting tool. However, the work material surface micrographs obtained withCC650show more defects compared to the ones obtained using CBN–100. The number of defects increases with increasing cutting speed. Layers of debris that have undergone severe deformation are observed on the machined surface. Such features are similar to the ones observed by Liew et al (2003). These defects may be a result of unstable built-up edge adhering unto the machined workpiece surface. The instability would be caused probably as a result of the high temperatures at the cutting tool–workpiece interface.

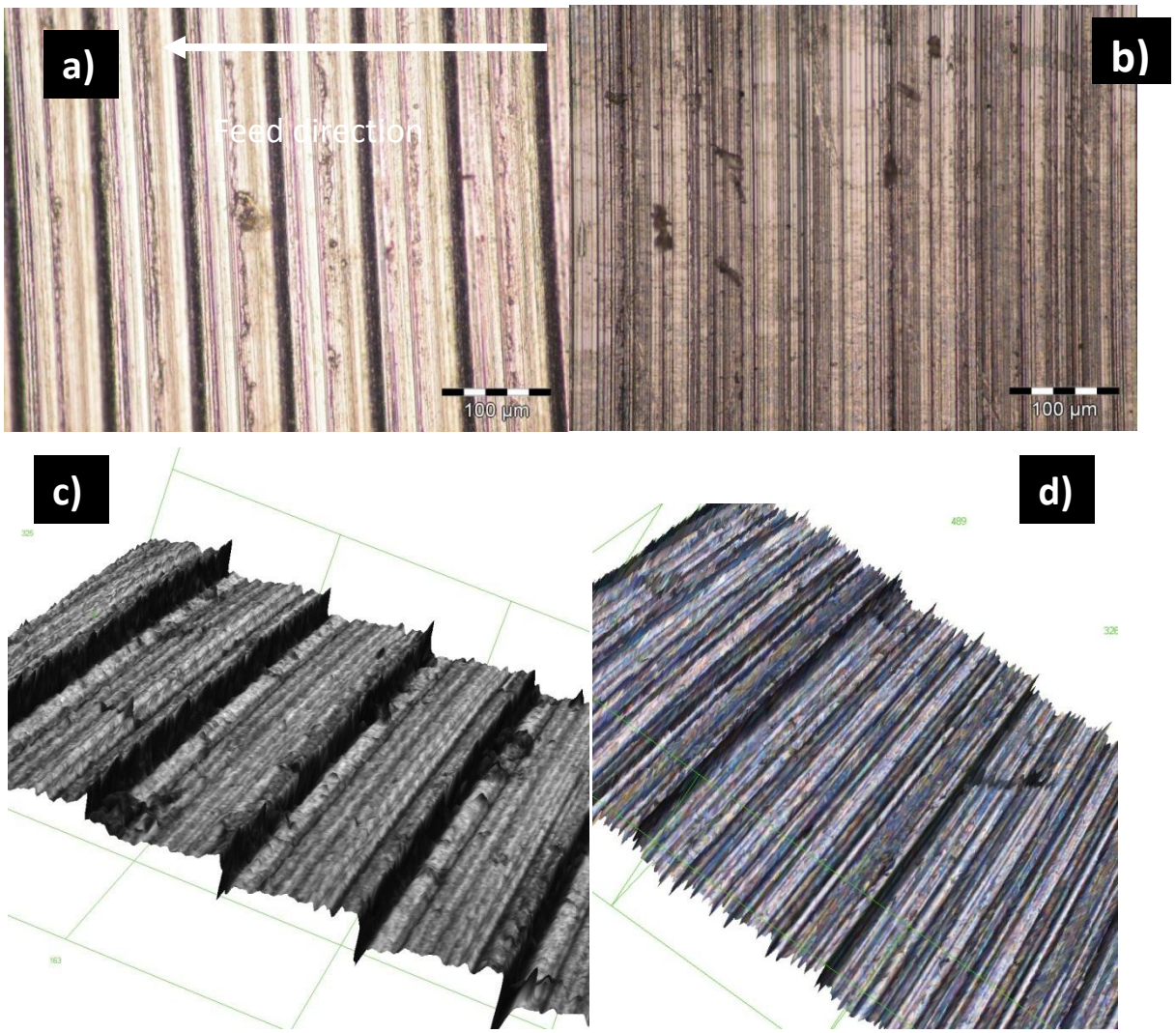

Figure 4-33 Machined surfaces a) CBN-100, 2D optical micrograph, b) CC650, 2D optical micrograph, c) CBN-100, 3D Optical micrograph, d) CC650, 3D optical micrograph, at cutting speed of 100 m/min, feed 0.1 mm/rev, DOC 0.1 mm

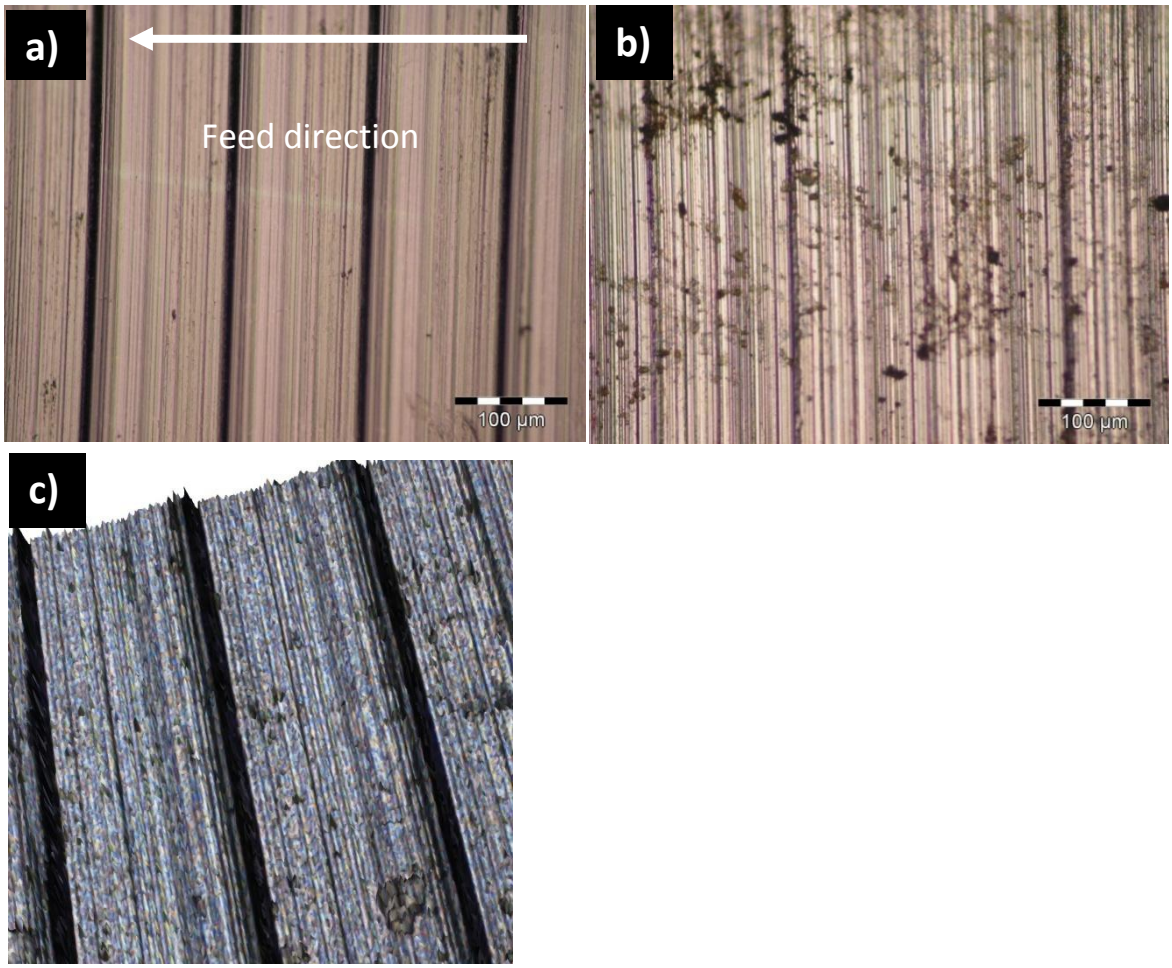

Figure 4-34 Machined surfaces a) CBN-100, 2D optical micrograph, b) CC650, 2D optical micrograph, c) CBN-100, 3D Optical micrograph, at cutting speed of 200 m/min, feed 0.15 mm/rev, DOC, 0.1 mm

4.3.5 Dimensional deviation

The difference between the measured diameter and the designed diameter, where a positive error indicates undercutting of a cylindrical work-piece, is known as the diameter error. For turned component parts, especially where cylindrical fits are involved, the dimensional error is an important quality characteristic (Rafair and Islam, 2009).The average diameter of the workpiece was checked for dimensional deviation after it was subjected to turning using the CBN–100 and CC650 cutting inserts. The result could be used for determining the most appropriate time for the tool to be discarded when considering the tolerance. Figure 4–35 shows the increase in the geometrical deviation (concentricity) of the workpiece as cutting progresses with the flank wear (measured in terms of length of cut). At the first pass, there was no deviation in the diameter of the workpiece machined using CBN–100 tool main while, at this pass, the workpiece increased slightly by 1 µm when CC650 tool was used. The

dimensional deviation of the workpiece increased rapidly at the third pass for the CBN–100 tool and second pass for the CC650 cutting tool. This rapid increase can be correlated to the rapid tool wear of both cutting tools at this point where the sharp edges of the tool breaks and a new cutting geometry is developed. This geometry produced a new nose radius with a decrease in the cutting edge effective height (h) (see Figure 2-24). At the end of nine passes, the dimensions of the final piece compared to the expected dimensions showed an increase by about 15 µm for CBN–100 and 32 µm for the CC650 cutting tool. This is as a result of the wear of the cutting tool. At the end of the nine passes the average tool wear for the CBN–100 cutting tool was 76µm and 165µm for CC650. The results obtained show clearly that cutting tool wear affects the geometrical deviation. As the tool becomes worn, the tool tip geometry changes. There is a loss of effective depth of cut resulting from the wear of the tool tip on the clearance side, leading to change of alignment between the cutting tool and the workpiece as dimensional and form errors are introduced. CBN–100 produces better dimensional accuracy due to its better wear resistance compared to the mixed ceramics.

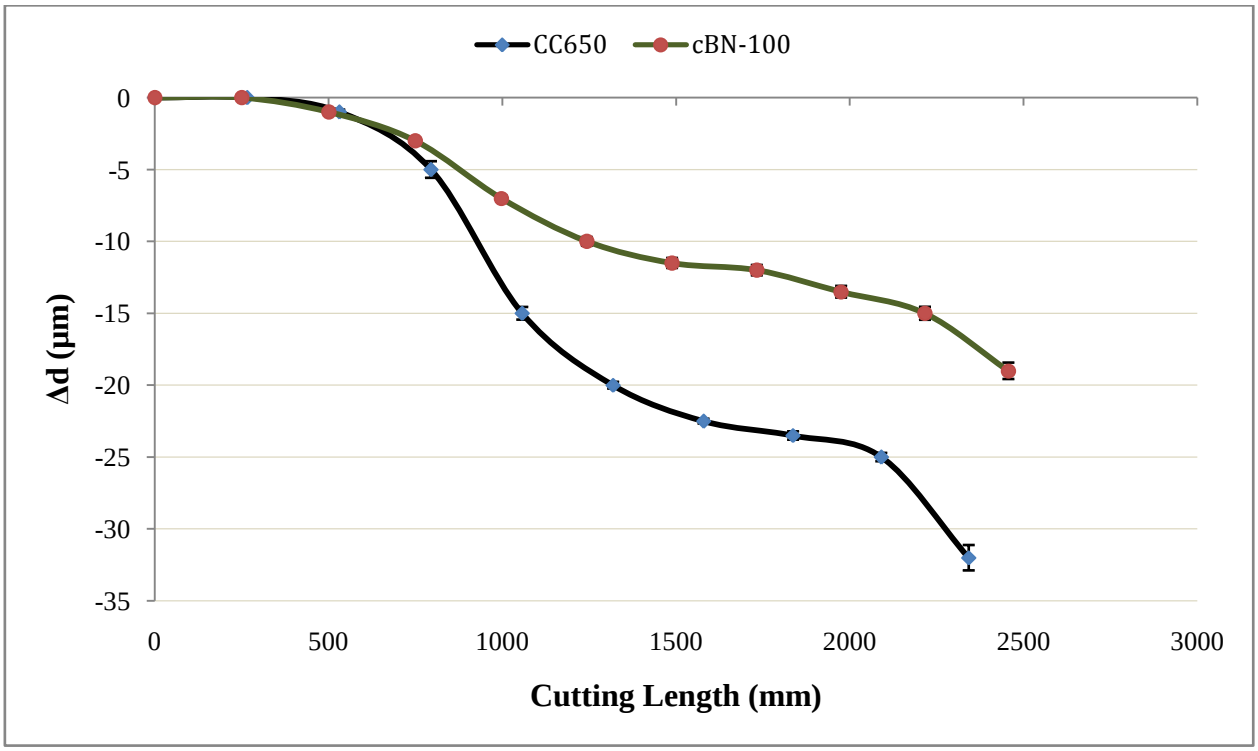

Figure 4-35 Dimensional deviation during hard turning using CBN-100and CC650 cutting tool at 200m/min

4.3.6 Waviness/Out of roundness

Roundness contributes to function and performance in many ways. It plays a significant role in the way parts are fitted together and where most especially lubrication film is to be maintained between mating components. The tool used to test out of roundness of the machining set-up (see Figure 4–36) consists basically of a dial gauge attached to a magnetic chuck. The initial results before the start of the machining process machining obtained from the CNC lathe shows insignificant waviness which represents relative rigidity of the lathe. Subsequently, after each turning using CBN–100 tool, the out of roundness was also tested. The minimum and maximum values recorded were 3.8 µm and 7.4µm respectively. This method to correlate the effect of the changes in the cutting tool as machining progresses resulting from the machining parameters for example, forces, wear, speed, feeds, on the machine rigidity.

Because of the brittleness of CBN–100 cutting tool (see Table 3–4), the tool is prone to chipping; thus, specific machine tool requirements, such as; rigidity, high power, and high precision, are important when using these tools for turning hardened steels. Furthermore, in achieving good surface part quality, a system with high rigidity clamping machine tools are required.

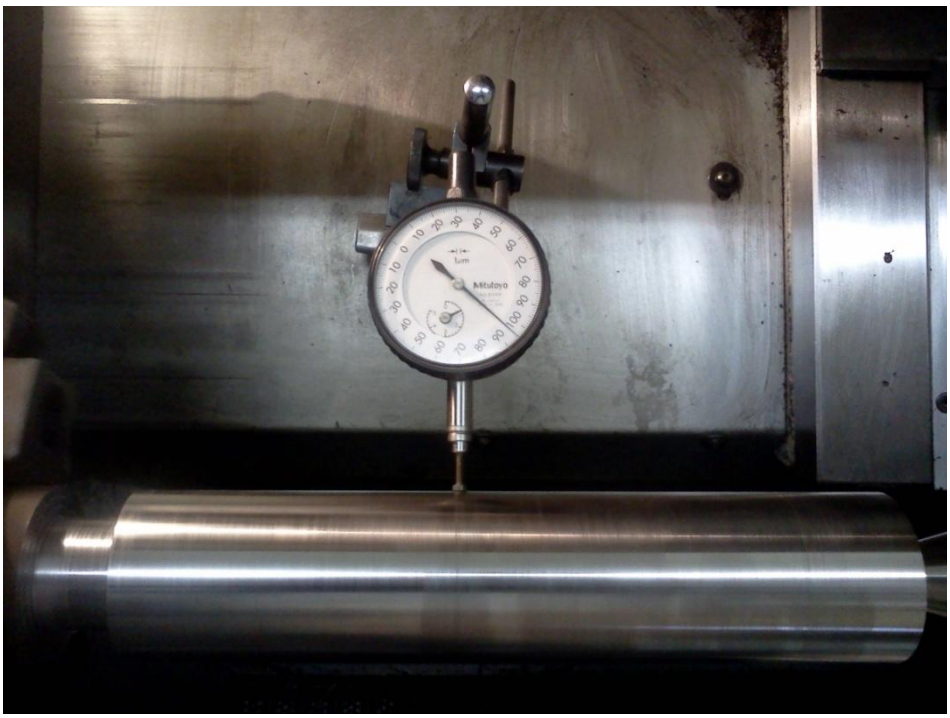

Figure 4-36 Tool set up to investigate the out of roundness produced on the cylindrical bar

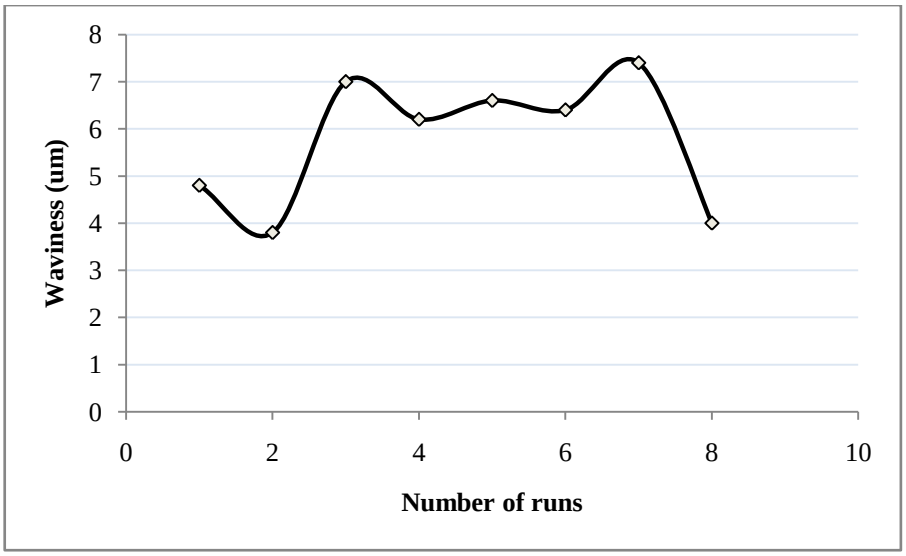

Figure 4-37 Waviness of tool set up at surface speed of 160 m/min

4.4 CHIP ANALYSIS

Figure 4–38 shows the optical micrograph of the chips produced by the cutting tools investigated at cutting speed of 100 m/min. Chips are formed by the shearing action at the shear plane. During the shearing action, many aspects of the cutting process are affected by the process of plastic deformation in the cutting zone, such as: surface finish, dimensional accuracy, cutting forces, temperature and tool life (Cep et al., 2008). The chip produced by the CBN–100 tool at a speed of 100 m/minis light brown in colour while the chip produced by CC650 is darker. The change in the colour of the chips produced is an indication of the heat caused by the intense temperature at the cutting zone. The CBN–100 tool has a higher thermal conductivity when compared to the CC650 cutting tool. This property enables it to conduct more heat away from the cutting zone; less heat is transmitted into the chips produced, thus the chips formed are lighter in colour.

Continuously cut chips, which entangle the tool holders, were produced at the cutting speed of 100 m/min by both cutting tools (see Figure 4–38). At the cutting speed of 150 m/min, continuous chip with darker colour was produced by the CBN–100 cutting tool, while the chips produced by CC650 were serrated. The formation of serrated chips was only observed with the CBN–100 cutting tool at cutting speeds above 200 m/min. The chips formed by CBN–100were slightly thinner compared to the ones formed using the CC650 cutting tool for all cutting speeds investigated. At high cutting speeds, above 200 m/min, segmented (saw-tooth) cutting chips were formed by both cutting tools. The formation of a saw-tooth

chip(shear localised, adiabatic shear and catastrophic shear) is normally observed when machining hardened materials with geometrically defined cutting tools (Nakayama et al., 1988; Poulachon and Moisan, 2000; Dogra et al., 2010; Grzesik, 2011).

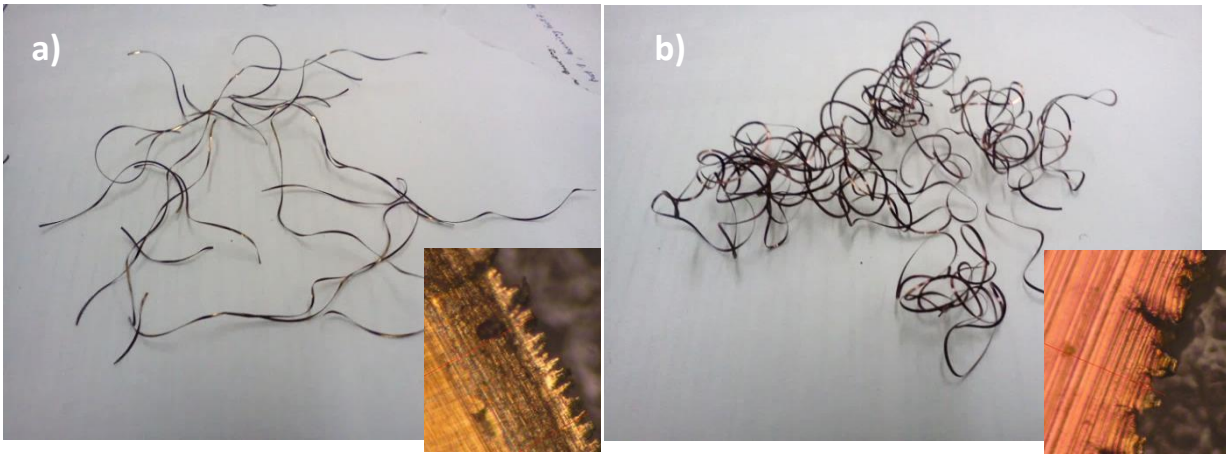

Figure 4-38 Typical chips formed by a) CBN-100, b) CC650, speed 100m/min, DOC, 0.1mm, feed, 0.1 mm/rev

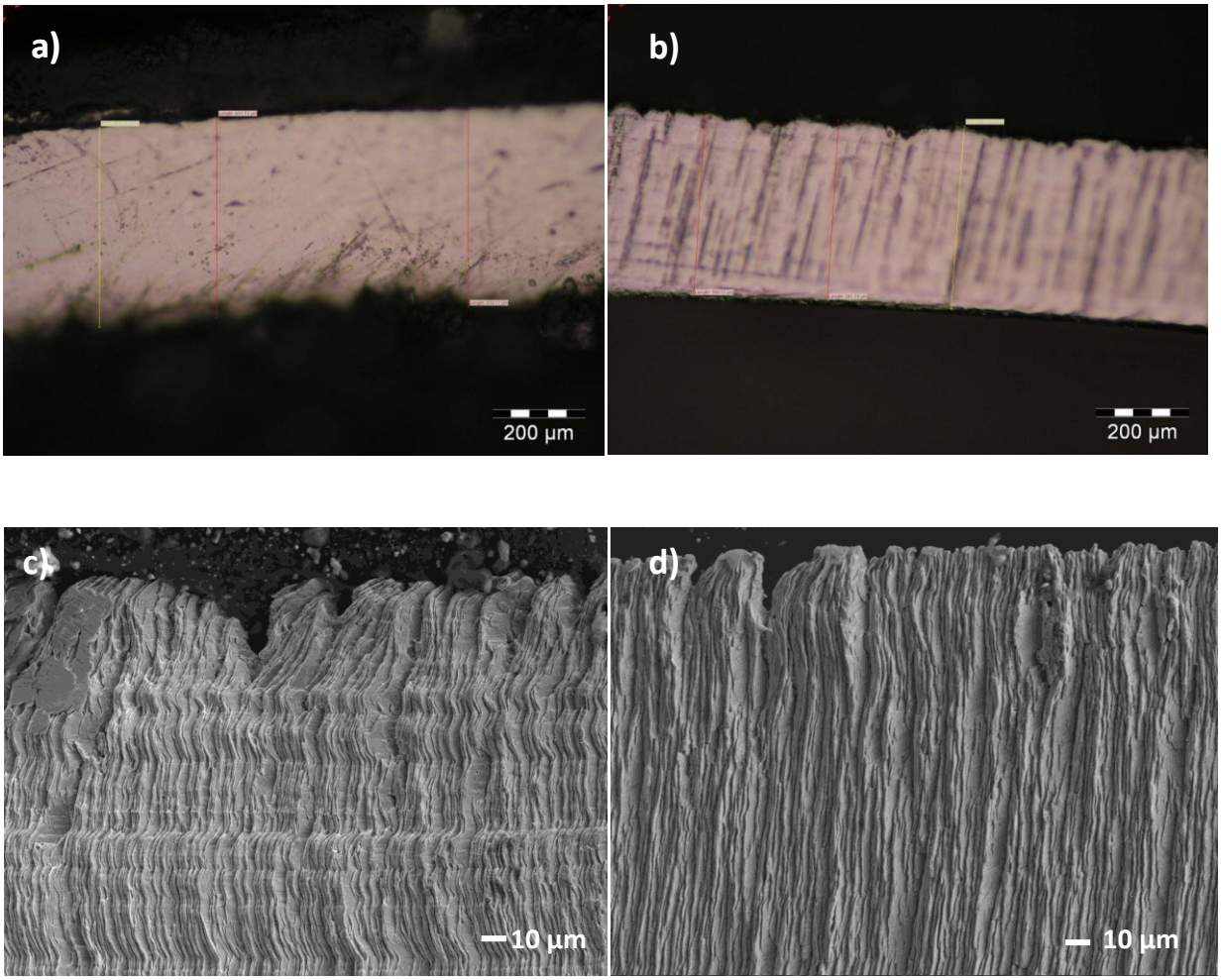

Figure 4-39 Optical micrograph of cutting chip at the free workpiece surface by a) CC650, b) CBN-100and SEM imaging c) CC650, d) CBN-100 at speed 100 m/min, feed 0.1 mm/rev, DOC 0.1mm

Figures 4–39c and d show the upper surface (free workpiece surface) of the chips, which is observed as jagged, with minute corrugations due to shear. Chips with slanting corrugations with lots of aperiodical cracks and outer edge breakages (into series of segments) were produced by the CC650 tool, very few outer edge breakages cab be observed with the CBN–100 tool. The upper side of the chips produced at cutting speed of 600 m/min are shown in Figures 4–40a (CC650) and b (CBN–100). The figure depicts a fully segmented chip where there is a more pronounced corrugation. At this cutting speed, the segment spacing becomes more periodic. The aperiodic variations in the segment spacing are as a result of thermal and elastic interaction between one and the next shear zones (Davies et al., 1997).

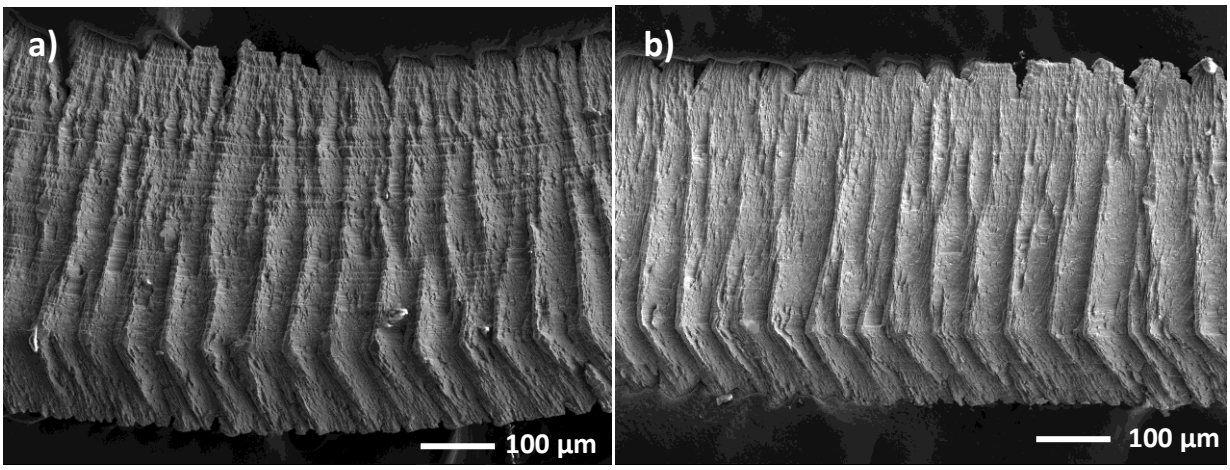

4-40 SEM micrograph of cutting chip by a) CC650 and b) CBN-100at 600 m/min, feed 0.1 mm/rev, DOC 0.1mm

The underside of the cutting chips produced by CBN–100 and CC650 cutting tools at the cutting speed of 100 m/min is shown in Figures 4–41and 4–42 respectively. The underside of chips produced by the CC650 tool (Figure 4–42) shows evidence of feed marks, debris (consisting mainly of broken pieces of the work material from the transferred layer) and small pits. Some of the chip removed is attached to the surface of the cutting tool by adhesion during the shearing process, while the chip undergoes plastic deformation. Similar trends were observed with the CBN–100 cutting tool as shown in Figure 4–41, except that the feed-marks were not pronounced. The EDS information of the chip produced by CBN–100 (Figure 4–41) shows an oxidation predominantly of elements in the work material and small traces of the cutting tool material with new compound such as SiO and AlO_3 formed. A similar result was obtained with the EDS information of the chip produced by CC650 depicting smearing mechanism of transfer film formation on the underside of the chip formed.

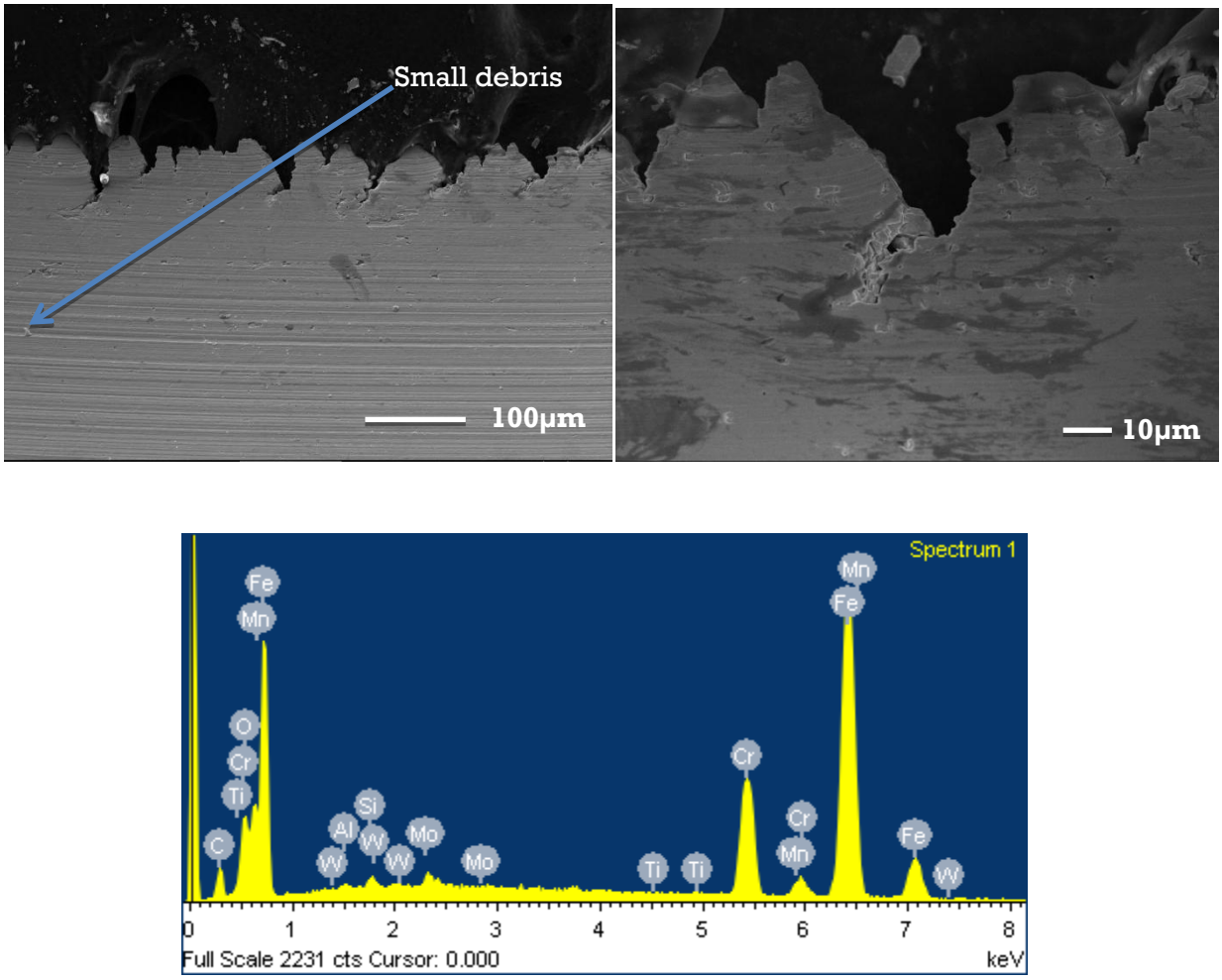

Figure 4-41 Underside SEM micrograph and EDAX pattern of cutting chips produced by CBN-100 at cutting speed 100 m/min

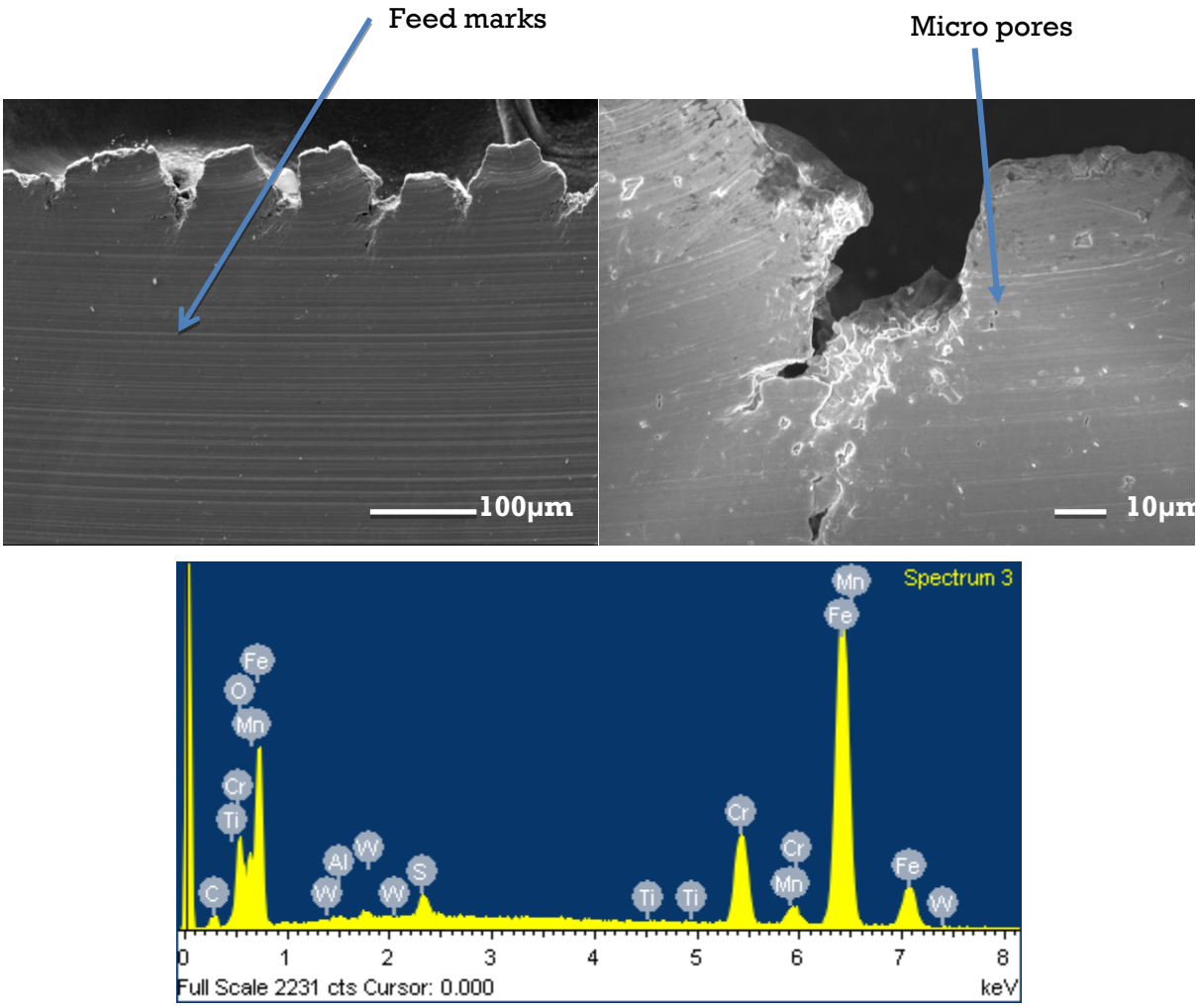

Figure 4-42 Underside SEM micrograph and EDAX pattern of cutting chips produced by CC650 at cutting speed of 100 m/min

The underside of the chip produced at cutting speed 600 m/min is shown in Figures 4–43a and b. White layer and debris were clearly observed in the underside of the chip. The intensity of the white layer and debris increased with increasing cutting speed resulting from excessive cutting tool wear and elevated cutting temperature at the cutting zone. During the machining of hardened steel parts, reports have shown appearance of white layers at the surfaces of both the workpiece and the underside of the chips (Chou and Evans, 1999; Poulachon et al., 2004).The formation of white layer is owing to microstructural changes in the chip, caused by the cutting tool, resulting from high mechanical energy and intense heat at the cutting zone (Salem, 2012).The white layer usually has high hardness (above 1000 HV) and is very brittle (Wang et al., 1999). The deep feed marks and white lines formed by the CC650 cutting tool are more pronounced owing to its rapid tool wear and abrasive marks on its flank face.

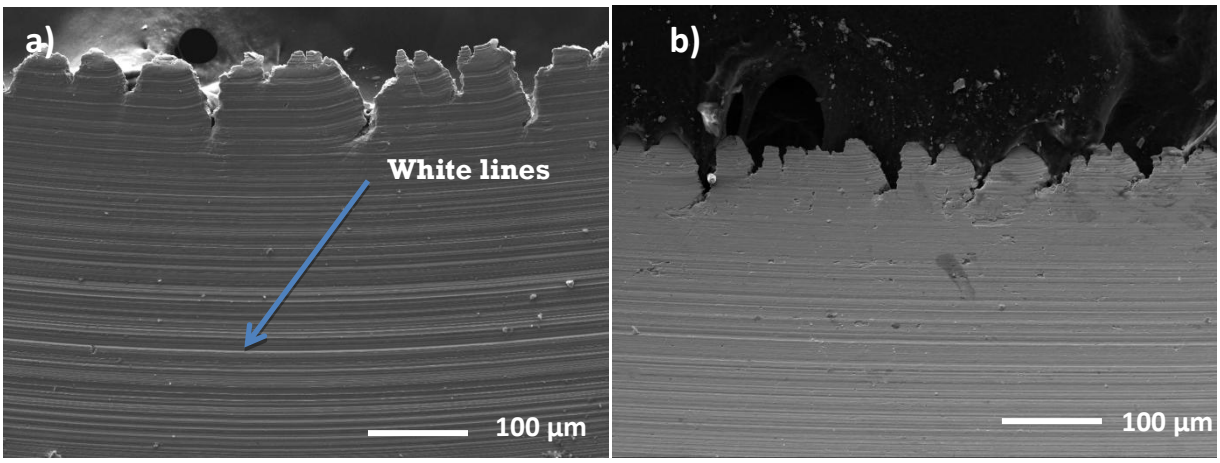

Figure 4-43 SEM micrograph of the chip underside a) CC650, b) CBN-100, at speed 600 m/min, feed 0.1 mm/rev and DOC 0.1 mm

Figures 4–44 and 4–45 present the optical micrographs of the main chip types observed at cutting speeds of 100 and 300 m/min respectively. At cutting the speed of 100 m/min, continuous chips were produced by CBN–100 and CC650 cutting tools, and they are characterized as non-oscillatory material flow. Slip band formation can be easily observed on the chips (see Figure 4–44b). Figures 4–45a and b show serrated or shear localized chips produced at the cutting speed of 300 m/min, and these chips are characterized as oscillatory material flow. The higher the cutting speed, the more the mean spacing of segmentation of the saw tooth (increased shearing bands) with considerable reduction in the width of the contact between each segments.

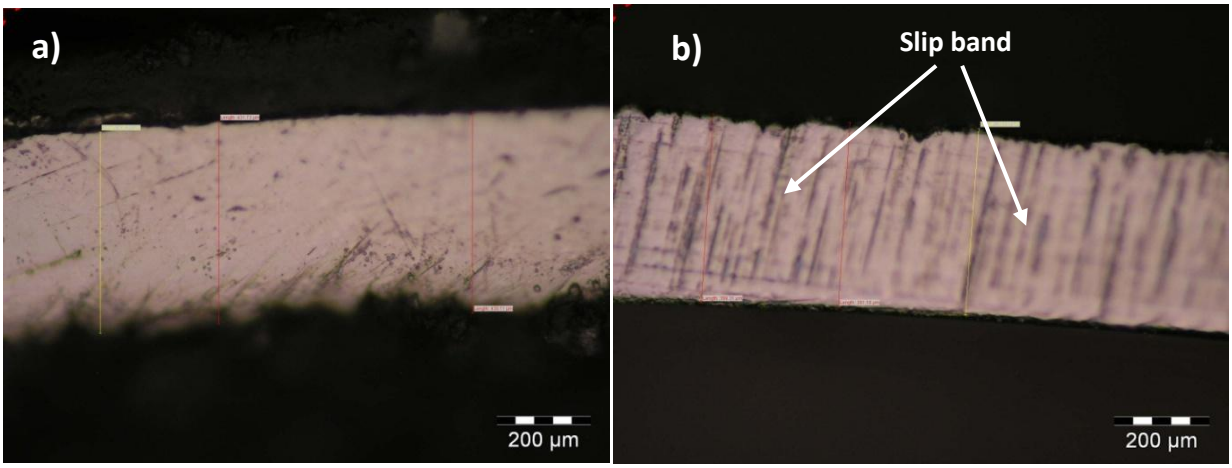

Figure 4-44Continuous chip produced by a) CC650 and b) CBN-100at 100 m/min

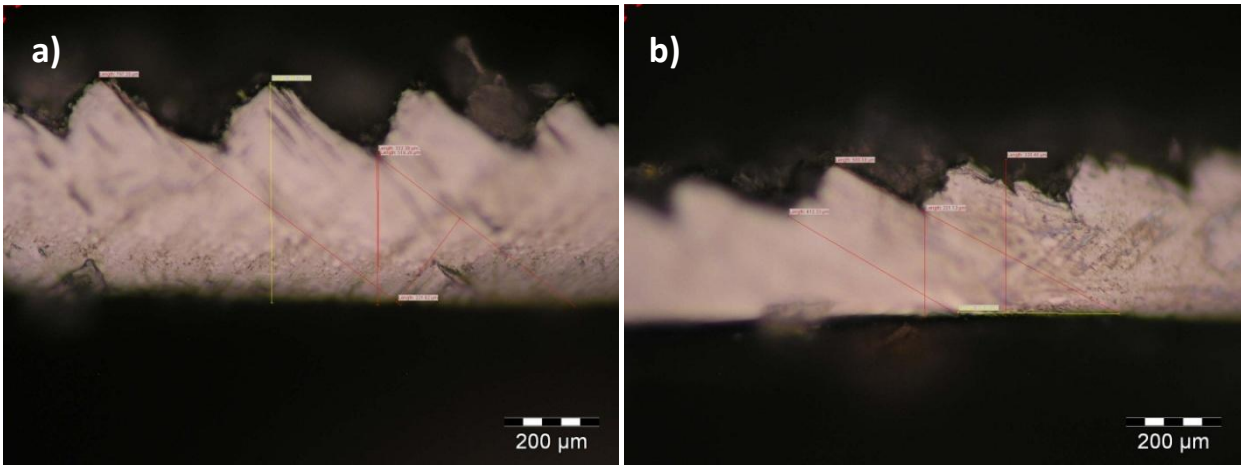

Figure 4-45 Serrated chip produced by a) CC650 and b) CBN-100 at 300 m/min

In hard turning, there are factors that favour the transition from continuous to saw-tooth chip formation; these include: increases in workpiece hardness, cutting speed, undeformed chip thickness, and flank land width with a decrease in tool rake angle. There is a gradual decrease in the average chip thickness during the transition from continuous to saw-tooth chip formation (Dogra et al., 2010).

Figures 4-46a–c show the SEM micrograph of the etched chip formed by the CBN–100 cutting tool at cutting speeds of 100 and 600 m/min, revealing the microstructure of the chip. The microstructure shows the distinct carbide grain in the martensitic matrix of the work material. The appearance of localized deformation of the primary deformation zone starts at low cutting speeds (Figure 4–46a) and becomes more visible at higher cutting speeds (Figure 4–46b). The parameters that mainly influence the chip morphology observed in this study are the cutting speed and the hardness of the material. In hard turning operations, high compression stresses occur on the work material and cutting tool (Dogra et al., 2010), because of the use of negative rake angle tools. Cracks instead of plastic deformation, was observed formed close to the chip primary shear zone as a result of the high compression stresses.
The intense shear localization in the primary deformation zone is as a result of the rise in the cutting temperature, which is a major contributing factor (Ezugwu and Tang, 1995; Salem et al., 2012). The primary shear zone and secondary shear zone are indicated in Figure 4–46b, with magnified view of these zones shown in Figures 4–47 and 4–48 respectively.

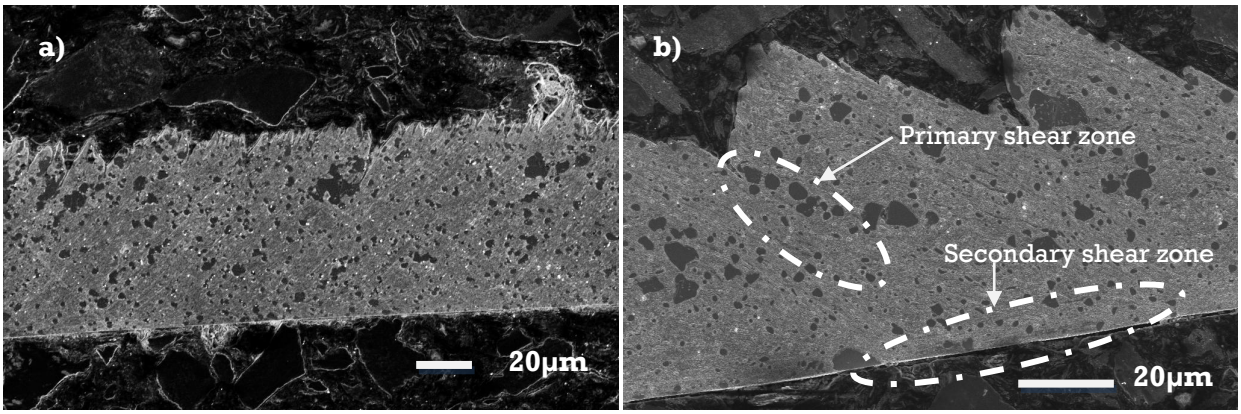

Figure 4-46 SEM image of etched chips formed by CBN-100 tool a) 100 m/min b) 600 m/min, feed 0.1 mm/rev, DOC 0.1 mm

The flow of plastically deformed tempered martensite lath (needle like structure) in the work material can be seen around the primary carbide in the primary and secondary shear zone in the microstructure of the cutting chips. The direction of the flow of the martensitic matrix is in the direction of the angle of shearing in the primary shear zone and horizontally in the secondary shear zone. For fully segmented chip (Figure 4–47 and 4–48), the mechanical properties of the material decreases during shearing in the primary and secondary shear zones, thus, possessing lower resistance to plastic deformation. The tempered martensite matrix is normally softer than the carbides, so they deform easily while the hardened carbide remained undeformed.

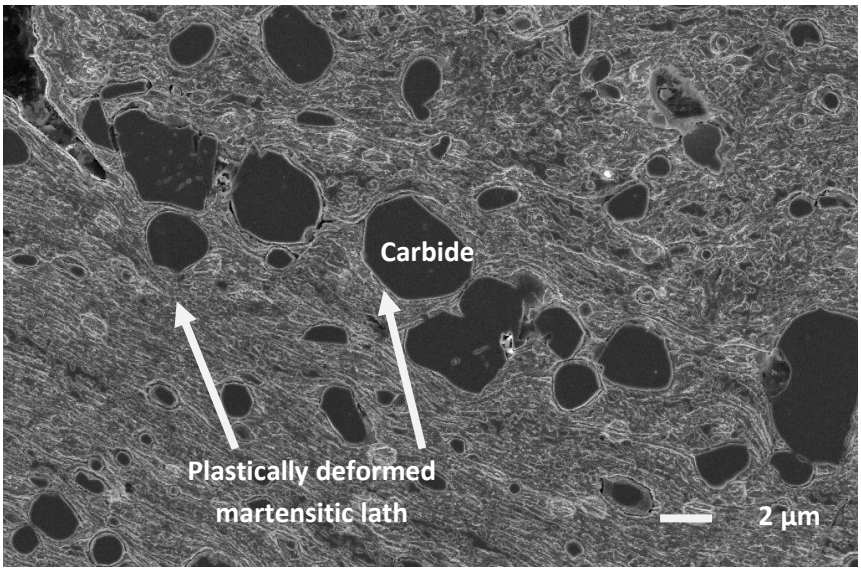

Figure 4-47 Enlarge view of primary shear zone (Magnification X 9,250)

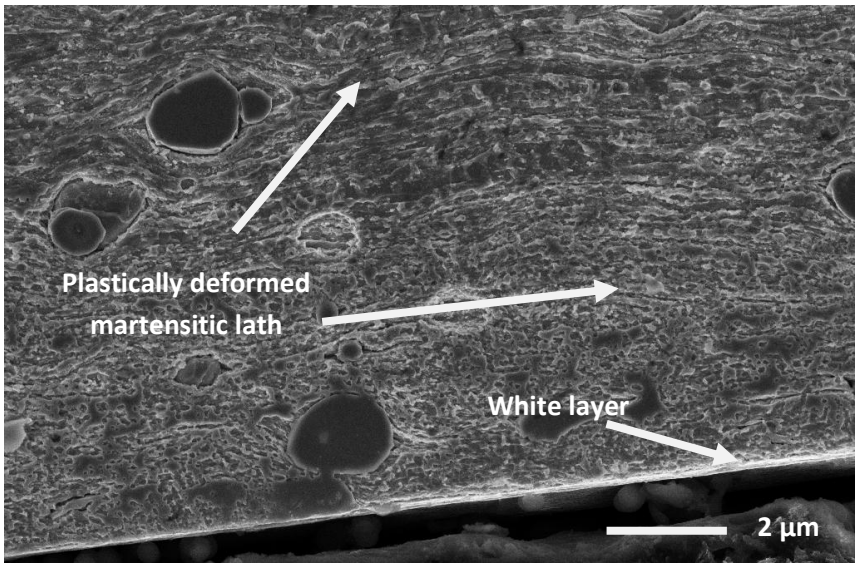

Figure 4-48 Enlarged view of secondary shear zone (Magnification X 22,000)

Cracks in the secondary shear zone were not observed in the chip sample investigated but evidence of clearly defined thin white layer was observed. Generally, white layer formation in the chip is common during hard turning and experimental investigations have been carried out to understand the properties and formation mechanisms of this white layer (Chou and Evans, 1999; Barry and Byrne, 2002; Morehead and Huang, 2007).

White layer is rapid microstructural transformation of the martensitic structure formed as a result of rapid heating from intensive heat sources localised in the field of cutting and quenching coupled with severe plastic deformation in the chip (Chou and Evans, 1999; Barry and Bryne, 2002; Salem et al., 2012).

The formation of white layer were also observed to be found on the machined surfaces of the workpiece investigated as a result of the combination of the factors such as the CBN–l00 tool with low thermal conductivity of the CBN–l00cutting tool and the rapid tool wear caused bu the high cutting speed.

Machining of the hardened stainless steel causes deformation with a decrease in the chip thickness as the cutting speed increases. The decrease in the thickness of the chips occurs during formation of segments.

Only the chip produced by the CBN–100 cutting tool was analysed statistically and the results are presented in this study. The relationship between the chip ratio (determined using Equation 3–7) and the cutting speed formed is shown in Figure 4–49. From the results, the chip thickness ratio observed is lower than 1 for both continuous and segmented chips.

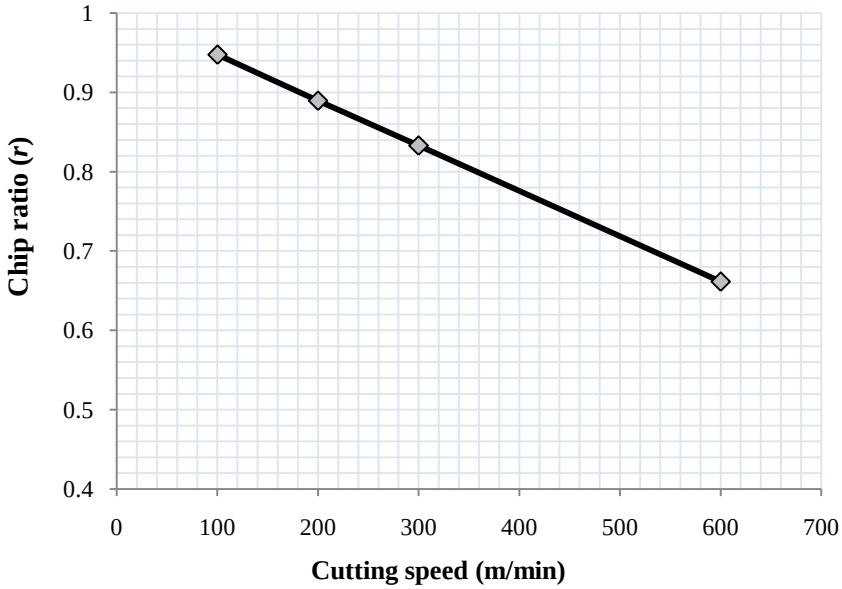

Figure 4-49 Evolution of cutting speed on chip ratio

Figure 4–50 shows the influence of the cutting speed on the shear strain (determined using Equation 3–11). As observed, the cutting speed shows greater influence in the shear strain and shear strain rate during segmented chip formation compared to its influence during the continuous chip formation. The plastic deformation within the localised areas of the segmented chip is quite high, which contributes to the rapid increase in the shear strain rate(determined using Equation 3–12) (see Figure 4–51). As deformation increases, there is an increase in the temperature in the shear zone, thus the shear strain hardening and the shear strain rate hardening increase the flow stress of the workpiece material in the shear zone (Qibiao et al., 2012). As observed, the intensity of plastic deformation significantly changes with increase in the cutting speed.

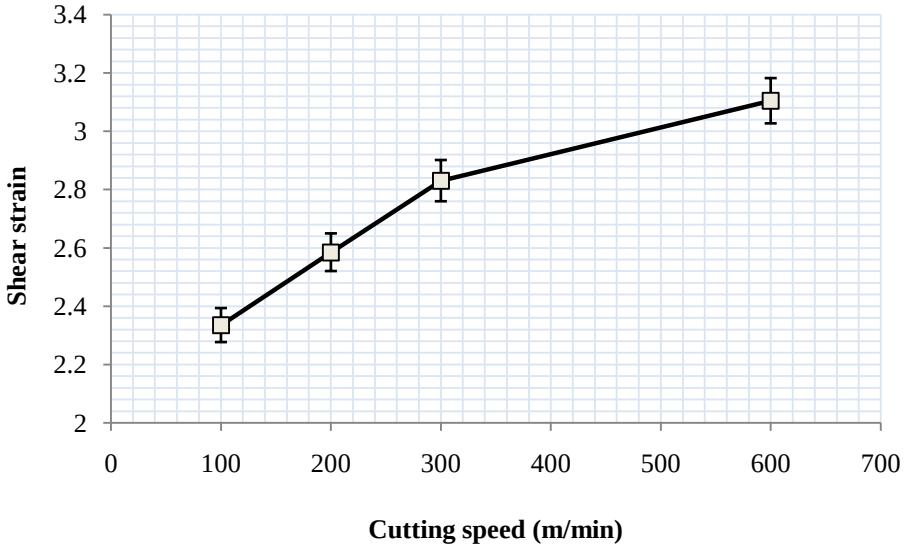

Figure 4-50 Influence of cutting speed on strain rate

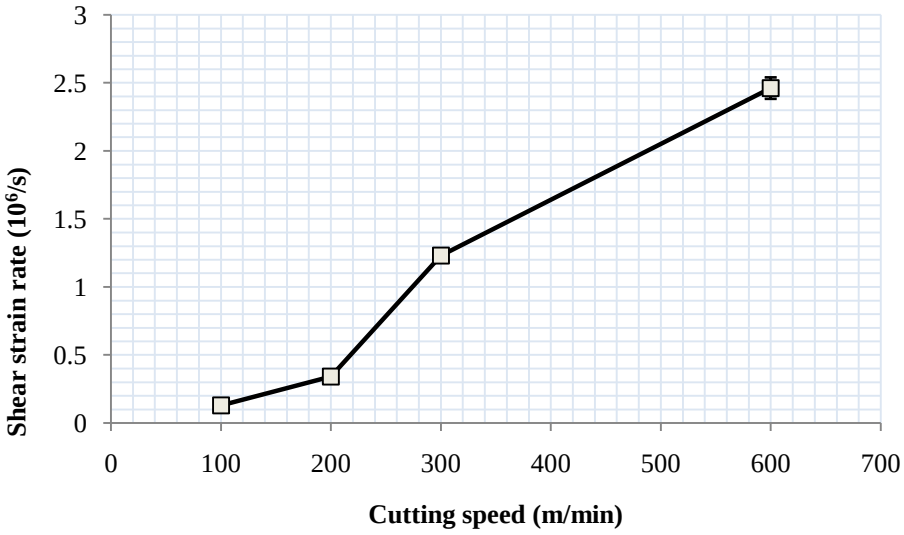

Figure 4-51 Influence of cutting speed on shear strain rate

The degree of segmentation is observed to increase as the cutting speed increases as a result of softening of the workpiece material, which leads to more adiabatic shearing in the primary zone of the chip formed, as seen with the chip formed at 600 m/min (See Figure 4–46) and this is confirmed in Figure 4–52.

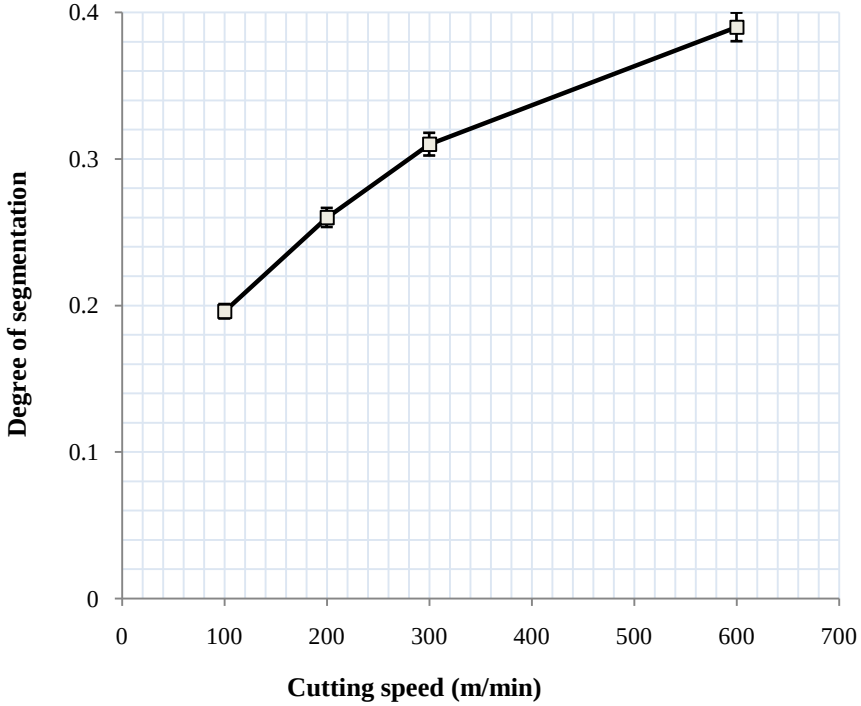

Figure 4-52 Degree of segmentation as a function of cutting speed for tool rake angle of -6º

4.5 MICROSTRUCTURAL CHARACTERISATION OF WORN CUTTING TOOL USING HRTEM

Two different samples from worn CBN–100 tool were selected for examination with an ultra-high resolution field emission scanning electron microscope (SEM), and transmission electron microscope (TEM), in order to understand the wear behaviour of the cutting tool through microstructural characterisation at submicron scale. Sample 1 was machined at cutting speed of 100 m/min, while sample 2 machined at 600 m/min. The choice of samples was to study the influence of the extreme cutting speed range on the degraded microstructure of the cBN cutting tool and observe possible chemical interactions between the cutting tool and the workpiece. The sample preparation procedures had been explained in Chapter 3.

4.5.1 SEM study (SAMPLE 1)

The SEM micrograph of the crater developed by sample 1 where a thin lamella was lifted out is shown in Figure 4–53 a. The thin lamella was taken out from an area close to the cutting edge of the cutting tool corresponding to an area where the temperature is expected to be the

highest. The chip flow direction, on the crater face of the cBN tool is indicated in Figure 4–53 a. From the figure, it is evident that there is a form of adhesion of the workpiece material on the crater of the cutting tool. The boundary layer between the adhered layer and the cBN tool is indicated in Figure 4–53b. The adhered layer is in full contact with the grains within the cBN tool. The adhered layer in the thin lift-out samples is in full contact with the grains within the cBN tool and is found to be in a stable condition, despite the sample preparation processing and handling of the samples. There is an indication of strong bond between the cutting tool and work material with no serious porosity or damaging in the boundary layer region between the tool and work material.

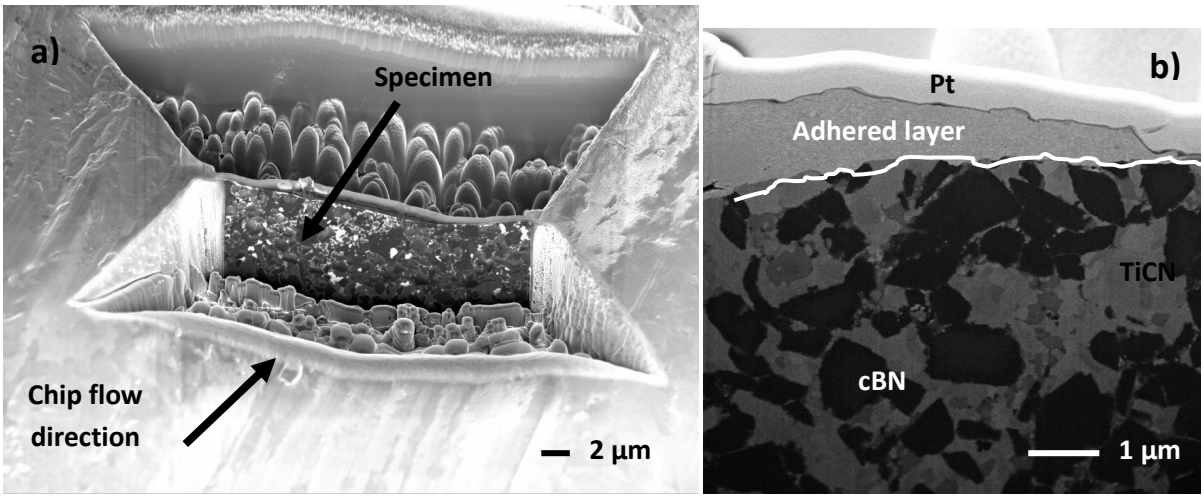

Figure 4-53 SEM micrograph of the specimen a) before lift out b) after lift out showing the adhered layer on cBN tool

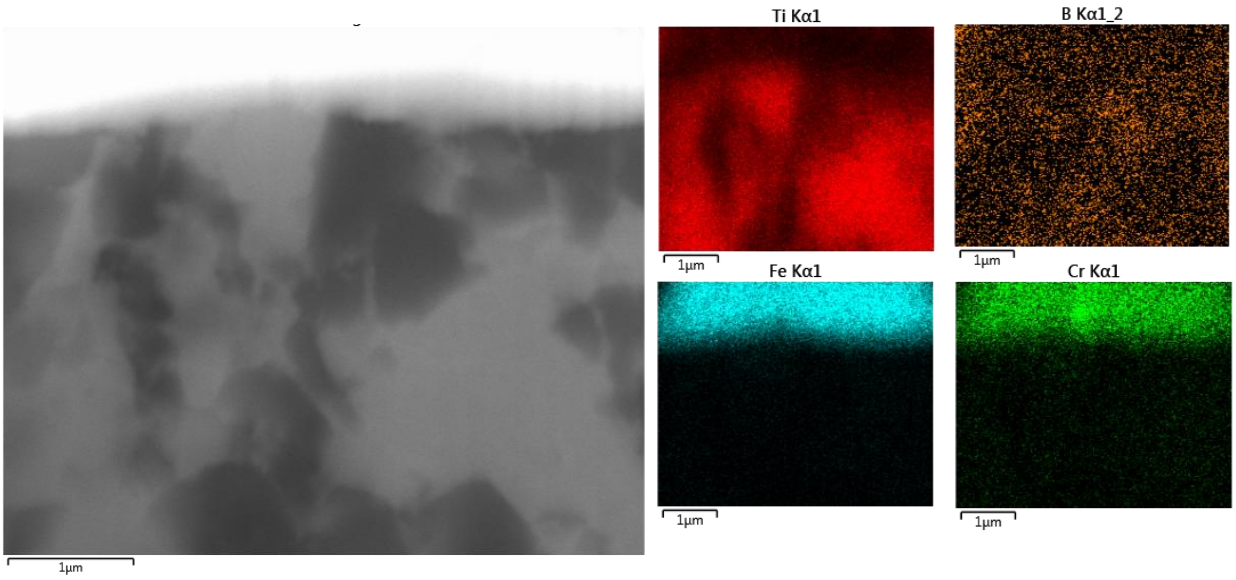

Figure 4-54 SEM micrograph and EDS mapping of specimen prepared by FIB-SEM

Figure 4–54 shows the SEM micrograph of the thin lift out specimen and the corresponding EDS elemental maps. The adhered layer thickness on the surface is about 1 µm in some areas and less than this in other areas resulting from the built up on the crater face of the cutting tool.

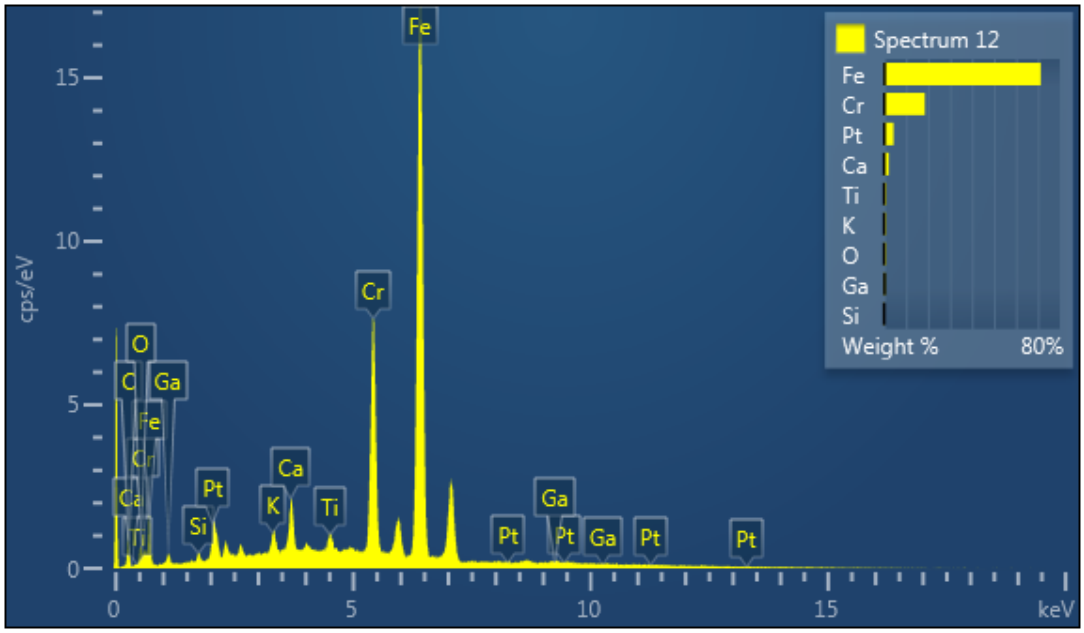

Figure 4-55 EDS analysis of work material

The elemental maps on the sample shown in Figure 4–54, confirm the presence of show the presence of Ti and B, in the cutting tool with Fe and Cr from the workpiece in the adhered layer; B is found to be in both the adhered layer and the cBN tool. The EDS point analysis of the adhered layer is shown inFigure 4–55, the adhered layer consist majorly of the work material that was transferred onto the surface of the cutting tool. Small traces (Ti) of the cutting tool identified the adhered layer. Most of the areas examined in the adhered layer consist of oxidised Fe. The predominant constituents of the work material in the boundary area to the cutting tool are Fe and Cr (Fe and Cr rich areas). These elements were also found in very small traces within the PcBN material but concentrated around the boundary between the adhered layer and the PcBN tool. Cr is found to be distributed in similar areas where Fe was found, but higher concentrations of Cr were found around the BN grains. There is also strong presence of oxygen in some other regions, most especially at the outer surface of the specimen. Similarly, some small traces of elements of the PcBN material were observed in the adhered layer, with large constituents of B and Al in the adhered layer. However, it is difficult to conclude the presence of chemical interaction of these elements from the work

material into the PcBN and vice versa with the SEM/EDX method due to the large probe diameter and also small amounts of elements (below 0.1 at %) are often difficult to detect.

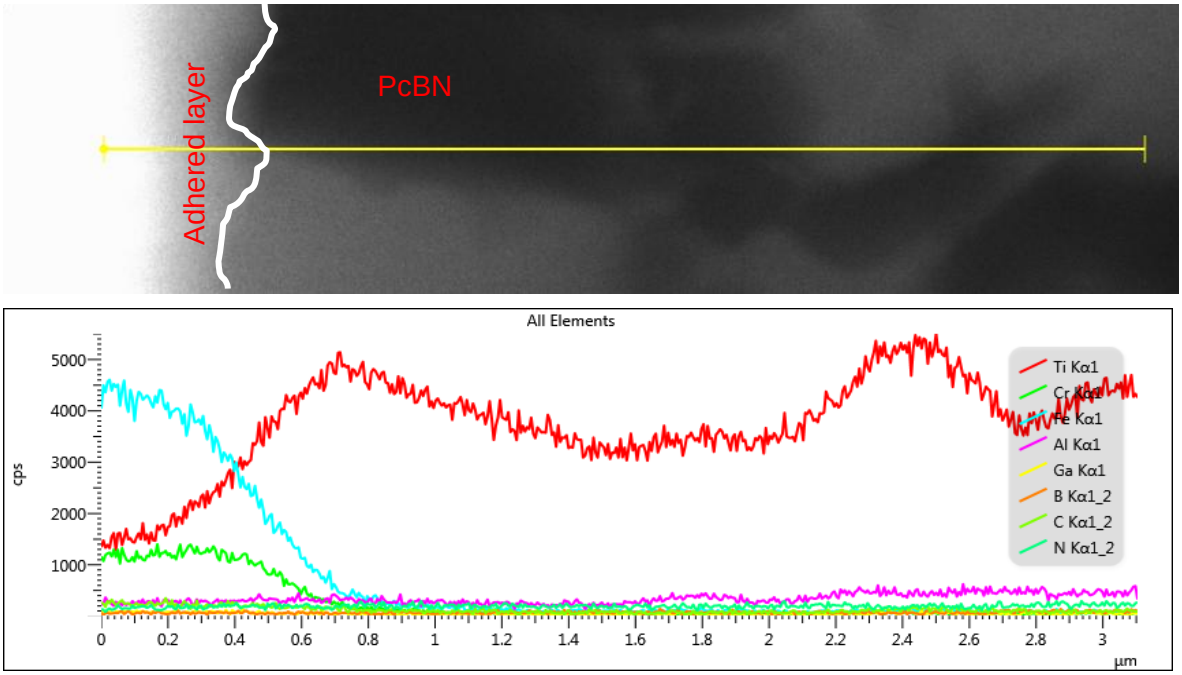

Figure 4-56 SEM Line scan diagram and EDAX analysis of sample 1

The SEM/ EDS line scan across the surface of the specimen in Figure 4–56. The figure shows the presence of Fe and Cr throughout the adhered layer and PcBN tool, with both elements decreasing after travelling for about 0.2 µm into the cBN tool. Fe concentration is found to be higher than the Cr in thecBN tool; which is attributed to its higher affinity to the PcBN material. Small traces of Ti were found more within the adhered layer, indicating some form of diffusion of Ti out of the cBN tool into the chip.

4.5.2 TEM study (SAMPLE 1)

Figure 4-57 shows the thin lamella cross-sectional STEM micrograph of the work material adhering on the PcBN cutting tool. The top surface contains the protective Pt layer, applied during FIB-SEM, followed by the adhered layer the cBN.

The EDS spot analysis of the lift-out specimen as indicated using A-F in Figure 4–58a and b shows presence of B, N, Ti, C, Al, O, Fe, Cr, Si, S, Mo. Table 4–1 shows the relationship between the constituents of work and cutting tool materials and the areas where they are

dominant. The small elements that were difficult to trace in using SEM were detected with the HRTEM. The Fe-rich areas were found in areas of TiC and AlB grains, with TiC having greater affinity for Fe in the work material as seen in Figure 4–59 b. The Fe in the work material had been shown to form Fe–Fe_2B eutectics with cBN (Klimenko et al., 1992), whereas, with its interaction with TiC binder, Fe–C pearlite-like structures were formed (Gimenez et al., 2007). According to Figure 4–59 b, the presence of high concentrations of Fe and oxygen in the microstructure, results to the possible formation of iron oxides. Si rich area was found in small quantities, most especially around the cBN grain boundary (Figure 4–59a). Si was not found in any other grain. There is tendency of Si being oxidised to be found as SiO_2 in the cBN grain areas. Similar observation was made by Chou et al., (2003) and Angseryd and Andren, (2011)**,** where the formation of SiO_2 and oxidised Fe was suggested during their investigation of adherent layer with XPS on the flank face. No traces of Fe or Cr were found in the vicinity of the cBN grain. The mobility of the Si and N in the work material may be a result of the effect of local thermal and pressure spikes during the turning operation**.** Oxidation of the elements was common in all the areas where the EDS spot analysis was conducted. O found in spot B shows that Fe-rich areas are oxidised in the surface. The oxidation is the sign of interaction of the Fe rich areas with the atmosphere during the turning operation.

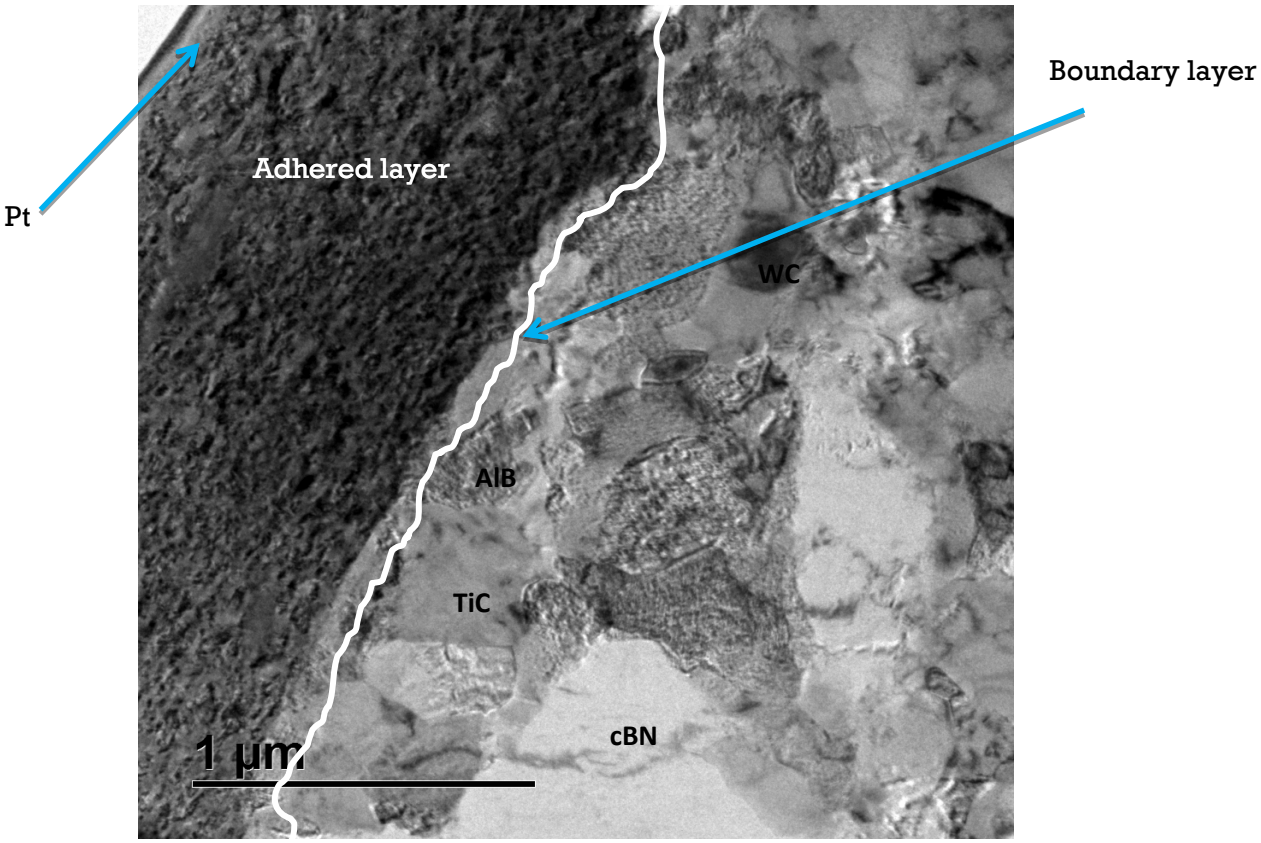

Figure 4-57 STEM micrograph of Sample 1

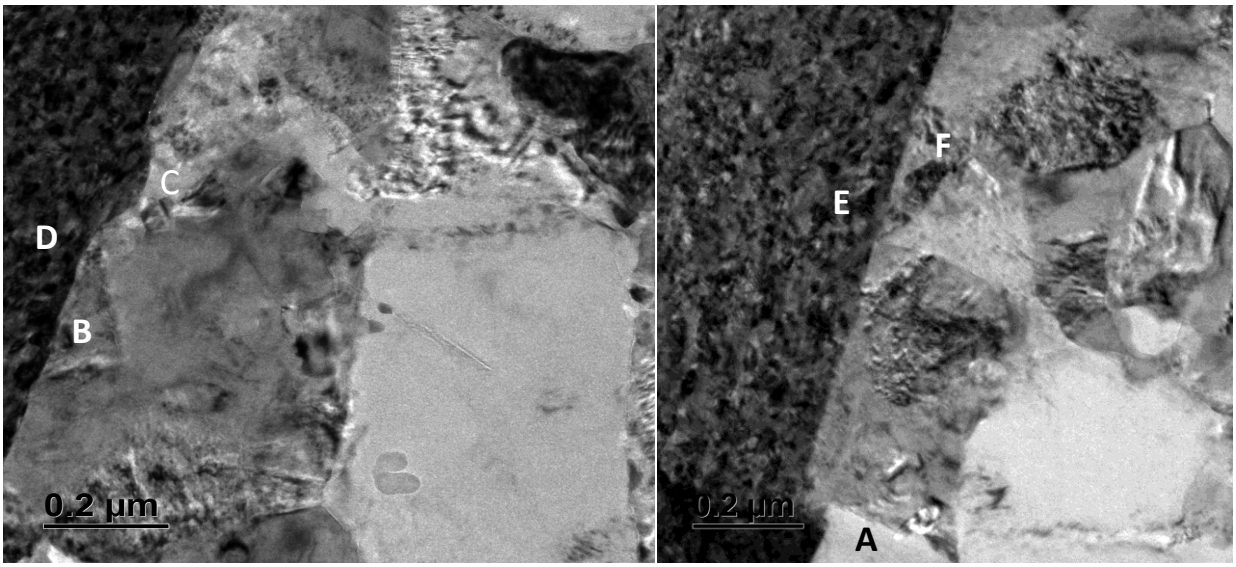

Figure 4-58 STEM micrograph of Sample 1 showing the EDS spot analysis

Table 4-1 EDS spot identification of most abundant elements in the sample

Spot	Area	Most abundant element	Remarks
A	cBN grain	B,N, Si, Ti	Si- rich area
B	TiC binder	Ti, Fe, O,C, Si, S	Fe-rich area
C	AlB	Al, Fe, Ti, O, C, B,N	High oxidation forming Al oxide, Fe rich
D	Adhered material	Fe, Cr, Si, Mo, C, O	
E	Adhered material	Fe, Si, Cr,	No traces of PcBN in work material
F	TiC binder + AlB	Ti, Al, Cr, Fe,C,	Cr-rich area

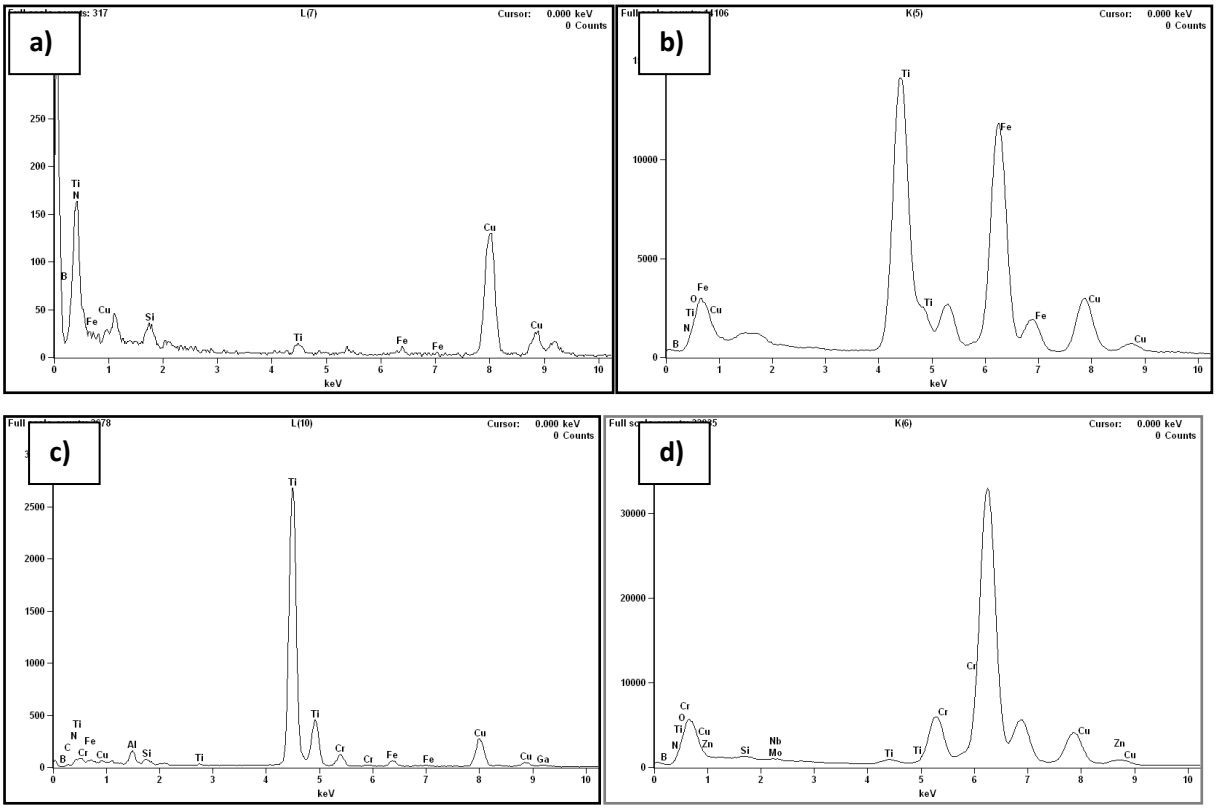

Figure 4-59 EDS Spot analysis of sample 1 lift-out specimen a) spot A, b) Spot B, c) spot F and d) spot D

No traces of B, N, Ti, Al at detectable levels were found in the adhered layer at areas close to the boundary area, with the PcBN cutting tool, though Zimmernamm et al. (1997) suggested the possibility of dissolution of BN into the flowing chip during tribochemical wear.

The SEM and TEM study clearly, confirm the strong chemical affinity of the work piece material with the CBN–100 cutting tool material even at low cutting speed where the cutting temperature at the chip–tool interface were expected to be much lower than when machined at high cutting speed.

The diffusion of elements (with formation of Fe–Fe_2B eutectics and Fe–C pearlite) in the work material into the PcBN tool most especially around its grain boundary could be responsible for the weakening of the grains and thus promoting grain pull out from the CBN–100 cutting tool during machining of the martensitic AISI 440 B stainless steel. The grain pull outs reduces the wear resistance properties of the cutting tool.

4.5.3 SEM study (SAMPLE 2)

The SEM micrograph of Sample 2 before lift out is shown in Figure 4-60. The adherent layer in Sample 2 is very thin (between 100–600 nm) compared to the ones found in Sample 1. When machining at much higher cutting speeds, there is a lot of crater wear on surface of the cutting tool. The elemental maps show the presence of Si, O, N, C, B, W, Cr, Fe, Ti and Al. The EDAX mapping analysis identified some traces of Fe and Cr in the adhered layer within PcBN tool from the workpiece material. Similarly, traces of Si can be found in the PcBN tool but cannot be fully established since it overlaps with other elements in the PcBN material. Presence of oxidation can be seen within the specimen, where both adhered layer and TiC grains exist (Figure 4–61).

In Sample 2, the cBN tool shows greater chemical affinity to the work material which was similarly observed by Angseryd et al., (2011) when machining at much higher cutting speed. This is a result of higher cutting temperatures between the tool chip interface when machining at high cutting speed, the elements in the work material have greater tendency of penetration into the cBN tool at elevated temperatures. From Figure 4–61, the SEM micrograph shows deeper penetration of Cr and Fe into the cBN tool which was not easily detected when machining at cutting speed of 100 m/min.

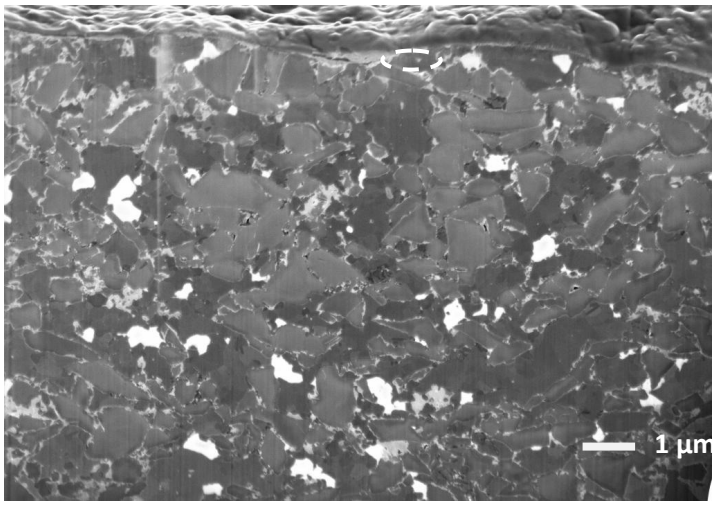

Figure 4-60 SEM micrograph of Sample 2

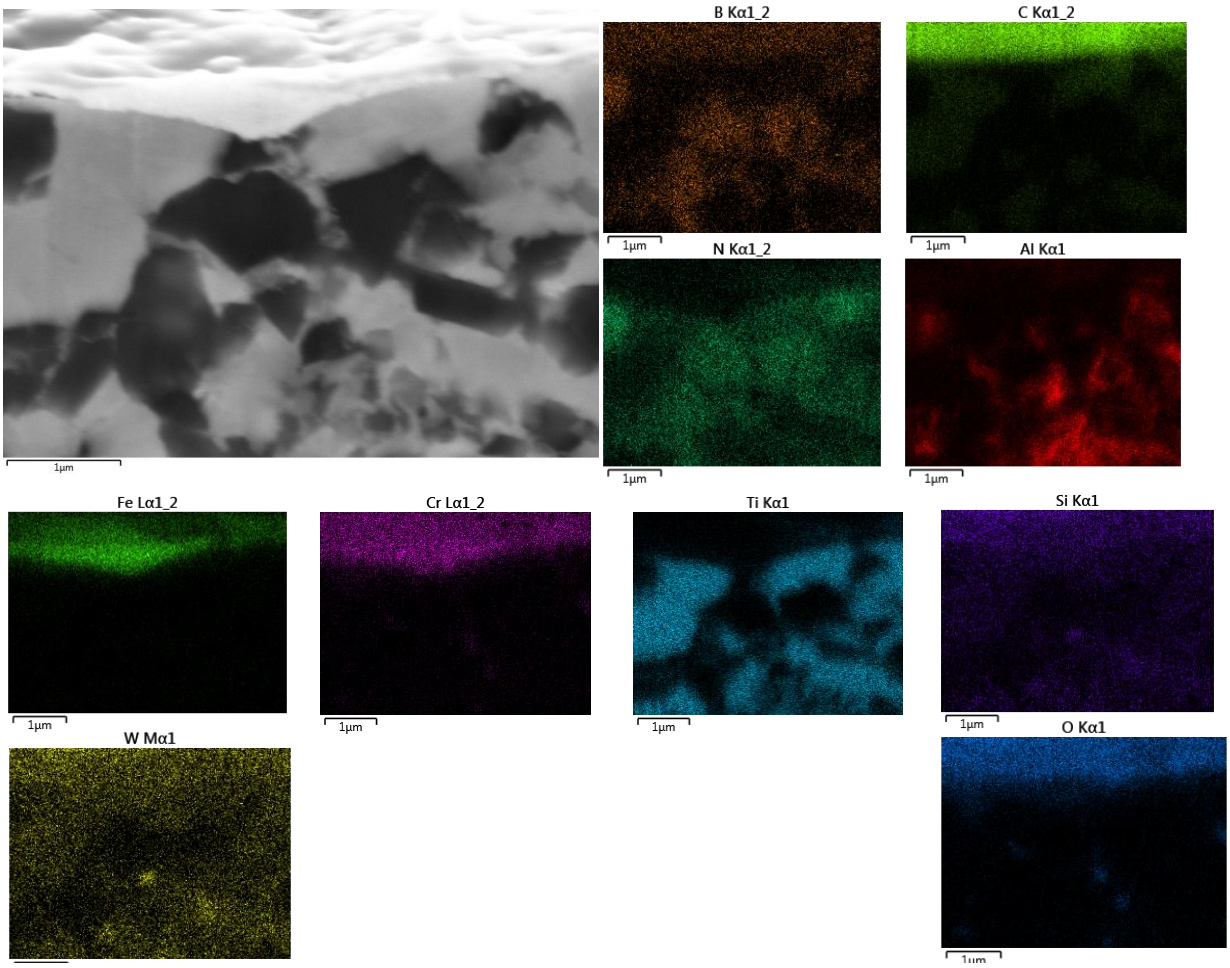

Figure 4-61 SEM micrograph and EDS elemental maps of sample 2

In the study by Barry and Byrne (2001), chemical wear was found to be the dominant wear mechanism with elements such as, Mn, Si, Al, O and S, in the adherent layer originating from the workpiece material. Consequently, inclusions such as, MnS, (Ca, Al) O and (Mn, Fe,

Ca)S, Si, were found in the adherent layer, which were not present in the steel workpiece material.

In this study, when machining using PcBN tool at high cutting speed, the dominant wear is found to be chemical wear; the wear is preceded by a chemical reaction in the contact zone, with some of the elements from the cutting tool detached and then removed by the chips flowing over the cutting edge. This phenomenon leads to rapid tool wear when machined at very high cutting speed and thus leading to rapid tool failure.

5 INDUSTRIAL APPLICATION

5.1 APPLICATION OF CBN TOOL FOR SPECIALISED FINISHING

For the purpose of industrial practice and comparison of the machining method, CBN-100 cutting tool performance was investigated as a finishing step during turning of hardened martensitic stainless steel.

5.1.1 Experimental Procedure

Hard turning experiments were carried out on martensitic AISI 440 B stainless steel with chemical composition as given in Table 3–1. The shape of cast before machining is given in Figure 5–1, while the machined final dimensions are given in Figure 5–2. The work material was cast close to the final dimensions, thus only a small volume of material needed to be removed by the turning process. The material was heat treated by quenching and tempering to achieve an average hardness of 44± 1.6 HRC. Machining trials were performed using a Hitachi Seiki – Hitech turn 23R III CNC lathe. Three different turning operations were selected for the machining of the part, the outer diameter (OD) turning, boring and grooving. To ensure good rigidity of the workpiece during machining, a clamping system was specially prepared by machining it to the shape of the workpiece, with small clearance to allow the workpiece to be easily inserted and removed.

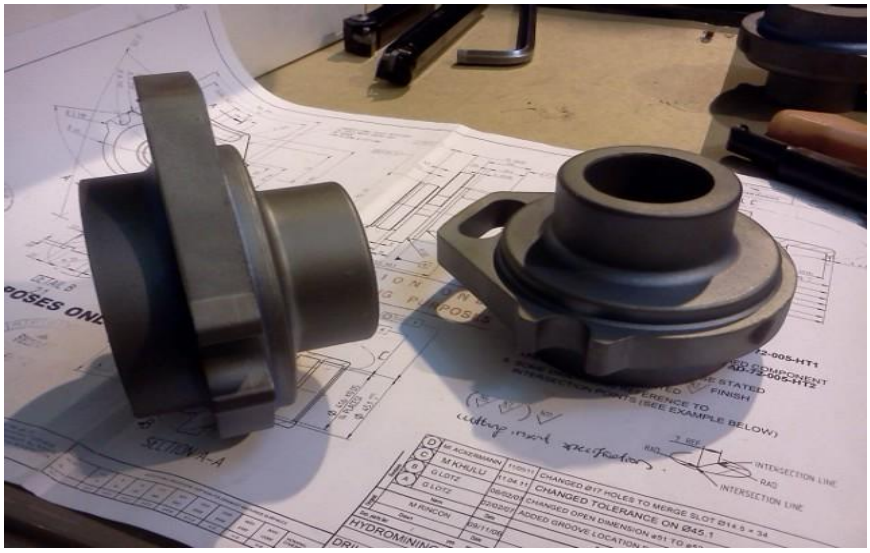

Figure 5-1Workpieces before machining

Inserts with three different shapes were used for the turning test. The inserts tool geometry and tool holders for roughing and finishing operations are given in Table 5–1. Rough turning was performed on the workpiece in the presence of coolant using an uncoated tungsten carbide cutting tool (IC 9250). The finishing was performed in dry cutting conditions using a CBN-10 cutting tool. The CBN-10 has the same material and properties as the CBN-100, but the material was brazed on a substrate. The three machining operations were outer diameter (OD) turning, facing boring, and grooving. All the inserts and tool holders were mounted in the turret before the commencement of the machining process so that the machining process was completed after a single cycle.

The machining process was performed at high speed, with the assumption that the parts would be mass produced. The machining conditions for roughing and finishing are given in Table 5-2. The depth of cut was kept constant at 2 mm for roughing and 0.3 mm for finishing. The sequence of the machining was facing, followed by OD turning, then boring and lastly grooving. The machining operations were repeated for the production of six identical parts.

After the end of the turning test, component surface finish was measured using a diamond stylus contact profilometers, in a two-dimensional (2D) and three-dimensional (3D) arrangements. The3D topographic maps of the machined surfaces were produced using scanning technique and the 3D measurements were determined over a scanned area of 10 mm × 0.5 mm by the means of a profilometer.A set of the 2D roughness parameters was determined by simple roughness measurements using a shop floor T8000 (Hommel Tester) instrument using probe TKU 300. Moreover, 3D measurements were carried out on the scanned area of 10 mm X 0.5 mm (OD) and 1.5 mm X 0.5 mm (groove) by means of the profilometer. The optical 3D image of the OD was taken using an Olympus LEXT OLS410 3D laser measuring microscope.

Table 5-1Insert geometry and tool holder with designated ISO code

OPERATIONS	INSERT GEOMETRY	TOOL HOLDER
Boring	WNGA 080408S	A25R PWLNR08
Facing and OD turning	WNGA 080408S	PWLNR 2020 KO8
Grooving (External)	LCMF 160304-0300E-LF	CFIR 2020 K03
Grooving (Internal)	LCGN 130304.0300S-LF	A20R-CGFR 1303

Table 5-2 Machining conditions

	Roughing				Finishing			
	Facing	**OD turning**	**Boring**	**Grooving**	**Facing**	**OD turning**	**Boring**	**Grooving**
Speed (m/min)	150	150	200	300	350	350	500	400
Feed (mm/rev)	0.35	0.35	0.15	0.1	0.1	0.1	0.1	0.1

5.1.2 Results and discussion

The final part machining sizing requirements with their tolerances are given in Figure 5–2. The image of the part after machining is shown in Figure 5–3.The surface roughness of the machined parts was measured in areas as indicated in Figure 5–3, with an average of five different points recorded. The average surface finish Ra of the outer diameter corresponds to 0.545$\pm$ 0.003 µm and the groove of the part 0.37 $\pm$ 0.002 µm. A lower value of surface roughness (about 32 % lower) was recorded for the bore of the component due to the machining process that was applied. The feed of the tool is only applied in the horizontal direction The surface roughness corresponds to the N6 and N5; ISO 1302: 1992 code (ISO CODE) which is applicable for bearing surfaces produced by grinding.

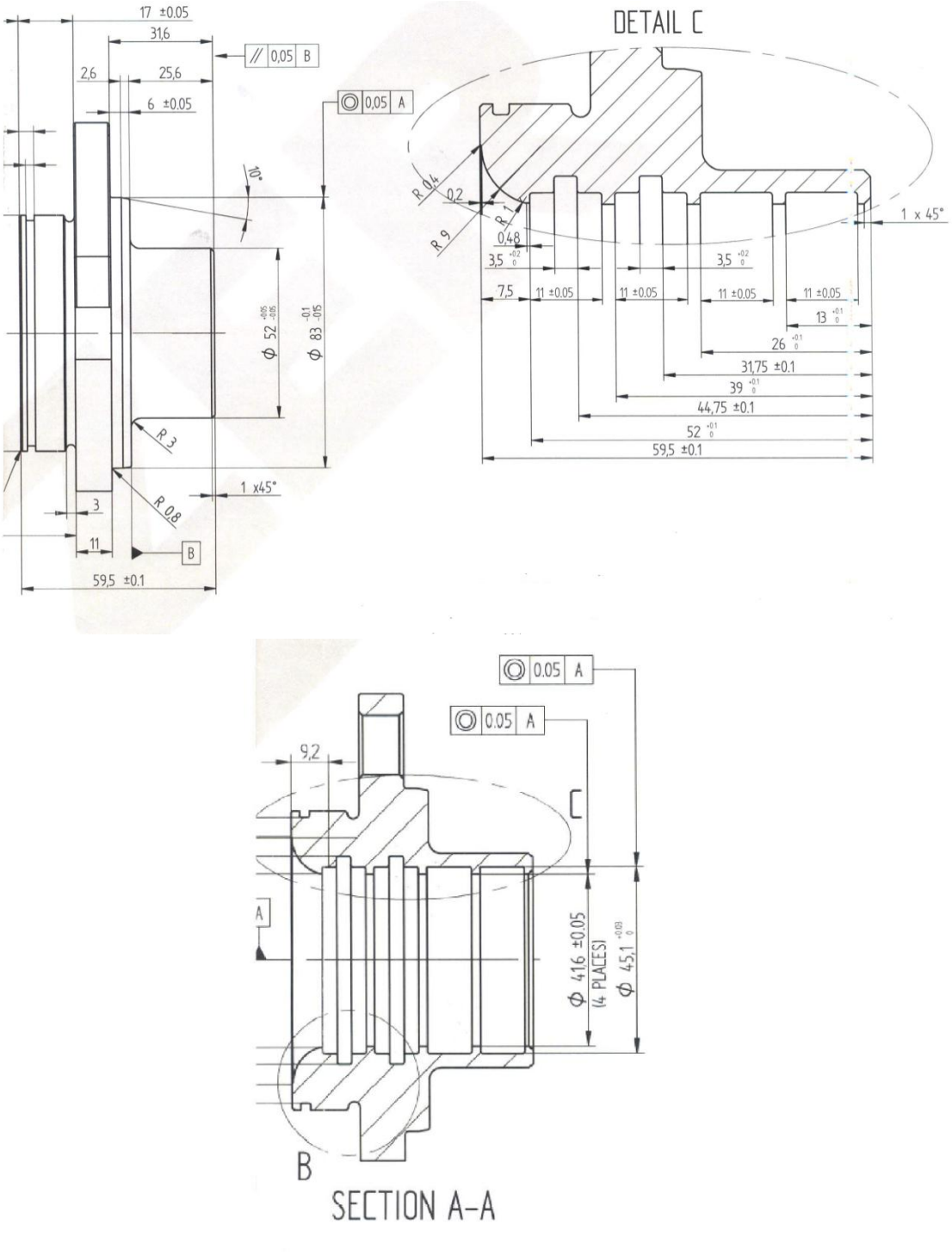

Figure 5-2 Detailed dimensions of final component, showing the part dimensions and tolerances

An measured 2D profiles and 3D topographies of the surfaces OD and bore are presented in Figures 5– 4 and 5–5 respectively. The measured 2D parameters (average of the parts machined) are presented in Table 5–3.

The ratio of Rt to Rz for the OD and groove of the machined components were about 1.466 and 1.083 respectively.The surface roughness peak height parameter Rp, showed a correlation with the maximum contact deformations, which are normally obtained during machining of rough surfaces. Thus, theratio Rp/Rt and Rv/Rt relatesthe surface profile resistance to abrasive wear and deformation between the contacting surfaces (Grzesik and Wanat, 2006).

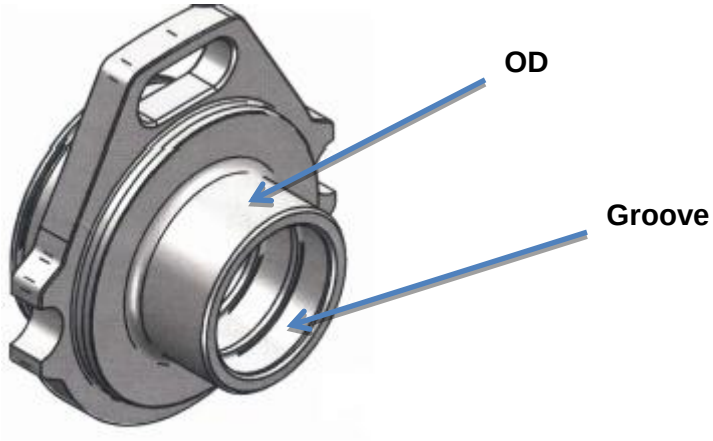

Figure 5-3 Points on machined components indicating areas where surface roughness were measured

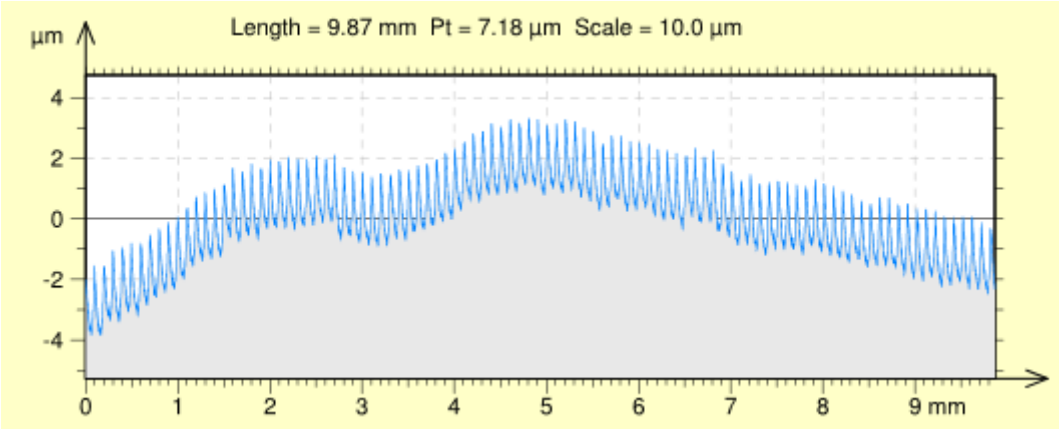

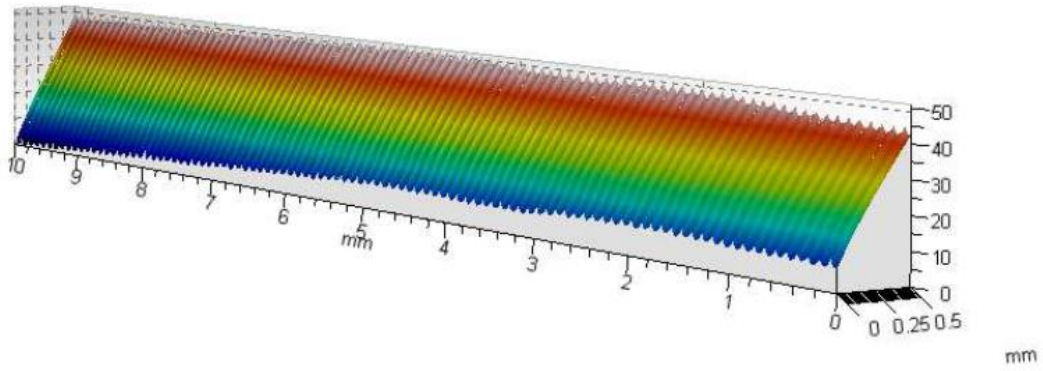

Figure 5-4 2D profiles and 3D topographies of OD Surface

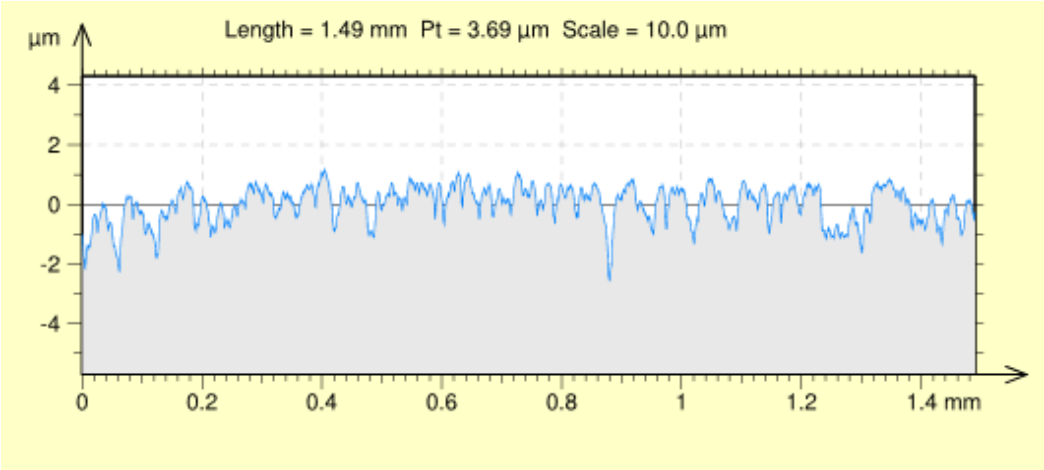

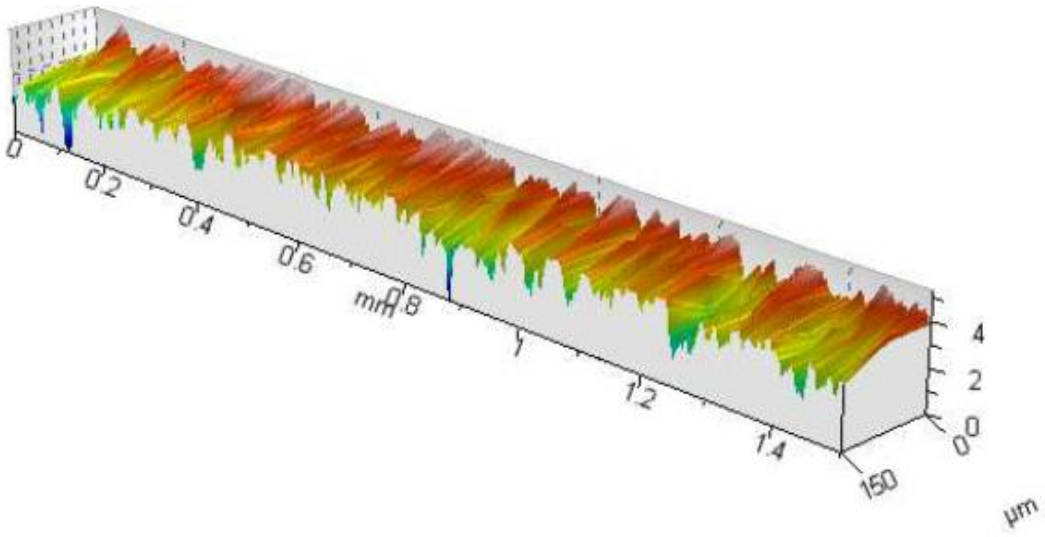

5-5 2D profiles and 3D topographies of the groove

Table 5-3 2D Parameters of Surfaces OD and bore

Parameters	Surface OD (µm)	Surface groove(µm)
$\mathbf{R_t}$	3.49	2.73
$\mathbf{R_z}$	2.38	2.52
$\mathbf{R_p}$	0.838	1.54
$\mathbf{R_v}$	1.55	0.975
$\mathbf{R_a}$	0.545	0.370
$\mathbf{R_q}$	0.644	0.472

Figure 5-6Component after machining

This result showed that a good surface finish can be produced using the cBN cutting tool in industrial machining conditions. The hard turning operations using cBN can be used for substituting traditional machining operations that involve the use of a grinding process after the turning operation is carried out. Consequently, the roughness falls within the high precision hard turning as required by the component after it would have been subjected to both turning and grinding, thus eliminating the grinding step necessary to manufacture this component.

The dimensional and geometrical accuracy of some selected areas of the machined component were measured after machining five identical parts, to observe deviation of the actual machined values from the dimensional requirements stipulated in the component design. The

dimensional deviation of the measured parts of the component in relationship to the length, diameter and concentricity are given in Table 5–4. The concentricity shows a maximum deviation of about 1 µm from the required deviation, the deviation in the straightness or length was between 14 and 18 µm, and the geometric deviation was between 0.135 and 0.21 µm. The results obtained confirmed an achievable and acceptable tolerance range of IT 5 within the machine tool shop during mass production of similar components.

Table 5-4 Dimensional deviation from specified

Characteristics	Size (mm)	Error (mm)
Length	31.75 ± 0.1	0.018
Diameter	52 ± 0.05	0.014
Length	11 ± 0.05	0.0135
Concentricity	0.005 A”	0.001
Diameter	45.1± 0.03	0.016
Diameter	41.6± 0.05	0.0206

The tight tolerance is as a result of the high stiffness and accuracy of the CNC machine coupled with the excellent properties of the cBN cutting tool, such as high abrasion and thermal shock resistance (Matsumoto et al., 1999; Bryne, 2003).

The overall surface finish and dimensional accuracy generated during the application of CBN-10 for machining the specified shape shows a component acceptable tolerance range with good surface finish similar to that of a grinding operation.

6 CONCLUSIONS AND RECOMMENDATIONS

6.1 CONCLUSIONS

In the manufacturing industry, components with high surface finish and precision are often required. In ensuring accurate reliability and lifetime during functionality of these parts, the surfaces are generally hardened. Hard turning provides the means for finish production of steels for achieving good geometrical machined part accuracy and surface finish using tougher tools (ceramics and PcBN) with high abrasion resistance and high heat conductivity.

The clearly unsatisfactory level of acceptance, by industry, of hard machining technology can be attributed partly to insufficient knowledge of tool wear, the component behaviour of hard machined surfaces, and the uncertainty about the attainable accuracies-to-size of parts machined. Little research has been done to explain the wear mechanisms of mixed alumina and PcBN cutting tools during hard turning of AISI 440 B stainless steel.

In the research reported here, the wear mechanism, cutting forces, surface roughness, and chip formationmechanism during hard-turning of martensitic AISI 440B stainless steel, using both mixed ceramic and cBN cutting tools, were studied. Investigation of the microstructure and chemical properties of the worn cutting cBN tool after machining is also presented in this study. The following conclusions can be drawn.

The cutting speed has the more significant effect on the flank wear than the depth of cut and the feed rate, where significant wear was observed with an increase/decrease in the cutting speed. Observing Figure 4–9 for CC650 cutting tool, for a given cutting length, flank wear appears to decrease as the feed rate increases. In the case of CBN–100 (Figure 4–10), flank wear initially decreases as feed rate increases from 0.05 to 0.1 mm/rev, and then increases as the feed rate is increases to 0.15 mm/rev. The high tool wear observed with low feed rate was attributed to the severe tool vibration experienced while machining at this feed. Feed rate of 0.1 mm/rev is however, recommended for finish turning owing to its moderate tool wear.

The ratio of the metal removed per unit flank wear is higher for the cBN tool at all cutting speeds. This is as a result of its better wear resistance, because of its high hot hardness and ability to retain its strength at higher cutting speeds and feed rates. The existence of adhesion and crater wear was found in the rake face of the cBN cutting tool, hence the investigation to

establish chemical interaction between the work material and the cutting tool at all the cutting speeds tested.

Tool wear is terminated by the wear on the flank face. The failure of mixed ceramic is predominantly by abrasive wear and cratering, while cBN fails by abrasive, adhesive and diffusionwear. The abrasive wear is caused by hard carbides particleswithin the *martensitic* matrixof the work material and pulled-out grains from the tool material.

The radial cutting force was found to be the highest as observed in the experiments which is typically observed during hard turning. Increase in the cutting speed leads to a decrease in the cutting forces caused by increase in the temperature at the cutting zone, thus leading to softening of the work material.

Better surface roughness Ra is produced by the mixed alumina tool but this material yields poorer surface quality with inclusions and debris on the machined surface, when compared to the surface produced by the PcBN cutting tool. The minimum and maximum values of the surface roughness values (Ra) of 0.51 and 1.13 µm and 0.63 and 1.44 µm were recorded for the mixed alumina and PcBN cutting tools respectively.

A simple method for determining the out of roundness and dimensional accuracy of the workpiece was developed. The dimensional accuracy of the machined part was correlated with the cutting tool wear to establish the effect tool wear on dimensional accuracy. Better dimensional accuracy of the machined part was obtained with the PcBN cutting tool compared with the one obtained by mixed alumina tool. This is a result of the better wear resistance of the PcBN cutting tool, since tool wear directly affect the geometrical deviation of any machined component.

The cutting chips produced are long, continuous and serrated at low cutting speeds for both the tools, but serrated and segmented as the cutting speed increased beyond 150 m/min. However, the chips formedwith the mixed ceramic tool showed a darker surface, resulting from oxidation caused by the higher temperatures generated during the machining process.

The chip formation mechanism for the work material (AISI 440B stainless steel) was developed with focus on the serrated chip model. The study observed the influence of the cutting speed on the chip ratio, shear strain, shear train rate and degree of segmentation of the chips formed. Microstructural analysis of the shear localized band during serrated chip

formation, governed by high speed and high temperature during the cutting process was investigatedto reveal deep understanding of the mechanism of the chip formation.

There was a gradual and continuous decrease in the average chip thickness during the transition from continuous to saw-tooth chip formation.

The appearance of localized deformation of the primary deformation zone started at low cutting speeds and became more visible at higher cutting speeds.

The flow of plastically deformed tempered martensite lath (needle like structure) in the work material could be seen around the primary carbide in the primary and secondary shear zone of the cutting chips. The direction of the flow of the martensitic lath was in the direction of the angle of shearing in the primary shear zone and horizontally in the secondary shear zone. The tempered martensite lath is normally softer than the carbides, so they deform easily with the hardened carbide remaining undeformed.

Cracks in the secondary shear zone were not observed in the chip sample investigated but evidence of clearly defined thin white layer was observed.

During machining of the work material, there was a decrease in the chip thickness as the cutting speed increased. The decrease in the thickness of the chips occurred during formation of segments; the chip ratio was lower than 1 for both continuous and segmented chips.

The degree of segmentation increased as the cutting speed increased as a result of softening of the workpiece material, which lead to more adiabatic shearing in the primary zone of the chip formed**.** Long and thin chips were formed with lower equivalent shear strain as opposed to turning soft steel.

From the SEM study, the elemental maps showed the presence of Ti, B, from the cBN tool and Cr, Fe, from the workpiece in the adhered layer. The EDAX point analysis identified the adhered layer consisting majorly from the workpiece material. Most of the areas in the adhered layer consisted of oxidised Fe. The predominant constituents of the work material in the boundary area to the cutting tool are Fe and Cr. These elements were also found in very small traces within the PcBN material but concentrated around the boundary between the adhered layer and the PcBN tool. Cr is found to be distributed in similar areas where Fe was found, but higher concentrations of Cr were found around the BN grains. Similarly, some

small traces of elements of the PcBN material were observed in the adhered layer, with constituents of B in the adhered layer. However, it is difficult to conclude the presence of chemical interaction of these elements from the work material into the PcBN and vice versa with the SEM/EDX method due to the large probe diameter and also small amounts of elements (below 0.1 at %) are often difficult to detect.

The SEM/ EDS line scan across the surface of the specimen showed the presence of Fe and Cr,in both the adhered layer and cBN tool; with Fe higher than Cr in the cBN tool. Small traces of Ti were found within the adhered layer indicating possible diffusion of Ti out from the cBN to the chip.

The small elements that were difficult to trace in using SEM were detected with the HRTEM. The TEM micrograph of the cross-sectional thin lamella showed that the boundary layer had a smooth profile with no sharp edges. The EDS spot analysis of the boundary layer in both adhered layer and the PcBN tool showed the presence of B, N, Ti, C, Al, O, Fe, Cr, Si, S and Mo. The Fe-rich areas were found in the vicinity of TiC and AlB grains, with TiC having greater affinity for Fe in the work material. Si-rich areas were also, though in small quantity, especially around the grain boundary.

The EDS maps of the sample obtained from the worn PcBN cutting tool used for machining at cutting speed of 600 m/min showed greater penetration of elements such as Fe and Cr into the work material compared to the sample obtained after machining at cutting speed of 100 m/min.

The diffusion of elements (with formation of Fe–Fe_2B eutectics and Fe–C pearlite) in the work material into the PcBN tool most especially around its grain boundary could be responsible for the weakening of the grains and thus promoting grain pull out from the CBN–100 cutting tool during machining of the martensitic AISI 440 B stainless steel. The grain pull outs reduces the wear resistance properties of the cutting tool, thus promoting rapid tool wear most especially at high cutting speeds.

This work clearly demonstrated that the PcBN cutting tool can be applied successfully for mass production of component in the manufacturing industry, where acceptable dimensional tolerance and surface finish can be obtained. The grinding process required for producing the

component investigated was completely eliminated with the use of the cBN tool applied, when machined at optimised machining parameters and rigid machine tool set-up.

The knowledge generated in this work should contribute towards improved design and processing of cutting tools, especially mixed alumina and PcBN for use in the machining of hardened stainless steel.

6.2 RECOMMENDATIONS

Future research is required to address the gaps and limitations presented in this work. The suggested recommendations are presented below.

The application of other cutting tools such as carbides and modified cutting tool can be applied in future study to understand its applicability during hard turning of martensitic AISI 440 B stainless steel.

An in-depth vibration analysis study should be performed on the machining set-up to understand its influence on the cutting tool wear and cutting forces at different machining conditions. This study will clearly identify the rapid tool failure through chipping of the cutting tool when machining at low feed rates and high cutting speeds.

During machining experimentation, the temperature at the cutting tool interface, was not investigated. Temperature measurements will provide betterinformation on the temperature when diffusion/ chemical wear occurs between the PcBN cutting tool and the workpiece by varying the cutting speed between the extremely low to extremely high limits.

The transitioning of the chip formation from continuous to serrated can also be correlated with the temperature measurements at the chip tool interface, to provide better understanding of the chip formation mechanism

The enhancement of both cBN and mixed ceramic cutting tool can be developed to increase its resistance to the forms of wear mechanisms as identified in this project.

Finally, the TEM study of the chemical interaction between the cBN and the workpiece at extreme high cutting speeds can be explored to further establish the effect of temperature during machining on diffusion and chemical wear of PcBN. The thermodynamic analysis of the chemical interaction is worth presenting in the future work.

REFERENCES

AB SandvikCoromant, *Hard Part Turning Guide*, p. 21.

Abrão, A.M., Aspinwall, D.K. & Wise, M.H.L. 1995. Tool life and workpiece surface integrity evaluations when machining hardened AISI H13 and AISI E52100 steels with conventional ceramic and PCBN tool materials. Wise, M.L.H., *Society of Manufacturing Engineers*, SME, MR95-195, Dearborn, MI, pp. 1–7.

Abrão, A.M., Ribeiro, J.L.S.&Davim, J.P. 2011. Surface integrity, Chapter 4, (pp. 115–141) in: Davim, J.P. (ed.). *Machining of Hard Materials.* London: Springer.

Almeida, C.H.D. &Abrão, A.M. 2002. Dimensional and geometric tolerances after machining case hardened AISI 5115 steel. *International Journal for Manufacturing Science and Technology*, vol. 3, pp. 92–109.

Ahn, S. &Kang, S. 2000. Formation of core/rim structures in TiCN–WC–Ni cermets via a dissolution and precipitation process. *Journal of the AmericanCeramic Society*, vol. 83(6),pp.1489–1494.

Angseryd, J., Elfwing, M., Olsson, E. & Andren, H.-O. 2009a. Detailed microstructure of cBN based cutting tool material. *International Journal of Refractory Metals and Hard Materials*, vol. 27, pp. 249-255.

Angseryd, J., Coronel, E., Elfwing, M, Olsson, E. &Andren, H.-O. 2009b. The microstructure of the affected zone of a worn PCBN cutting tool characterised with SEM and TEM.*Wear*, vol. 267, pp.1031–1040.

Angseryd, J.& Andrén, H.-O.2011. An in-depth investigation of the cutting speed impact on the degraded microstructure of worn PCBN cutting tools. *Wear*, vol. 271 (9–10),pp. 2610–2618.

Anthony, D.J. 1990. Concepts of polycrystalline diamond tooling for the woodworking industry, *Proceedings of the First International Symposium on Tooling for the Wood Industry*, Raleigh, NC.

Arrazola, P.J. &Ozel, T. 2007.Numerical modelling of 3D hard turning using arbitrary LagrangianEulerian finite element method.*International Journal of Machining and Machinability of Materials*, vol. 3(3), pp.238–249.

Arsecularatne, J.A., Zhang,L.C. & Montross,C. 2006. Wear and tool life of tungsten carbide, PCBN and PCD cutting tools, *International Journal of Machine Tools and Manufacture*, vol. 46 (5), pp. 482–491.

Arunachalam, R.M., Mannan, M.A. &Spowage, A.C. 2004. Surface integrity when machining age hardened Inconel 718 with coated carbide cutting tools. *International Journal of Machine Tools and Manufacture*, vol. 44, pp. 1481–1491.

ASM Handbook. 1994.*Surface Engineering*, ASM International, vol. 5, Materials Park, 1994.

Astakhov, V. P. 2006. *Tribology of Metal Cutting*(1st Ed), In Tribology and Interface Engineering. London: Elsevier.

Astakhov, V.P.& Davim, J.P.2008. Tools (geometry and material) and tool wear. In: Davim, J.P. (eds) *Machining, Fundamentals, and Recent Advances*. London: Springer-Verlag, pp. 29–57.

Ávila, R.F. &Abrão, A.M. 2001. The effect of cutting fluids on the machining of hardened AISI 4340 steel. *Journal of Material Processing Technology*, vol. 119, pp. 21–26.

Awaji,H., Choi, A. & Yagi, E. 2002. Mechanisms of toughening and strengthening in ceramic-based nanocomposites, *Mechanics of Materials*, vol.34 (7), pp. 411–422.

Bachrathy, D., Janka, R.M. &Mezaros, I. 2010.Optimal cutting speeds and surface prediction in interrupted high precision hard turning.*Proceedings of the 7th International Conference on Mechanical Engineering 2010*, pp.241–246.

Barlow, L.D & Du Toit, M. 2011.Effect of Austenitizing heat treatment on the microstructure and hardness of martensitic stainless steel AISI 420.*Journal of Materials Engineering and Performance*, vol. 21, (7), pp.1327–1336.

Barry, J, &Byrne, G. 2001. Cutting tool wear in the machining of hardened steels. Part II. Cubicboron nitride cutting tool wear. *Wear*, vol.247, pp. 152–160.

Barry, J. &Bryne, B. 2002. TEM study on the surface white layer in two turned hardened steels.*Materials Science Transaction A*, vol. 325 (1–2), pp. 356–364.

Bartarya, G. & Choudhury, S.K. 2012.Effect of cutting parameters on cutting force and surface roughness during finish hard turning AISI52100 grade steel.*Proceedings of the 5th CIRP Conference on High Performance Cutting 2012*,Procedia CIRP 1, pp.651–656.

Bawa, H.S. 2004. CNC machine tools. In: *Manufacturing processing II*. pp. 233–246.

Benga, G.C. &Abrao, A.M. 2003.Turning of hardened 100Cr6 bearing steel with ceramic and PCBN cutting tools.*Journal of Material Processing Technology*, vol. 143–144, pp.237–241.

Benko, E., Stanislaw, J.S., Królicka, B., Wyczesany, A. & Barr, T.L. 1999.cBN-TiN, cBN-TiC composites: chemical equilibria, microstructure and hardness mechanical investigations,*Diamond and Related Materials*, vol. 8, pp. 1838–1846.

Benko, E., Barr, T.L., Hardcastle, S., Hoppe, E., Bernasik, A. &Morgiel, J. 2001. XPS study of the cBN–TiC system, *Ceramics International*, vol. 27, pp. 637–643.

Benko, E., Klimczyk, P., Morgiel, J., Wlochowicz, A. & Barr, T.L. 2003.Electron microscopy investigations of the cBN–Ti compound composites. *Materials Chemistry and Physics*,vol. 81(2–3), pp.336-40.

Ber, A. &Porat, R. 1990. New approach of cutting tool materials-Cermet(Titanium carbonitride-based material) for machining steels, *Annals of the CIRP*, vol. 39, pp.71–75.

Bergman, F., Hedenqvist, P.&Hogmark, S. 1994. 3-Body Abrasion of Selected PM High Speed Steels.*Tribologia*, vol. 13, pp. 3–15.

Bhadeshia, H.K. &Honeycombe, R.W. 2006.*Steels microstructure and properties*, 3rd ed. London: Elsevier,pp. 264–267.

Bramfitt, B.L. 2002. *Metallographer's Guide: Practice and Procedures for Irons and Steels*, ASM International, OH, USA.

Brydson, R. 2001. *Electron energy-loss spectroscopy*. Microscopy Handbooks 48, Royal Microscopy Society Microscopy Handbooks. BIOS Scientific Publishers Ltd, p. 136.

Bohler N685 Extra, Available: http://www.bohler.at/deutsch/files/downloads/N685DE.pdf

Boothroyd G.& W.A. Knight, W.A. 1989.*Fundamentals of Machining and Machine tools*, 2nd ed. New York: Marcel Dekker.

Bouacha, K., Yallese, M.A., Mabrouki, T. &Rigal, J.F. 2010.Statistical analysis of surface roughness and cutting forces using response surface methodology in hard turning of AISI 52100 bearing steel with CBN tool.*International Journal of Refractory Metals and Hard Materials*, vol. 28(3), pp.349–361.

Buchholz, S.,Farhat, Z.N.,Kipouros, G.J. &Plucknett,K.P.2012. The reciprocating wear behaviour of TiC–Ni3Al cermets, *International Journal of Refractory Metals and Hard Materials*, vol. 33, pp. 42–52.

Bushlya, V., Zhou, J., Avdovic, P. & Stahl, J. 2013. Performance and wear mechanisms of whisker-reinforced alumina, coated and uncoated PCBN tools when high-speed turning aged Inconel 718, *International Journal of Advanced Manufacturing Technology*. Vol. 66(9-12), pp. 2013-2021.

Bushlya, V.M., Gutnichenko, O.A., Zhou, J. M., Ståhl, J.-E. & Gunnarsson, S. 2014. Tool wear and tool life of PCBN, binderless cBN and wBN-cBN tools in continuous finish hard turning of cold work tool steel, *Journal of Superhard Materials*, vol. 36 (1), pp. 49–60.

Byrne, G., Dornfeld, D.&Denkena, B. 2003.Advancing cutting technology.*Annals of CIRP*,vol.52 (2),pp.483–507.

Can, N. &Andersin, S.A. 2006. Cubic Boron Nitride Compact, *Patent, World Intellectual Property Organization, International Bureau,* WO 2006/046125 A1, PCT/IB2005/003221, 4 May 2006.

Caydas, U. 2009. Machinability evaluation in hard turning of AISI 4340 steel with different cutting tools using statistical methods.*Journal of Engineering Manufacture*, vol. 224, pp.1043–1055.

Cep, R., Neslusan, M. &Barisic, B. 2008. Chip formation analysis during hard turning.*Strojarstvo,*vol. 50(6), pp. 337–346.

Ceramics, *Sandvik Coromant*, 2006, Available at: http://www.sandvik.coromant.com/en-gb/knowledge/materials/cutting_tool_materials/ceramics/pages/default.aspx.

Childs, T.H.C., Maekawa, K., Obikawa, T. & Yamane, Y. 2000.*Metal machining theory and applications*. London: Arnold.

Chou, Y.K. & Evans, C.J.1997.Tool wear mechanism in continuous cutting of hardened tool steels. *Wear*, vol.212, pp. 59–65.

Chou, Y.K.& Evans, C.J. 1999. White layers and thermal modelling of hard turned surfaces.*International Journal of Machine Tools and Manufacture*, vol. 39(12),pp. 1863–1881.

Chou, Y.K., Evans,C.J.&Barash, M.M. 2003. Experimental investigation on CBN turning of hardened AISI 52100 steel.*Journal of Materials Processing Technology,* vol. 134,pp. 1–9.

Claussen, N., Rühle, M. &Heuer, A.H. 1984. *Science and Technology of Zirconia II*. In: Advances in Ceramics, vol. 12, (eds), Columbus, OH: American Ceramic Society.

Clayton, R., Chen, S. &Lefort, G. 2005. New bit design, cutter technology extend PDC applications to hard rock drilling, *Proceedings ofSPE/IADC Drilling Conference, Amsterdam, Netherland, 23-25 February, 2005.*

Coelho, R.T., Silva, L.R., Braghini Jr., A. &Bezerra, A.A. 2004. Some effects of cutting edge preparation and geometric modifications when turning INCONEL 718TM at high cutting speeds. *Journal of Material Processing Technology*, vol. 148, pp.147–153.

Cook, N.H. 1973. Tool wear and tool life, ASME Journal of Engineering for Industry, vol. 95, pp. 931–938.

D' Errico, G.E., Bugliosi, S., Cuppiui, D. &Guglielmi, E. 1997.A study of cermets' wear behaviour.*Wear*,vol. 203–204, pp.242–246.

Da Silva, R.B., Machado, A.R., Ezugwu, E.O., Bonney, J. &Sales, W.F. 2013. Tool life and wear mechanisms in high speed machining of Ti–6Al–4V alloy with PCD tools under various coolant pressures, *Journal of Materials Processing Technology*, vol. 213(8), pp. 1459–1464.

Dacian, T. & Hoi Pang, N. 2013.*In situ* lift-out dedicated techniques using FIB–SEM system for TEM specimen preparation, *Micron*, vol. 44, pp.115–119.

Davidge, R.W., Brook, R.J., Gambler, F., Poorteman, M., Leriche, A., O'Sullivan, D. et al. 1997. Fabrication, properties, and modelling of engineering ceramics reinforced with nanoparticles of silicon carbide. *Brazilian Ceramics Transaction*,vol. 96, pp. 121–7.

Davies, M.A., Burns, T.J. & Evans, C.J. 1997. On the dynamics of chip formation in machining hard metals. *Annals of CIRP*, vol. 46(1), pp. 25–30.

Davim, J.P. &Figueira, L. 2007. Comparative evaluation of conventional and wiper ceramic tools on cutting forces, surface roughness, and tool wear in hard turning AISI D2 steel. *Proceedings of the Institution of Mechanical Engineers, Part B: Journal of Engineering Manufacture*, vol. 221, pp.625–633.

Dawson, T.G.&Kurfess, R.T. 2001.Hard turning, tool life, and surface quality,*Transactions of NAMRI/SME*, vol. 29, pp. 175-182

DeGarmo, E.P., Black, J.T. & Kohser, R.A. 2003. *Materials and Processes in Manufacturing* (9th ed.). Wiley.

De Godoy, A.V.&Diniz, A.E. 2011.Turning of interrupted and continuous hardened steel surfaces using ceramic and CBN cutting tools.*Journal of Materials Processing Technology*, vol. 211, pp.1014–1025.

Deming, M., Young, B. Ratliff, D. 1993. Turning grey cast iron with PcBN cutting tools, *Diamond & CBN UltrahardMaterials Symposium*, IDA, September 29–30, 1993, pp. 131–142.

Derby, B. 1998. Ceramic nanocomposites: mechanical properties. *Current Opinion in Solid State& Materials Science*, vol. 3, pp. 490–495.

Dereli, T. &Filiz, I.H. 2000.Allocating optimal index positions on tool magazines using genetic algorithms.*Robotics Autonomous Systems*, vol. 33, pp. 155–167.

Diniz, A.E., Oliveira, A.J. &Ursolino, D.J. 2009.Hard turning of continuous and interruptedsurfaces using CBN and ceramic tools.*Journal of Material Processing Technology*, vol. 209,pp. 5262–5270.

sDogra, M., Sharma, V.S., Sachdeva, A., Suri, N.M. & Dureja, J.S. 2010. Tool wear, chip formation and workpiece surface issues in CBN hard turning: A review,

International Journal of Precision Engineering and Manufacturing. vol. 11 (2), pp 341–358.

Dubec, J., Neslusan, M., Micietova, A. & Cillikova, M. 2013. Influence of flank wear on decomposition of cutting forces in turning, *MM Science Journal*, pp. 448-451. [Available at: www.mmscience.eu/content/www_mmscience_cz_201317.pdf]

El-Wardany, T. I., Kishawy, H.A.&Elbestawi, M.A. 2000. Surface integrity of die material in high speed hard machining, Part 1: Micrographical analysis. *Journal of Manufacturing Science and Engineering*, vol. 122 (4), pp.620–631.

Elbestawi, M.A., Chen, L., Becze, C.E. & El-Wardany, T.I. 1997. High-speed milling of dies and moulds in their hardened state.*Annals ofClRP*, vol. 46(1), pp. 57–62.

Eredel, B.P. 1998. *New dimensions in manufacturing*. Cincinnati: Hanser Gardner.

Ettmayer, P., Kolaska, H., Lengauer, W. & Dreyer, K. 1995.TiCNcermets metallurgy and properties.*International Journal of Refractory Metals Hard Materials*, vol. 13, pp.343–51.

Ezugwu, E.O. & Tang, S.H. 1995.Surface abuse when machining cast iron (G-17) and nickel-base superalloy (Inconel 718) with ceramic tools.*Journal of Materials Processing Technology*, vol. 55, pp. 63–69.

Ezugwu, E.O. &Wang, Z.M. 1997.Titanium alloys and machinability – a review.*Journal of Materials Processing Technology*, vol. 68, pp. 262–274.

Flink, A., Saoubi, A.M., Giuliani, F., Sjolen, J., Larsson, T., Persson, P., Johansson, M.P. &Hultman, L. 2009. Microstructural characterization of the tool-chip interface enabled by fused ion beam and analytical electron microscopy.*Wear*, vol. 266 (11–12), pp.1237–1240.

Fnides, B.,Aouici, H. &Yallese,M.A. 2008. Cutting forces and surface roughness in hard turning of hot work steel X38CrMoV5-1 using mixed ceramic. *Mechanika*, vol. 2(70), pp.73–78.

Fnides, B., Yallese, M.N., Mabrouki, T. &Rigal, J.F. 2011. Application of response surface methodology for determining cutting force model in turning hardened AISI H11 hot work tool steel, *Sadhana, Indian Academy of Sciences*, vol. 36 (1), pp.109–123.

Friemuth, T. 2002. HerstellungspanenderWerkzeuge,Fortschr.-Ber.VDI Reihe 2, Nr. 615, Dusseldorf, VDI-Verlag, zugl.HabilitationsschriftUniversitat Hannover.

Gaitonde, V.N., Karnik, S.R., Figueira, L. &Davim, J.P. 2009.Machinability investigations in hard turning of AISI D2 cold work tool steel with conventional and wiper ceramic inserts.*International Journal of Refractive Metal and Hard Material*, vol. 27, pp. 754–763.

Giannuzzi, L.A. & Stevie, F.A. 2005.Introduction to focused ion beams.In: Giannuzzi, Stevie (eds),*Instrumentation, Theory, Techniques and Practice*, Springer.

Giménez, S., Van der Biest, S.O. &Vleugels,J. 2007. The role of chemical wear in machining iron based materials by PCD and PCBN super-hard tool materials.*Diamond and Related Materials*, vol. 16 (3), pp. 435–445.

Gopalsamy, B.M., Mondal, B. & Ghosh, S. 2009. Taguchi method and ANOVA: An approach for process parameters optimization of hard machining while machining hardened steel.*Journal of Scientific and Industrial Research*, vol. 68, pp.686–695.

Gosiger, 2012, Fundamentals of hard turning: An in-depth look at the process, pp. 1–26 [Available at: info.gosiger.com/Portals/139128/docs/GOS_WP_HardTurning_F.pdf].

Graham, G.A., Bradley, J.P., Bernas, M., Stroud, R.M., Dai, Z.R., Floss, C., Stadermann, F.J., Snead, C.J. &Westphal, A.J. 2004.Focused ion beam recovery and analysis of

interplanetary dust particles (IDPs) and stardust analogues.*Lunar and Planetary Science XXXV*, Houston, [Online.] Available at: http://www.lpi.usra.edu/meetings/lpsc2004/pdf/2044.pdf

Griffiths, B. 2001. Manufacturing surface technology. In: *Surface Integrity and Functional Performance*. London: Penton Press.

Groover, M.P. 2010.Theory of metal machining. In: *Fundamentals of Modern Manufacturing: Materials, Processes, and Systems*. John Wiley and Sons INC., pp. 438–502.

Gruss, W.W. &Friederich, K.M. 1994. Cermets cutting tools. In: Whitney, E.D. & Whitney, E.D. (eds), *Ceramic cutting tools: Materials development and performance*, pp. 63, Elsevier Inc.

Grzesik, W. 2008. Machining of hard materials. In: Davim, P. (ed.)*Machining fundamentals and advances*. London: Springer, pp. 97–126.

Grzesik, W. 2009. Wear development on wiper Al2O3–TiC mixed ceramic tools in hard machining of high strength steel.*Wear*, vol. 266 (9-10), pp.1021–1028.

Grzesik, W. 2011, Mechanics of cutting and chip formation. In: Davim, P. (ed.), *Machining of hard materials*, London: Springer, pp. 97–126.

Grzesik, W. & Wanat, T. 2005. Comparative assessment of surface roughness produced by hardmachining with mixed ceramic tools including 2D and 3D analysis.*Journal of Materials Processing Technology*, vol. 169,pp.364–371.

Grzesik, W. & Wanat, T. 2006. Hard turning of quenched alloy steel parts using conventional and wiper ceramic inserts. International Journal of Machine Tools and Manufacture, vol. 46, pp. 1988–1995.

Grzesik, W. &Zalisz, Z. 2008. Wear phenomenon in the hard steel machining using ceramic tools.*Tribology International*, vol. 41 (8), pp. 802–812.

Habig, K.-H. 1980. *Wear and hardness of materials*. Carl Hanser, München.

Hallberg, L. 2010.Recycling on the rise.*Cutting Tool Engineering*, vol. 62(10), pp. 60–64. [Online.] Available at: http://www.ctemag.com/aa_pages/2010/101005_SandvikRecycling.html

Hamade, R.F., Manthri, S.P., Pusavec, F., Zacny, K.A., Taylor, L.A., Dillon Jr., O.W., Rouch, K.E. &Jawahir, I.S. 2010.Compact core drilling in basalt rock using PCD tool inserts: Wear characteristics and cutting forces.*Journal of Materials Processing Technology*, vol. 210(10), pp.1326–1339.

Haosheng. L., Su, W. &Kratz, H. 2007.FFT and wavelet-based analysis of the influence of machine vibrations on hard turned surface topographies.*Tsinghua Science and Technology*, vol. 12(4), pp. 441–446.

Harris, T.K., Brookes, E.J.&Taylor, C.J. 2004.The effect of temperature on the hardness of polycrystalline cubic boron nitride cutting tool materials.*International Journal of Refractory Metals & Hard materials*, vol. 22, pp. 105–110.

Hasan, S. &Tamizhmanii, S. 2010. Tool flank wear analysis on AISI 440 C martensitic stainless steel by turning.*International Journal of Material Formation*, vol. 3, pp.427–430.

Hastings, W.F. &Oxley, P.L.B. 1976. Predicting tool life from fundamental work material properties and cutting conditions,*Annals of CIRP*, vol. 25, pp.33–38.

He, N., Lee, T.C., Lau, W.S. & Chan, S.K.2002.Assessment of deformation of a shear localised chip in high speed machining. *Journal of Material Processing Technology*, vol. 129(1–3), pp. 101–104.

Heath, P.J.1986.Properties and uses of AMBORITE. *Industrial Diamond Review*, vol. 46, pp.120–127.

Heath, P.J. 1989. Ultrahard Tool Materials, In: ASM International Handbook Committee, Metals Handbook (9thed.), vol. 16, Machining. ASM International, USA, pp. 105–117.

Hsu, F.C., Tai, T.Y., Vo, V.N., Chen, S.Y &Chen, Y.H. 2013. The machining characteristics of polycrystalline diamond (PCD) by Micro-WEDM,*Procedia CIRP*, vol. 6, pp.261–266.

Huang, Y. & Liang, S.Y. 2003.Cutting forces modeling considering the effect of tool thermal property-application to CBN hard turning, International.*Journal of Machine Tools Manufacturing*, vol. 43, pp.307 - 315.

Huang, Y. & Liang, S. Y. 2004a.Modelling of CBN tool flank wear progression in finish hard turning.*ASME Journal of Manufacturing Science and Engineering*, vol. 126, pp.98–106.

Huang, Y. & Liang S.Y. 2005.Modeling of cutting forces under hard turning conditions considering tool wear effect.Transactions of ASME, *Journal of Engineering Manufacture,* 127, pp.262–70.

Huang, Y., Chou, Y. K. & Liang, S. Y. 2007.CBN tool wear in hard turning: A survey on research progresses. *International Journal of Advanced Manufacturing Technology*, vol. 35(5–6), pp.443–453.

ISO 3685, 1993, Tool-Life Testing with Single-Point Turning Tools, Annex G, p. 41.

Jacobson, S. 1994. Applications of a new model for the abrasive wear resistance of multiphase materials, composites and coated materials. Paper presented at the Austrib '94, Perth, Australia, 1994.

Jacobson, M., Dahlman, P. &Gunnberg, F. 2002. Cutting speed influence on surface integrity of hard turned bainite steel. *Journal of Material Processing Technology*, vol. 128, pp.318–323.

Jaworska, L., Rozmus, M., Królicka, B. & Twardowska, A. 2006. Functionally graded cermets,*Journal of Achievements in Materials and Manufacturing Engineering*, vol. 17 (1–2), pp. 73–76.

Jian, L. 2006. The focused-ion-beam microscope-more than a precision ion milling machine.*Journal of Management*,vol. 58, pp.27–31.

Jiang, W., More, A.S., Brown, W.D. &Malshe, A.P. 2006. AcBN-TiN composite coating for carbide inserts: Coating characterization and its applications for finish hard turning, *Surface & Coatings Technology*,vol. 201, pp.2443–2449.

Jones C.T., and L.A. Bryan. 1987. Programmable control. In: *Manufacturing High Technology Handbook*. New York: Marcel Dekker, pp. 255–298.

Juneja B.L., Sekhon, G.S. & Seth N. 2003. Machining process and machine tools. In:*Fundamentals of CNC metal cutting and machine tools*, 2nd ed. New Age International Publishers, pp. 2–69.

Jung, J. & Kang, S. 2004. Effect of ultra-fine powders on the microstructure of Ti(CN)–xWC–Ni cermets. *ActaMaterialia*. vol. 52,pp.1379–1386.

Kamruzzaman, M. & Dhar, N.R. 2008. The effect of applying high-pressure coolant (HPC) jet in machining of 42CrMo4 steel by uncoated carbide inserts, *Journal of Mechanical Engineering*, vol. 39 (2), pp. 71–77.

Karpat, Y. &Ozel, T. 2007.3D FEA ofhard turning, investigation of PCBN cutting tool micro geometry effect.*Transaction of NAMRI/SME*, vol. 35,pp.1–8.

Katuku, K. 2009. Exploring the possibilities of extending the application of PCBN cutting tools to the machining of ADI through the understanding of wear meachanisms. PhD. Dissertation, University of the Witwatersrand.

Kishawy, H.A. & Elbestawi, M.A. 1999. Effects of process parameters on material side flow during hard turning. *International Journal of Machine Tools & Manufacture*, vol. 39 (7), pp. 1017–1030.

Klimenko, S.A., Mukovoz, Y.A., Lyashko, V.A., Vashchenko, A.N. &Ogorodnik, V.V. 1992.On the wear mechanism of cubic boron nitride base cutting tools.*Wear*, vol. 157, pp.1–7.

Klocke, F. & Kuchle, A. 2011.Fundamentals of cutting. In: *Manufacturing processes 1 Cutting, RWTH* (ed.). Berlin, Heidelberg: Springer-Verlag, pp. 39–94.

Ko, T. J. & Kim, H.S. 2001.Surface integrity and machinability in intermittent hard turning.*International Journal of Advance Manufacturing Technology*, vol. 18, pp.168–175.

Konig, W., Komanduri, R., Tonshoff, H. K. &Ackershoff, G. 1984. Machining of hard materials, *Annals of the CIRP*, vol. 39 (1), pp. 417–427.

Konig, W. & Lauscher, J. 1986. Turning of cast iron using silicon nitride ceramics: Wear behaviour and cutting forces. *V.D.I.Z.*, vol. 128 (11), pp. 415–420.

Konig, W., Klinger, M. &Link, R. 1990.Machining hard material with geometrically defined cutting edges-field of application and limitations.*Annals of CIRP*, vol. 39(1), pp.61–64.

Konig, W., Berktold, A. & Koch, K.F. 1993. Turning versus grinding: a comparison of surface integrity aspects and attainable accuracies, *Annals of ClRP*, vol. 42, pp. 39–43.

König, W. &Neises, N. 1993a. Turning TiAl6V4 with PCD,*Industrial Diamond Review*, 53 (1), pp.85–88.

König, W., &Neises, A. 1993b.Wear mechanisms of ultra-hard non-metallic cutting tools, *Wear* vol. 162–163, pp. 12–21.

Kopac, J., Stoic, A. &Lucic, M. 2006.Dynamic instability of the hard turning process.*Journal of Achievements in Materials and Manufacturing Engineering*, vol. 17, pp.1–2.

Kosaraju, S., Anne, V. &Ghanta, V. 2011. Effect of rake angle and feed rate on cutting forces in an orthogonal turning process, *Proceedings of the International Conference on Trends in Mechanical and Industrial Engineering, ICTMIE'2011*, Bangkok, Dec., 2011.

Koshy, P., Dewes, R.C. &Aspinwall, D.K. 2002. High speed end milling of hardened AISI D2 tool steel (~58 HRC). *Journal of Material Processing Technology*, vol. 127, pp. 266–273.

Kramer, B.M. 1987. On tool material for material for high speed machining, *Journal ofEngineering for Industry-Transactions of the ASME,*vol. 109, pp. 87–91.

Kumar, A., Raja Durai, A., & Sornakumar, T. 2003. Machinability of hardened steel using alumina based ceramic cutting tools. *International Journal of Refractory Metals and Hard Materials*, vol.21(3), pp. 109–117.

Kumar, A., Durai, A. R. &Sornakumar, T. 2006.The effect of tool wear on tool life of alumina-based ceramic cutting tools while machining hardened martensitic stainless steel.*Journal of Materials Processing Technology*, vol. 173, pp.151–156.

Kundrak, J., Karpuschewski, B., Gyani, K. &Bana, V. 2008.Accuracy of hard turning.*Journal ofMaterial Processing Technology*, vol. 202, pp.328–338.

Lahiff, C., Gordon, S. & Phelan, P. 2007. PCBN tool wear modes and mechanisms in finish hard turning, *Robotics and Computer-Integrated Manufacturing*, vol. 23 (6), pp. 638–644.

Lalwani, D.I., Mehta, N.K. & Jain, P.K. 2008. Experimental investigations of cutting parameters influence on cutting forces and surface roughness in finish hard turning

of MDN250 steel, *Journal of Materials Processing Technology*, vol. 206, pp. 167–179.

Lee, M., Horne, J. & Tabor, D. 1979. Proceedings of the International Conference on wear of materials, ASME, New York, pp. 460–469.

Lee, M.R., Bland, P.A. & Graham, G. 2003. Preparation of TEM samples by focused ion beam (FIB) techniques: applications to the study of clays and phyllosilicates in meteorites.*Mineralogical Magazine*, vol. 67, pp.581–592.

Liew, W.Y.H., Ngoi, B.K.A. & Lu, Y.G. 2003. Wear characteristics of PCBN tools in the ultra-precision machining of stainless steel at low speeds,*Wear*, vol. 254, pp.265–277.

Lima, J.G., Avila, R.F., Abrao, A.M. & Paulo D.S. 2005. Hard turning: AISI 4340 high strength low alloy steel and AISI D2 cold work tool steel.*Journal of Materials Processing Technology*, pp.388–395.

Lin, Z.C. &Chen, D.Y. 1995. A study of cutting with a CBN tool. *Journal of Material Processing Technology*, vol. 49, pp. 149–64.

Lin, Z.C. & Yang, C.B. 1994.Evaluation of machine selection bythe AHP method.*Journal of Material Processing Technology*, vol. 57, pp. 253–258.

Lin, H. M., Liao, Y. S. & Wei, C. C. 2008."Wear behavior in turning high hardness alloy steel by CBN tool". *Wear*, vol. 264 (7–8), pp. 679–684, 2008.

Liu, Z.Q. &Ai, X. 2005. Cutting tool materials for high speed machining. *Progress in Natural Science: Materials International*, vol. 15, pp. 777–83.

Liu, J., Vohra Y.K., Tarvin J.T. &Vagarali, S.S. 1995. Cubic-to-rhombohedral transformation in boron nitride induced by laser heating: In situ Raman-spectroscopy studies, *Physical Review B Condensed matter and materials physics*, vol. 51 (13), pp. 8591–8594.

Liu, Z.Q., Ai, X., Zhang, H., Wang, Z.T.& Wan, Y. 2002. Wear patterns and mechanisms of cutting tools in high-speed face milling. *Journal of Material Processing Technology*, vol. 129(1–3), pp. 222–226.

Liu, N., Han, C.L., Xu, Y.D., Chao, S., Shi, M. & Feng, J.P. 2004. Microstructures and mechanical properties of nanoTiN modified TiC-based cermets for the milling tools. *Materials Science and EngineeringA*, vol. 382, pp.122–31.

Liu, Z.Q., Wan, Y.& Ai, X. 2004. Recent Developments in Tool Materials for High Speed Machining. *Materials Science Forum*, vol. (471–472), pp. 438–442.

Lo Castco, S., Lo Valvo, E. & Ruisi, V.F. 1993, Wear mechanisms of ceramic tools, *Wear*, vol. 160, pp. 227–235.

López de Lacalle, L.N., Lamikiz, A., Fernández de Larrinoa, J. &Azkona, I. 2011. Advanced Cutting Tools,In: Davim, J.P. (ed.), *Machining of Hard Materials*. London: Springer-Verlag, pp. 33–65.

Luo, S.Y., Liao Y.S. & Tsai Y.Y. 1999. Wear characteristics in turning high hardness alloy steel by ceramic and CBN tools.*Journal of Materials Processing Technology*, vol. 88,pp.114–121.

Markarow, A.D. 1976.*Optimization of Cutting Processes*. Moscow: Mashinostroenie.

Matsumoto, Y., Hashimoto, F. &Lahoti, G. 1999.Surface integrity generated by precision hard turning.*Annals of CIRP*, vol. 48(1), pp. 59–62.

Merchant, M.E. 1945. 'Mechanics of metal cutting process: Part I orthogonal cutting and a type-2 of chip', *Journal of Applied Physics*, vol. 16, pp. 267–275.

Mohlfeld, A. 2000.*Dry drilling with PVD-coated carbide tools*.PhD. Dissertation, Universität Hannover.

Momper, F. 1987. Flexible production with ceramics, *Production Engineer*, vol. 66 (5), pp. 18–19, [Available at: ieeexplore.ieee.org/stamp/stamp.jsp?arnumber=4938141].

Morehead, M.D. & Huang, Y. 2007.Chip morphology characterization and modeling in machining hardened 52100 steels, *Machining Science and Technology: An International Journal*, vol. 11, pp. 335–354.

Mookherjee, R.&Bhattacharyya, B. 2001.Development of an expert system for turning and rotating tool selection in a dynamic environment.*Journal of Material Processing Technology*, vol. 113 pp. 306–311.

Motorcu, A.R., 2011. Tool life performances, wear mechanisms and surface roughness characteristics when turning austenised and quenched AISI 52100 bearing steel with ceramics and CBN/TiC cutting tools, *Indian Journal of Engineering Material Science*, vol. 8, pp. 137–146.

Nakayama, K., Arai, M. & Kanda, T. 1988.Machining characteristic of hard materials. *CIRP Annals – Manufacturing Technology*,vol. 37, pp. 89–92.

Narutaki, N. & Yamane, Y. 1979.Tool wear and cutting temperature of CBN tools in machining of hardened steels. *Annals of CIRP*, vol. 28, pp. 23–8.

Neslusan, M., Sipek, M. & Mrazik, J. 2012. Analysis of chip formation during hard turning through acoustic emission, *Material Engineering*, vol. 19, pp. 1–11.

Neo, K.S., Rahman, M., Li, X.P., Khoo, H.H., Sawa, M. & Maedan, Y. 2003.Performance evaluation of pure CBN tools for machining of steel.*Journal of Material Processing Technology*, vol. 140, pp. 326–31.

Newman, S.T., Nassehi, A.. Xu, X.,Rosso, R., Wang, L., Yusof, Y. Ali, L.,Liu, R., Zheng, L. Y., Kumar, S., Vichare, P. &Dhokia, V. 2008.Strategic advantages of interoperability for global manufacturing using CNC technology, *Robotics and Computer-Integrated Manufacturing*, vol. 24, pp. 699–708.

Niihara, K., Nakahira, A., 1990. Particulate strengthened oxide by the circles. The predicted toughening factor a nanocomposites. In: Vincenzini, P. (ed.)*Advanced Structural Inorganic Composites*. Trieste: Elsevier, pp. 637–664.

Noordin, M.Y., Kurniawan, D. & Sharif, S. 2006. Hard turning of stainless steels using wiper coated carbide tool.*International Journal of Precision Technology*, vol. 1, pp.75–84.

Noordin, M. Y., Venkatesh,V.C. & Sharif, S. 2007.Dry turning of tempered martensitic stainless tool steel using coated cermet and coated carbide tools.*Journal of Materials Processing Technology*, pp.83–90.

Noordin, M. Y., Kurniawan, D., Tang, Y.C. &Muniswaran, K. 2012. Feasibility of mild hard turning of stainless steel using coated carbide tool.*International Journal of Advance Manufacturing Technology*, vol. 60, pp.853–863.

North, B. 1989.Indexable metal cutting inserts. Factors influencing machining and their controls, *Proceedings of an international conference and workshop*, Cincinnati, Ohio, 12–14 September 1989, pp. 33–42

Nurul Amin, A.K.M., Ismail, A.F.&Nor-Khairusshima,M.K., 2007. Effectiveness of uncoated WC–Co and PCD inserts in end milling of titanium alloy—Ti–6Al–4V, *Journal of Materials Processing Technology*, vol. (192–193), pp. 147–158.

Okubo, S., Fukui, K., Akiyama, M. & Liang, W. 1999. Bit wear and cutting force in rock cutting. *Journal of the Mining and Materials Processing Institute of Japan*, vol. 115(9), pp. 669– 676.

Opitz, H. &Konig, W. 1967. On the wear of cutting tools *Proceedings of the 8th International MTDR Conference*, pp.173–190.

Orloff, J., Swanson, L., Utlaut, M. &Utlaut, M.W. 2002.*Physics of liquid metal ion sources.* InHigh resolution focused ion beams: FIB and its applications, Kluwer Academic Publishers, pp.21–77.

OzelT.,Hsu, T. &Zeren, E. 2005. Effects of cutting edge geometry, workpiece hardness, feed rateand cutting speed on surface roughness and forces in finish turningof hardened AISI H13 steel. *International Journal of Advances in Manufacturing Technology*, vol. 25, pp. 262–269.

Pal, S.&Chakraborty, D. 2005. Surface roughness prediction in turning usingartificial neural network,*Neural Computing Application*, vol. 14, pp. 319–324.

Pastor, H. 1987.Present status and development of tool materials: part 1. Cutting tools, *International Journal of Refractory Metals and Hard Materials*, vol. 6, pp.196–209.

Pavel, R., IoanMarinescu, I., Deis, M. & Pillar, J. 2005.Effect of tool wear on surface finish for a case of continuous and interrupted hard turning.*Journal of Materials Processing Technology*, vol. 170, pp.341–395.

Peng, Y., Miao, H., Peng, Z. 2013. Development of TiCN-based cermets: Mechanical properties and wear mechanism, *International Journal of Refractory Metals and Hard Materials*, vol. 39, pp. 78–89.

Pezzotti, G. & Muller, W.H. 2002. Micromechanics of fracture in a ceramic/metal composite studied by in situ fluorescence specroscopy I: foundations and stress analysis. *Continuum Mechanics and Thermodynamics*, vol. 14(1), pp. 113–126.

Phaneuf, M.W. 1999. Applications of focused ion beam to materials science specimens. *Micron* vol. 30,pp.277–288.

Philbin, P. & Gordon, S. 2005.Characterisation of the wear behaviour of polycrystalline diamond (PCD) tools when machining wood-based composites, *Journal of Materials Processing Technology*, vol. 162–163, pp.665–672.

Poulachon, G.&Moisan, A.L. 2000. Hard turning: chip formation mechanisms and metallurgical aspects. *Transaction of the ASME*, vol. 122, pp. 406–412.

Poulachon, G., Moisan, A. & Jawahir, I.S. 2001. Tool-Wear Mechanisms in Hard Turning with Polycrystalline cubic Boron Nitride Tools, *Wear*, vol. 250 (1-12), pp. 576-586

Poulachon, G., Bandyopadhyay, B.P., Jawahir, I.S.,Pheulpin, S. & Seguin, E. 2004.Wear behaviour of CBN tools while turning various hardened steels. *Wear*, vol. 256 (3-4), pp. 302–10.

Puretz, J., Orloff, J. & Swanson, L. 1984. Application of focused ion beams to electron beam testing of integrated circuits. *Proceedings of SPIE –The International Society for Optical Engineering*, vol. 471, pp.38–46.

Qibiao, Y., Zhanqiang, L. & Bing, W. 2012.Characterisation of chip formation during machining 1045 steel, *International Journal of Advance Manufacturing Technology*, vol. 63, pp. 881–886.

Rafai, N.H. &Islam, M.N. 2009.An investigation into dimensional accuracy and surface finish achievable in dry turning.*Machining Science and Technology*, vol. 3(4), pp.571–589.

Rao P.N., 2013. Machine tools. In: *Manufacturing technology volume 2, Metal cutting and Machine tools*, 3rd ed. India: McGraw Hill Education, pp. 80–106.

Rech, J., 2006. A multi-view approach to the tribologicalcharacterization of cutting tool coatings for steels in highvelocity dry turning, *International Journal for Machiningand Machinability ofMaterials*, vol.1, pp. 27–44.

Rech, J. &Moisan, A. 2003.Surface integrity in finish hard turning of case-hardened steels.*International Journal of Machine Tools and Manufacturing*, vol. 43, pp.543–550.

Recht, R.F. 1964. Catastrophic thermoplastic shear.*Journal of Applied Mechanics*, vol. 86, pp. 186–193.

Richard, W. 2009. Focused Ion Beam (FIB) combined with SEM and TEM: Advanced analytical tools for studies of chemical composition, microstructure and crystal

structure in geo-materials on a nanometre scale, *Chemical Geology*, vol. 261, pp. 217–229.

Richt, C. 2009. Hard turn toward efficiency.*Gear SolutionsMagazine*, issue 4: pp. 22–30.

Risbood, K.A., Dixit, V.S. &Sahasrabudhe, A.D. 2003.Prediction of surface roughness and dimensional deviation by measuring cutting forces and vibrations in turning process.*Journal of Materials Processing Technology*, vol. 132, pp.203–214.

Rong, X.Z. & Yano, T. 2004.TEM investigation of high-pressure reaction-sintered cBN–Al composites.*Journal of Material Science*, vol. 39, pp.4705–4710.

Rosemar, B.S., Álisson, R. M., Emmanuel, O. E., John, B. &Wisley, F.S. 2013. Tool life and wear mechanisms in high speed machining of Ti–6Al–4V alloy with PCD tools under various coolant pressures, *Journal of Materials Processing Technology*, vol. 213 (8), pp.1459–1464.

Salem, B., Bayraktar, E, Boujelbene, M. &Katundi D.2012. Effect of cutting parameters on chip formation in orthogonal cutting,*Journal of Achievements in Materials and Manufacturing Engineering*, vol. 50 (1), pp. 7–17.

Salleh, S.H., Omar, M.Z., Syarif, J., Ghazali, M.J., Abdullah, S. &Sajuri, Z. 2009. Investigation of microstructures and properties of 440c martensitic stainless steel, *International Journal of Mechanical and Materials Engineering (IJMME)*, vol. 4(2), pp. 123–126.

Sales, W.F., Costa, L.A., Santos, S.C., Diniz, A.E., Bonney, J. &Ezugwu, E.O. 2009.Performance of coated, cemented carbide, mixed-ceramicand PCBN-H tools when turning W320 steel.*International Journal of Advanced Manufacturing Technology*, pp.660–669.

Seah, K.H.W., Rahman, M. & Lee, C.H. 1995. Comparing the effectiveness of coatings on carbide and cermet cutting tool inserts. *Journal of Material Science and Technology*, vol. 11, pp.269–275.

SECO. 2003. *Secomax PCBN technical guide* (www.secotools.com) Fagersta:SECO Tools AB, pp. 41.

Shao, X., Liu, S., Zhang, L. & Lin, Z. 2013.Simulation of workpiece deformation caused byreleasing the clamping force, *Transactions of the Canadian Society for Mechanical Engineering*,vol. 37 (3), pp. 703–712.

Sharman, A.R.C.,Amarasinghe, A. & Ridgway, K. 2008. Tool life and surface integrity aspect when drilling and hole making in Inconel 718. *Journal of Material ProcessingTechnolology*, vol. 200, pp. 424–432.

Shaw, M.C. 1984. *Metal Cutting Principles*. Oxford: Oxford Science.

Shaw, M.C. & A. Vyas, A. 1998. The Mechanism of Chip Formation with Hard Turning Steel, *CIRP Annals - Manufacturing Technology*, vol. 47 (1), pp. 77–82.

Shihab, S.K., Khan, Z.A., Mohammad A. & Siddiquee, A.N. 2014. A review of turning of hard steels used in bearing and automotive applications, *Production and Manufacturing Research*, vol. 2 (1), pp. 24 – 49.

Schneider, J. & Richter, G. 1999. New developments in ceramic cutting tools and theirapplications, *Proceedings of 2nd International German and French Conference HighSpeed Machining*, Darmstadt, pp. 249–253, March 1999.

Sieben, B., Wagner, T. &Biermann, D. 2010.Empirical modelling of hard turning of AISI 6150 steel using design and analysis of computer experiments.*Production Engineering, Resources and Development*, vol. 4, pp.115–125.

Smallman, R. E. & Ngan, A.H.W. 2007. *Non-metallics 1-Ceramics, glass, glass –ceramics,* In: Physical Metallurgy and Advanced Materials, 7th Ed. Butterworth-Heinemann, Burlington, MA, pp. 513–545.

Stephenson. D. A., & Agapiou, J.S. 2006. *Metal cutting operations in Metal Cutting Theory and Practice,*2nded. Boca Raton, FL: Taylor and Francis Group, pp. 17–70.

Stevenson, R. 1992. The morphology of machining chips formed during low speed quasi-orthogonal machining of CA 360 Brass and a model for their formation, *Journal of Manufacturing Science and Engineering*, vol. 114 (4), pp. 404–411.

Sobiyi, K.K. 2011. Machining of Powder Metal Titanium, MSc. Dissertation, Stellenbosch University.

Sobiyi, K., Sigalas, I., Akdogan, G. & Turan, Y. 2015. Performance of mixed ceramics and CBN toold during hard turning of martensitic stainless steel, *International Journal of Advanced Manufacturing Technology*, vol. 77 (5), pp. 861–871.

Song, S.X., Ai, X., Zhao, J.& Huang, C. 2002. Al2O3/Ti(C0.3N0.7) cutting tool material *Materials Science and Engineering A*, No. 356, pp. 43–47.

Sourmail, T. & Bhadeshia, H.K.D.H. 2005. Stainless steels. University of Cambridge, Available at: http://www.msm.cam.ac.uk/phase-trans/2005/Stainless_steels/stainless.html.

Suresh, R., Basavarajappa, S. & Samuel, G.L. 2012. Predictive modeling of cutting forces and tool wear in hard turning using response methodology, proceedings of International conference on modelling optimisation and Computing (ICMOC-2012), *Procedia Engineering*, vol. 38, pp.73–81.

Surjya K. & Chakraborty, D. 2005. Surface roughness prediction in turning using artificial neural network,*Neural Computing and Applications,* vol. 14, pp.319–324.

Thamizhmanii, S. & Hasan, S. 2008a. Investigating flank wear and cutting force on hard steels by CBN cutting tool by turning, *Proceedings of the World Congress on Engineering 2008,* vol. III WCE 2008, July 2–4, 2008, London, U.K.

Thamizhmanii, S. & Hasan, S. 2008b. Measurement of surface roughnessand flank wear on hard martensiticstainless steel by CBN and PCBN cutting tools, *Journal of Achievements in Materials and Manufacturing Engineering*, vol. 31, pp.415–431.

Thamizhmanii, S, Bin Omar, B., Saparudin, S. & Hasan, S. 2008. Surface roughness analyses on hard martensitic stainless steel by turning, *Journal of Achievements in Materials and Manufacturing Engineering*, vol. 26(2), pp.139–142.

Thiele, J.D. &Melkote, S.N. 1999.Effect of cutting edge geometry and workpiece hardness on surface generation in the finish hard turning of AISI 52100 steel.*Journal of Materials Processing Technology*, vol. 94, pp. 216–226.

Thomas, T.R., 1999, *Rough Surfaces*, 2nd ed. London: Imperial College Press.

Trent, E. M. & Wright, P.K. 2000.Cutting tool materials III, Ceramics, CBN,Diamond. In: *Metal cutting*, 4thed. Woburn, MA: Butterworth-Heinemann, pp. 227–249.

Tönshoff, H.K., Zinngrebe, M. & Kemmerling,M. 1986. Optimization of Internal Grinding by Microcomputer-Based Force Control, *CIRP Annals - Manufacturing Technology*, vol. 35(1), pp. 293–296,

Tönshoff, H.K., Wobker, H. & Brandt, D. 1995.Hard turning influences on workpiece properties.*Transactions of NAMRI/SME*, vol. 23, pp.215–220.

Tönshoff, H. K., Arendt, C. & Ben, A. R. 2000.Cutting of hardened steel.*Annals of CIRP*, vol. 49(2), pp.547–566.

Verhoeven, J.D.2007.*Stainless steel for knife makers in Steel Metallurgy for the Non-Metallurgist,* ASM International, Materials Park OH, pp.209–212.

Walker, L.S., Marotti, V.R., Rafiee, M.A. Koratkar, N. & Corral, E. 2011. Toughening in Graphene Ceramic Composites, *ACS Nano*, vol. 5(4), pp. 3182–3190.

Walmsley, J.C. & Lang, A.R. 1987.A transmission electron microscope study of a cubic boron nitride-based compact material with AlN and AlB2 binder phase.*Journal of Material Science,* vol. 22(11), pp. 4093–102.

Wang, Y., Lei, T. &Liu, J. 1999. Tribo-metallographic behaviour of high carbon steels in dry sliding III. Dynamic microstructural changes and wear, *Wear*, vol. 231, pp. 20–37.

Wang, X., Wang, W., Huang, Y., Nguyen, N. &Krishnakumar, K. 2008.Design of neural network-based estimator for tool wear modelling in hard turning.*Journal of Intelligent Manufacturing*, vol.19, pp.383–396.

Wayne, S.F. & Buljan, S.T. 1990. Wear of ceramic cutting tools in Ni-based super alloy machining. *Tribology Transaction*, vol. 33, pp.618–626.

Weidow, J. 2005.*The microstructure of sintered cubic boron nitride (cBN) with binder*. Master Thesis. Göteborg, Sweden: Chalmers University of Technology.

Weinz, E.A. 1980. Mono- and polycrystalline diamond and boron nitride tools, *Precision Engineering*, vol. 2(1), pp. 33–37.

Williams, D.B. & Carter, C.B. 1996.*Transmission electron microscopy*: A textbook for materials science. Plenum Press, pp. 649–653.

Wirth, R. 2009. Focused Ion Beam (FIB) combined with SEM and TEM: Advanced analytical tools for studies of chemical composition, microstructure and crystal structure in geomaterials on a nanometre scale, *Chemical Geology*, vol. 261, pp. 217–229.

Witney, D. 1994. *Ceramic cutting tools: materials, development and performance*. Park Ridge, NJ:Noyes Publications.

Wright, P.K. & Bagchi, A. 1981. Wear mechanisms which dominate tool life in machining. *Journal of applied metal working*, vol. 1, pp. 15–23.

Wuyi, C., Cutting Force and Surface Finish When Machining Medium Hardness Steel Using CBN Tools, *International Journal of Machine Tools and Manufacture,* vol. 40, pp. 455–466, 2000.

Xie, J.Q., Bayoumi, A.E. &Zbib, H.M. 1995. Analytical and experimental study of shear localisation in chip formation in orthogonal machining, *Journal of Material Engineering Performance*, vol. 4(1), pp. 32–39.

Yih-Fong, T. 2006.Parameter design optimisation of computerised numerical control turning tool steels for high dimensional precision and accuracy.*Journal of Materials and Design*, vol. 27, pp.665–675.

Ying P., Hezhuo, M. &Zhijian, P. 2013. Development of TiCN-based cermets: Mechanical properties and wear mechanism. *International Journal of Refractory Metals and Hard Materials*, vol. 39, pp.78–89.

Zhang, L.X. 2009.Brazing temperature andtime effects onthemechanical properties of TiC cermet/Ag–Cu–Zn/steel joints.*Material Science and Engineering A*, vol. 428, pp. 24–33.

Zhang, Y.Z., JieZhong, Q.Y., Peng, W.2009. Effect of carbon content and cooling mode on the microstructure and properties of Ti(C,N)-based cermets. *International Journal of Refractory Metals & Hard Materials*, vol. 27, pp.1009–1013.

Zhang, X., Senthil Kumar, A., Rahman, M., Nath, C. &Liu, K. 2011.Experimental study on ultrasonic elliptical vibration cutting of hardened steel using PCD tools, *Journal of Materials Processing Technology*, vol. 211 (11), pp. 1701–1709.

Zhao, J. & Ai X. 2006. Fabrication and cutting performance of an Al 2 O 3 –(W, Ti)C functionally gradient ceramic tool. *International Journal of Machining and Machinability of Materials*, vol. 1, pp. 277–86.

Zhao, J., Yuan, X. &Zhou, Y. 2010. Cutting performance and failure mechanisms of an Al2O3/WC/TiC, micro- nano-composite ceramic tool, *International Journal of Refractory Metals & Hard Materials*, vol. 28, pp. 330–337.

Zhao, Y.C, Wang, M.Z. 2007. Cubic BN sintered with Al under high temperature and high pressure. *Chinese Physics Letters*, vol. 24(8), pp. 2412–2414.

Zheng-Fei, H. & Zhen-Guo, Y. 2003. Identification of the precipitates by TEM and EDS in X20CrMoV12.1 after long-term service at elevated temperature, *Journal of Materials Engineering and Performance*,vol. 12(1), pp. 106–111.

Zhou, J.M., Andersson, M. & Stahl, J.E. 2003.The monitoring of flank wear on the CBN tool in the hard turning process. *International Conference on Mechanical Engineering.*vol 22, pp.697–702.

Zhou, J. M., Anderson, M. & Stahl, J. E. 2004.Identification of cutting errors in precision hard turning process.*Journal of Materials Processing Technology*, pp.746–750.

Zhou, J. M., Hognas, S. & Stahl, J. 2010.Improving waviness of bore in precision hard turning by pressurized coolant.*International Journal of Advanced Manufacturing Technology*, vol. 49, pp.469–474.

Zimmermann, M., Lahres, M., Viens, D.V.&Laube, B.L. 1997. Investigations of the wear of cubic boron nitride cutting tools using Auger electron spectroscopy and X-ray analysis by EPMA,*Wear*, vol. 209, pp. 241–246.

ZumGahr, K.-H. 1987. Basics of wear. In: *Metallic and non-metallic materials and their processing methods compared*. VDI Report 600.3, pp. 29–55. VDI, Düsseldorf.

APENDIX A: Copyright permissions

1. CHOU AND EVANS 1997

ELSEVIER LICENSETERMS AND CONDITIONS

Aug 22, 2014

This is a License Agreement between Kehinde Sobiyi ("You") and Elsevier ("Elsevier") provided by Copyright Clearance Center ("CCC"). The license consists of your order details, the terms and conditions provided by Elsevier, and the payment terms and conditions.

All payments must be made in full to CCC. For payment instructions, please see information listed at the bottom of this form.

Supplier Elsevier Limited

The Boulevard, Langford LaneKidlington, Oxford, OX5 1GB, UK

Registered Company Number1982084

Customer name Kehinde Sobiyi

Customer address

Room 406 Richard Wards Building Johannesburg, Gauteng 2050

License number 3451890064648

License date Aug 18, 2014

Licensed content publisher Elsevier

Licensed content publication Wear

Licensed content title

Tool wear mechanism in continuous cutting of hardened tool steels

Licensed content author: Y.Kevin Chou,Chris J. Evans

Licensed content date 30 November 1997

Licensed content volume number 212

Licensed content issue number 1

Number of pages 7

Start Page 59

End Page 65

Type of Use: reuse in a thesis/dissertation

Portion: figures/tables/illustrations

Number of figures/tables/illustrations: 1

Format: both print and electronic

Are you the author of this Elsevier article? No

Will you be translating? No

Title of your thesis/dissertation Hard turning of martensitic AISI 440B stainless steel

Elsevier VAT number: GB 494 6272 12

Permissions price: 0.00 USD

VAT/Local Sales Tax: 0.00 USD / 0.00 GBP

Total: 0.00 USD

2. AHN AND KANG 2000

License Number: 3451881274395

License date: Aug 18, 2014

Licensed content publisher: John Wiley and Sons

Licensed content publication: Journal of the American Ceramic Society

Licensed content title

Formation of Core/Rim Structures in Ti(C,N)-WC-Ni Cermets via a Dissolution and Precipitation Process

Licensed copyright line Copyright © 2004, John Wiley and Sons

Licensed content author Sun-Yong Ahn,Shinhoo Kang

Licensed content date:Dec 20, 2004

Start page 1489

End page 1494

Type of use Dissertation/Thesis

Requestor type University/Academic

Format: Electronic

Portion: Figure/table

Number of figures/tables: 1

Original Wiley figure/table number(s):Figure 1

Will you be translating? No

Title of your thesis / dissertation Hard turning of martensitic AISI 440B stainless steel

Total 0.00 USD

3. GRZESIK AND WANAT 2006

License number 3451890359769

License date Aug 18, 2014

Licensed content publisher Elsevier

Licensed content publication International Journal of Machine Tools and Manufacture

Licensed content title

Surface finish generated in hard turning of quenched alloy steel parts using conventional and wiper ceramic inserts

Licensed content author W. Grzesik,T. Wanat

Licensed content date December 2006

Licensed content volume number 46

Licensed content issue number 15

Number of pages 8

Start Page 1988

End Page 1995

Type of Use reuse in a thesis/dissertation

Intended publisher of new work other

Portion: figures/tables/illustrations

Number of figures/tables/illustrations1

Format: both print and electronic

Are you the author of this Elsevier article? No

Will you be translating? No

Title of your thesis/dissertation Hard turning of martensitic AISI 440B stainless steel

Elsevier VAT number GB 494 6272 12

Permissions price 0.00 USD

VAT/Local Sales Tax 0.00 USD / 0.00 GBP

Total 0.00 USD

4. BOUACHA ET AL. 2010

License number 3451881412697

License date Aug 18, 2014

Licensed content publisher Elsevier

Licensed content publication

International Journal of Refractory Metals and Hard Materials

Licensed content title

Statistical analysis of surface roughness and cutting forces using response surface methodology in hard turning of AISI 52100 bearing steel with CBN tool

Licensed content author Khaider Bouacha,Mohamed Athmane Yallese,Tarek Mabrouki,Jean-François Rigal

Licensed content date May 2010

Licensed content volume number 28

Licensed content issue number 3

Number of pages 13

Start Page 349

End Page 361

Type of Use reuse in a thesis/dissertation

Intended publisher of new work other

Portion: figures/tables/illustrations

Number of figures/tables/illustrations1

Format: both print and electronic

Are you the author of this Elsevier article? No

Will you be translating? No

Title of your thesis/dissertation Hard turning of martensitic AISI 440B stainless steel

Elsevier VAT number GB 494 6272 12

Permissions price 0.00 USD

VAT/Local Sales Tax 0.00 USD / 0.00 GBP

Total 0.00 USD

5. SALES ET AL. 2009

License Number 3384031242636

License date May 08, 2014

Licensed content publisher Springer

Licensed content publication

The International Journal of Advanced Manufacturing Technology

Licensed content title

Performance of coated, cemented carbide, mixed-ceramic and PCBN-H tools when turning W320 steel

Licensed content author W. F. Sales

Licensed content date

Jan 1, 2008

Volume number 41

Issue number 7

Type of Use Thesis/Dissertation

Portion: Figures

Author of this Springer article No

Order reference number None

Original figure numbers Figure 10

Title of your thesis / dissertation Hard turning of martensitic stainless steel

Total 0.00 USD

6. GRZESIK 2008

License Number 3435871085787

License date Jul 25, 2014

Licensed content publisher Springer

Licensed content publication Springer eBook

Licensed content title Machining of Hard Materials

Licensed content author Wit Grzesik

Licensed content date Jan 1, 2008

Type of Use Thesis/Dissertation

Portion: Figures

Author of this Springer article No

Order reference number None

Original figure numbers Figure 4.26

Title of your thesis / dissertation Hard turning of martensitic AISI 440B stainless steel

Total 0.00 USD

7. BARLOW 2011

License Number 3435890475383

License date Jul 25, 2014

Licensed content publisher Springer

Licensed content publication

Journal of Materials Engineering and Performance

Licensed content title

Effect of Austenitizing Heat Treatment on the Microstructure and Hardness of Martensitic Stainless Steel AISI 420

Licensed content author L. D. Barlow

Licensed content date Jan 1, 2011

Volume number 21

Issue number 7

Type of Use Thesis/Dissertation

Portion: Figures

Author of this Springer article No

Order reference number None

Original figure numbers Figure 4

Title of your thesis / dissertation Hard turning of martensitic AISI 440B stainless steel

Total 0.00 USD

8. ASTAKHOV ET AL. 2006

License Number 3451870494606

License date Aug 18, 2014

Licensed content publisher Springer

Licensed content publication Springer eBook

Licensed content title

Tools (Geometry and Material) and Tool Wear

Licensed content author Viktor P. Astakhov

Licensed content date Jan 1, 2008

Type of Use Thesis/Dissertation

Portion: Figures

Author of this Springer article No

Order reference number None

Original figure numbers Figure 2.6

Title of your thesis / dissertation Hard turning of martensitic AISI 440B stainless steel

Total 0.00 USD

9. KLOCKE 2011

License Number 3451880674535

License date Aug 18, 2014

Licensed content publisher Springer

Licensed content publication Springer eBook

Licensed content title Fundamentals of Cutting

Licensed content author Professor Dr.-Ing. Dr.-Ing. E.h. Dr. h.c. Dr. h.c. Fritz Klocke

Licensed content date Jan 1, 2011

Type of Use Thesis/Dissertation

Portion: Figures

Author of this Springer article No

Order reference number None

Original figure numbers Figures 3.21, 3.40 and 3.45

Title of your thesis / dissertation Hard turning of martensitic AISI 440B stainless steel

Total 0.00 USD

10. DOGRA ET AL. 2010

License Number 3384030242322

License date May 08, 2014

Licensed content publisher Springer

Licensed content publication

International Journal of Precision Engineering and Manufacturing

Licensed content title

Tool wear, chip formation and workpiece surface issues in CBN hard turning: A review

Licensed content author Manu Dogra

Licensed content date Jan 1, 2010

Volume number 11

Issue number 2

Type of Use Thesis/Dissertation

Portion: Figures

Author of this Springer article No

Country of republication other

Order reference number None

Original figure numbers Figures 1 , 2

Title of your thesis / dissertation Hard turning of Martensitic steel

Total 0.00 USD

APPENDIX B: TEM Micrographs

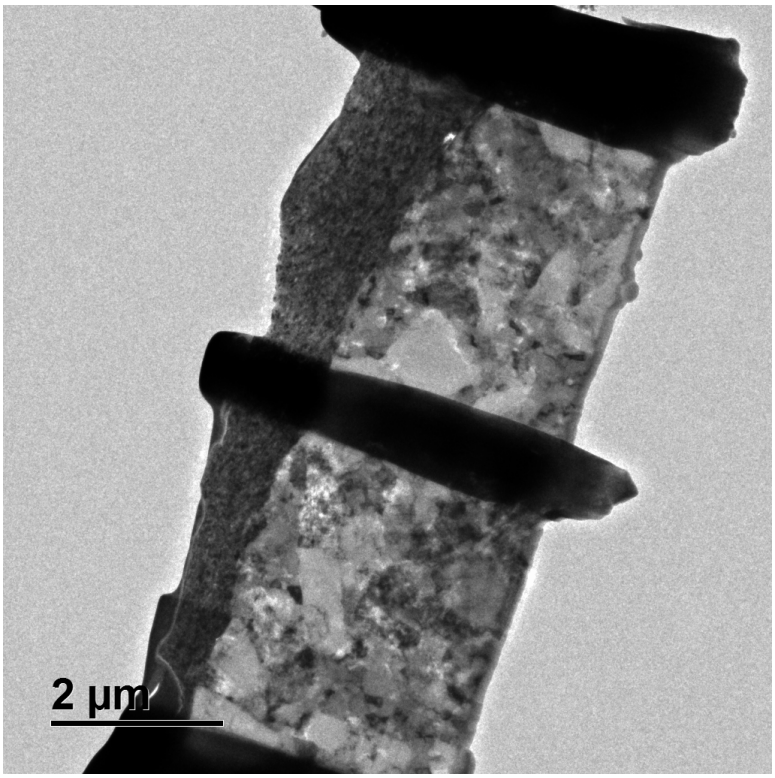

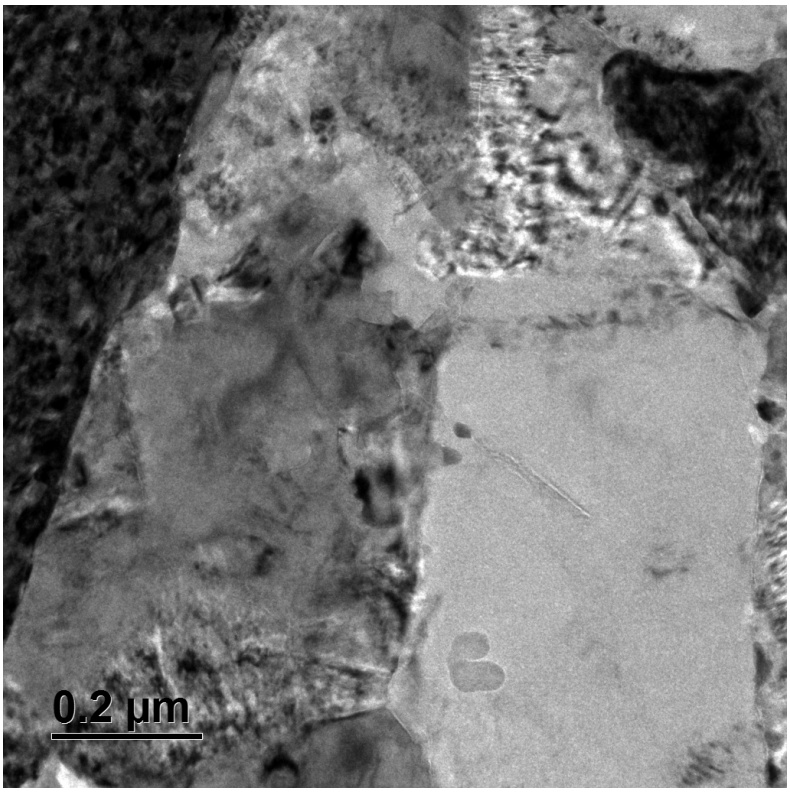

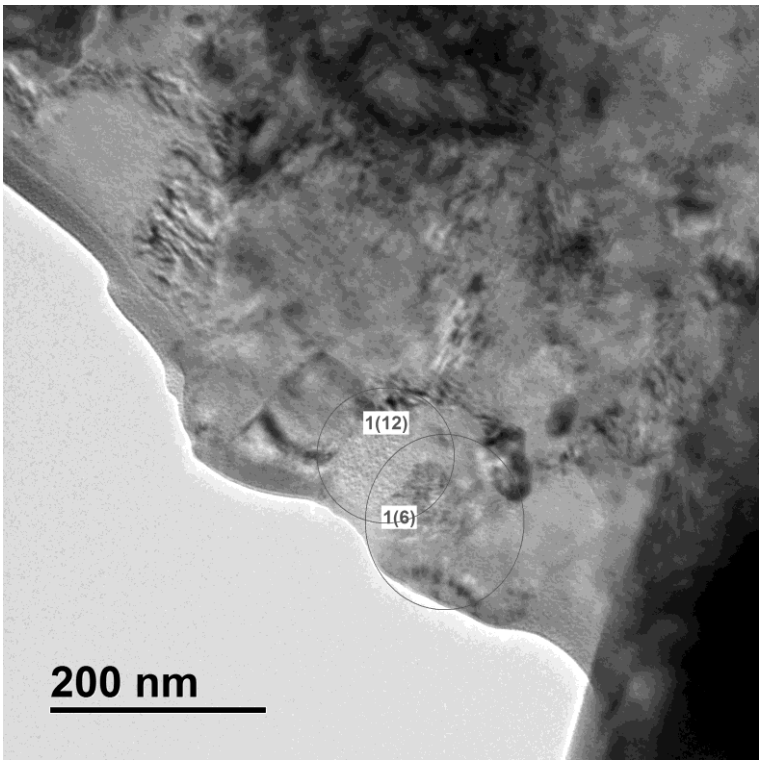
1(12)
1(6)
200 nm

APPENDIX C: CNC MACHINING CODE

1. WITS TRIALS

```
/ G 28 U0;
/ G 28 W0;
G 50 S 3000;
G0  X 250. Z  100. T01 01;
G96 S150 M04;
G00 X170. Z3.;
X145.;
G1 Z-134. F0.1;
G0 X170.;
X250. Z100. T0300;
M30;
%
```

2. INDUSTRIAL APPLICATION TRIALS

```
N3 G0 T300;
G50 S800;
G96 S150 M3;
G0 X56. Z.5;
G1 X35. F.35;
G0 X88. W.5;
Z -24.6;
G1 X57. F.25;
G0 X88. W.5;
Z – 25.3;
G1 X57. F .35;
G0 Z2.;
X 52.5;
G1 Z-23.1;
G2 44.4 Z-25.3 R2.2;
G0 X82.4 W.5;
G1 Z -25.3 F.35;
X 83.5 W -2.6 F.25;
Z -31.3;
X 150. F.25;
G0 X150. Z100.;
M1;
;
```

APPENDIX D: cBN AND MIXED CERAMICS GRAIN SIZE MEASUREMENT

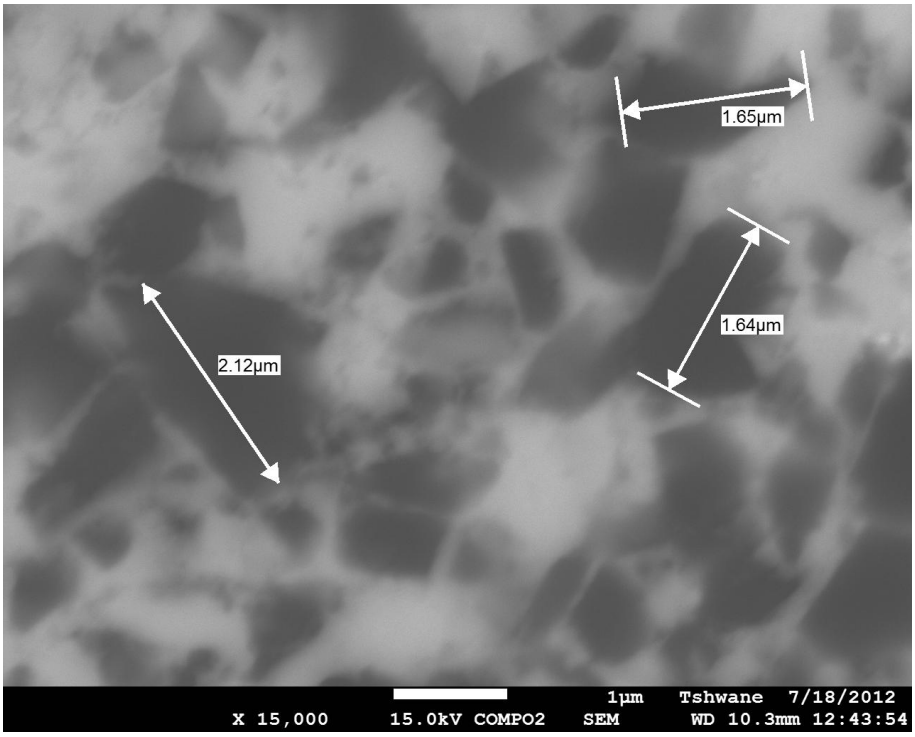

PcBN: cBN grain size measurement

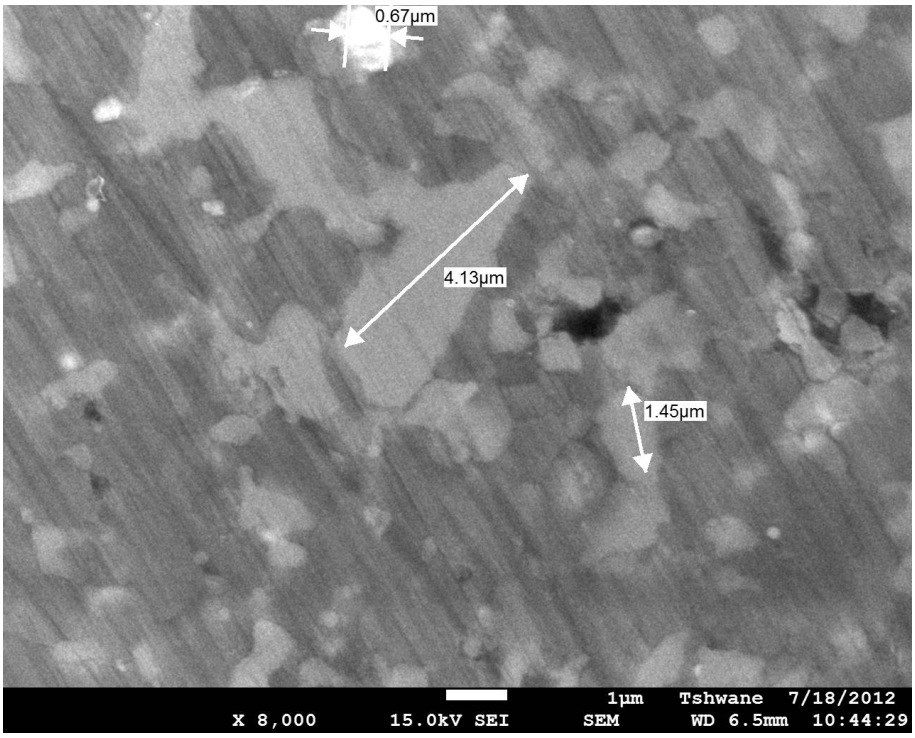

Mixed Ceramics: TiC grains size measurement